Electronic Theses and Dissertations

Theses, Dissertations, and Major Papers

1-1-1971

Part One. A study of the dissolution of tin tubes in hydrochloric acid solutions. Part Two. A potentiostatic investigation of the polarization and cathodic protection of tin tubes in hydrochloric acid solutions.

x

PART ONE. A STUDY OF THE DISSOLUTION OF TIN TUBES
IN HYDROCHLORIC ACID SOLUTIONS

PART TWO. A POTENTIOSTATIC INVESTIGATION OF THE
POLARIZATION AND CATHODIC PROTECTION OF
TIN TUBES IN HYDROCHLORIC ACID SOLUTIONS

A Dissertation
Submitted to the Faculty of Graduate Studies Through the
Department of Chemical Engineering in Partial Fulfilment
of the Requirements for the Degree of
Doctor of Philosophy at the
University of Windsor

by

David S.P. Poa

Windsor, Ontario
1971

UMI Number: DC52684

INFORMATION TO USERS

The quality of this reproduction is dependent upon the quality of the copy submitted. Broken or indistinct print, colored or poor quality illustrations and photographs, print bleed-through, substandard margins, and improper alignment can adversely affect reproduction.

In the unlikely event that the author did not send a complete manuscript and there are missing pages, these will be noted. Also, if unauthorized copyright material had to be removed, a note will indicate the deletion.

UMI®

UMI Microform DC52684
Copyright 2009 by ProQuest LLC.
All rights reserved. This microform edition is protected against unauthorized copying under Title 17, United States Code.

HBX 5938

APPROVED BY: _Alex Snyff_

W Youdefis

W G Allind

W Callina

H S Foyle

367720

ACKNOWLEDGMENTS

TABLE OF CONTENTS

vi

vii

viii

LIST OF TABLES

LIST OF FIGURES

x

xi

xiii

PART ONE

A STUDY OF THE DISSOLUTION OF TIN TUBES

IN HYDROCHLORIC ACID SOLUTIONS

1

ABSTRACT

Horizontally positioned tin tubes, with hydrodynamic entry and exit lengths, were incorporated into a closed loop flow circuit, which was designed for the kinetic study of the dissolution of tin in aerated and deaerated hydrochloric acid solutions circulating through the system.

The effects of total tin ion concentration in the bulk solution; acid concentration, temperature, oxygen concentration, flow velocity of the corroding solution, and the variation of the inside diameter and length of the tin tubes on the dissolution rate of tin in HCl solutions were investigated.

Because the dissolution of tin in aerated hydrochloric acid solutions appears to occur through three simultaneous processes (hydrogen evolution, oxygen depolarization, and an autocatalytic reaction), the experimental results obtained in this investigation have been analyzed in terms of three parallel effects. Over the range of conditions studied the dissolution rate of tin has been correlated by an empirical rate equation showing the contributions of the three possible processes.

Low temperature coefficients and significant effects of fluid velocity indicate that diffusional mass transfer

2

effects play a significant role in the overall dissolution process.

CHAPTER I

INTRODUCTION

The systematic study of corrosion and corrosion prevention is quickly becoming an important engineering science. People have learned that it is more economical to prevent corrosion initially by proper material selection and protective systems rather than pay for replacements and repairs made necessary by the damages of corrosion. Consequently, the corrosion engineer has established himself as a necessary member of the industrial engineering team.

The challenge in Chemical Engineering lies in predicting the behaviour of a given material in a given environment. For many years, corrosion technology was an art rather than a science, with experience and empirical data the only tools available. Stimulated and facilitated by parallel advances in other fields of technology and science, the present trend is toward deepening the understanding of the mechanisms of corrosion and the physical laws which govern corrosion processes in the hope of improving predictions by a coherent theoretical model of physical and chemical behaviour.

In recent years, many investigators have studied the mechanism and kinetics of the dissolution of metals with rotating cylindrical systems. Empirical correlations have been established and various criteria have been postulated for different situations for prediction of dissolution rates. A

4

survey of the literature indicates that little data exist for the interpretation of the mechanism and kinetics of dissolution of metals in recycling flow systems.

In studies on the dissolution and corrosion rates of rotating metal cylinders, Lui[53] found the dissolution rate of tin to be directly proportional to the square root of the surface area of the specimen, while Bodner[12] observed that the dissolution rate of titanium increased with 3/4 power of the surface area of the metal sample. There are examples of other correlations between metal dissolution rate and sample surface area.[63,82] Interpretations of these correlations are open to question. The effects of cylinder diameter and length have never been incorporated into these correlations, although the significance of these factors should not be ignored.

The present work was undertaken with the following aims in mind: (a) to experimentally establish correlations between physical properties of a system, geometrical and hydrodynamic conditions, and rates at which metallic tin is dissolved from the inner surface of a tube into the hydrochloric acid flowing through a recycling system; (b) to compare the rate correlations from this flow system with those obtained from rotating cylindrical systems, and examine whether they share any important characteristics.

The particular system studied, tin-hydrochloric acid was chosen for reasons of convenience and simplicity. Previously, using rotating cylindrical systems, very extensive and

systematic studies on the dissolution rates of tin in HCl solutions were done by Lui,[53] and the present author.[63] These works provide readily available rate correlations which facilitate the second objective. Also, high purity tin can be easily obtained and cast into any desired geometry. Hydrochloric acid is one of the simpler acids and there is precise information available concerning many of its physical properties.

CHAPTER II

LITERATURE REVIEW

Over the last three decades, a large number of articles has appeared in the literature on the general problem of dissolution and corrosion rate of metals. Since the purpose of this study is to obtain a better understanding of the dissolution kinetics of tin in HCl solutions flowing through a recycling system, the following survey will review only those papers pertinent to this subject.

A. Kinetic Studies of Metal Dissolution

Lu and Graydon[51,52] studied the mechanism and kinetics of copper dissolution in aqueous ammonium hydroxide and aqueous sulfuric acid solutions. Weeks and Hills[89] investigated the initial corrosion rate of copper in HCl solutions. Their work was extended by Gnyp.[33] Other systematic researches on the dissolution kinetics of metals including brass, by Kagetsu and Graydon[40] and Bumbulis and Graydon,[16] titanium, by Bodner,[12] and iron, by Taneja[82] have been carried out. Using rotating metal cylinders, the above investigators studied the rate of metal dissolution as a function of temperature, oxygen partial pressure, rotational speed, sample surface area, corroding solution volume, and acid concentration. Over a wide range of conditions, all of them found an autocatalytic effect, with dissolution rate increasing with increasing metal ion concentration in solution.

7

B. General Review of Studies on Tin Dissolution

As early as 1813, the dissolution of tin in acid solutions was examined by Berzelius.[8,9] According to his report, tin dissolves in deaerated hydrochloric and sulfuric acid solutions in the stannous form with the evolution of hydrogen gas.

The effect of oxygen on tin dissolution in various acidic media was studied by Whitman and Russel.[92] Their results showed that, in most cases, oxygen acts as a depolarizer, and if added to acids, will increase the attack on tin. In the absence of air or other oxidizing agents, tin was very resistant to dilute acids. This is because tin has a high hydrogen overpotential, and becomes quickly polarized by hydrogen which prevents the flow of current that accompanies corrosion.

Kohman and Sanborn[44] reported that, in air-free solutions, tin is depolarized by increasing the temperature of the solution, and hydrogen evolution occurs. The effect of temperature on the corrosion of tin in acid solutions was investigated by Khitrov and Shotalova.[43] The rate of tin corrosion in 1-7M solutions of hydrochloric acid and sulfuric acid was observed to increase with increasing temperature. The increase of corrosion rate with increasing temperature is associated with a fall in hydrogen overpotential, decrease in polarization, decrease in viscosity of the solution, and destruction of protective films.

The phenomenon of localized corrosion of tin was examined electrochemically by Hoar.[38] He studied the attack on tin by

nearly neutral solutions containing numerous different anions and cations. Brennert[14] investigated the formation of "black spots" on tin in sodium chloride, sulphate, and nitrate solutions. Britton and Michael[15] studied the local corrosion of tin in chloride solutions. Their results showed that the formation of black spots was an actual building up of the oxide film originally present on the tin surface. Anodic attack at a weak spot on the oxide film covering the metal would not cause tin cations to pass into liquid, but rather cause an increase in the film thickness by deposition of oxide and hydroxide. After a certain time the accumulated acidity at these points apparently became sufficient for the formation of soluble stannous ions, which ruined the film so that break-down occurred with the formation of black spots. The blackness of these spots, according to Britton, was probably due to the absence of reflection from the locally roughened surface.

Hagymas and Quintin[34] studied the corrosion of tin in sulfuric acid. In 0.1 to 1.0 M solutions the hydrogen overvoltage on the tin electrode did not vary with acid concentration. Kohman and Sanborn[44] also reported that there was no apparent influence of acid concentration on the corrosion of tin in air-free solutions.

Probably the most extensive and systematic investigation on the dissolution of tin was done by Lui.[53] He reported that over a wide range of conditions the dissolution of tin in hydrochloric acid solutions proceeds in two autocatalytic

stages with the rate during each stage being dependent on the square root of the tin ion concentration in the corroding solution. His work was extended by this auther.[63]

C. Hydrodynamic and Diffusional Mass Transfer Effects

A review of the literature concerning the relative movement between the corroding solution and metal surface in corrosion processes is given on the following pages.

In 1921 Friend[29] studied the effect of velocity on iron dissolution using a stirrer method and a weight-loss technique. He found that in natural water the corrosion rate decreased with increasing velocity and at high velocity no weight losses were observed. However, in acid solutions the corrosion rate increased with increasing velocity. The rate of dissolution of a rotating disc in dilute acid with no depolarizer was found to be linear with rotational speeds up to 4,000 r.p.m.

Speller and Kendall[75] investigated the flow of natural water in steel pipes in 1923 and published results contradictory to those of Friend. They observed that the corrosion rate was low in the laminar flow region, increased rapidly in the transition region, and continued to increase but at a lower rate in the turbulent region.

Romeo et al.[69], in 1958, reported that for turbulent flow, in small steel pipes, the corrosion rate was found to be proportional to the velocity raised to the power of 0.88.

Roethelli and Brown[72] rotated steel specimens in oxygenated water. Their results showed an increase in the

corrosion rate at low velocities followed by a decrease at
intermediate velocities. At higher velocities the corrosion
rate once more increased with increase in velocity. This
rate enhancement they attributed principally to erosion. The
minimum at intermediate velocities was due to a change in the
corrosion product, ferrous ions being oxidized to ferric.

Both Whitman[91] and Wilson[94], in 1913, stated that velocity
was important in determing the thickness of the film through
which oxygen must diffuse.

Makrides and Hackerman[55], using a stirrer technique to
investigate the behaviour of iron in hydrochloric acid,
observed that the dissolution rate was small and independent
of the stirrer speed in air-free solutions, but showed a
marked dependence on stirrer speed when oxygen was present.

Hatch and Rice[37], in 1945, stressed the importance of
velocity as a means of regulating the rate of supply of oxygen
or inhibitor to a corroding surface. They investigated the
problem by using a weight loss technique on a mild steel pipe
in aerated tap water. At high values of Reynolds number the
corrosion rate attained a steady value. The oxygen was being
supplied to the metal surface in sufficient quantities for
the actual rate of cathodic discharge to be the controlling
step.

Ross and Jones[71], in 1962, studied the effect of flow on
mild steel in sulfuric acid with and without added inhibitors.
They observed that;

(1) dissolution rate $\propto$ (Re)$^{\frac{1}{2}}$ for laminar flow conditions.

(2) dissolution rate $\propto$ (Re) for turbulent flow conditions.

At Re values of 100,000, the dissolution rate still increased rapidly, the systems apparently still being diffusion controlled. It was not stated whether the system was oxygenated, and if so, to what degree.

The dissolution of rotating steel specimens in 1.0M H_2SO_4 was studied by Uhlig[84] under both aerated and deaerated conditions. In deaerated acid low carbon iron corroded at the same rate at all flow velocities. This was attributed to the activation energy of the cathodic reaction being the controlling factor. In aerated acid, velocity very much accelerated corrosion but at a decreasing rate as the velocity increased.

Levich[49] was one of the first workers to present his findings in terms of dimensionless groups. He studied rotating disc electrodes and derived the following expression for the thickness of the Nernst diffusion layer;

$$\delta = 1.62 \left(\frac{\rho D}{\mu} \right)^{.33} \left(\frac{\mu}{\rho \omega} \right)^{.50}$$
$$= 1.62 \, (Sc)^{-.33} (Re)^{-.50}$$

where: δ = diffusion layer thickness;

ω = angular velocity of the electrode;

Riddiford and Bircumshaw[68] reported on the kinetics of dissolution of zinc in aqueous iodine solutions. The rate of dissolution was found to be a function of the stirrer speed. The reactions being diffusion controlled, they established the following relationships between the dissolution constant

k and the stirrer speed;

$$k = 0.0103 \text{ (r.p.m.)}^{0.50}$$

or in dimensionless groupings

$$Nu = 0.558 \text{ (Re)}^{0.56} \text{(Sc)}^{0.27}$$

Wilke et al[93] evaluated mass transfer coefficients for free convection from limiting currents and correlated their data by;

$$Nu_{av} = 0.66 \text{ (Sc)}^{0.25} \text{(Gr)}^{0.25}$$

The results were in good agreement with those predicted from the boundary layer theory for mass transfer by free convection.

In 1954, Eisenberg et al[25] investigated the dissolution of metal cylinders by varying, systematically, the rotational speed, the limiting current, and the cylinder diameter. It was possible to correlate their results by;

$$Nu = 0.079 \text{ (Re)}^{0.70} \text{(Sc)}^{0.356}$$

Makrides[54] used the rotating electrode technique in his study of the anodic dissolution of iron in sulfuric acid and ferric sulphate solutions. He expressed the dependence on hydrodynamic flow conditions at a constant oxidant concentration as;

$$E = \beta_a \log v^{(1 - \varphi)} + \text{const.}$$

Where v = linear velocity

φ = const.

β_a = Tafel slope

Lin et al[50], in 1951, and Von Shaw et al[87], in 1963, studied several diffusion controlled processes under forced flow conditions using circular tube flow systems. In the laminar region their results were in excellent agreement with the Leveque[47] heat transfer equation in which the Prandtl group was replaced by the Schmidt group;

$$Nu = 1.614 \ (Re)^{1/3} \ (Sc)^{1/3} (\frac{d}{L})^{1/3}$$

In the region of turbulent flow, Von Shaw, Reiss, and Hanratty[87] expect the average Nusselt number in circular tubes to be given by;

$$Nu_{av} = 0.276 \ (Re)^{0.58} (Sc)^{0.33} (\frac{d}{L})^{0.33}$$

Cornet et al[20] studied the effect of flow rate on a copper tube in 2.1N H_2SO_4. They found that at high Reynolds numbers there was little increase in corrosion with increase in flow rate. This behaviour was attributed to control by a slow cathodic discharge process. In laminar flow the system was diffusion controlled. Cornet's group correlated their data in the turbulent region by;

$$Nu = 0.053 \ (Re)^{0.68} (Sc)^{0.33}$$

Wranglen and Nilsson[95], in 1962, studied cathodic deposition on horizontal plates under forced convection. Under limiting current density conditions they expressed their results as;

$$Nu = 0.34 \ (Re)^{0.50} (Sc)^{0.33} \text{ for laminar flow, and}$$

$$Nu = 0.17 \ (Re)^{0.60} (Sc)^{0.33} \text{ for turbulent flow}$$

Two papers published recently, one by Ibl[39] in 1959 and the other by Elder and Wranglen[26] in 1964, present theoretical studies of the application of dimensional analysis to electrochemistry. The latter paper gives a detailed theoretical treatment of mass transfer at plane plate electrodes under conditions of both forced and natural convection.

The agreement between the results of all investigations is quite good considering the difficulty of the problem. In general the power of the Reynolds number varies from 0.50 to 0.70, and the Schmidt number from 0.25 to 0.356 under turbulent flow conditions. Most of the later workers have compared their correlations with standard heat transfer correlations and obtained excellent agreement.

CHAPTER III

THEORY

In the first section of this chapter, the mechanism of dissolution of a metal in electrically conductive solutions (electrolytes) is briefly presented by examining a typical case of electrochemical corrosion - dissolution of metal in hydrochloric acid solutions. In the second section, effects of diffusional mass transfer on the dissolution process are discussed. The reason for this special emphasis is that previous workers[53,63] found the reaction of tin with hydrochloric acid to be mass transport controlled.

A. Reaction Mechanism

It was established many years ago that metals corrode in aqueous environments by an electrochemical mechanism. On a piece of metal that is corroding there are both anodic and cathodic sites. These may be permanently separated from each other, but in many instances the whole of the metal surface consists of anodic and cathodic sites which are continually shifting. At an anodic site an oxidation process occurs through a loss of electrons and the metal goes into solution by a reaction that can be depicted as (for example):

$$Sn - 2e \longrightarrow Sn^{++}$$
$$\text{(metal)} \qquad\qquad \text{(ionized in solution)}$$

At a cathodic site a reduction process occurs (a gain of electrons). This will result in the reduction of dissolved

16

oxygen or the liberation of hydrogen gas (particularly from acid solutions) or other less common reactions. The two most common reactions can be depicted as:

$$O_2 + 4e + 2H_2O \longrightarrow 4OH^-$$

$$2H^+ + 2e \longrightarrow H_2$$
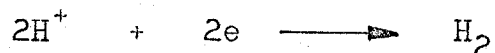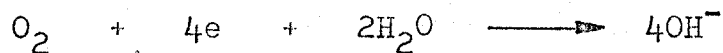
Very detailed descriptions of the mechanism of dissolution of metals were given elsewhere by Taneja[82] and this author[63].

The fundamental mechanism of such a process can be represented in the following manner:

1. The dissolution of a metal, capable of existing in two oxidation states, by a hydrogen evolution process can be described in terms of the following elementary stages:

a. First, when an acid such as hydrochloric acid dissolves in water, we have

$$HCl + H_2O \longrightarrow H_3O^+ + Cl^-$$
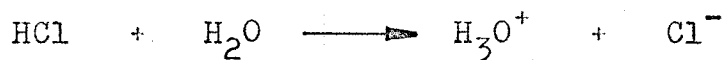
The bulk solution, therefore, consists of water molecules, hydronium ions, and chloride ions. In general, contact between two immiscible phases is accompanied by an increased concentration in the fluid phase close to the interface. This tendency leads to the formation of a "diffusion layer". Therefore, when a metal is placed in the deaerated acid solution, the hydrogen ions will diffuse through this layer, from the bulk solution to the metal-solution interface,

$$H_b^+ \longrightarrow H_i^+$$

where subscript b denotes bulk solution, and subscript

i denotes metal-solution interface. (Hereafter we use H^+

instead of H_3O^+ for convenience.)

  b. The adsorption of hydrogen ions on the metal surface

$$H^+_i \; + \; \underset{*}{M} \; \rightleftharpoons \; \underset{*}{M}\text{-}H^+_s$$

where $\underset{*}{M}\text{-}H^+_s$ denotes a hydrogen ion adsorbed on an active

site, $\underset{*}{M}$,on the metal surface:

  c. Discharge of adsorbed hydrogen ions by virtue of

electron transfer through the metal:

   (c1) Electrons transferred from a neighbouring vacant

site on the metal surface

$$\overset{H^+}{\underset{*}{|}}_{M} - \underset{*}{M} - \underset{*}{M} - M - \overset{H^+}{\underset{*}{|}}_{M} - \longrightarrow \overset{H}{\underset{*}{|}}_{M} - M - M^{++} - M - \overset{H}{\underset{*}{|}}_{M} -$$

   (c2) Electrons transferred directly from the surface

atoms on which adsorption occurred

$$\underset{*}{M}\text{-}H^+_s \; \longrightarrow \; \underset{*}{M^-}H_s$$

  d. Formation of molecular hydrogen from atomic hydrogen,

by one of the following possible modes:

   (d1)

$$\overset{H}{\underset{*}{|}}_{M} - \underset{*}{M} - M^{++} - M - \overset{H}{\underset{*}{|}}_{M} - \longrightarrow \underset{*}{M} - M - M^{++} - M - \overset{H_2}{\underset{*}{|}}_{M} -$$

   (d2) $2\,(\,\underset{*}{M^+}\text{-}H_s) \; \longrightarrow \; \underset{*}{M^{++}_s} \; + \; \underset{*}{M}\text{-}H_{2\,s}$

(d3)
$$M^+\underset{*}{-}H_s \quad + \quad H_i^+ \quad \longrightarrow \quad M^{++}\underset{*}{-}H_{2_s}$$
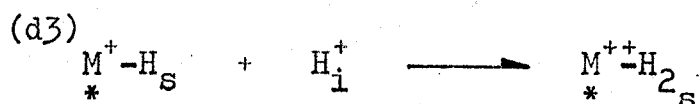
e. The removal of molecular hydrogen from the metal surface by one or more of the following possibilities:

(e1) Dissolution of molecular hydrogen into the solution at the metal-solution interface

$$M\underset{*}{-}H_{2_s} \quad \longrightarrow \quad M_* \quad + \quad H_{2_{i,dissolved}}$$
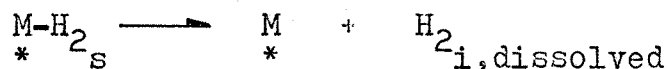
(e2) Absorption of molecular hydrogen from the metal surface into the lattice structure of the metal

$$
\begin{array}{ccccc}
 & \underset{*}{-M-}H_2 & & & -\underset{*}{M}- \\
 & | & & & | \\
-M - & M - M - M - & \longrightarrow & -M - & M \underset{H_2}{} M - M - \\
| & |\quad|\quad| & & | & |\quad| \quad| \\
-M - & M - M - M - & & -M - & M - M - M -
\end{array}
$$
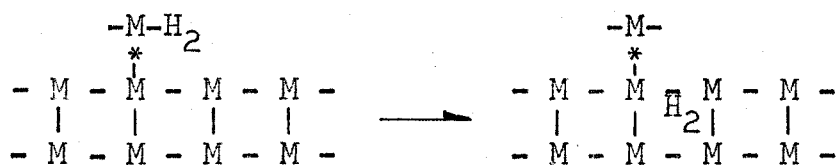
(e3) Formation of hydrogen gas bubbles on the metal surface and their subsequent detachment from the metal surface

$$n(\ M\underset{*}{-}H_2) \quad \longrightarrow \quad M\underset{*}{-}(H_2)_n \quad + \quad (n-1)M_*$$

$$M\underset{*}{-}(H_2)_n \quad \longrightarrow \quad M_* \quad + \quad (H_2)_n$$
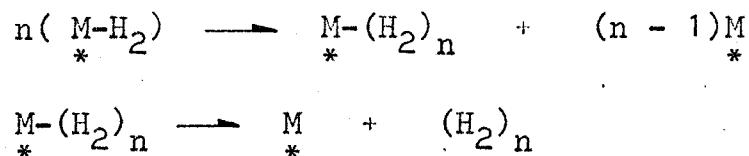
where $M\underset{*}{-}(H_2)_n$ represents a hydrogen gas bubble attached on the metal surface:

f. Desorption of metal ions from the metal surface

$$M_s^{++} \quad \rightleftharpoons \quad M_i^{++}$$
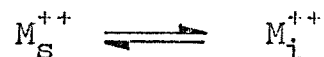
g. Diffusion of metal ions(probably hydrated) from the metal-solution interface to the bulk solution

$$M_i^{++} \quad + \quad nH_2O \quad \longrightarrow \quad M^{+\pm}nH_2O$$
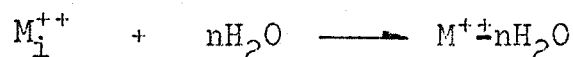
2. In aerated solutions, two other processes can occur together with hydrogen evolution, namely, oxygen depolarization and autocatalysis.

Investigations[23,45,83] have shown that the following successive stages are in good agreement with experimental data for the reaction of oxygen depolarization:

a. Diffusion of molecular oxygen from the bulk solution to the metal-solution interface

$$O_{2_b} \longrightarrow O_{2_i}$$
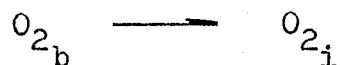
where b denotes bulk solution, and i denotes metal-solution interface.

b. Adsorption of oxygen on the metal surface; there are two types of adsorption possible for oxygen on metal surface[13,80]:

(b1) Molecular adsorption

$$M_* + O_{2_i} \rightleftharpoons M\text{-}O_{2_s}^*$$

(b2) Dissociative adsorption

$$2M_* + O_{2_i} \rightleftharpoons 2(M\text{-}O_s^*)$$
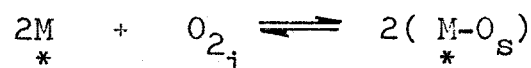
c. Formation of a mono-valent oxygen ion

(c1)

$$\underset{-M - \overset{M\text{-}O_2}{\overset{*}{M}} - M - M -}{} \longrightarrow \underset{-M - \overset{M^+O_2^-}{\overset{*}{M}} - M - M -}{}$$

(c2)

$$\underset{-M - \overset{M\text{-}O}{\overset{*}{M}} - M - \overset{M\text{-}O}{\overset{*}{M}} -}{} \longrightarrow \underset{-M - \overset{M^+\text{-}O^-}{\overset{*}{M}} - M - \overset{M^+\text{-}O^-}{\overset{*}{M}} -}{}$$

d. Formation of perhydroxyl radical or hydroxyl radical

(d1)

$$M^+_{*}\text{-}O_{2}^{-}{}_{s} + M\text{-}H^{+}_{*}{}_{s} \longrightarrow M^{+}_{*}\text{-}HO_{2}{}_{s} + M_{*}{}_{s}$$

(d2)

$$M^{+}_{*}\text{-}O^{-}_{s} + M\text{-}H^{+}_{*}{}_{s} \longrightarrow M^{+}_{*}\text{-}HO_{s} + M_{*}{}_{s}$$
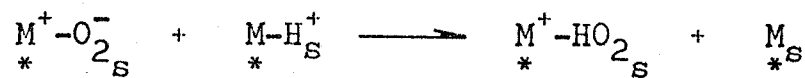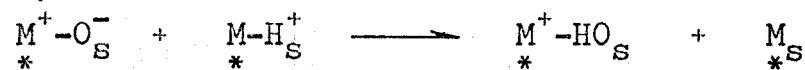
e. Formation of perhydroxyl ion by virtue of electron transfer

$$M^{+}_{*}\text{-}HO_{2}{}_{s} \longrightarrow M^{++}_{*}\text{-}HO_{2}^{-}{}_{s}$$
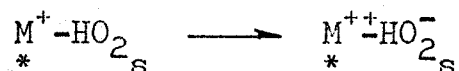
f. Formation of hydrogen peroxide by one of the following possibilities:

(f1)

$$M^{++}_{*}\text{-}HO_{2}^{-}{}_{s} + M\text{-}H^{+}_{*}{}_{s} \longrightarrow M\text{-}H_{2}O_{2}{}_{*}{}_{s} + M^{++}_{*}{}_{s}$$

(f2)

$$2(\,M^{+}_{*}\text{-}HO\,) \longrightarrow M\text{-}H_{2}O_{2}{}_{*}{}_{s} + M^{++}_{*}{}_{s}$$

g. Reduction of hydrogen peroxide with the formation of hydroxyl ions. This step is itself a complex process and can be further broken down into the following sequence:

(g1) Reduction of hydrogen peroxide to hydroxyl ion and hydroxyl radical

$$M\text{-}H_{2}O_{2}{}_{*}{}_{s} \longrightarrow M^{+}_{*}\text{-}HO_{s} + OH^{-}_{i}$$
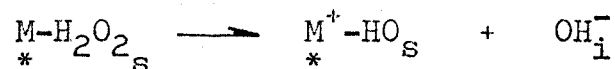
(g2) Reduction of hydroxyl radical to hydroxyl ion

$$M^{+}_{*}\text{-}HO_{s} \longrightarrow M^{++}_{*}{}_{s} + OH^{-}_{i}$$
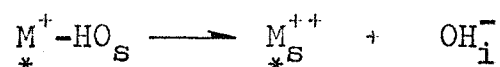
h. Desorption of the metal ions from the metal surface

$$M^{++}_{*}{}_{s} \rightleftharpoons M^{++}_{i}$$
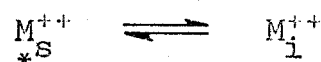
i. Diffusion of the metal ions from the metal-solution interface to the bulk solution

$$M_i^{++} + nH_2O \longrightarrow M^{++}-nH_2O_{bulk}$$

Many of these elementary stages are experimentally proven facts. For instance, the existance of mono-valent oxygen ions (O_2^-) in the cathodic reduction of oxygen in aqueous solutions has been verified by Krasilshchikov[45].

3. For metals that can exist in two or more oxidation states in acidic media, an autocatalytic reaction should be considered as a possibility. The following reaction scheme is suggested as a possible mechanism for this process when the ion of higher oxidation state is quadrivalent of the type M^{++++}:

a. An oxidation process[1] caused by dissolved oxygen with the formation of peroxide intermediate according to

$$M^{++} + O_2 + 2H^+ \longrightarrow M^{++++} + H_2O_2$$
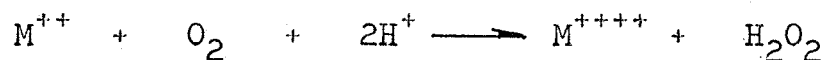
This process can occur in the bulk of the solution, at the metal-solution interface, or at the metal surface
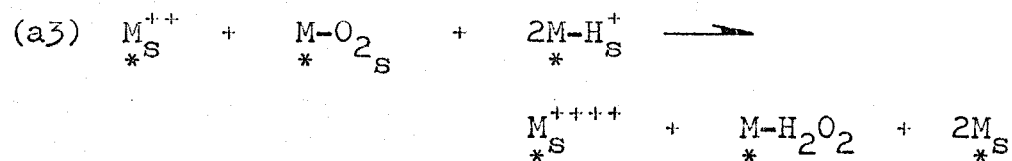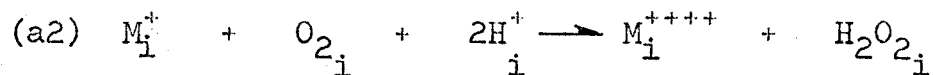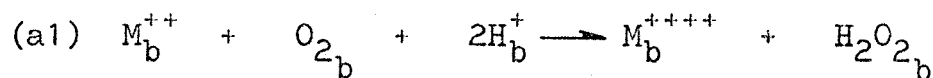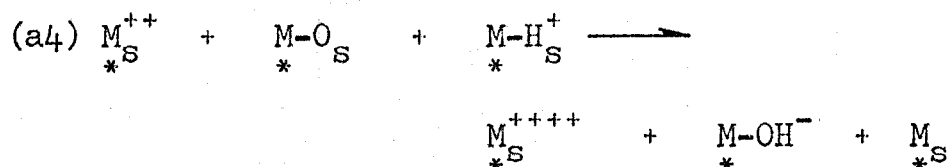
(a1) $M_b^{++} + O_{2_b} + 2H_b^+ \longrightarrow M_b^{++++} + H_2O_{2_b}$

(a2) $M_i^{++} + O_{2_i} + 2H_i^+ \longrightarrow M_i^{++++} + H_2O_{2_i}$

(a3) $M_{*s}^{++} + M-O_{2_s} + 2M-H_{*s}^+ \longrightarrow$

$$M_{*s}^{++++} + M-H_2O_2 + 2M_{*s}$$

$$(a4) \quad M_{*s}^{++} + M\text{-}O_{*\,s} + M\text{-}H_{*\,s}^{+} \longrightarrow$$

$$M_{*s}^{++++} + M\text{-}OH_{*}^{-} + M_{*s}$$

b. An oxidation process caused by the peroxide intermediates[67] (produced in stage a and in the oxygen depolarization reaction) according to

$$M\text{-}H_{*\,s}^{+} + M_{i}^{++} + H_2O_{2\,i} \longrightarrow M_{i}^{++++} + M\text{-}OH_{*\,s}^{-} + H_2O$$

or

$$M\text{-}H_{*\,s}^{+} + M_{*s}^{++} + M\text{-}H_2O_{2\,*\,s} \longrightarrow$$

$$M_{*s}^{++++} + M\text{-}OH_{*\,s}^{-} + M\text{-}H_2O_{*\,s}$$
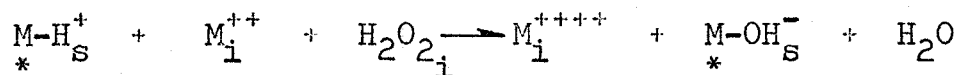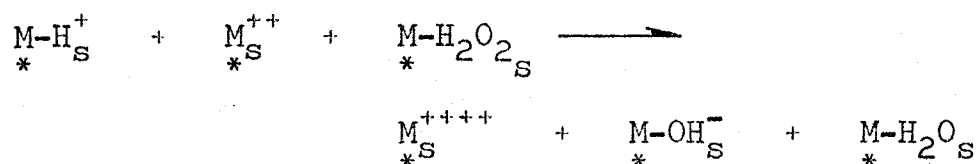
c. An equilibrium[7] between metal ions of higher and lower oxidation states by virtue of electron transfer, either at the metal surface or at the metal-solution interface:

(c1)

$$\begin{array}{ccccc} -M_{*}^{++} & -M_{*}^{++} & M_{*}\text{-} & & -M_{*}^{++++} & -M - M_{*} \\ | & | & | & & | & | & | \\ -M - M - M - M - M\text{-} & \rightleftharpoons & -M - M - M - M - M\text{-} \end{array}$$

(c2)

$$M_{i}^{++++} + M_{*s} \rightleftharpoons 2M_{i}^{++}$$
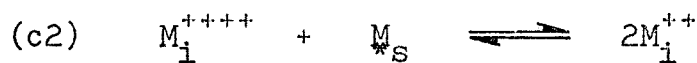
Stages a, b, and c constitute an autocatalytic reaction sequence.

B. Mass Transfer in Electrochemical Dissolution Processes

1. Fundamental Equations

The laws of transport in dilute electrolytic solutions have been known for many years and have been discussed in detail elsewhere[11,48]. The flux of a species is

due to migration in an electric field, diffusion in a concentration gradient, and convection with the fluid velocity.

$$N_j = -z_j u_j FC_j \nabla \Phi \quad - \quad D_j \nabla C_j \quad + \quad vC_j \quad \text{(I-3-1)}$$

where N_j = flux of species j (mole/cm.^{2}-sec)

z_j = charge number of species j

u_j = mobility of species j(sq.cm.-mole/joule-sec)

F = Faraday's constant(coulomb/equiv.)

C_j = concentration of species j(mole/c.c.)

Φ = electrostatic potential(volt)

D_j = diffusion coefficient of species j(sq.cm./sec)

v = fluid velocity(cm./sec.)

A material balance for a small volume element leads to the differential conservation law:

$$\frac{\partial C_j}{\partial t} = -\nabla \cdot N_j \quad + \quad R_j \quad \text{(I-3-2)}$$

where R_j = homogeneous rate of production of species j (mole/c.c.-sec)

Since reactions are frequently restricted to the surfaces of electrodes, the bulk reaction term R_j is often zero in electrochemical systems. To a very good approximation the solution is electrically neutral hence

$$\sum_j z_j C_j = 0 \quad \text{(I-3-3)}$$

The current density in an electrolytic solution is due to the motion of charged species:

$$i = F\sum_j z_j N_j \quad \text{(I-3-4)}$$

where i = current density(amp/sq.cm.)

These laws provide the basis for the analysis of electro-chemical systems. The flux relation, Equation(I-3-1), defines transport coefficients – the mobility u_j and the diffusion coefficient D_j of an ion in a dilute solution. Many electrochemical systems involve flow of the electrolytic solution. The fluid velocity is to be determined from the Navier-Stokes equation

$$\rho \left(\frac{\partial v}{\partial t} + v \cdot \nabla v \right) = -\nabla p - \mu \nabla^2 v + \rho g \qquad (I-3-5)$$

where ρ = fluid density(gm./c.c.)

p = fluid pressure(gm./cm.-sec^2.)

μ = fluid viscosity(gm./cm.-sec.)

g = gravitational acceleration(cm./sec^2.)

and the continuity equation

$$\nabla \cdot v = 0 \qquad (I-3-6)$$

For the reaction of minor species in a solution containing excess supporting electrolyte, it should be permissible to neglect the contribution of ionic migration to the flux of the reacting ions, so that Equation(I-3-1) becomes

$$N_j = -D_j \nabla c_j + v c_j \qquad (I-3-7)$$

and substitution into Equation(I-3-2) yields

$$\frac{\partial c_j}{\partial t} + v \cdot \nabla c_j = D_j \nabla^2 c_j \qquad (I-3-8)$$

This is the general equation of convective diffusion.

For a full solution of the equations of hydrodynamics and

convective transfer, we must also know the boundary and
initial conditions that satisfy the different systems under
consideration. It would, of course, be more satisfactory to
obtain a complete solution of these equations, but, this is,
in most cases,impossible. Therefore, in practice, most of the
work in this field has been done by dimensional analysis and
empirical approach.

2. Nernst Diffusion Layer Theory

Essential to the understanding of convective transfer
problems is the concept of the diffusion layer. Frequently,
due to the small value of the diffusion coefficient, the
concentrations differ significantly from their bulk values
only in a thin region near the surface of an electrode.
According to Nernst[61], a practically stationary liquid layer
must be assumed in contact with the electrode surface,
regardless of whether the electrolytic solution is stirred or
not. Within this layer molecular diffusion and ionic transport
are of primary importance to the transport process, while
outside this layer the convective transport dominates and the
concentration is maintained at a constant value by convection.
The concentration gradient was assumed to be linear and
related to the solute mass transfer flux N_j by the equation

$$N_j = \frac{D_j}{\delta} (C_i - C_b) \qquad\qquad (I\text{-}3\text{-}9)$$

where C_i = concentration of species j at the solution-
electrode interface(mole/c.c.)

C_b = concentration of species j in bulk solution (mole/c.c.)

δ = diffusion layer thickness(cm.)

In general, the flux N_j of the ions through a cross section parallel to the surface and away from the surface is additively composed of the diffusion term and the migration term. The flux is therefore, given by

$$N_j = D_j \frac{(C_i - C_b)}{\delta} + \frac{i \cdot t_j}{z_j \cdot F} \qquad (I-3-10)$$

where t_j = transport number of species j

Nernst's theory postulates that the liquid is stationary within the diffusion layer, which is contrary to experimental data obtained for fluid flow near solid surfaces[48]. In reality the transition from diffusion to convection takes place continuously. Furthermore, the theory does not allow quantitative predictions to be made as to the dependence of δ on the flow conditions.

3. Application of Dimensional Analysis

The diffusional flux is now usually written in the form[62]

$$N_j = k_j(C_i - C_b) \qquad (I-3-11)$$

where k_j = mass transfer coefficient of species j.

The value of k_j can be determined by dimensional analysis and the correlations have the general form

$$Nu = const.(Re)^\alpha (Sc)^\zeta \qquad (I-3-12)$$

for forced convection

and $$Nu = const.(Gr)^{\gamma} (Sc)^{\epsilon} \qquad (I\text{-}3\text{-}13)$$

for natural convection

The exponents α, ζ, γ, and ϵ are determined by experiment where the dimensionless groups are

$$\text{Grashof number, } Gr = \frac{gL^{3}\Delta\rho}{\rho}\left(\frac{\rho}{\mu}\right)^{2}$$

$$\text{Reynolds number, } Re = \frac{Lv\rho}{\mu}$$

$$\text{Nusselt number, } Nu = \frac{k_{1}L}{D}$$

$$\text{Schmidt number, } Sc = \frac{\mu}{\rho D}$$

where L = characteristic length(cm.)

The physical significance of the dimensionless groups is of interest. The Reynolds number is defined as the ratio of the non-viscous or inertial forces to the viscous forces acting on the element of fluid. At low values of Reynolds number the inertial forces are small compared with the viscous forces and the flow is streamlined. At high values of Reynolds number the inertial forces predominate and the flow becomes turbulent.

The Schmidt number is the ratio of the fluid property governing the transfer of momentum by viscous forces, the kinematic viscosity, to the fluid property governing mass transfer by diffusion, the diffusivity.

It is possible to obtain the dimensionless correlations (I-3-12) and (I-3-13) by;

(a) direct dimensional analysis,

(b) writing the fundamental equations of motion and

diffusion in dimensionless terms,

and (c) employing the Prandtl-Taylor or Chilton-Colburn

extensions of the Reynolds Analogy as applied to

mass transfer.

By analogy with their j_H factor for heat transfer Chilton

and Colburn deduced a factor for mass transfer j_D and showed

that the two were approximately equal. Thus it is possible

to calculate mass transfer coefficients from data obtained

from heat transfer experiments[62].

4. Diffusional Mass Transfer in a Circular Tube

In this section we consider a special simple case

as an example of the application of the dimensional analysis

method by writing the fundamental equations of motion and

diffusion in dimensionless terms. Consider the steady

isothermal flow of an acid solution inside a tube of circular

cross section as shown in Figure I-3-1.
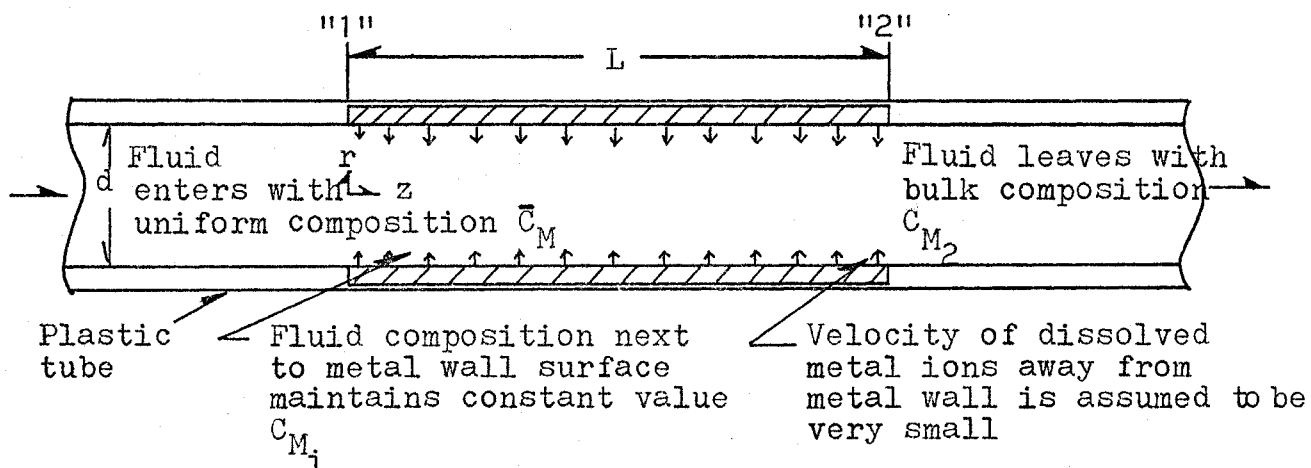
FIGURE I-3-1. Mass Transfer in a Tube With a Soluble
Metal Wall.

Assume that the flow pattern is fully established and the velocity distribution is known at plane "1" and that the fluid concentration is uniform at $\bar{C}_M$ in the region $z < 0$. From $z = 0$ to $z = L$, the tube is made of a metal or other soluble solid, which dissolves slowly and maintains the liquid composition along the dissolving surface at constant value C_{M_i}. We further assume that the physical properties ρ, μ, and D_M are constant.

The diffusional mass transfer at the solution-metal interface can be described by starting from Equation (I-3-7).

$$N_M = -D_M \nabla C_M \quad + \quad v_z C_M \qquad (I-3-14)$$

in this case $j = M$, and at the metal surface, within the diffusion layer, the fluid velocity is very small and the term $v C_M$ can be neglected. Therefore, the flux of M away from the metal surface is

$$N_M = -D_M \nabla C_M = -D_M \frac{\partial C_M}{\partial r} \qquad (I-3-15)$$

The total molar rate of addition of species M by diffusion over the whole metal tube surface between plane "1" and "2" in Figure I-3-1 is given by the following expression, valid for either laminar or turbulent flow:

Total molar rate of addition of species M

$$= \int_0^L \int_0^{2\Pi} \left(D_M \frac{\partial C_M}{\partial r} \bigg|_{r=R} \right) R d\theta \, dz \qquad (I-3-16)$$

where R is the radius of the tube.

But from Equation (I-3-11), we have

$$N_M = k_M \left(C_{M_i} \quad - \quad \bar{C}_{M_b} \right)$$

and therefore;

The total molar rate of addition of species M

$$= k_M A (C_{M_i} - \bar{C}_{M_b})$$

$$= k_M \Pi L d (C_{M_i} - \bar{C}_{M_b}) \qquad (I-3-17)$$

where d denotes the inside diameter of the metal tube, and A denotes the inner surface area of the metal tube.

Substitution of Equation(I-3-17) into Equation(I-3-16) gives

$$k_M = \frac{1}{\Pi L d (C_{M_i} - \bar{C}_{M_b})} \int_0^L \int_0^{2\Pi} (D_M \frac{\partial C_M}{\partial r}\bigg|_{r=R}) R d\theta \, dz \qquad (I-3-18)$$

This equation can be reduced to a dimensionless form by introducing the dimensionless quantities; $r^* = r/d$, $z^* = z/d$, and $C_M^* = (C_M - C_{M_i})/(\bar{C}_{M_b} - C_{M_i})$. Using these quantities in the equation and rearranging it gives

$$Nu = \frac{k_M d}{D_M} = \frac{1}{2\Pi L/d} \int_0^{L/d} \int_0^{2\Pi} (-\frac{\partial C_M^*}{\partial r^*}\bigg|_{r^*=\frac{1}{2}}) d\theta \, dz^* \qquad (I-3-19)$$

The general equation of convective diffusion for any species is

$$\frac{\partial C}{\partial t} + v \cdot \nabla C = D\nabla^2 C \qquad (I-3-20)$$

This equation can be simplified if radial symmetry is present to the convective diffusion equation in cylindrical coordinates

$$\frac{\partial C}{\partial t} + v_r\left(\frac{\partial C}{\partial r}\right) + v_z\left(\frac{\partial C}{\partial z}\right)$$

$$= \frac{\partial}{\partial z} (D \frac{\partial C}{\partial z}) + D\left(\frac{\partial^2 C}{\partial r^2}\right) + \frac{D}{r}\left(\frac{\partial C}{\partial r}\right)$$

$$(I-3-21)$$

This equation may now be reduced to dimensionless form by introducing a characteristic flow velocity U_o , which is the uniform velocity of the solution in the tube.

Multiplying Equation (I-3-21) by $\frac{1}{U_o C_o}$, where C_o is the uniform concentration in the bulk of the solution, we have

$$\frac{1}{d}\left(\frac{\partial \frac{C}{C_o}}{\partial \frac{tU_o}{d}}\right) + \frac{v_r}{U_o d}\left(\frac{\partial \frac{C}{C_o}}{\partial \frac{r}{d}}\right) + \frac{v_z}{U_o d}\left(\frac{\partial \frac{C}{C_o}}{\partial \frac{z}{d}}\right)$$

$$= \frac{D}{U_o d^2}\cdot\left(\frac{\partial^2 \frac{C}{C_o}}{\partial \frac{z^2}{d^2}}\right) + \frac{D}{U_o d^2}\left(\frac{\partial^2 \frac{C}{C_o}}{\partial \frac{r^2}{d^2}}\right) + \frac{D}{U_o d^2 (\frac{r}{d})}\cdot\left(\frac{\partial \frac{C}{C_o}}{\partial \frac{r}{d}}\right)$$

$$(I-3-22)$$

Introducing the dimensionless quantities; $v_r^* = v_r/U_o$, $v_z^* = v_z/U_o$, $t^* = tU_o/d$, $r^* = r/d$, $z^* = z/d$, and $C^* = C/C_o$, we obtain

$$\frac{\partial C^*}{\partial t^*} + v_r^*\left(\frac{\partial C^*}{\partial r^*}\right) + v_z^*\left(\frac{\partial C^*}{\partial z^*}\right)$$

$$= \frac{D}{U_o d}\left(\frac{\partial^2 C^*}{\partial r^{*2}}\right) + \frac{D}{U_o d}\left(\frac{\partial^2 C^*}{\partial z^{*2}}\right) + \frac{D}{U_o d r^*}\left(\frac{\partial C^*}{\partial r^*}\right)$$

$$(I-3-23)$$

The dimensionless ratio, $Pe = \frac{U_o d}{D}$, is known as the Peclet number. Introducing the Peclet number into Equation (I-3-23), we have

$$\frac{\partial c^*}{\partial t^*} + v_r^*\left(\frac{\partial c^*}{\partial r^*}\right) + v_z^*\left(\frac{\partial c^*}{\partial z^*}\right)$$

$$= \frac{1}{Pe}\left[\frac{\partial^2 c^*}{\partial r^{*2}} + \frac{\partial^2 c^*}{\partial z^{*2}} + \frac{1}{r^*}\left(\frac{\partial c^*}{\partial r^*}\right)\right]$$

$$(I-3-24)$$

But $Pe = \dfrac{U_o d}{D} = \dfrac{U_o L}{\nu}\cdot\dfrac{\nu}{D} = Re\cdot Sc$. Therefore, Equation (I-3-24) becomes

$$v_r^*\frac{\partial c^*}{\partial r^*} = \frac{1}{Re\cdot Sc}\left(\frac{\partial^2 c^*}{\partial r^{*2}} + \frac{\partial^2 c^*}{\partial z^{*2}} + \frac{1}{r^*}\cdot\frac{\partial c^*}{\partial r^*}\right) - v_z^*\frac{\partial c^*}{\partial z^*} - \frac{\partial c^*}{\partial t^*}$$

$$(I-3-25)$$

Equation (I-3-25) shows clearly

$$\frac{\partial c^*}{\partial r^*} = \psi(Re,\ Sc) \qquad\qquad (I-3-26)$$

and consequently, Equation (I-3-19) is of the form

$$Nu = \Psi(Re,\ Sc,\ d/L)$$

or $\qquad Nu = const.(Re)^m (Sc)^n \left(\dfrac{d}{L}\right)^p \qquad\qquad (I-3-27)$

where the exponents, m, n, and p for the dissolution of metal tubes of circular cross section can be experimentally determined. Previous workers[39,87,95] showed that m varies between 0.4 and 0.8, n between 0.3 and 0.4, and p between 0.3 and 0.4.

CHAPTER IV

EXPERIMENTAL

A. Equipment

    1. Design of Liquid Recycle System and Accessories

        The schematic diagram of the experimental equipment is shown in Figure I-4-1. The flow system is a closed loop which was constructed from plexiglas tubing. A three-fifteenth horsepower Dynalab Model 4-MD magnetic drive pump, capable of delivering 660 gal./hr. water against 3 feet head, was used to circulate the corroding solution.

        Adjustment of the electrolyte flow rate was achieved by means of globe valve B in the pump by-pass. Two rotameters equipped with stainless steel floats provided an indication of actual flow rates.(One was calibrated to 4 USGPM of 1.0N HCl at 25°C and the other to 15 USGPM.)

        The 20-litre QVF glass supply tank was equipped with an immersion Vycor brand glass heater, a thermo-regulator thermometer, a Teflon coated stirrer, and a gas saturation system. The 35-litre polypropylene make-up tank was equipped with a Teflon coated electric stirrer.

        The test section, mounted in a horizontal position, was located on the downstream side of the pump. The only part of the system on the suction side was about 6 feet of PVC pipe leading from the top supply tank to the pump. This meant, that if any leaks developed, escaping electrolyte

34
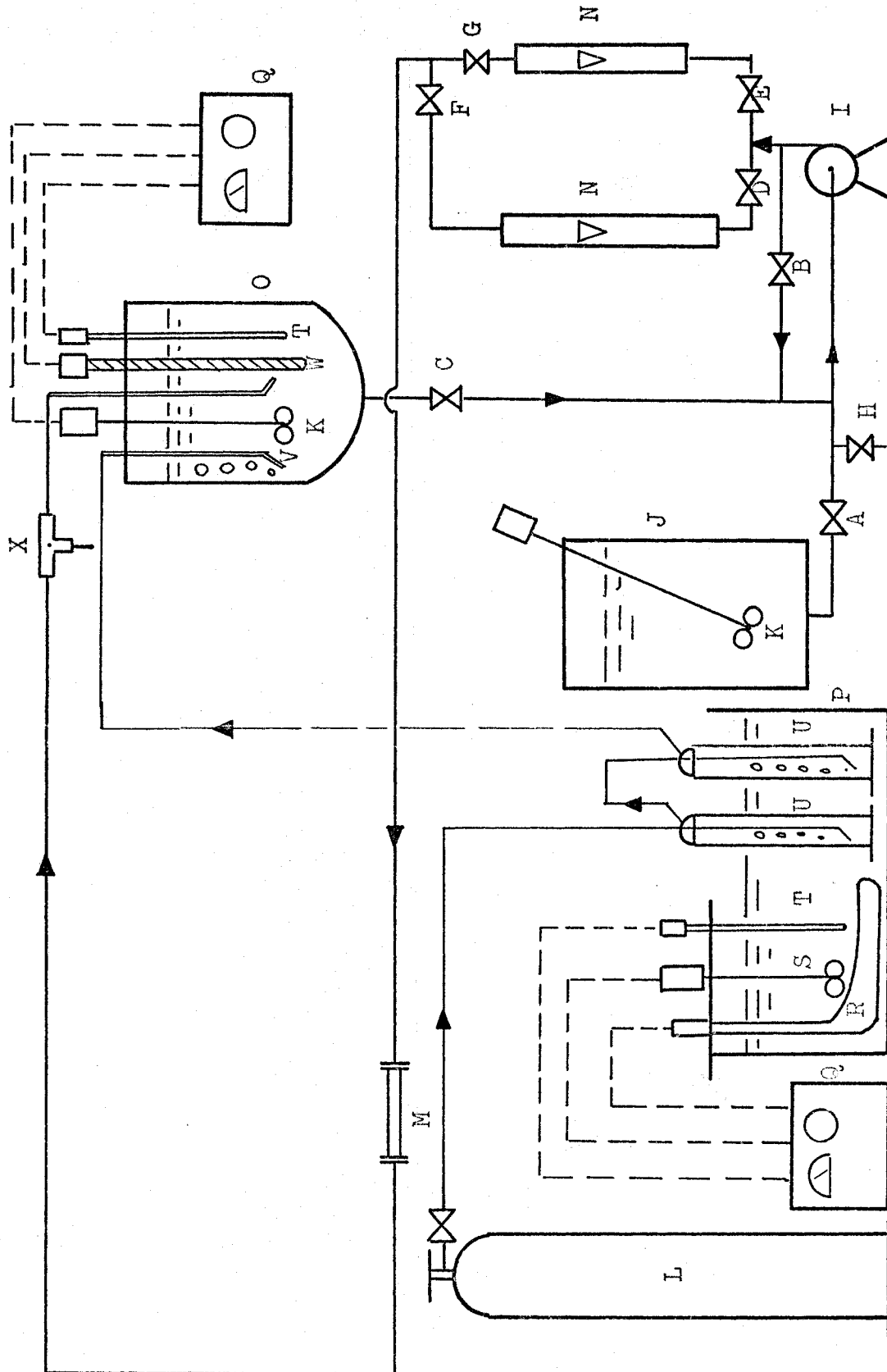
FIGURE I-4-1. SCHEMATIC DIAGRAM OF FLUID RECYCLE SYSTEM

LEGEND - For Figure I-4-1

A, F, G, H - PVC ball valves

D, E, B   - PVC globe valves

C   - QVF glass globe valve

I   - Sealless, magnetic drive pump

J   - Make-up tank, 35 litre, polypropylene

K   - Teflon coated electric stirrer

L   - Compressed gas cylinder

M   - Test section

N   - Rotameter

O   - Supply tank, QVF glass, 20 litre

P   - Constant temperature water bath

Q   - Relay

R   - Electric heating coil

S   - Stirrer

T   - Thermo-regulator thermometer

U   - Glass washing tower

V   - Gas dispersion tube

W   - Vycor brand glass heater

X   - Thermometer

would be easier to see than air being drawn into the system.

Eight feet of clear plexiglas piping immediately preceded the test section to allow development of the hydrodynamic boundary layer. Three feet of clear plexiglas piping immediately followed the test section to ensure steady flow in the test section.

Gas saturation of the acid solution was achieved by passing the appropriate gases from compressed gas cylinders through a series of wash bottles containing HCl solution of the same concentration as in the supply tank. All wash bottles were kept at the same temperature as the corroding solution by immersing them in a constant temperature bath.

The return inlet to the supply tank was located below the solution surface and directed away from the gas dispersion tube to prevent large gas bubbles from being drawn into the system.

A thermometer, incorporated near the return inlet by means of a polypropylene T-piece, provided a check on the temperature variation of the system.

Except for the calming and test section, the circulation loop consisted only of standard half inch plexiglas and PVC pipes, valves, and joints. As a result of the choice of materials and equipments the only metal components contacting the corroding solution other than the surface of the test section are two Type 304 stainless steel floats in the rotameters. The dissolution of Type 304 stainless steel in

dilute HCl solution (up to 6.0N) is negligible.

2. Details of Test Section Construction

A detailed drawing, illustrating the design and materials used in the construction of the test section, is provided as Figure I-4-2.

Tin bars, originally about 1.02 cm. in diameter, were melted and remoulded into 1 inch and 1.5 inch diameter rods under argon gas in a vacuum furnace. Tin tubes of 0.25 to 1.0 inch inside diameter, 2.5 to 5.5 inches in length were produced from these remoulded tin rods.

Pairs of spigot were machined from 1.5 and 2 inch diameter polypropylene rods to different dimensions to accommodate the tin tubes.

Both ends of the tin specimen were recessed into the spigots and secured firmly with plastic cement. In addition, functioning as watertight seals, two Teflon washers were placed between the end surfaces of tin specimen and the stopping edges of the spigots.

Before any test section assembly was incorporated into the system, it was held together, under pressure, so that any Teflon washers projecting beyond the inner surface could be machined flush with the tube walls.

3. Temperature Control and Measurement

The temperature control of the corroding solution was achieved by setting the desired temperature on the thermoregulator-thermometer which sensed the temperature

POLYPROPYLENE SPIGOT JOINT

TIN TUBE

TEFLON WASHER
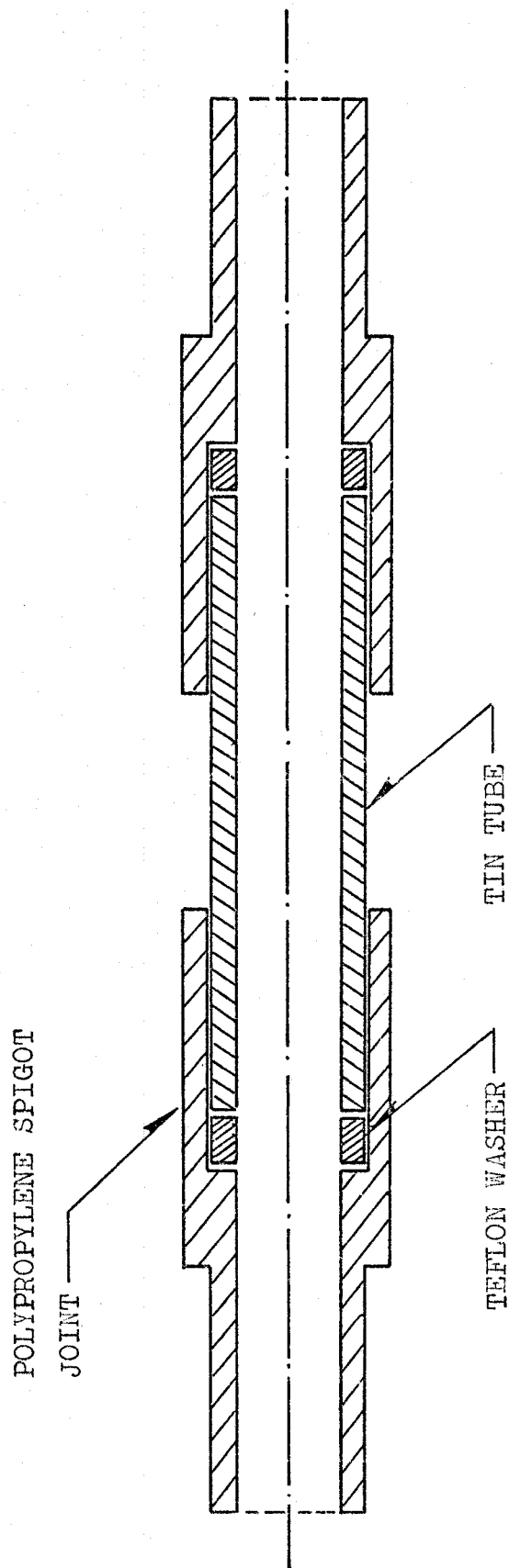
FIGURE I-4-2. DETAILED DRAWING OF TEST SECTION

variation of the corroding solution and maintained it at the set-point by activating a 500 watt immersion Vycor brand glass heater through a relay. The temperature control used in this system was supplied by the Chemical Rubber Company who claimed that it was capable of controlling the temperature within $\pm$ 0.01°C.

The temperature of the solution at the return inlet was also checked and recorded. If the difference between this temperature reading and the temperature reading of the bulk solution exceeded 0.1°C the average value would then be used for data analysis.

B. Chemicals and Materials

The Analar grade tin bars used in this study were supplied by British Drug House LTD. The purity of metal was 99.92 per cent tin. The exact analysis according to the manufacturer showed 0.01 per cent lead, 0.0025 per cent copper, 0.002 per cent bismuth, 0.002 per cent iron, 0.004 per cent total foreign metals, 0.0001 per cent arsenic, and 0.025 per cent antimony.

Hydrochloric acid and all other reagents used were of analytical grade. Dilute HCl solutions were made with distilled water.

C. Procedure

1. Experimental Preparation

The two rotameters were calibrated by maintaining a particular reading and measuring the volume of effluent

collected during a known time interval. Details of rotameter
calibration are given in Appendix 1.

The make-up tank and the QVF glass supply tank were also
calibrated. The liquid capacities at different liquid levels
were measured and marked.

Before the tin tube was integrated into the flow system
it was polished manually to 3/0 emery paper smoothness(average
surface roughness less than 20 microinches) and washed
initially with distilled water and dried with filter paper,
then washed with acetone for degreasing, and finally rewashed
with distilled water. After each run, the tin tube was washed
and dried. A check on the material balance was maintained by
weighing the clean dry tin tube before and after each run.

When not in use, the tin tube was filled with distilled
water. At the start of a run, 0.5N HCl was flushed through
for about 5 minutes. This removed any oxide built up during
storage in distilled water.

2. Procedure for Dissolution Run

The HCl solutions were made up and mixed in the
make-up tank with valves A and H closed(refer to Figure I-4-1).
Valves A, D, E, F, and G were then opened, valve C closed, and
the solution was pumped from the make-up tank into the supply
tank. After the volume of solution in the system was adjusted
by letting the excess solution drain through valves D, E, F,
and G into the make-up tank, valve A was closed and C opened.
At this stage the system was operational. The appropriate gas

was then introduced into the solution through the dispersion tube.

After the solution was flushed overnight, the temperature control system and the stirrer in the supply tank were switched on. During the time required for the acid solution to reach the desired temperature, the test section was prepared and connected to the flow system as previously described.

After the solution reached the desired temperature, the pump was switched on and the flow rate was regulated by adjusting valves B, D, and E.

A 5 ml. sample of the corroding solution was withdrawn for routine analysis at convenient intervals of time from the top supply tank. For every sample of corroding solution withdrawn, an equal volume of HCl solution of the same concentration was added to the supply tank to minimize solution volume change during the dissolution run.

Tin concentrations were determined by means of a Jarrell-Ash Model 82-526 Maximum Versatility Atomic Absorption Spectrophotometer. Details of the analytical procedure are given in Appendix 2.

Upon termination of a dissolution run, the system was drained of corroding solution, flushed with city water three or four times and then flushed with distilled water once. The test section was then disconnected from the system and stored in distilled water until further use.

CHAPTER V

EXPERIMENTAL RESULTS AND DISCUSSION

A. Method of Analysis of Experimental Data; A Typical

Example

In Chapter III details of the mechanism of dissolution of
a metal, capable of existing in two oxidation states in acid
solutions, were presented. On the basis of that discussion the
following characteristics of dissolution can be visualized:

The corroding solution concentration-time plot for the
dissolution of such a metal in aerated solutions will show an
autocatalytic effect, with dissolution rate increasing with
increasing metal ion concentration in solution. The over-all
dissolution rate is a combination of the following three
parallel corrosion effects: hydrogen evolution, oxygen
depolarization, and autocatalysis. The rates of hydrogen
evolution and oxygen depolarization are independent of the
metal ion concentration in the solution(zero order dependency
on metal ion concentration). Therefore, the corroding solution
concentration-time plots for these two reactions should be
straight lines. The oxygen depolarization and autocatalytic
reactions can occur only when oxygen gas is introduced into
the solution. The autocatalytic effect is negligible at the
initial stage because no metal ions are present in the solution
at the start of a dissolution process.

The analysis of the dissolution data obtained in this

43

study is based on the above discussion with experimental data recalculated to a metal dissolved per unit surface area basis. A typical model of this analysis is illustrated in Figure I-5-1, where OA shows the plot of the rate data for the dissolution of tin in deaerated hydrochloric acid solution, a condition under which only hydrogen evolution can occur. Curve OC shows the rate data obtained under the same conditions as those of OA except that the acid solution was air saturated.

The shape of OA, a straight line, conforms to a zero order plot of metal ion concentration vs time. The exponential concentration-time plot of curve OC is a confirmation of an autocatalytic process. The straight line OB has been drawn asymptotically to curve OC at its initial stage where autocatalysis is negligible. This linearity essentially represents an extrapolation of the initial corrosion rate under aerobic conditions in the absence of autocatalysis.

The total area under curve OC is divided by straight lines OA and OB into three regions, each of which corresponds to a specific effect on the over-all dissolution reaction as shown in Figure I-5-1, where slope of line OA = r_1, slope of line OB = $r_1 + r_2$, and slope of curve OC = $r_1 + r_2 + r_3$. (r_1, r_2, and r_3 are the reaction rates in moles of metal dissolved per square centimeter per minute for hydrogen evolution, oxygen depolarization, and autocatalysis respectively.)

This analysis provides a pattern for the interpretation of the tin dissolution data obtained during this investigation.
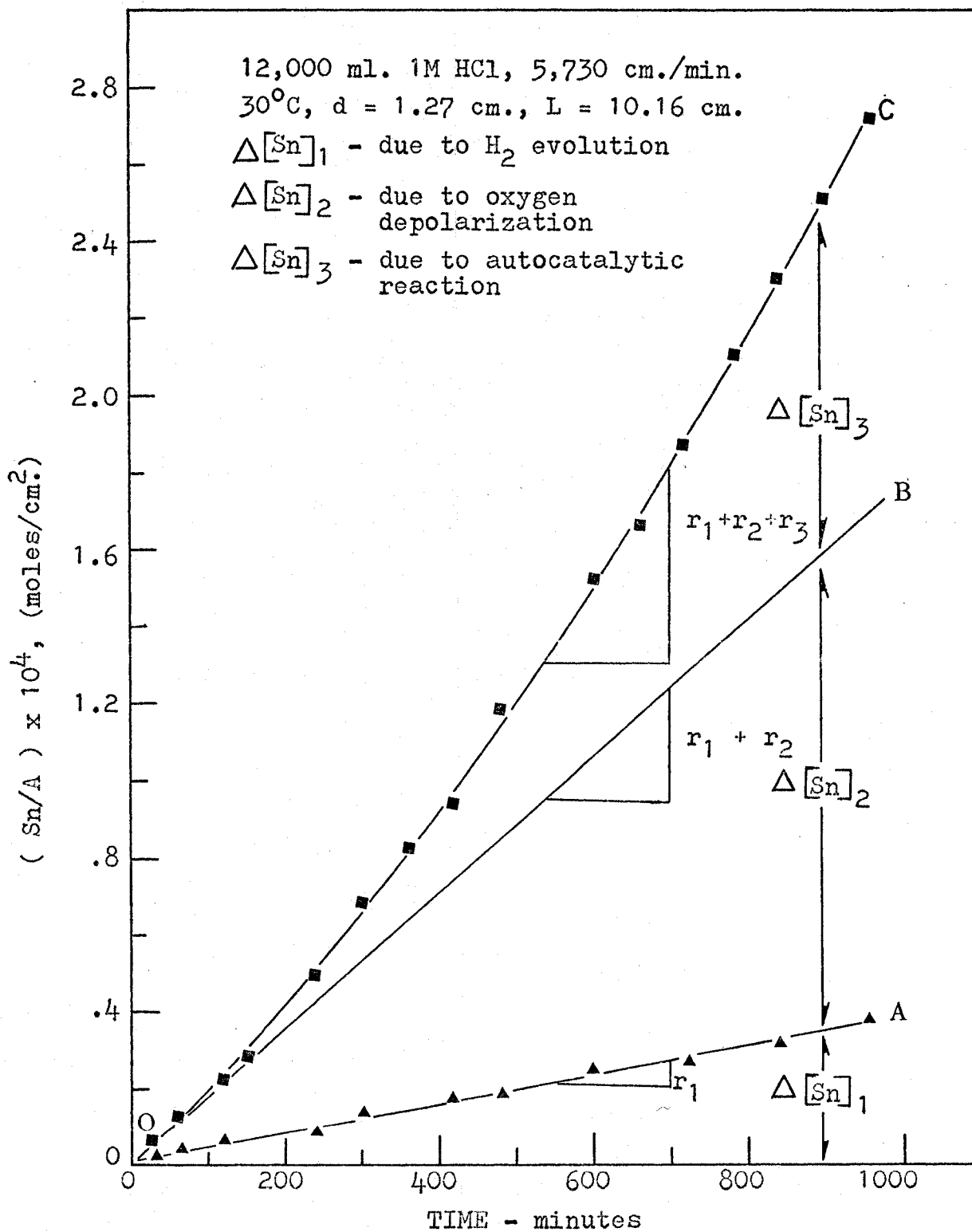
FIGURE I-5-1. A PROPOSED GRAPHICAL ANALYSIS FOR TIN
DISSOLUTION IN HCl SOLUTIONS

B. Reproducibility

In order to check the reproducibility of experimental determinations duplicate runs were made under various conditions. A typical plot of a duplicate run is shown in Figure I-5-2.

C. Effects of Different Factors on the Dissolution Rate of Tin

1. Rate Dependence on Tin Ion Concentration

As shown in Figure I-5-3, the autocatalytic dissolution effect, which is represented by the difference in tin ion concentration between curve OC and the linear zero-order initial rate plot OB as shown in Figure I-5-1, can be correlated by a half-order plot. The reaction rate of autocatalysis, r_3, is proportional to the total tin ion concentration in the bulk solution raised to the 0.5 power. Experimental evidence shows that the autocatalytic reaction becomes important only after an elapsed time of 40 to 120 minutes. The beginning of noticeable autocatalysis, as determined by the deviation from the asymptotic line OB in Figure I-5-1, depends on the dissolution conditions, but in general the bulk tin ion concentration must be greater than 0.35×10^{-4} moles/litre.

2. Rate Dependence on Fluid Velocity

The effect of the velocity of the acid solution flowing through the tube was studied for velocities ranging from 1,175 to 16,600 cm./min. in tin tubes of different

12,000 ml. 1N HCl, T = 30°C
v = 4,150 cm./min.
d = 1.27 cm.   L = 10.16 cm.
AIR
▲ – RUN A
O – RUN B
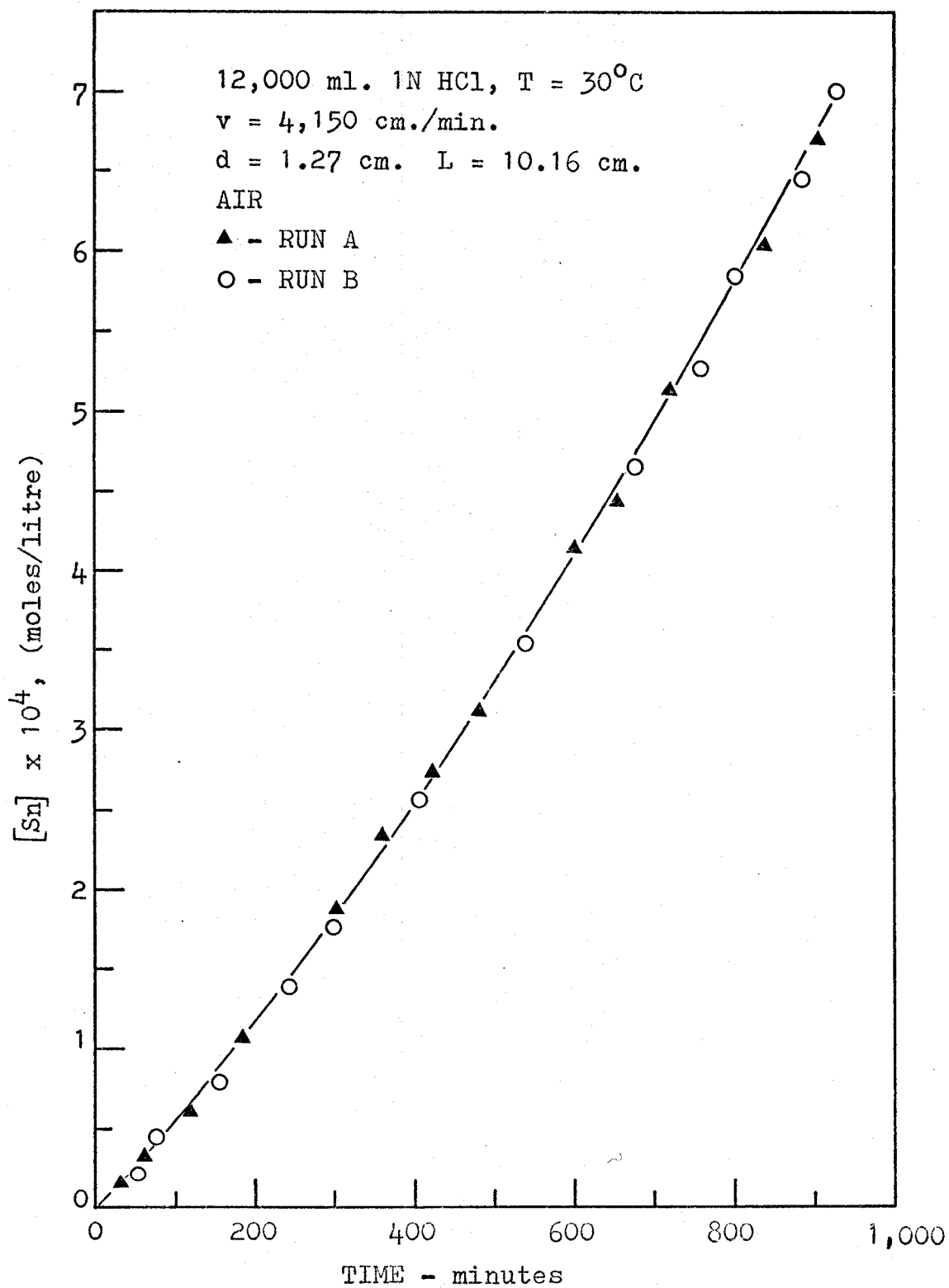
FIGURE I-5-2.   REPRODUCIBILITY OF EXPERIMENTAL DATA
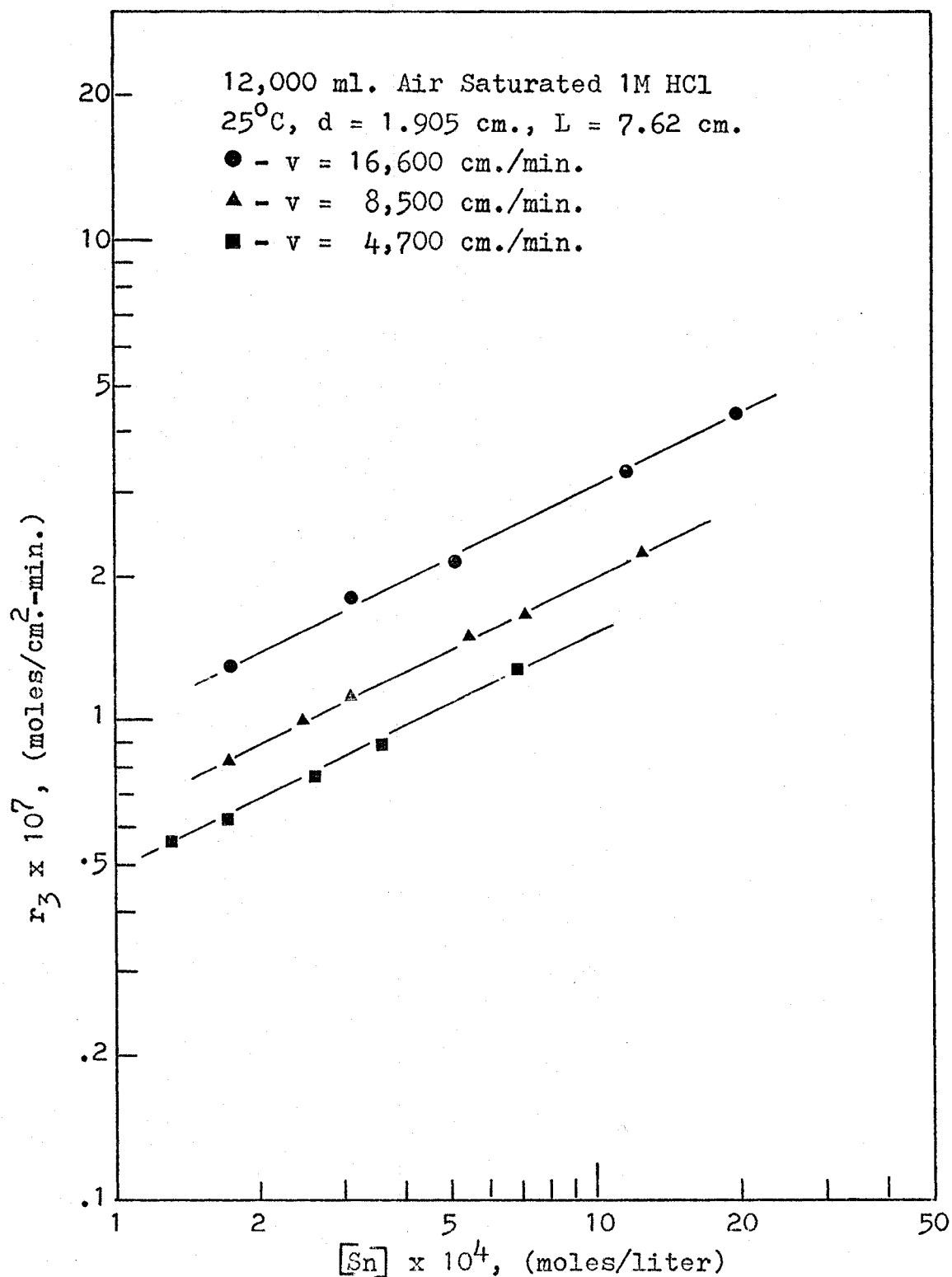
FIGURE I-5-3. DISSOLUTION AS FUNCTION OF TIN ION
CONCENTRATION IN THE BULK SOLUTION
(FOR AUTOCATALYTIC REACTION)

diameters and lengths, at three different temperatures.

The results shown in Figures I-5-4, I-5-5, and I-5-6 indicate that r_1, the reaction rate for hydrogen evolution, r_2, the reaction rate for oxygen depolarization, and r_3, the reaction rate for autocatalysis are proportional to fluid velocity raised to the 0.67, 0.59, and 0.61 powers respectively.

This behaviour indicates that resistance to diffusional mass transfer is operative for the range of velocities **(turbulent flow in all cases) investigated.**

3. Rate Dependence on Temperature

The rate dependence on temperature was studied over the range 25 to 50°C under nitrogen, air, and oxygen saturation at four different flow velocities. The results are illustrated by the Arrhenius' activation energy plots shown in Figures I-5-7, I-5-8, and I-5-9.

The temperature variations correspond to apparent activation energies of 4.25 kcal per mole for the hydrogen evolution reaction, 5.45 kcal per mole for the oxygen depolarization reaction, and 5.8 kcal per mole for the autocatalytic reaction. These low values of activation energy suggest that the temperature coefficients for these reactions are low and the controlling step is more likely physical than chemical.

4. Effect of Hydrochloric Acid Concentration

The effect of hydrochloric acid concentration was studied in aerated and deaerated solutions over the
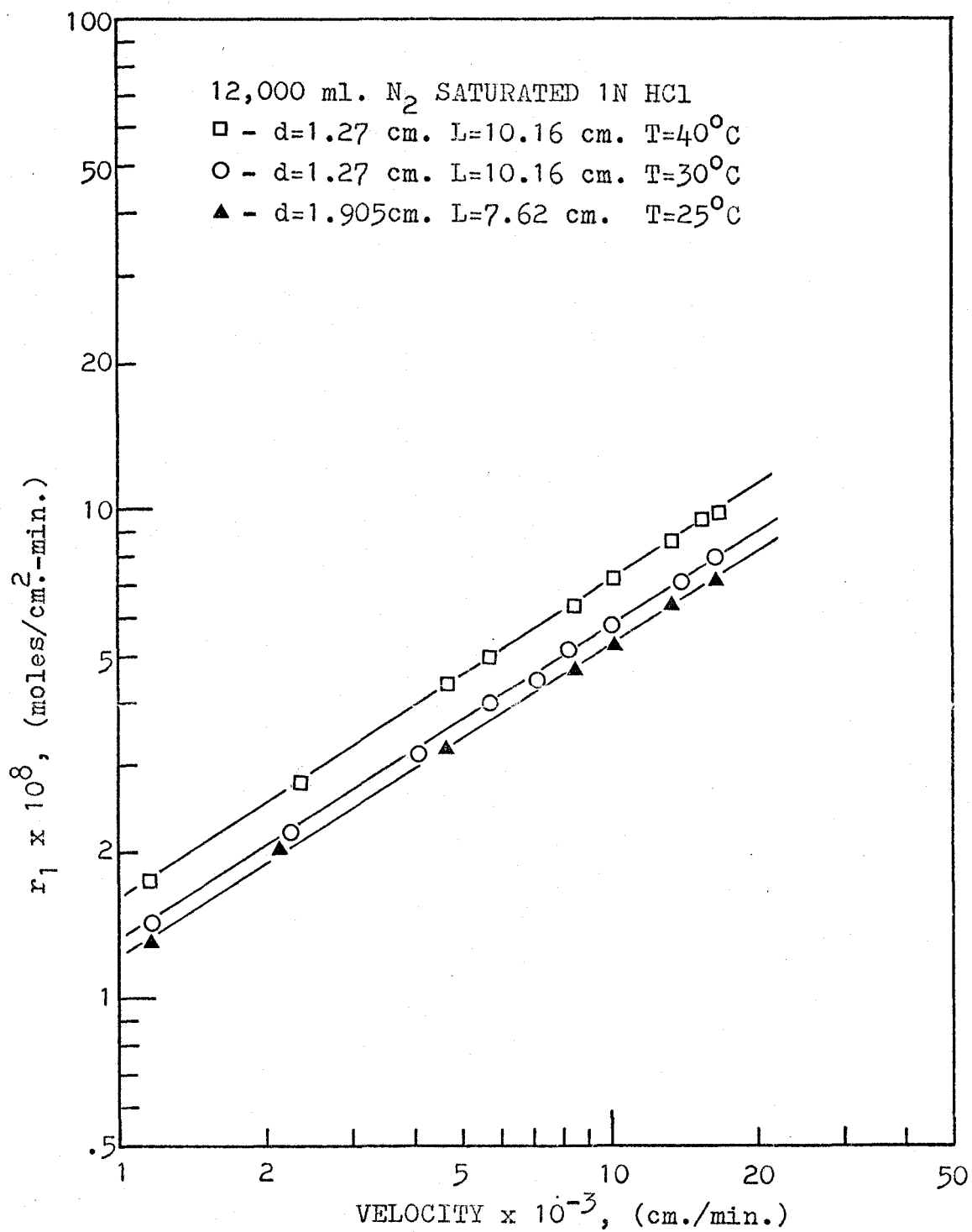
FIGURE I-5-4. DISSOLUTION AS FUNCTION OF FLUID
VELOCITY(FOR H_2 EVOLUTION REACTION)
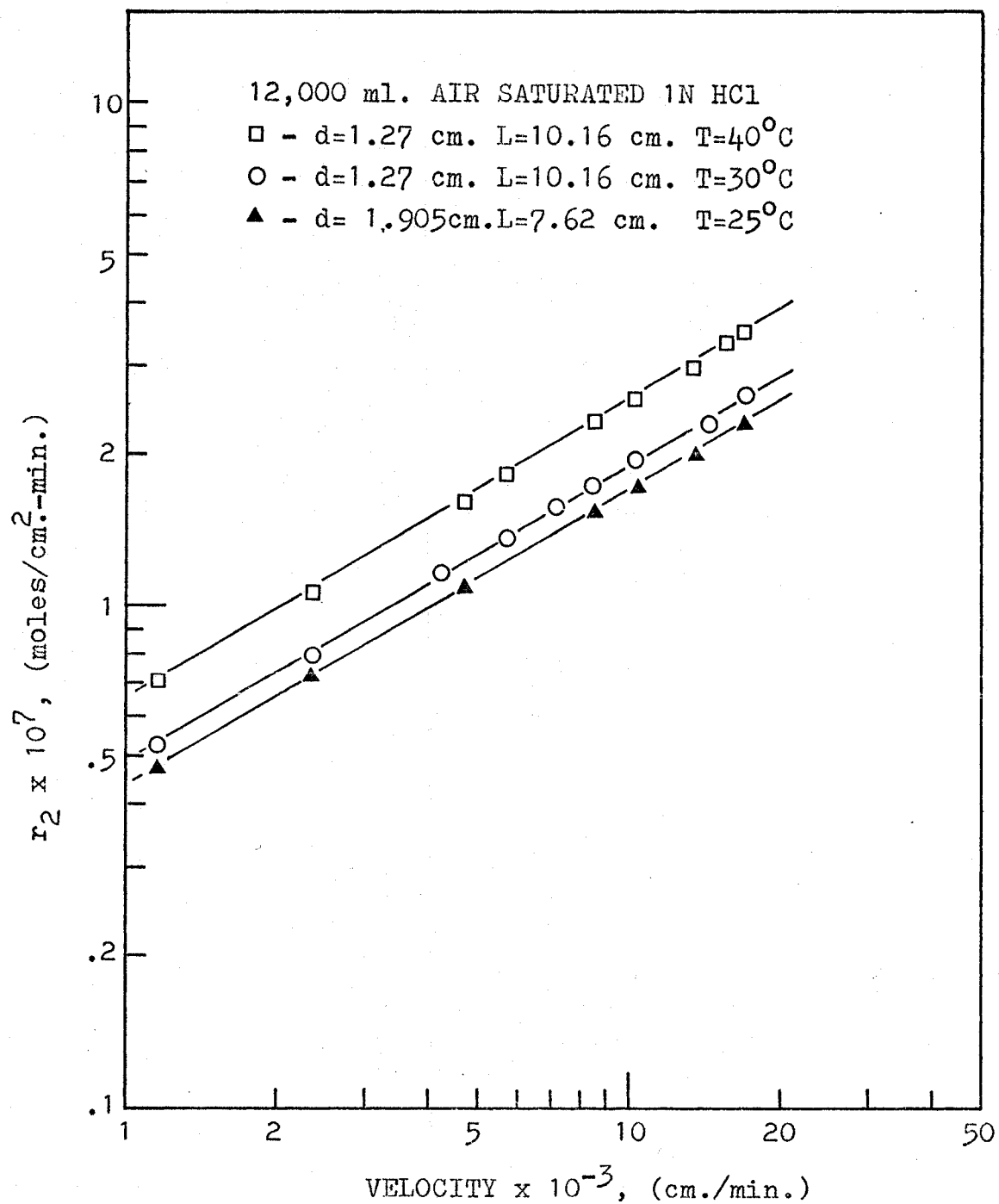
FIGURE I-5-5. DISSOLUTION AS FUNCTION OF FLUID
VELOCITY(FOR OXYGEN DEPOLARIZATION
REACTION)
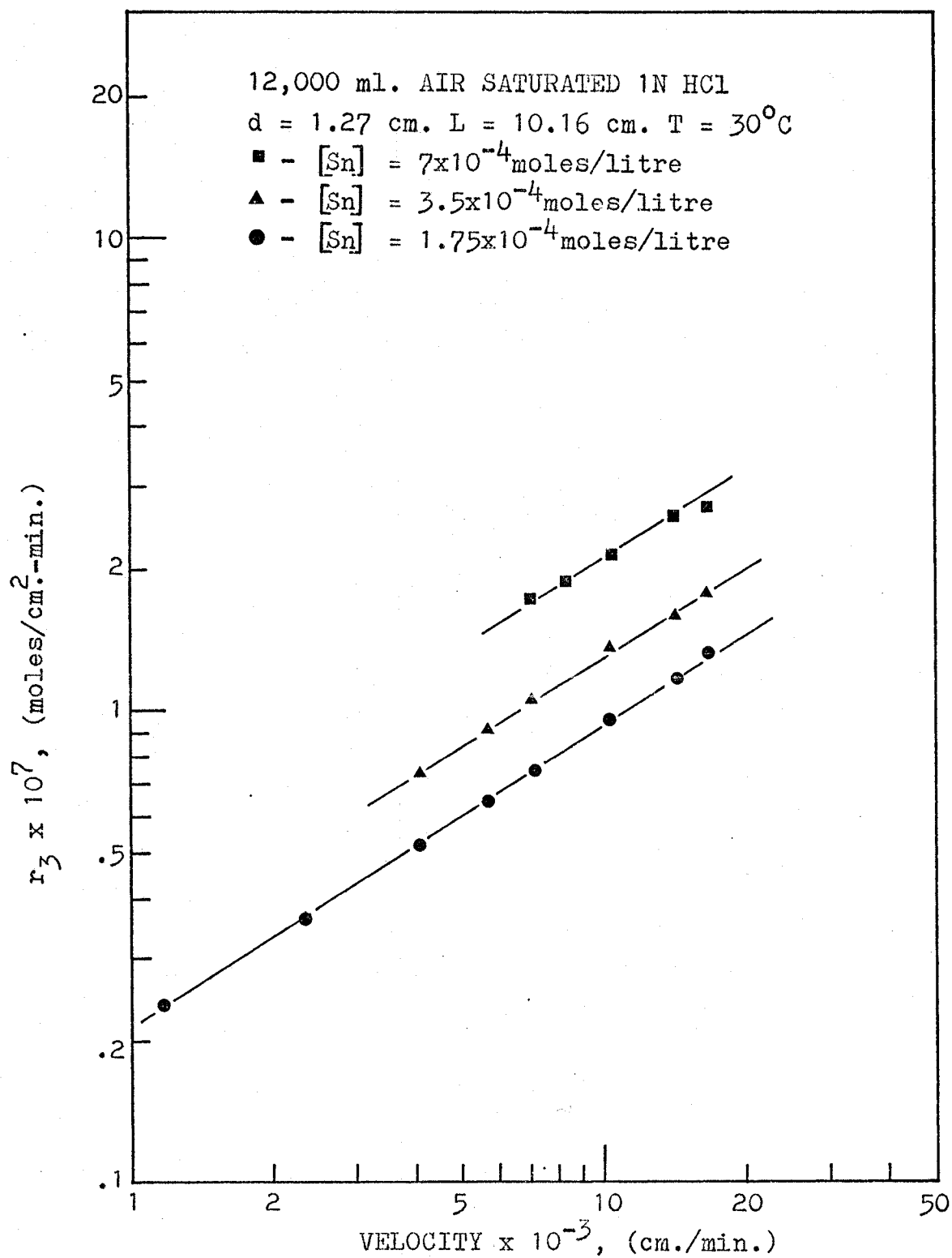
FIGURE I-5-6. DISSOLUTION AS FUNCTION OF FLUID
VELOCITY(FOR AUTOCATALYTIC REACTION)
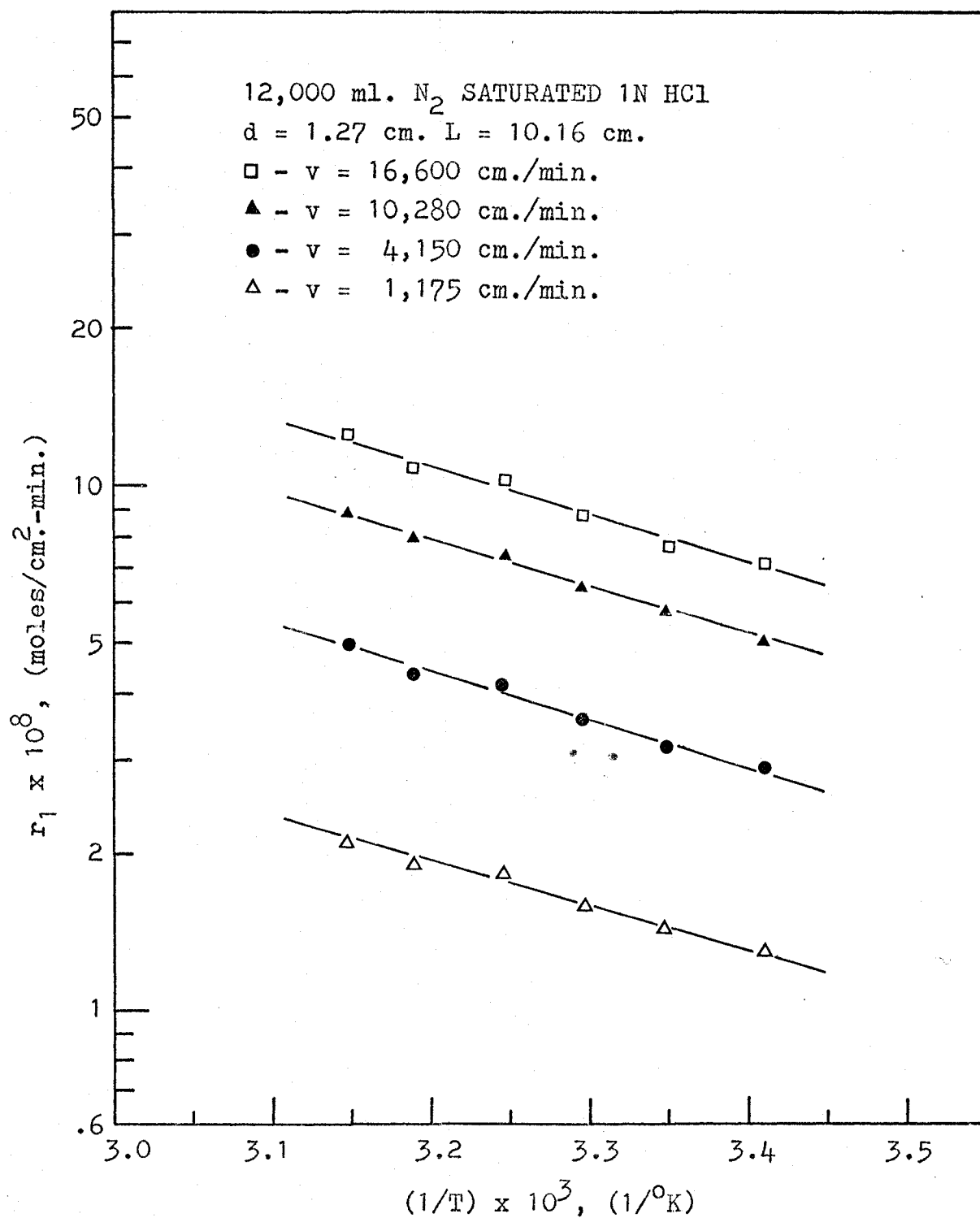
FIGURE I-5-7. DISSOLUTION AS FUNCTION OF TEMPERATURE
(FOR HYDROGEN EVOLUTION REACTION)

12,000 ml. AIR SATURATED 1N HCl
d = 1.27 cm. L = 10.16 cm.
□ – v = 16,600 cm./min.
▲ – v = 10,280 cm./min.
● – v = 4,150 cm./min.
△ – v = 1,175 cm./min.
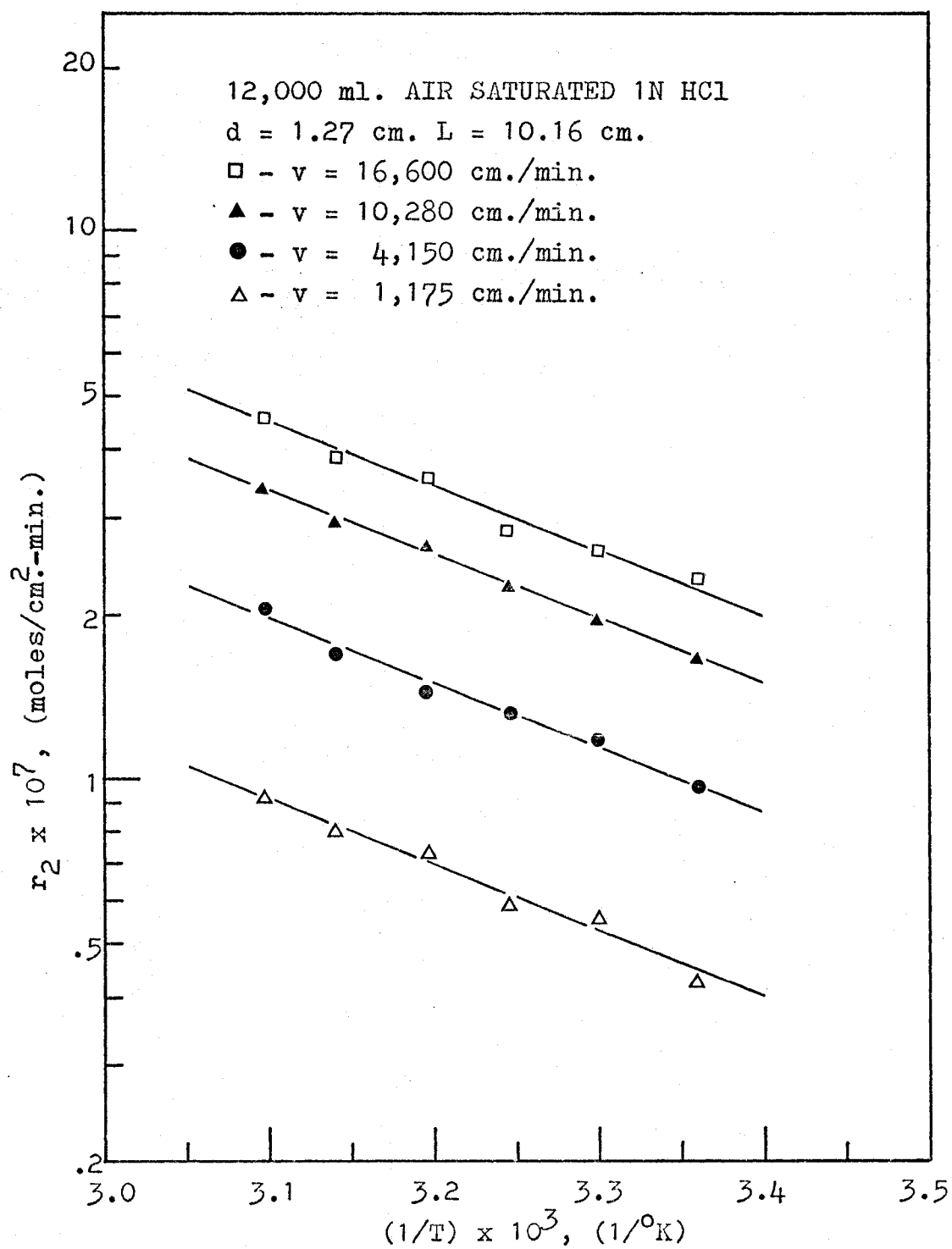
FIGURE I-5-8.   DISSOLUTION AS FUNCTION OF TEMPERATURE
(FOR OXYGEN DEPOLARIZATION REACTION)
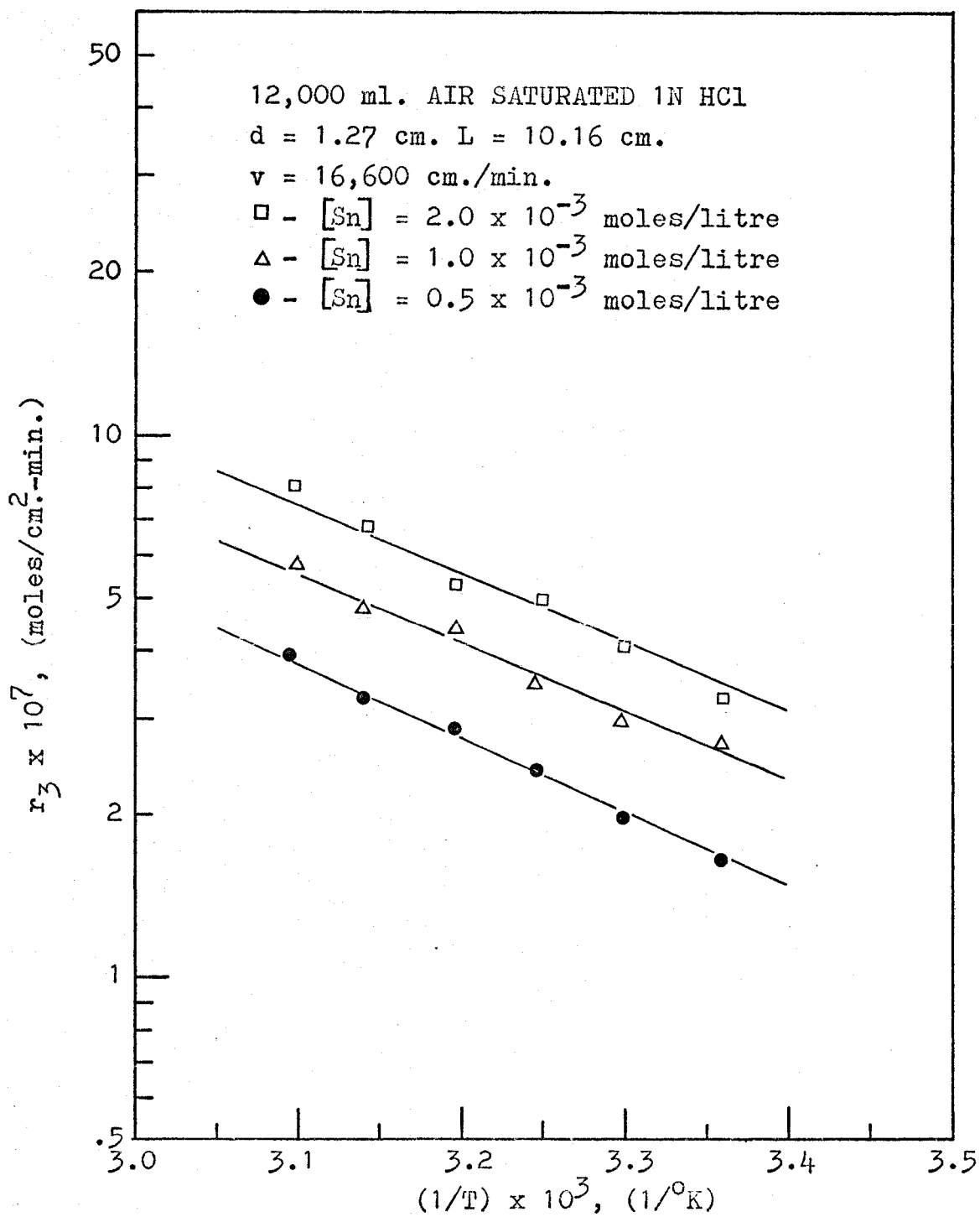
FIGURE I-5-9.   DISSOLUTION AS FUNCTION OF TEMPERATURE
(FOR AUTOCATALYTIC REACTION)

concentration range 0.10 to 4.0 M HCl. Analysis of the data obtained in these investigations shows that the rate of dissolution of tin tubes is essentially independent of HCl concentration. Table I-5-1 indicates that there is no apparent trend for r_1, r_2, and r_3 over the range of concentration studied.

TABLE I-5-1

Effect of HCl Concentration on Tin Dissolution

$T = 30^{\circ}C$, $v = 16,600$ cm./min., d = 1.27 cm.

$L = 10.16$ cm., $[Sn] = 2.0 \times 10^{-3}$ moles/litre

HCl (N)	a_{HCl} (N)	r_1 ($\frac{moles}{cm^2-min.}$)	r_2 ($\frac{moles}{cm^2-min.}$)	r_3 ($\frac{moles}{cm^2-min.}$)
0.10	0.079	7.93×10^{-8}	2.60×10^{-7}	4.05×10^{-7}
0.25	0.194	7.32 -	2.35 -	4.18 -
0.33	0.253	6.95 -	2.50 -	3.96 -
0.50	0.379	7.15 -	1.95 -	3.85 -
0.75	0.586	7.65 -	2.05 -	4.22 -
1.00	0.809	6.82 -	2.86 -	3.75 -
2.00	2.018	7.95 -	2.25 -	4.15 -
3.00	4.080	7.20 -	1.85 -	4.20 -
4.00	7.280	6.75 -	2.55 -	3.80 -

Dissolution rates independent of acid concentration were also reported by other investigators[16,44,52]. This behaviour is an indication that the diffusion of hydrogen ions from the bulk solution to the solution-metal interface and the adsorption of hydrogen ions on the active sites on the tin surface are fast steps. Therefore, the variation of hydrogen ion concentration in the bulk solution has little influence on the dissolution rates of tin in hydrochloric acid solutions.

5. Effect of Oxygen Partial Pressure in Gas Phase

The variation of the concentration of oxygen in the gas mixtures used to saturate the acid solutions and purge the flow system was achieved by adjusting the ratio of volumetric flow rates of oxygen and nitrogen from gas cylinders.

The influence of oxygen concentration on the dissolution rate was determined by saturating the acid solutions with air, and gas mixtures of oxygen and nitrogen. The proportion of oxygen in these gas mixtures was varied over the range 0 to 1.0. This investigation was performed at three different velocities; 16,600cm./min., 10,280 cm./min., and 4,150 cm./min.

The results shown in Figures I-5-10 and I-5-11 indicate that the rate of dissolution can be well correlated in terms of the square root of the oxygen partial pressure in the gas phase with which the solution is equilibrated. The reaction rates r_2 and r_3 are directly proportional to the square root of the oxygen partial pressure. This behaviour suggests that the adsorption of oxygen on the metal surface is possibly of the dissociative type.

6. Effect of Tube Inside Diameter

The effect of the inside diameter of the tube was studied over the range 0.953 to 2.54 cm., under nitrogen and air saturation, and at the following three flow velocities; 1,175 cm./min., 5,730 cm./min., and 16,600 cm./min. It was found that the dissolution rate in moles/cm^2-min. decreased
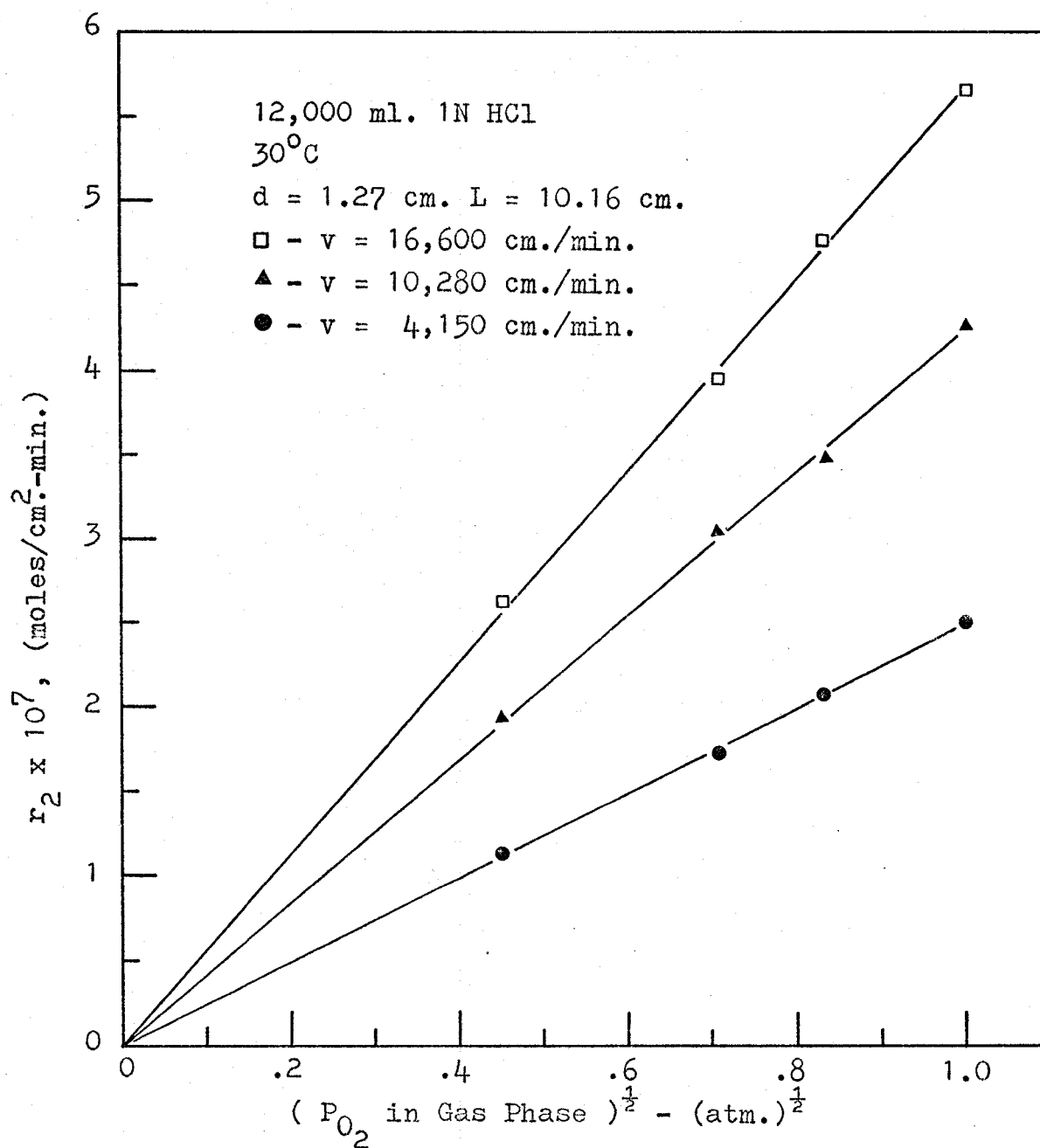
FIGURE I-5-10. DISSOLUTION AS FUNCTION OF OXYGEN
CONCENTRATION(FOR OXYGEN DEPOLARIZATION)
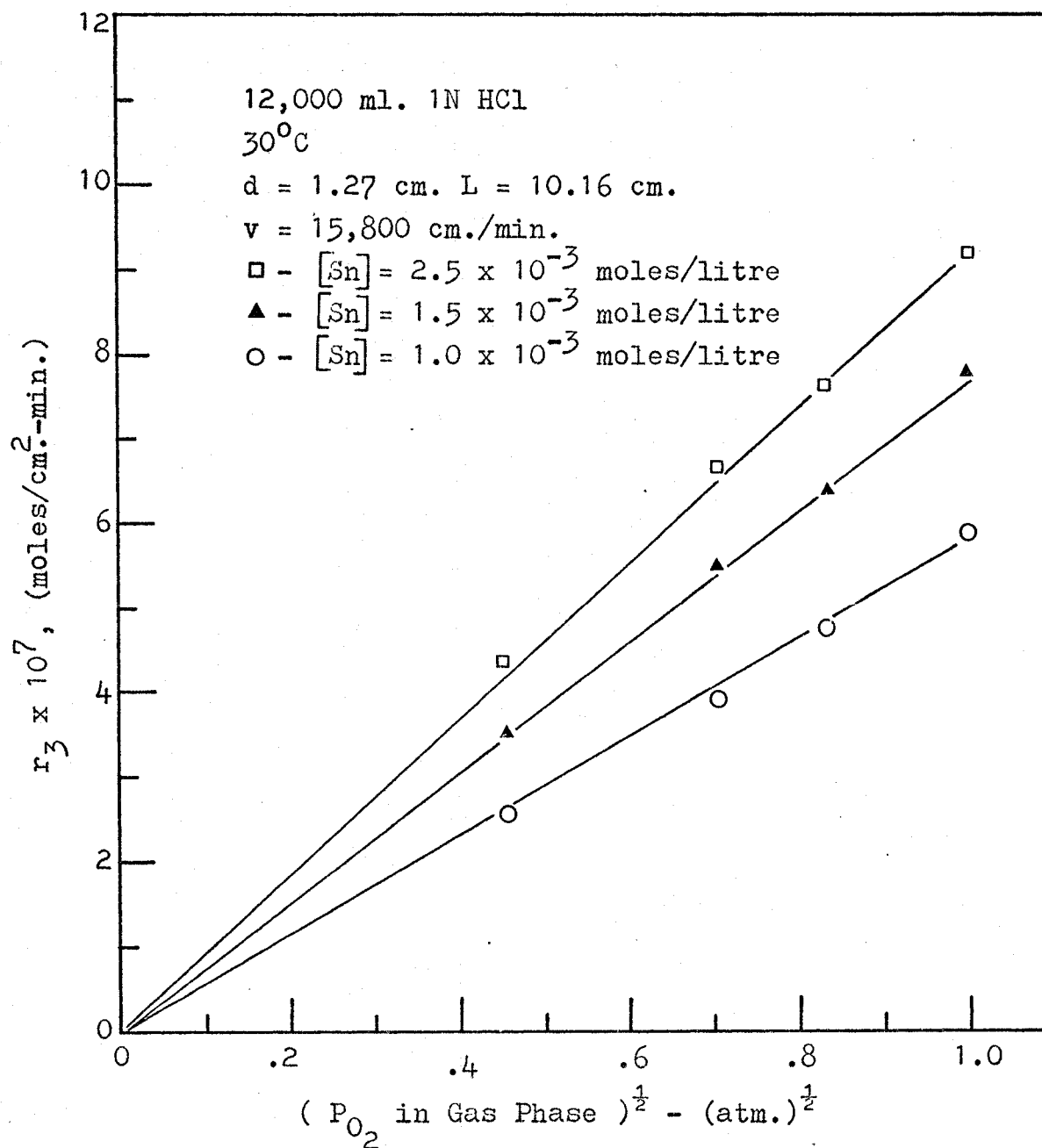
FIGURE I-5-11. DISSOLUTION AS FUNCTION OF OXYGEN
CONCENTRATION (FOR AUTOCATALYTIC REACTION)

slightly with increasing tube diameter.

The results given in Figures I-5-12, I-5-13, and I-5-14 show that r_1, r_2, and r_3 are proportional to $d^{-0.05}$, $d^{-0.11}$, and $d^{-0.10}$ respectively.

This behaviour can be explained by the effect of tube diameter on the thickness of the diffusion layer δ.

Levich[48], who examined the case of the inside surface of a tube serving as the reaction surface under conditions of both laminar and turbulent flow through the tube, derived the following relationships for the thickness of the diffusion layer:

$$\delta \propto (d)^{1/3}$$

for laminar flow

and
$$\delta \propto (d)^{1/8}$$

for turbulent flow

The range of Reynolds number encountered in this study is between 3,940 - 74,500. As a result all experimental data fall within the region of turbulent flow. Therefore, according to Levich, the relationship, $\delta \propto (d)^{1/8}$, should hold true for this investigation. In other words, the diffusional mass transfer flux should follow the relationship; $N \propto (d)^{-1/8}$.

A comparison of the results obtained in this investigation with the above relationship shows that they are of the right order of magnitude.

7. Effect of Tube Length

The effect of tube length on the dissolution rate
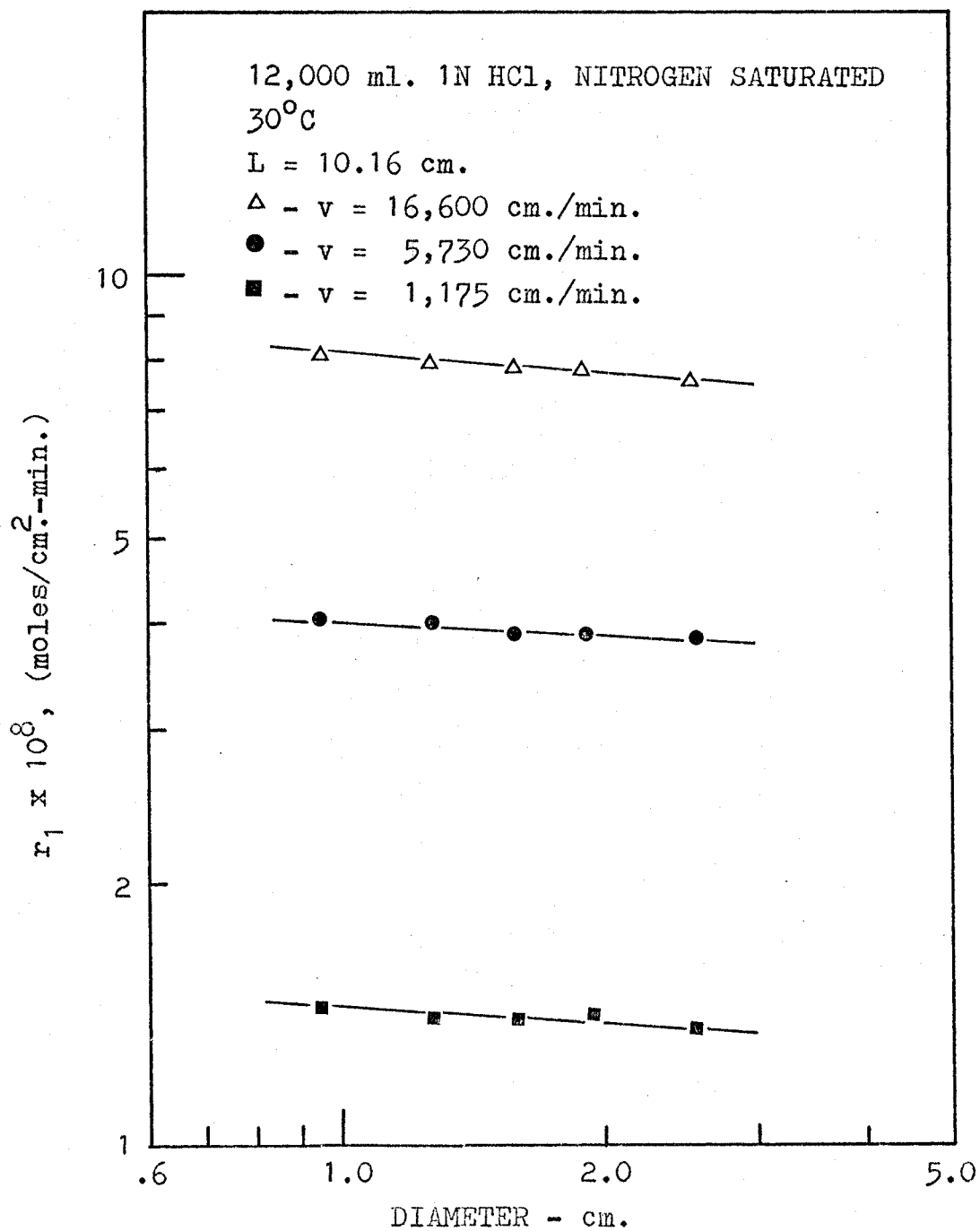
FIGURE I-5-12. DISSOLUTION AS FUNCTION OF TUBE
INSIDE DIAMETER(FOR H_2 EVOLUTION)
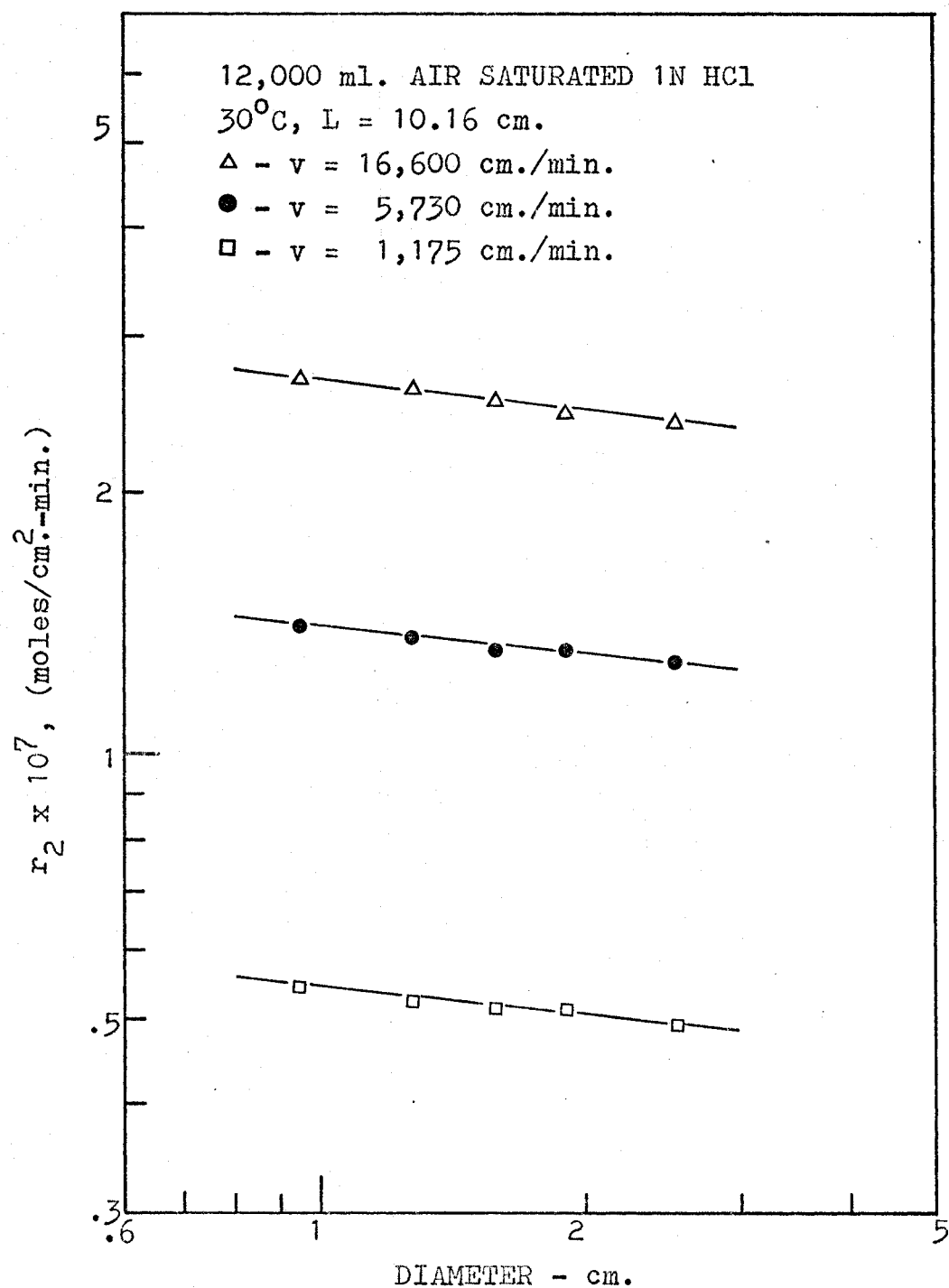
FIGURE I-5-13. DISSOLUTION AS FUNCTION OF TUBE INSIDE DIAMETER(FOR OXYGEN DEPOLARIZATION)
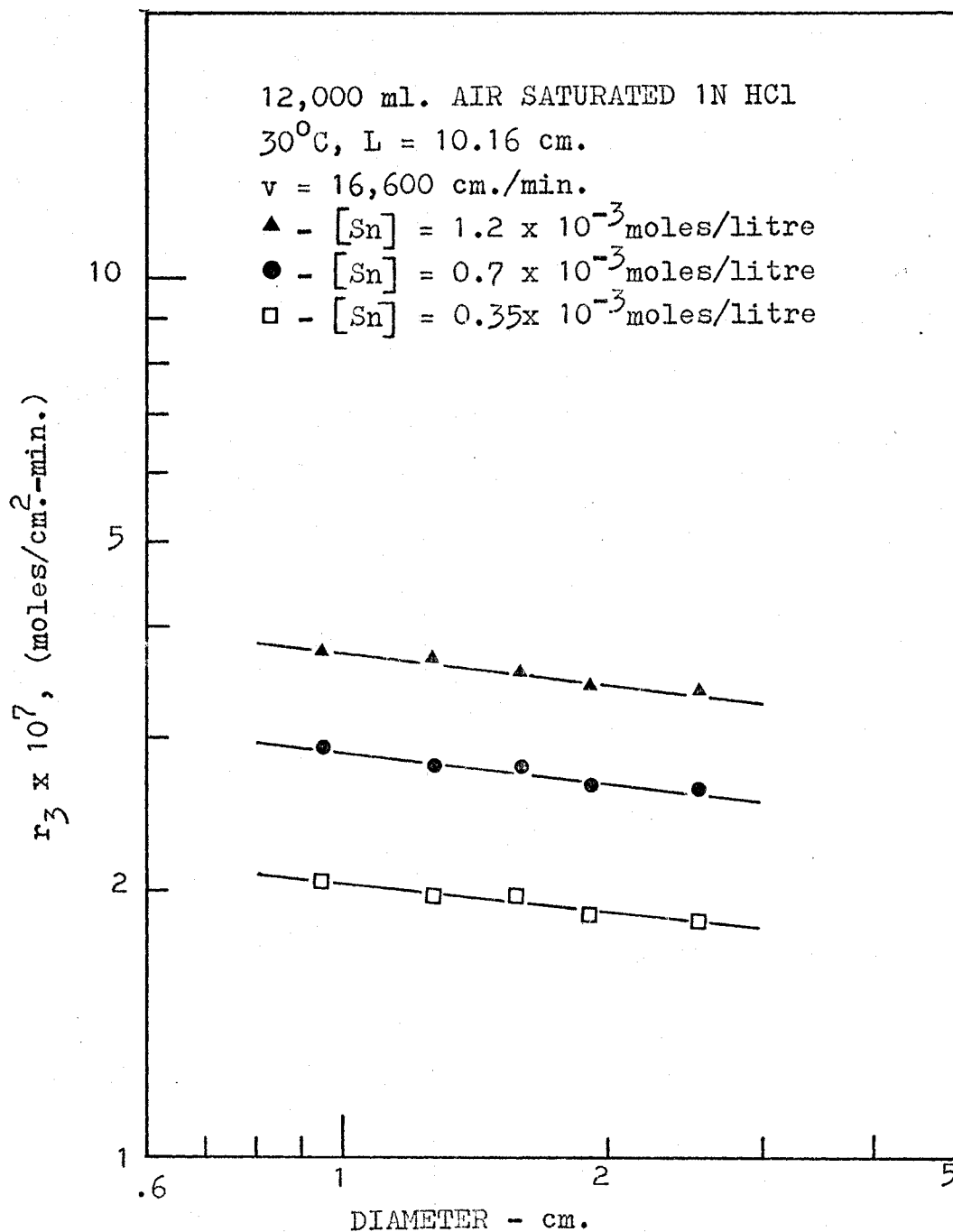
FIGURE I-5-14. DISSOLUTION AS FUNCTION OF TUBE
INSIDE DIAMETER(FOR AUTOCATALYTIC
REACTION)

was studied over the range 5.075 - 13.950 cm., under nitrogen and air saturation, at 30 and 40°C, and at the following three flow velocities: 2,350 cm./min., 8,300 cm./min., and 16,600 cm./min.

Figures I-5-15, I-5-16, and I-5-17 show that the rates of dissolution are influenced by the length of the tube. The reaction rates, r_1, r_2, and r_3 are proportional to $L^{-0.30}$, $L^{-0.33}$, and $L^{-0.32}$ respectively.

This phenomenon can be interpreted in terms of a progressive decrease of concentration gradient of reacting species in the immediate vicinity of the metal surface as the solution moves from one edge of the tube to the other edge.

According to Levich[48], the diffusional mass transfer flux, against the inside surface of a tube, is a function of the distance along the tube in the inlet section of the mass transfer entry region. It extends for a distance of about 100 diameters for laminar flow. The mass transfer region is much shorter in turbulent than in laminar flow. Von Shaw, Reiss, and Hanratty[87], indicate that this length ranges from 2 diameters to 0.5 diameters as the Reynolds number varies from 5,000 to 75,000.

D. Proposed Mechanism for the Dissolution of Tin in Hydrochloric Acid Solutions

On the basis of the established experimental results, tin dissolution may now be interpreted in terms of the following mechanism:
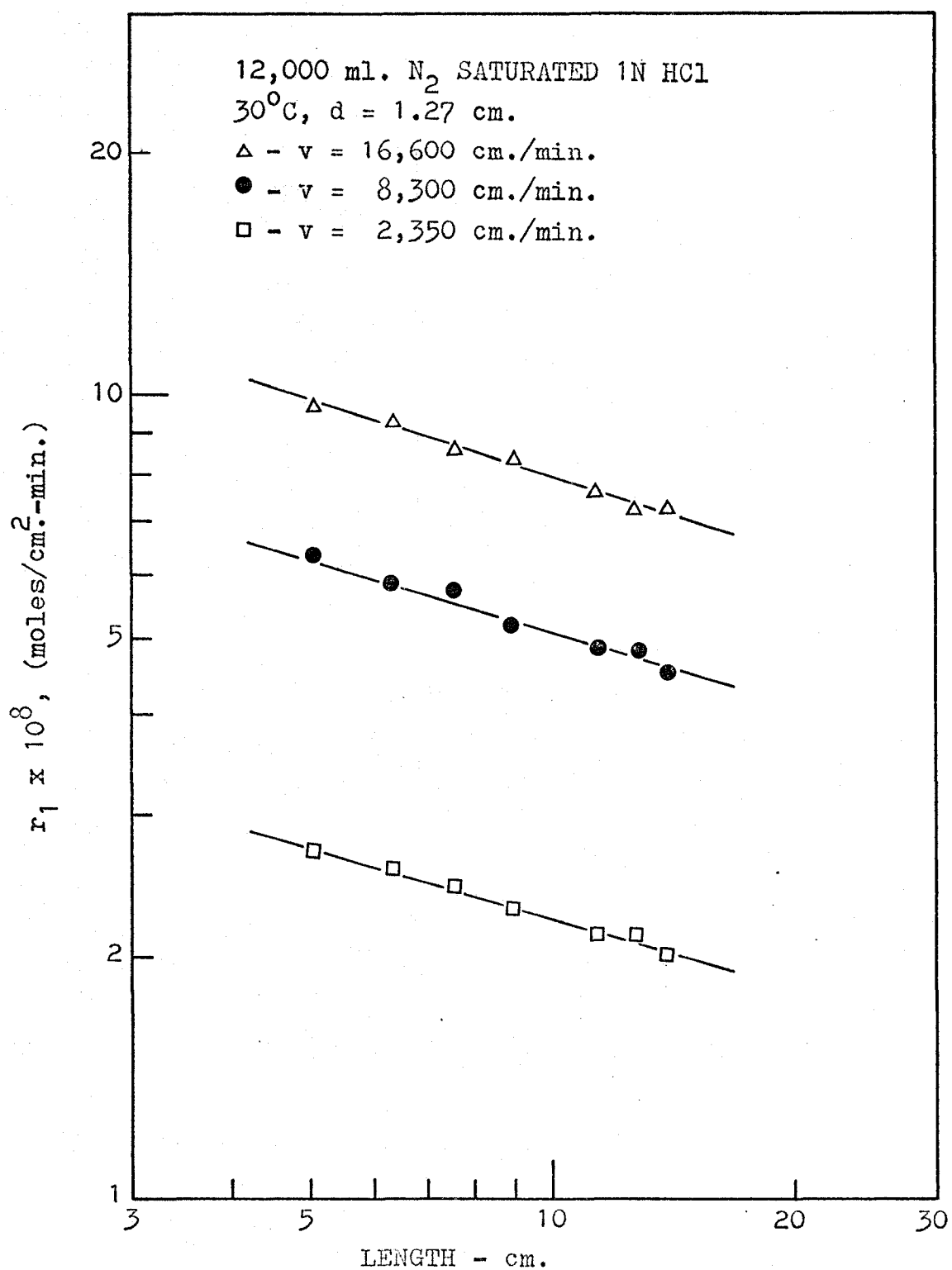
FIGURE I-5-15.   DISSOLUTION AS FUNCTION OF TUBE
LENGTH (FOR H_2 EVOLUTION)
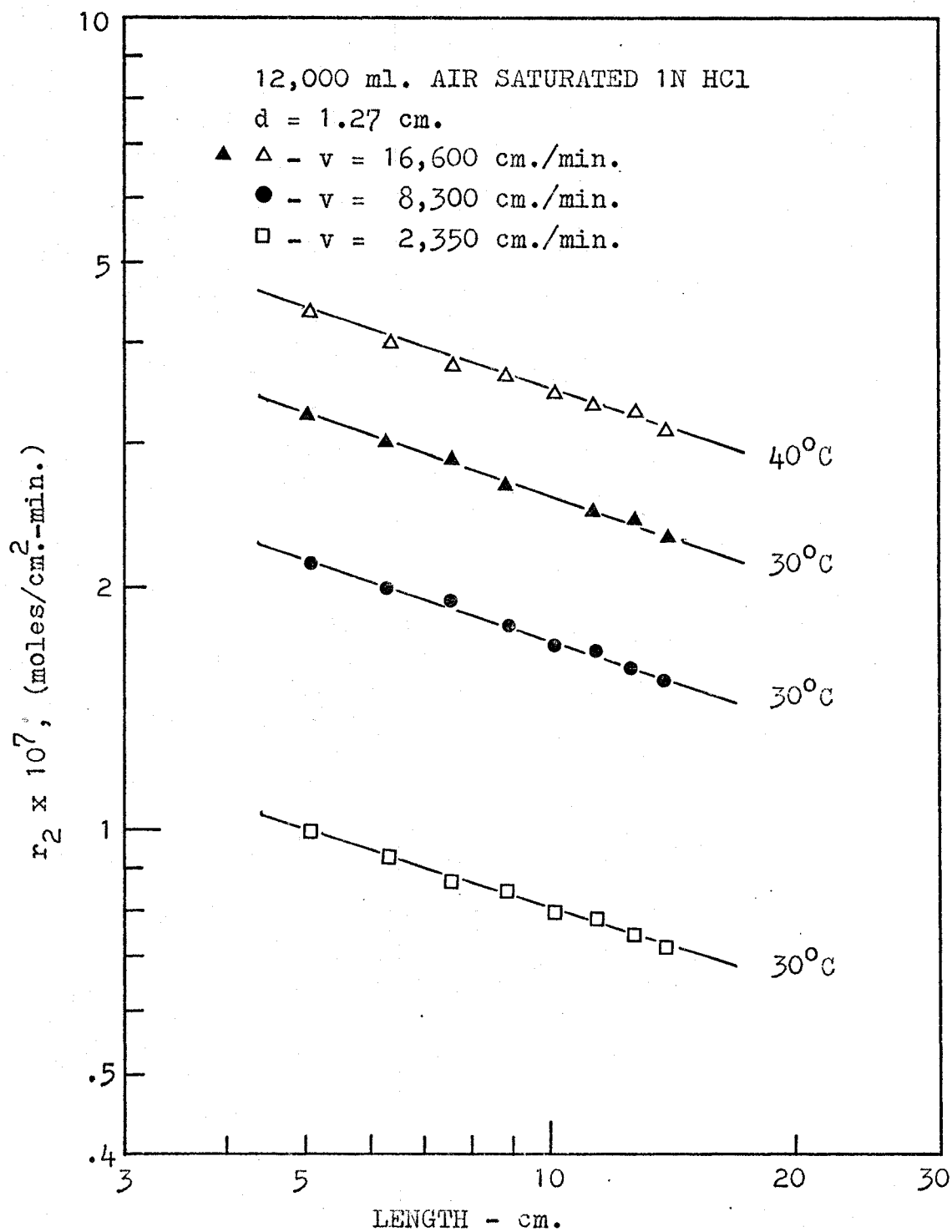
FIGURE I-5-16. DISSOLUTION AS FUNCTION OF TUBE LENGTH (FOR OXYGEN DEPOLARIZATION)
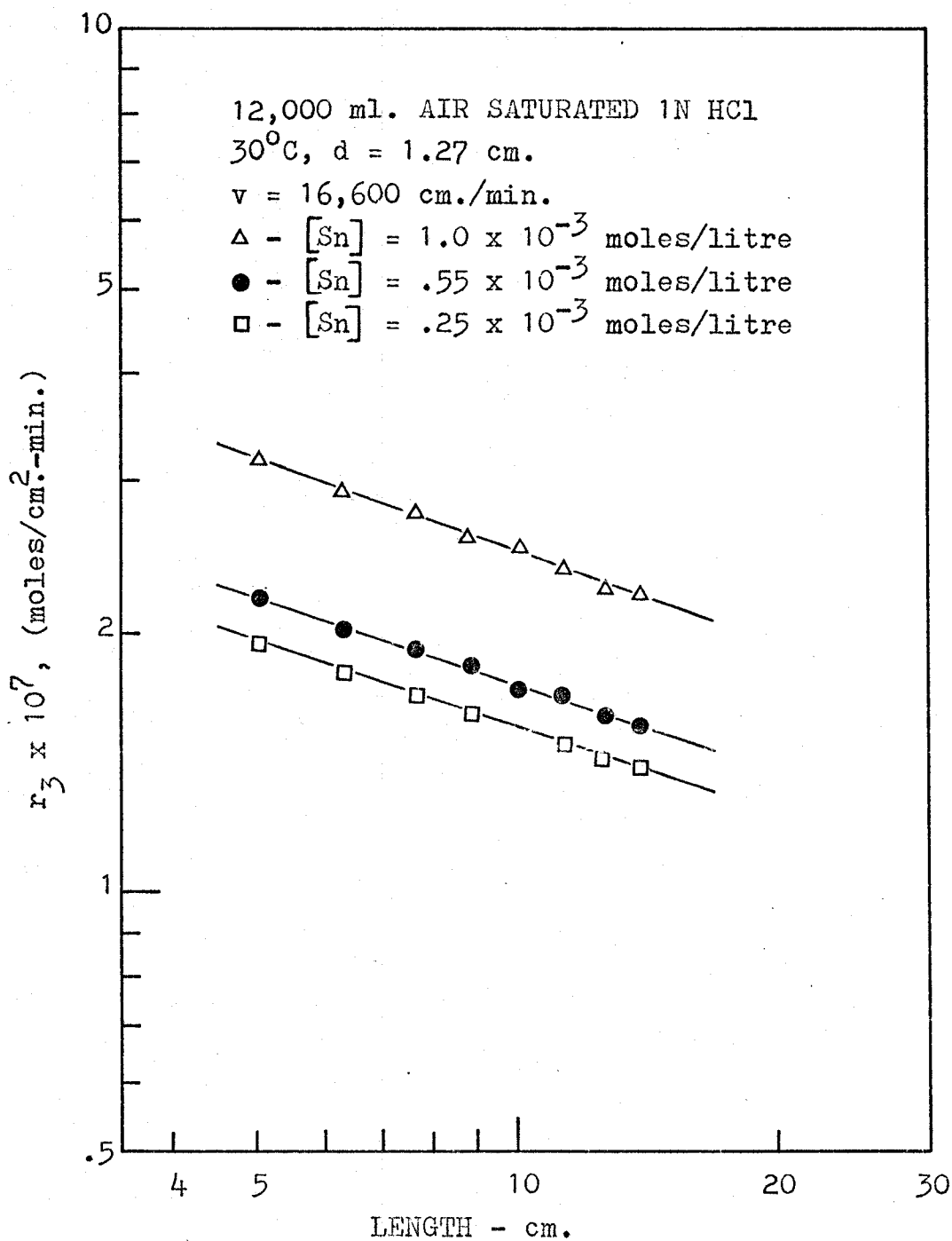
FIGURE I-5-17. DISSOLUTION AS FUNCTION OF TUBE
LENGTH(FOR AUTOCATALYTIC REACTION)

1. The reaction scheme proposed for the hydrogen evolution reaction is:

a. Diffusion of hydrogen ions from the bulk solution to the metal-solution interface
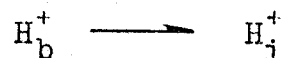
$$H_b^+ \longrightarrow H_i^+$$

b. Adsorption of hydrogen ions on the metal surface
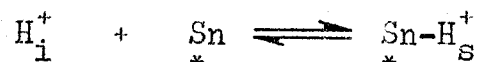
$$H_i^+ + Sn_* \rightleftharpoons Sn-H_s^+_*$$

c. Discharge of adsorbed hydrogen ions by virtue of electron transfer through the metal:

(c1) Electrons transferred from a neighbouring vacant site on the metal surface

$$\overset{\overset{H^+}{|}}{-Sn_*-Sn-Sn_*-Sn-\overset{\overset{H^+}{|}}{Sn_*}-} \longrightarrow \overset{\overset{H}{|}}{-Sn_*-Sn-Sn^{++}_*-Sn-\overset{\overset{H}{|}}{Sn_*}-}$$

(c2) Electrons transferred directly from the surface atoms on which adsorption occurred

$$Sn-H_s^+_* \longrightarrow Sn^+_*-H_s$$

d. Formation of molecular hydrogen from atomic hydrogen, by one of the following modes:

(d1)

$$\overset{\overset{H}{|}}{-Sn_*-Sn-Sn^{++}_*-Sn-\overset{\overset{H}{|}}{Sn_*}-} \longrightarrow -Sn_*-Sn-Sn^{++}_*-Sn-\overset{\overset{H_2}{|}}{Sn_*}-$$

(d2) $$2\,(Sn^+_*-H_s) \longrightarrow Sn^{++}_{*s} + Sn-H_{2s}_*$$

(d3) $$Sn^+_*-H_s + H_i^+ \longrightarrow Sn^{++}_*-H_{2s}$$
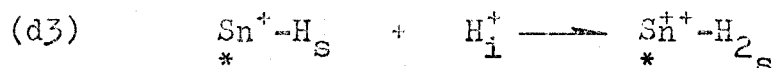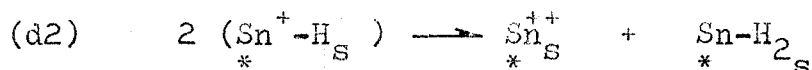
e. Removal of hydrogen molecules from the metal surface, either by dissolution into the solution or by the formation of gas bubbles and their subsequent detachement from the metal surface.

(e1) $\underset{*}{Sn}-H_2{}_s \longrightarrow \underset{*}{Sn}_s + H_2{}_{i,dissolved}$

(e2) $n\,(\,\underset{*}{Sn}-H_2{}_s\,) \longrightarrow \underset{*}{Sn}-(H_2)_{n_s} + (n-1)\underset{*}{Sn}$

$\underset{*}{Sn}-(H_2)_{n_s} \longrightarrow \underset{*}{Sn} + (H_2)_n$
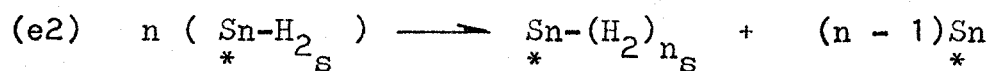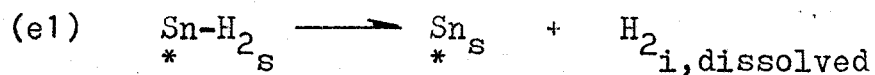
where $\underset{*}{Sn}-(H_2)_{n_s}$ represents a hydrogen gas bubble attached on the metal surface.

f. Desorption of stannous ions from the metal surface to the metal-solution interface

$$\underset{s}{Sn}^{++} \rightleftharpoons Sn_i^{++}$$
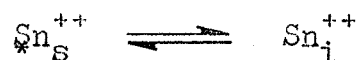
g. Diffusion of hydrated stannous ions from the metal-solution interface to the bulk solution

$$Sn_i^{++} + nH_2O \longrightarrow Sn^{++}-nH_2O_{bulk}$$

2. In aerated hydrochloric acid solution, the dissolution of tin is accelerated by two other simultaneous reactions. These are oxygen depolarization and autocatalysis.

The mechanism proposed for the oxygen depolarization can be described by the following elementary stages:

a. Diffusion of oxygen from the bulk solution to the metal-solution interface

$$O_2{}_b \longrightarrow O_2{}_i$$

b. A dissociative adsorption of oxygen on the metal surface

$$O_{2_i} + 2 \underset{*}{Sn} \rightleftharpoons 2 (\underset{*}{Sn}-O_s)$$
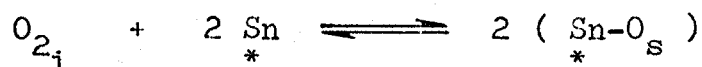
c. Formation of mono-valent oxygen ions by virtue of electron transfer

$$\underset{*}{Sn}-O_s \longrightarrow \underset{*}{Sn}^+-O_s^-$$

d. Formation of hydroxyl radical

$$\underset{*}{Sn}^+-O_s^- + \underset{*}{Sn}-H_s^+ \longrightarrow \underset{*}{Sn}^+-HO_s + \underset{*}{Sn}_s$$

e. Formation of hydrogen peroxide

$$2 (\underset{*}{Sn}^+-OH) \longrightarrow \underset{*}{Sn}-H_2O_{2_s} + \underset{*}{Sn}_s^{++}$$

f. Reduction of hydrogen peroxide with formation of hydroxyl ions
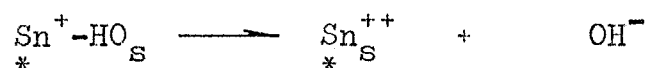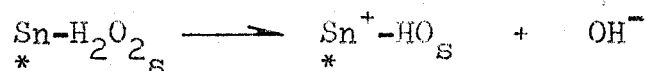
$$\underset{*}{Sn}-H_2O_{2_s} \longrightarrow \underset{*}{Sn}^+-HO_s + OH^-$$

$$\underset{*}{Sn}^+-HO_s \longrightarrow \underset{*}{Sn}_s^{++} + OH^-$$

g. Desorption of stannous ions from the metal surface to the metal-solution interface

$$\underset{*}{Sn}_s^{++} \rightleftharpoons Sn_i^{++}$$
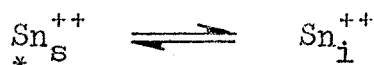
h. Diffusion of hydrated stannous ions from the metal-solution interface to the bulk solution

$$Sn_i^{++} + nH_2O \longrightarrow Sn^{++}-nH_2O_{bulk}$$
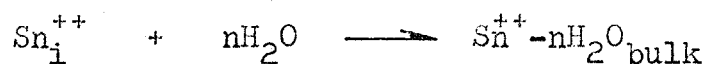
3. The following reaction scheme is proposed for the autocatalytic process:

a. An oxidation process[1] caused by dissolved oxygen

with the formation of peroxide intermediate according to

$$Sn_{*i}^{++} + O_{2i} + 2H_i^+ \longrightarrow Sn_{*i}^{++++} + H_2O_{2i}$$
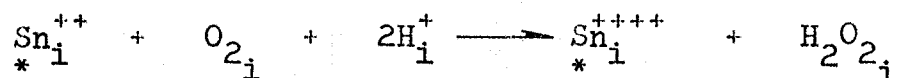
b. An oxidation process caused by the atomic oxygen adsorbed on the metal surface with the formation of hydroxyl ion

$$Sn_{*s}^{++} + Sn-O_{*s} + Sn-H_{*s}^+ \longrightarrow Sn_{*s}^{++++} + Sn-OH_{*s}^- + Sn_{*s}$$

c. An oxidation process caused by the peroxide intermediates[67] (produced in stage a and in the oxygen depolarization reaction) according to

$$Sn-H_{*s}^+ + Sn_{*i}^{++} + H_2O_{2i} \longrightarrow Sn_i^{++++} + Sn-OH_{*s}^- + H_2O$$

or

$$Sn-H_{*s}^+ + Sn_{*s}^{++} + Sn-H_2O_{2s} \longrightarrow Sn_{*s}^{++++} + Sn-OH_{*s}^- + Sn-H_2O_{*s}$$
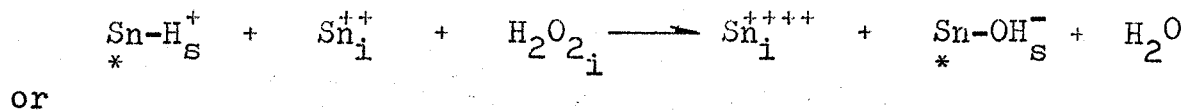
d. An equilibrium[7] between the stannous and stannic ions is established at all times at the metal surface by virtue of electron transfer:

$$Sn_{*s} + Sn_i^{++++} \rightleftharpoons 2 Sn_i^{++}$$
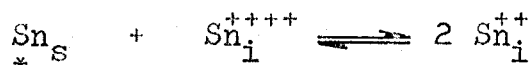
As reported by other investigators[53,56], the specimen surface became coated with a grayish film during tin dissolution in acidic media. Chemical analysis[56] and X-ray diffraction analysis[53] of the surface film showed that it consisted of redeposited pure tin.

E. Empirical Rate Equation for Tin Dissolution

The experimental data for the dissolution of tin in hydrochloric acid solutions in the presence or absence of

oxygen may be summarized by the following equation:

$$\frac{1}{A}\frac{dSn}{dt} = \frac{V}{A}\frac{d[Sn]}{dt}$$

$$= k_1^o [HCl]^o (v)^{.67} (d)^{-.05} (L)^{-.30} e^{-\frac{4250}{RT}}$$

$$+ k_2^o [HCl]^o (v)^{.59} (d)^{-.11} (L)^{-.33} (P_{O_2})^{.50} e^{-\frac{5450}{RT}}$$

$$+ k_3^o [HCl]^o (v)^{.61} (d)^{-.10} (L)^{-.32} (P_{O_2})^{.50} [Sn]^{.50} e^{-\frac{5800}{RT}}$$

where the dissolution rate, $\frac{1}{A}\frac{dSn}{dt}$, is expressed in moles

of tin dissolved per square centimeter of metal surface per

minute. The tin ion concentration, $[Sn]$, is expressed in

moles per litre. The values of k_1^o, k_2^o, and k_3^o have been found

to be 3.37×10^{-7}, 3.05×10^{-5}, and 6.45×10^{-4} respectively. The

detailed calculations are given in Appendix 3.

Therefore, the empirical rate equation for the dissolution

of tin in HCl solutions can be established as:

$$\frac{1}{A}\frac{dSn}{dt} = \frac{V}{A}\frac{d[Sn]}{dt}$$

$$= 3.37 \times 10^{-7} [HCl]^o (v)^{.67} (d)^{-.05} (L)^{-.30} e^{-\frac{4250}{RT}}$$

$$= 3.05 \times 10^{-5} [HCl]^o (v)^{.59} (d)^{-.11} (L)^{-.33} (P_{O_2})^{.50} e^{-\frac{5450}{RT}}$$

$$= 6.45 \times 10^{-4} [HCl]^o (v)^{.61} (d)^{-.10} (L)^{-.32} (P_{O_2})^{.50} [Sn]^{.50} e^{\frac{-5800}{RT}}$$

in which the third term(autocatalysis) applies only after an

elapsed time of 40 to 120 minutes. The beginning of noticeable

autocatalysis depends on the dissolution conditions, but in

general the bulk tin ion concentration must be greater than

0.35×10^{-4} moles/litre.

Range of experimental conditions:

$$T = 298.15 - 323.15 °K$$
$$v = 1,175 - 16,600 \text{ cm./min.}$$
$$d = 0.953 - 2.54 \text{ cm.}$$
$$L = 5.075 - 13.950 \text{ cm.}$$
$$V = 8,000 - 14,000 \text{ ml.}$$
$$P_{O_2} = 0 - 1.0 \text{ atm.}$$
$$[HCl] = 0.1 - 4.0 \text{ M}$$

An example of the application of the above empirical rate equation to predict the changes in tin ion concentration in the corroding solution is given in Appendix 4.

CHAPTER VI

SUMMARY AND CONCLUSIONS

A. Comparison of Present Results with Previous Work

In earlier studies with rotating cylindrical systems[63],

experimental data were correlated by the following empirical

rate equation designed to express the changes in tin ion

concentration in the corroding solution:

$$\frac{d[Sn]}{dt} = 5.31 \times 10^{-7} \frac{A}{V} [HCl]^{0} (v)^{.98} e^{-\frac{3060}{RT}}$$

$$+ 2.88 \times 10^{-5} \frac{A}{V} [HCl]^{0} (v)^{.98} (P_{O_2})^{.50} e^{-\frac{3660}{RT}}$$

$$+ 1.25 \times 10^{-1} \frac{(A)^{.50}}{V} [HCl]^{0} (v)^{n} (P_{O_2})^{.50} (\Delta[Sn]_3)^{.50} e^{-\frac{5440}{RT}}$$

where: n = 0.30 for $2,840 < v < 21,230$ cm./min.

n = 0.90 for $21,230 < v < 34,100$ cm./min.

Rearranging the above equation gives

$$\frac{1}{A} \frac{dSn}{dt} = 5.31 \times 10^{-7} [HCl]^{0} (v)^{.98} e^{-\frac{3060}{RT}}$$

$$+ 2.88 \times 10^{-5} [HCl]^{0} (v)^{.98} (P_{O_2})^{.50} e^{-\frac{3660}{RT}}$$

$$+ 1.25 \times 10^{-1} \frac{[HCl]^{0}}{(A)^{.50}} (v)^{n} (P_{O_2})^{.50} (\Delta[Sn]_3)^{.50} e^{-\frac{5440}{RT}}$$

The rate equation obtained in the present investigation

is very similar to the above correlation. Both rate equations

show that, (a) the dissolution rate of tin is independent of

the hydrochloric acid concentration, (b) in aerated acid

solutions, the dissolution reactions show an autocatalytic

74

effect, with dissolution rate increasing with increasing tin ion concentration in corroding solution, and the autocatalytic process shows a half order dependence on tin ion concentration, (c) the rates of oxygen depolarization and autocatalytic processes are proportional to the square root of the oxygen partial pressure, and (d) there is no direct proportionality between the dissolution rate and the apparent surface area of the dissolving metal for the autocatalytic component.

The respective values of apparent activation energies appearing in these two equations fall within the same order of magnitude. It is also interesting to note that the values of activation energies in both correlations show the same important characteristic; that is, the hydrogen evolution process has a smaller value of activation energy than those of the oxygen depolarization and autocatalytic processes.

The low activation energy, along with independence on hydrogen ion concentration and other chemical factors, but significant dependence on flow velocity suggest that the hydrogen evolution component is essentially under diffusional mass transfer control. (Probably the diffusion of hydrated tin ions from the metal-solution interface to the bulk solution is a very slow step.)

Because the rates of the oxygen depolarization and autocatalytic processes are proportional to oxygen partial pressure raised to the 0.5 power, it would appear that the adsorption of oxygen on the metal surface is a dissociative

type, and also a slow step. Therefore, the oxygen depolarization and autocatalytic processes have a combination of physical(the diffusion of hydrated tin ions from the metal-solution interface to the bulk solution) and chemical(the dissociation of oxygen molecules on adsorption) slow steps involved in their elementary stages. In other words, the oxygen depolarization and autocatalytic processes are under mixed control.

Significant differences are shown between the effect of velocity on dissolution rates from cylindrical and tubular specimens. For the rotating cylindrical system, the reaction rates are proportional to peripheral velocity raised to the 0.90 - 0.98 powers.(The rate of the autocatalytic process is proportional to peripheral velocity raised to the 0.30 power for a narrow range of lower velocities.) For the tubular flow system the reaction rates are proportional to linear velocity of the corroding solution raised to the 0.59 - 0.67 powers. This difference in magnitude of the flow velocity effect is probably due to the significant differences in flow patterns in these two systems. The flow pattern in the recycling flow system was well established, while that in the rotating cylindrical system was made far more complex by the baffles incorporated into the solution container[63]. The violent turbulence of the corroding solution caused by these baffles surely enhanced the effect of velocity on diffusional mass transfer. Therefore, the same apparent increase in

relative movement between the metal surface and corroding solution would cause a much higher turbulence (consequently a much larger effect on dissolution rate of tin) in the case of the rotating cylindrical system than in the tubular flow system.

B. Comparison of Present Results with Mass Transfer Correlations

Diffusional mass transfer correlations for the dissolution of solids into fluids moving through a tube of circular cross section, as discussed in Chapter III, have the following general form:

$$Nu = const.(Re)^m(Sc)^n(\frac{d}{L})^p \qquad (I-6-1)$$

where the exponents m, n, and p are usually determined experimentally.

To compare some of the characteristics of the rate equation obtained in this investigation with those of the above general correlation, consider the case of any general dissolution run of tin in HCl solution. At any given instant, the following properties of the corroding solution; temperature, oxygen partial pressure, and tin ion concentration are fixed. Under these conditions, the empirical rate equation reduces to

$$\frac{d[Sn]}{dt} = c_1 \cdot (v)^{.67}(d)^{-.05}(L)^{-.30}$$
$$+ c_2 \cdot (v)^{.59}(d)^{-.11}(L)^{-.33}$$
$$+ c_3 \cdot (v)^{.61}(d)^{-.10}(L)^{-.32} \qquad (I-6-2)$$

where c_1, c_2, and c_3 are constants.

With some further assumptions and rearrangements, the above equation can be converted to the following form:

$$\frac{k_L d}{D} = Nu = c_1' \cdot (Re)^{.67}(Sc)^{.67}\left(\frac{d}{L}\right)^{.29}$$

$$+ c_2' \cdot (Re)^{.59}(Sc)^{.59}\left(\frac{d}{L}\right)^{.31}$$

$$+ c_3' \cdot (Re)^{.61}(Sc)^{.61}\left(\frac{d}{L}\right)^{.30} \qquad (I-6-3)$$

where c_1', c_2', and c_3' are constants. (A detailed derivation along with the necessary assumptions is given in Appendix 5.)

Equation(I-6-3) is essentially similar to Equation(I-6-1). This general agreement is an indication that some very slow diffusional mass transfer step (or steps) is involved in the dissolution processes of tin in hydrochloric acid solutions.

C. Conclusions

1. The dissolution of tin in hydrochloric acid solutions appears to occur through three parallel reaction paths. In deaerated acid solutions there is a single slow hydrogen evolution process. In aerated acid solutions there are three simultaneous reactions; hydrogen evolution, oxygen depolarization, and an autocatalytic process. The last reaction becomes significant only after sufficient tin has been dissolved to create a tin ion concentration of about 0.35×10^{-4} moles/litre.

The hydrogen evolution process is essentially under diffusion control, while the oxygen depolarization and autocatalytic processes are under mixed control, because they

have a combination of slow physical and chemical steps involved in their elementary stages.

2. On the basis of the experimental results it is reasonable to believe that, (a) the diffusion of hydrogen ions from the bulk solution to the solution-metal interface and the adsorption of hydrogen ions on the metal surface are fast steps;

$$H_b^+ \xrightarrow{\text{fast}} H_i^+$$

$$H_i^+ + \underset{*}{Sn} \underset{\text{}}{\overset{\text{fast}}{\rightleftharpoons}} \underset{*}{Sn}\text{-}H_s^+$$
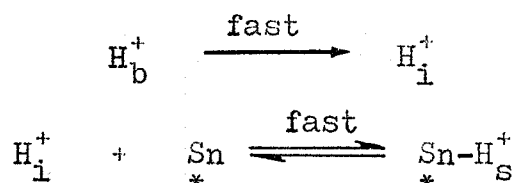
(b) the adsorption of oxygen on the tin surface is a dissociative type of adsorption, and is probably a slow step,

$$O_{2_i} + 2 \underset{*}{Sn} \overset{\text{slow}}{\rightleftharpoons} 2 \underset{*}{Sn}\text{-}O_s$$
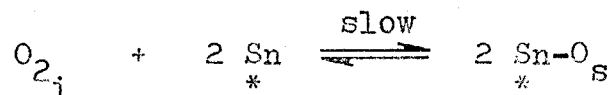
and (c) the diffusion of hydrated tin ions from the metal-solution interface to the bulk solution is a slow step.

$$Sn_i^{++} + n\ H_2O \xrightarrow{\text{slow}} Sn^{++}\text{-}nH_2O_{bulk}$$
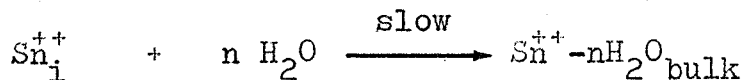
3. The dissolution rate of tin in HCl solutions is not directly proportional to the inner surface area of the tin tube. It is, instead, a function of the inside diameter and length of the tin tube.

4. Formation of gray film on the tin surface was observed. Other investigators[53,63,67] have reported this film to be composed of pure tin.

5. The stannous species, stannic species equilibrium:

$$\underset{*}{Sn}_s \quad + \quad Sn_i^{++++} \quad \rightleftharpoons \quad 2 \; Sn_i^{++}$$
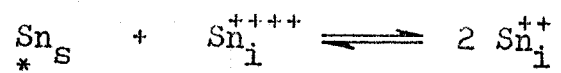
is assumed to be established at the metal surface very quickly.

PART TWO

A POTENTIOSTATIC INVESTIGATION OF THE POLARIZATION
AND CATHODIC PROTECTION OF TIN TUBES IN HYDROCHLORIC
ACID SOLUTIONS

81

ABSTRACT

A horizontally mounted tubular electrolysis cell, incorporated into a closed loop flow circuit, was used for the potentiostatic investigation of the polarization and cathodic protection of tin tubes in aerated and deaerated hydrochloric acid solutions.

The counter electrode consisted of a coaxial length of 17 s.w.g. platinum wire.

Some preliminary studies on stationary tin cylinders immersed in HCl solutions were carried out to determine the magnitude of the required protection current and the appropriate potential range likely to be encountered.

For both the stationary and flow systems plots of potential-log(current density) showed well defined linear portions (Tafel lines). The values of the Tafel constants, β_a and β_c, given by the slopes of these Tafel lines decreased with increasing hydrochloric acid and oxygen concentrations and flow velocities of the corroding solutions.

The corrosion current (I_c) of tin in HCl solutions, as determined by the intersections of the anodic and cathodic Tafel lines, was found to be proportional to the fluid velocity raised to the 0.65 power, and also directly proportional to the square root of the oxygen concentration, but essentially independent of the hydrochloric acid concentration.

82

The relationships between imposed cathodic potential on the tin tubes, protection current densities, and dissolution rates of tin were presented in the form of $[Sn]$-electrode potential-protection current density plots.

The experimental results showed that cathodic protection of tin can be achieved in both aerated and deaerated HCl solutions. The protection current requirements increased with increasing oxygen concentrations, flow velocities, acid concentrations, and temperatures of the corroding solutions.

CHAPTER I

INTRODUCTION

The application of cathodic protection is encountered in many industrial and civic facilities such as petroleum, gas, and water pipelines, hulls of ships, chemical storage tanks, boilers, heat exchangers, cooling towers, drying cylinders in paper-making machines, and other equipment.

Cathodic protection is perhaps the most effective of all approaches to corrosion abatement. By means of an externally applied electric current, the corrosion rate is reduced virtually to a negligible value, thus a buried or immersed metallic structure can be maintained in a corrosive environment for an indefinite time without deterioration.

This technique is usually concerned with the protection of ferrous materials, because these constitute the bulk of the objects that are used in industrial situations. As a result of this general dependence on iron containing metals, most of the earlier works, on the applicability of cathodic protection to control corrosion, have been done with ferrous materials in a variety of systems. A survey of the literature indicates that little attention has been paid to the study of cathodic protection of tin in electrolytic solutions.

In the application of cathodic protection, either in industrial or research projects, the coupled anode is usually connected externally to the system which is under protection.

84

There are two important disadvantages to this type of connection. The first results from the uneven protection-current distribution on the metal surface of the protected structure. As a result the most accessible parts of the structure are made more cathodic than necessary, while the current density on the metal surface of the least accessible parts is insufficient to offer protection. The second disadvantage is due to the inability of the protection current to enter electrically screened areas such as interiors of water condenser tubes and inner pipe surfaces of double pipe heat exchangers.

This study was conducted to investigate the applicability of cathodic protection to control corrosion of tin in HCl solutions under controlled flow patterns. This was accomplished through the following program:

1. Experimental examination of the behaviour of tin samples during anodic and cathodic polarization.

2. Experimental measurements to determine the dissolution rate of tin as a function of imposed cathodic potential.

3. Experimental measurements to determine the dependence of protection-current density on temperature, corroding solution velocity, acid concentration, and oxygen partial pressure.

An additional purpose of this study was to seek a way of obviating the difficulties presented by uneven protection-current distribution and electrically screened areas. To achieve this objective, a coaxial length of platinum wire

was used as the counter electrode(i.e. an internally coupled anode was employed in the specially constructed tubular electrolysis cell).

CHAPTER II

LITERATURE REVIEW

A. Electrochemical Theory of Corrosion

In aqueous media, metallic corrosion is the result of basic electrochemical reactions which can be separated into two or more partial reactions. These partial reactions are divided into two classes: anodic reactions and cathodic reactions.

The electrode at which oxidation reactions occur is called the anode[85]. An example of anodic reaction is:

$$Sn \longrightarrow Sn^{++} + 2e^- \qquad (II-2-1)$$

This reaction is the basis of the corrosion of tin.

The electrode at which chemical reduction occurs is called the cathode[85]. One of the commonest cathodic processes during corrosion is that of hydrogen evolution:

$$2 H^+ + 2e^- \longrightarrow H_2 \qquad (II-2-2)$$
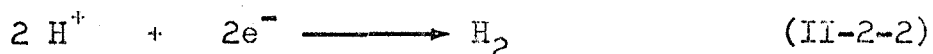
To view the over-all reaction, one combines the oxidation and reduction reactions.

$$Sn + 2 H^+ \longrightarrow Sn^{++} + H_2 \qquad (II-2-3)$$
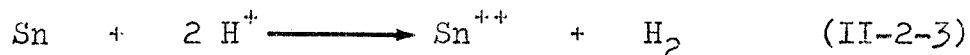
1. Thermodynamics of Electrochemical Corrosion Processes

In any electrochemical corrosion reaction, the driving force is the potential difference which exists between the anode and cathode.

For these electrode potential calculations, the concept

87

of standard half-cell potentials has been developed[85].

Arbitrarily, the hydrogen electrode has been universally

chosen as the standard reference electrode, and assigned a

standard potential of zero volts at all temperatures. The

standard potential of an electrode, E^O, is that potential

which exists between the electrode and a standard hydrogen

electrode when all reactants and products are at unit activity.

If the activity of any of the products or reactants is not

unity, a new electrode potential can be calculated from the

Nernst equation:

$$E = E^O + \frac{RT}{nF} \ln \frac{a_{ox.}}{a_{red.}} \qquad \text{(II-2-4)}$$

where:

E^O = standard electrode potential, volts

E = electrode potential, volts

R = gas constant, cal./g.mole-^{O}K

T = absolute temperature, ^{O}K

F = Faraday,coulomb/g.equiv.

n = number of electrons transferred in the reaction

$a_{ox.}$ = activity of oxidized species

$a_{red.}$ = activity of reduced species

The potential of a reaction is related to its free energy
by[28,73]:

$$\Delta G = -nFE \qquad \text{(II-2-5)}$$

where ΔG is the change in free energy for the reaction.

A negative value for the change in free energy corresponds

to a spontaneous reaction[28,73]. It can be seen also from

Equation(II-2-5) that a reaction which has a positive potential will proceed as written.

The application of thermodynamic principles to corrosion studies has been further generalized by means of potential-pH plots. Pourbaix and his co-workers[31,65,66] have calculated the phases at equilibrium for metal-water,and for other systems at $25^\circ C$, from the chemical potentials of the species concerned in the equilibrium, and have expressed the data in the form of equilibrium diagrams having pH and potential, E, as ordinates.

The main uses of the potential-pH diagrams are (1) predicting the spontaneous direction of reactions, (2) estimating the composition of corrosion products, and (3) predicting environmental changes which will prevent or reduce corrosion attack[73].

The potential-pH diagrams for tin have been constructed by Deltombe, Zoubov, Vanleugenhaghe, and Pourbaix[65]. These diagrams predict a domain of passivation in moderately acid, neutral and slightly alkaline solutions, in the pH range between 3.5 to 9.0. This passivation would correspond to the metal being covered with a protective film of stannic oxide in the absence of substances capable of forming soluble complexes with tin or insoluble compounds. On the other hand, acid solutions and moderately alkaline solutions(pH value between about 0 and 12) are passivated if they contain oxidizing agents capable of raising the potential to about +0.2v in acid media to -0.7v in alkaline media. From these

diagrams it also appears to be possible to bring about the cathodic protection of tin by lowering its potential to values included between two well defined limits, which are about -0.3 and 1.0 v in very acid solutions, and -1.1 and -1.8 v in very alkaline solutions.

Potential-pH diagrams are subject to the same limitations as any thermodynamic calculations. They represent equilibrium conditions and hence can not be used to predict the velocity of a possible reaction.

2. Kinetics of Electrochemical Corrosion Processes

One of the keystones of electrochemistry is Faraday's law which relates chemical change and electrical energy[27]. For every equivalent of chemical reaction 96,500 coulombs must pass through the cell. This equivalence between chemical reaction and electrical charge makes it possible to write the rates for electrochemical reactions in terms of electrical currents.

The discussion of the kinetics of electrochemical reactions is based largely on the mixed potential theory of electrode kinetics as stated by Wagner and Traud[88]. The basic assumptions of this theory are (a) the kinetics of the various partial reactions can be treated separately and (b) no net current flows from an electrode which is in equilibrium or at steady state. The condition of no net current flow means the total rate of reduction must equal the total rate of oxidation on the electrode surface if the electrode is at steady state

or equilibrium.

The relationship between exchange-reaction rate and current density can be directly derived from Faraday's law:

$$\lambda_{oxd.} = \lambda_{red.} = \frac{i_o}{nF} \qquad (II-2-6)$$

where $\lambda_{oxd.}$ and $\lambda_{red.}$ are the equilibrium oxidation and reduction rates and i_o is the exchange-current density.

When a reaction is forced away from equilibrium, the potential at which the reaction is occuring changes. The amount by which the potential changes is the overvoltage, defined as[77]:

$$\eta = E_{eq.} - E_i \qquad (II-2-7)$$

where:

   η = overvoltage, volts

   $E_{eq.}$ = equilibrium potential, volts

   E_i = polarized(current flowing) potential, volts

The current applied to cause the departure from equilibrium is the net rate of reaction. Thus:

$$i_{app.} = \Sigma i_a - \Sigma i_c \qquad (II-2-8)$$

where:

   i_a = anodic current density, amp./cm^2

   i_c = cathodic current density, amp./cm^2

   $i_{app.}$ = applied current density, amp./cm^2

The overvoltage, exchange-current density, and the rates of the various partial processes can be related in the form of a chemical rate equation[73].

$$i_a = i_o exp(\frac{2.3\eta_A}{\beta a}) \qquad (II-2-9a)$$

$$i_c = i_o \exp\left(\frac{2.3\eta_A}{\beta_c}\right) \qquad \text{(II-2-9b)}$$

where β_a and β_c are constants (Tafel constants) of the system and may be equal to one another. For corrosion and electrochemical studies, Equation(II-2-9) is usually written in logarithmic form[79] and called the Tafel equation[81].

$$\eta_A = -\beta_c \log i_c/i_o = \beta_a \log i_a/i_o \qquad \text{(II-2-10)}$$

where: η_A = activation overvoltage, volts

In Figure II-2-1, polarization curves have been constructed for a reaction whose rate is described by Equation(II-2-9), which may be applied whenever corrosion is solely electro-chemical and governed by activation overvoltage[28].
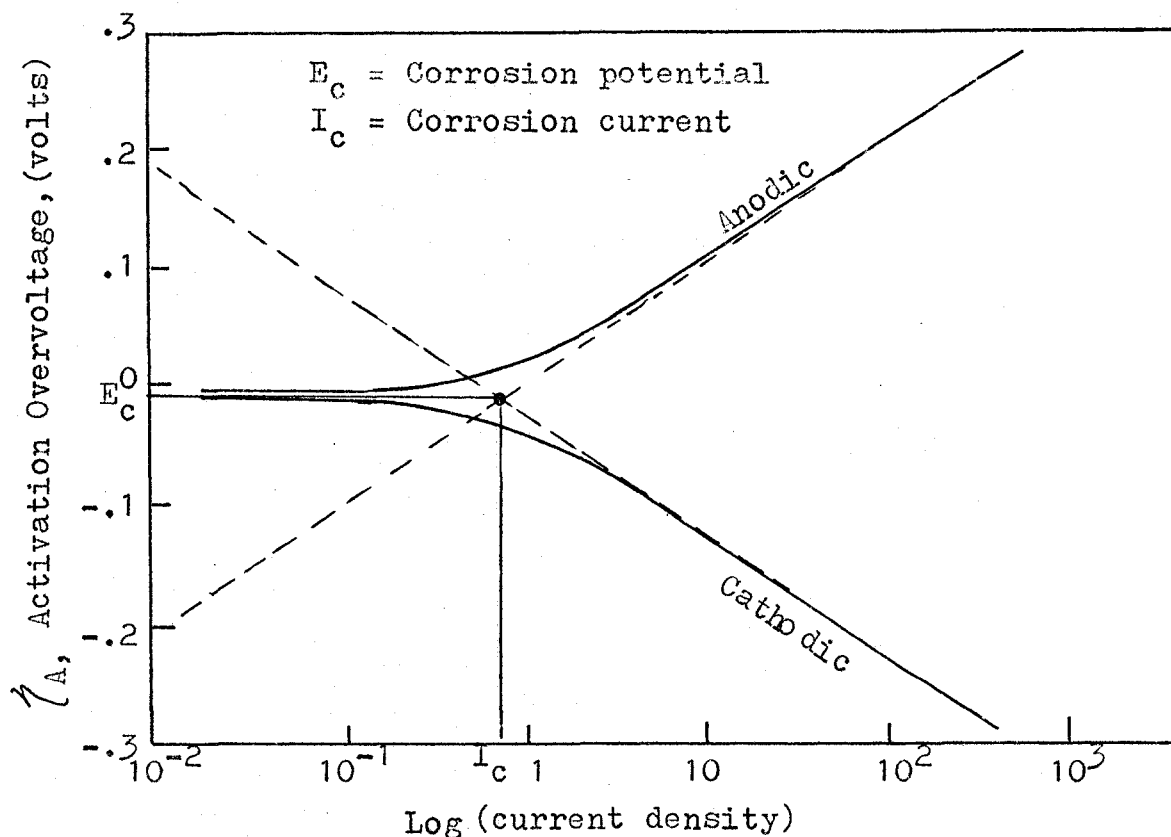
Figure II-2-1. Activation Polarization Curve for a Reversible Electrode

In Figure II-2-1, the zero-net-current point for a reversible system is the equilibrium potential. In a corroding system, the no-current point is the corrosion potential[28].

Besides activation polarization, it is possible to have concentration polarization at an electrode.

Concentration polarization occurs when one or more of the reactants are consumed at an electrode faster than they can be supplied from the bulk of the solution or when products accumulated at the electrode surface. The rate of the reaction is then limited by diffusion of ions or dissolved species toward or from the metal-solution interface. This limiting rate can be expressed as a current density(the limiting current density i_L) by the equation[73]:

$$i_L = \frac{DnF}{\delta} \Delta C \qquad \text{(II-2-11)}$$

where:

i_L = limiting current density, amp./cm^2.

D = diffusion coefficient of reacting species, cm^2/sec.

ΔC = concentration difference between ions in the bulk solution and that at the metal-solution interface.

The amount of concentration polarization overvoltage, η_c, is related to the limiting current density by the equation[77]:

$$\eta_C = \frac{RT}{nF} \log\left(1 - \frac{i}{i_L} \right)$$
(II-2-12)

where: η_C= concentration polarization overvoltage, volts

A schematic plot of this equation is shown in Figure II-2-2. It is seen that concentration polarization does not become effective until the net reduction current density approaches the limiting current density[28].
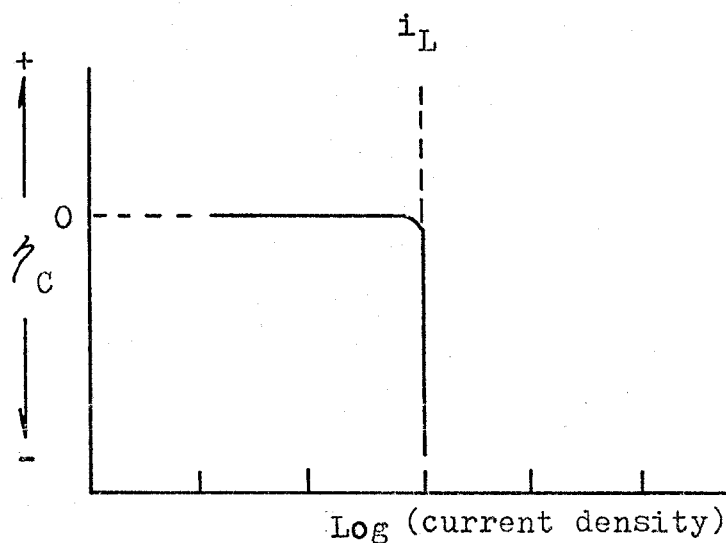
Figure II-2-2. Concentration Polarization Curve
(Reduction Process)

It was observed[46] that, in practice, both activation and concentration polarization usually occur at an electrode. At low reaction rates, activation polarization usually controls, while at higher reaction rates(higher current densities) concentration polarization becomes controlling.

For corrosion reactions it is usually sufficient to consider the measured overvoltage to be the sum of the

concentration and activation overvoltage[79]:

$$\eta_T = \eta_A + \eta_C + \eta_R \qquad (II\text{-}2\text{-}13)$$

The last term in Equation(II-2-13), η_R , is the resistance polarization which is merely an error produced by the potential measuring circuit. It is important only at high current densities or in high resistance solutions.

During reduction processes such as hydrogen evolution or oxygen reduction, both types of polarization are present, and the over-all equation for the overvoltage of the reduction process is formed by combining Equations (II-2-10) and (II-2-12):

$$\eta_T = \eta_A + \eta_C$$
$$= -\beta_c \log i_c/i_o + 2.3 \frac{RT}{nF} \log(1 - \frac{i}{i_L}) \qquad (II\text{-}2\text{-}14)$$

Equation(II-2-14) is graphically illustrated in Figure II-2-3.
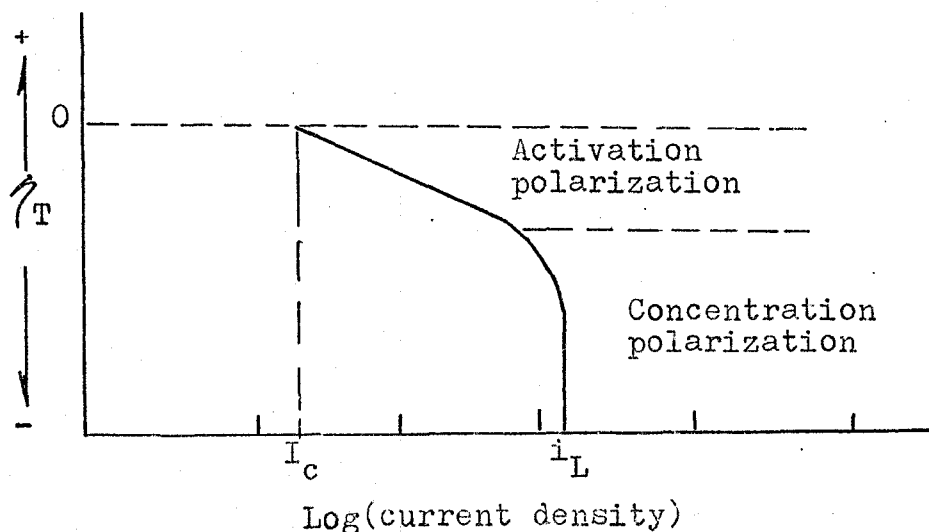
Figure II-2-3. Combined Polarization Curve - Activation and Concentration Polarization (Reduction Process)

B.   Polarization Studies of Tin

In 1938 Kerr[42] investigated the formation of oxide
films on tin during anodic polarization in sodium hydroxide
solutions.   He observed that the nature (such as colour,
composition, etc.) and the rates of growth of the films
depended on various factors, including alkali concentration,
temperature, and current density.   He also found that, in
the presence of oxidizing agents such as chromates, chlorates,
etc., the anodic polarization curves showed that tin became
passive for any current density.

In 1968 Hampson and Spencer[35] examined the anodic
polarization of tin in potassium hydroxide solutions.   They
reported that the orientation of the anode played an important
part in the observed behaviour; permanent passivity occurred
when the potential rose to that required for oxygen evolution
from a film of stannic oxide.   In potassium hydroxide
solutions of concentration higher than 7M, anodic films
formed with less and less dependence on mass transfer in the
electrolyte.

In 1963 Ross and Firoiu[70] studied the cathodic
polarization behaviour of tin in potassium hydroxide
solutions at four concentrations and three temperatures.
They reported that the hydrogen overvoltage values, obtained
in solutions of 0.01, 0.05, 0.10, and 1.0 N KOH, were in
full agreement with Tafel's equation.   The slope of the

potential-log(current density) plots, β , was 0.12v at 25°C for all concentrations. The effect of temperature was investigated at 25°, 40°, and 55°C in 0.1N KOH solution. The hydrogen overvoltage decreased by approximately 2mv/$^\circ$C, whilst the constant β increased approximately in direct ratio to the absolute temperature.

C. Cathodic Protection of Metals

The rate of electrochemical corrosion of buried or immersed metallic structures can be reduced by cathodic polarization or by contact with an additional electrode serving as an anode relative to the corroding system. This phenomenon has long been known(first noted by Davy[22] in 1824) and serves as a basis for a wide spectrum of protective methods, generally known as cathodic protection. It is accomplished (a) by cathodic polarization through the application of an impressed potential from an external source such as a d-c generator or a rectifier, or (b) by connecting the metal to be protected with another metal which has a more negative(active) electrochemical potential[3,28,59].

Many different theories have been advanced to explain the mechanism of cathodic protection. Evans[27] assumed that the basic reason for cathodic protection was the formation of alkali which would produce protective hydroxide films on cathodically polarized surfaces.

Harker et al[36] have expressed opinions that to obtain complete protection it is sufficient to provide a cathodic

current density equal to the total local current density on the metal surface. Cathodic protection, according to these authors, is due to a reverse electrolysis of the dissolving metal. Later, similar points of view on the mechanisms of cathodic protection were expressed by Mears and Brown[57,58].

Stender, Artamonov, and Bogoyavlenskii[76] suggested an entirely different approach. They proposed that cathodic protection could be explained by the fact that the atomic hydrogen evolved on the protected surface during cathodic polarization completely tied up the oxygen diffusing to the corroding surface. This retardation process would limit the access of the corroding surface to the oxygen essential for depolarization. However, this does not completely explain the mechanism of cathodic protection. For instance, it is well known that cathodic protection can be attained in the absence of oxygen and also in acid media where the oxygen supply is not the controlling factor of corrosion.

In general, the principles of cathodic protection may be explained by considering the corrosion of a typical metal M in an acid environment. The electrochemical reactions occuring are the dissolution of the metal and the evolution of hydrogen gas:

$$M \longrightarrow M^{n+} + ne^- \qquad (II-2-15)$$

$$2 H^+ + 2e^- \longrightarrow H_2 \qquad (II-2-16)$$
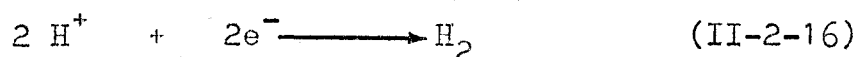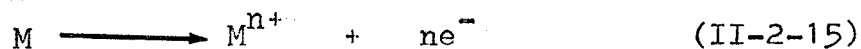
Cathodic protection is achieved by supplying electrons to the metal structure to be protected. Examination of

Equations(II-2-15) and (II-2-16) indicates that the addition

of electrons to the metal will tend to suppress metal

dissolution and increase the rate of hydrogen evolution. If

current is considered to flow from (+) to (-), as in

conventional electrical theory, then a structure is protected

if current enters it from the electrolyte. Figure II-2-4

illustrates cathodic protection by supplying an external current

to the corroding metal on the surface of which local action

cells operate. Current leaves the auxiliary anode and enters

both the cathodic and anodic areas of the corroding surface,

returning to the source of d-c current B. Thus the corroding

metal will be made more negative by electrons flowing to it.

These electrons will attract the positive ions and thus reduce

the tendency for these ions to go into solution (i.e. corrosion

rate will be reduced).

Electrolyte

Auxiliary
Anode

Corroding
Metal
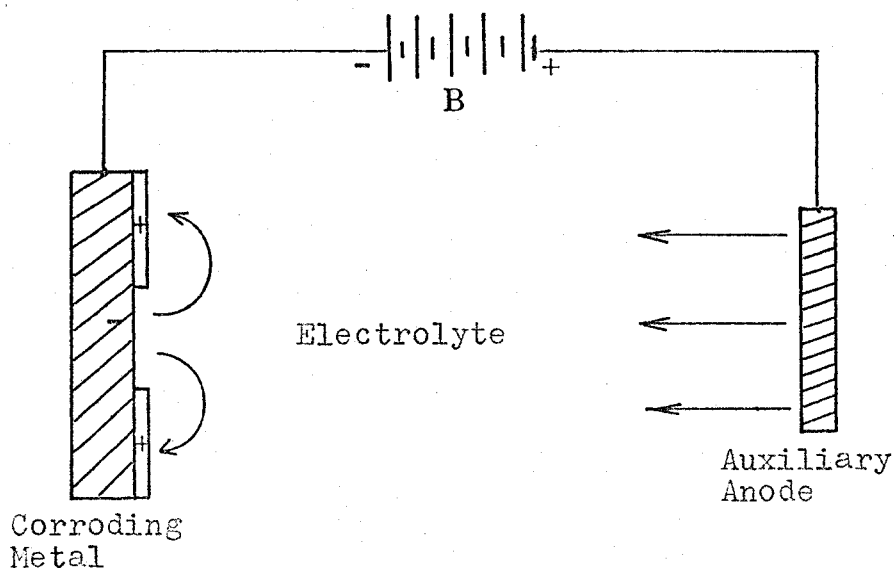
Figure II-2-4. Cathodic Protection by Superposition of
                Impressed Current on Local Action Current

There are three mechanisms which cause reduction of corrosion when cathodic protection is applied[73]:

1. The potential of the metal is lowered so that cathodic processes actually occur on all surface areas of the metal, i.e. $M \longrightarrow M^{n+} + ne^-$ is prevented.

2. The electrolyte adjacent to the metal surface becomes more alkaline owing to the reduction of oxygen or hydrogen ions, and for ferrous metals this increase in pH will cause inhibition of corrosion.

3. The increase in pH will cause the precipitation of insoluble salts, i.e. $CaCO_3$ and $Mg(OH)_2$, which may deposit on the metal surface and produce a protective film.

D. Current Density Requirements for Cathodic Protection

The current density required to protect a metal surface is usually determined empirically, because it depends on a large number of factors. According to Stern[78], Shreir[73], Morgan[59], and Tomashov[83], the current requirement depends to a large extent on the following environmental factors;

1. Oxygen accessibility. This factor is associated with oxygen concentration in the electrolyte and degree of turbulence. The latter reduces the thickness of the diffusion layer through which the oxygen must diffuse. In highly turbulent oxygenated liquids substantially higher current densities are required to protect an uncoated metal surface.

2. The nature of the electrolyte. In the presence of high concentrations of cathode depolarizers very large current

densities may be required to produce protection. The most important instance is that of acid solutions in which hydrogen ions can be discharged.

3. The temperature of electrolyte. Because an increase in temperature of the electrolyte is associated with a fall in hydrogen overvoltage, increase in depolarization, decrease in viscosity of the solution, and destruction of protective film, the current requirement is usually increased with increase in temperature.

E. Overprotection

Current used in excess of that required does no good, and may do harm to metals. In 1931 Akimov[4] observed that in a case of extraordinarily high protection current in the cathodic protection of Duralumin in a 3% solution of NaCl, instead of the expected increase in the protective action there occurred just the reverse. This overprotection phenomenon was later also observed by Slomyanskaya[74] with stainless steel in sea water. Muller[60] pointed out that the rate of dissolution of chromium in acid solutions can be increased by cathodic polarization. Kabanov and Kokoulina[41],in 1958, observed that the cathodic protection of iron and stainless steel by high current densities in nitric acid solutions can considerably increase their rates of dissolution.

It is generally accepted that the negative protective effect(overprotection) is caused by the destruction of the protective film and reactivation of the metal by one of the

following destructive actions:

1. Chemical dissolution of the protective oxide films by the alkali formed at the cathode during cathodic polarization (as may occur with amphoteric metals such as aluminum).

2. Cathodic reduction of the protective film(for metals with not too high negative potential - Cu, Ni, Fe).

3. Purely mechanical destruction of the protective film by the liberation of hydrogen on the cathode.

The critical cathodic current density at which the negative protective effect appears depends on the operating conditions of the protected metal surface.

F. Studies on Cathodic Protection

Most of the earlier work on the applicability of cathodic protection to control corrosion was done with ferrous materials. In addition, the emphasis was generally focussed on special applications under very limited experimental conditions.

Recently, a systematic study of cathodic protection of a rotating vertical Monel cylinder in a 4% aqueous solution of sodium chloride was carried out by Cornet and Kappesser[21]. They observed that at -0.97v vs S.C.E. the Monel cylinder was cathodically protected from chemical attack in aerated sea water. Constant voltage runs at this potential were made to determine the correlation of Sherwood number with Reynolds number for the diffusion of oxygen to the surface of the cylinder under limiting current conditions.

The anodic behaviour of tin in alkaline solutions plays
an important part in the process of tin-plating and has been
the subject of various studies, because over half of the tin
produced goes into coating other metals, primarily steel to
make the tin can. The cathodic behaviour of tin in acid
media has not been paid much attention.

G. Polarization Studies Employing Potentiostatic Techniques

A potentiostat, as the name implies, maintains an
electrode at a pre-set potential with respect to a reference
electrode. If the potential drifts from this value, an error
signal is generated, amplified, and fed to an output stage
where the error is corrected by changing the current to the
auxiliary electrode[24].

A schematic diagram of a potentiostatic circuit for use
in the study of metallic polarization behaviour is shown
in Figure II-2-5.
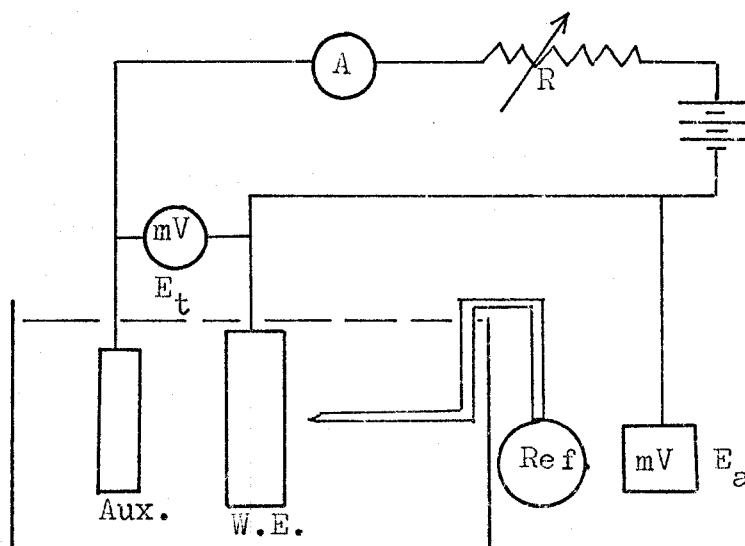
Figure II-2-5. Electric Circuit for Polarization
Measurements

The metal sample is termed the working electrode(W.E.) and current is supplied to it by means of the auxiliary electrode composed of some inert material such as platinum. Current is measured by means of an ammeter A, and the potential of the working electrode is measured with respect to a reference electrode. In practice, current is increased by reducing the value of the variable resistance R.

To obtain polarization curves, the metal sample is made the cathode or anode by adjusting the potential of the sample to the desired potential which is then maintained between the working electrode and the reference electrode. This is accomplished by automatic regulation of the current which flows between the auxiliary electrode and the working electrode. After the desired potential is adjusted, the current is allowed to stabilize and noted[24]. A new potential is set, and the process is repeated until the desired portion of the polarization curve is obtained.

The chief use of a potentiostat is in elucidating the kinetics and mechanism of corrosion processes. This normally involves the study of potential-current characteristics as a function of the corroding system and of time[90].

CHAPTER III

EXPERIMENTAL

A. Details of the Design of the Stationary System

The following is a description of the equipment used for conducting preliminary polarization measurements and cathodic protection tests of tin in stationary HCl solutions. These preliminary experiments were carried out to determine the proper potential range, and the magnitude of the required protection current likely to be encountered in order to limit the surface area of the specimens to be used in the flow system, so that the current output would fall well within the range of the potentiostat.

1. The Assembly of the Test Cell

The test cell was assembled as shown in Figure II-3-1. The cell consisted of a 1,500 ml. reaction vessel fabricated from plexiglas pipe and plate. The four sockets on the top cover were used to hold the test electrode, gas bubbler, counter electrode, and reference electrode probe. The reference electrode probe was connected by a salt bridge of KCl to a saturated calomel reference electrode contained in a separate constant temperature water bath. A description of the preparation of the saturated calomel electrode used in this study is given in Appendix 6.

2. Test Electrode Design

The design of the test electrode is shown in

105

Figure II-3-1. Schematic Diagram of Stationary Test Cell Assembly

LEGEND

A — counter electrode
B — counter electrode lead
C — test electrode (tin bar)
D — test electrode lead
E — reference electrode probe
F — salt bridge
G — gas bubbler
H — test cell

Figure II-3-2.

3. The Counter Electrode

The counter electrode was an eight inch length of 17 s.w.g. platinum wire.

4. The Potentiostat

The potentiostat used in this study was a Model 4700M Research potentiostat produced by Magna Corporation, Santa Fe Springs, Calif. The essential features of the circuit of this potentiostat are shown in Figure II-3-3.

The principle of operation of this potentiostat is that a desired potential is pre-set into the potential control circuit. The potential difference between the reference and test electrode is then read and balanced against this pre-set potential. The difference or error signal is fed into the Control Amplifier. The resultant control signal varies the output of the Current Supply as necessary to maintain the pre-set potential. A chopper circuit is incorporated into the Control Amplifier to counteract any drift and to prevent accumulation of error signal. Because of the extremely high input impedance, essentially no current is drawn through the reference electrode, and its potential remains stable. Specifications of the Model 4700M potentiostat are given in Appendix 7.

B. Details of the Design of the Flow System and the Tubular Electrolysis Cell

1. Design of the Liquid Recycle System and its Accessories

Copper wire

Copper nut

Teflon washer

Teflon tube

5"

0.125"

Teflon washer

3"

Tin bar

0.3"
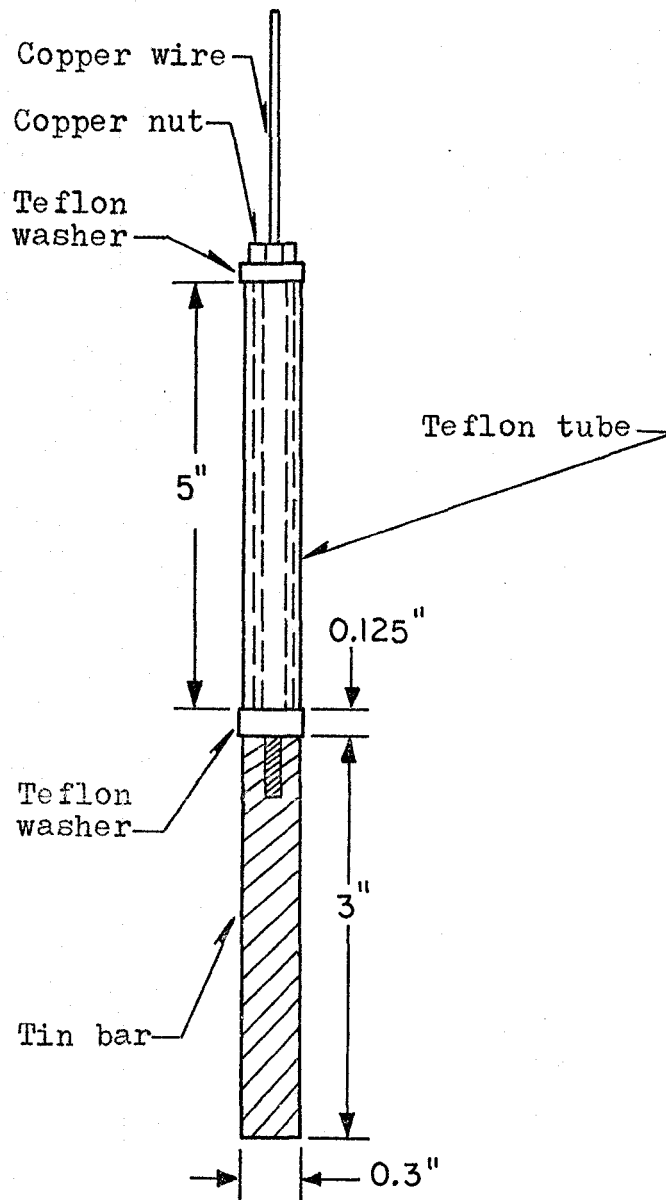
Figure II-3-2. Schematic Diagram of Test Electrode
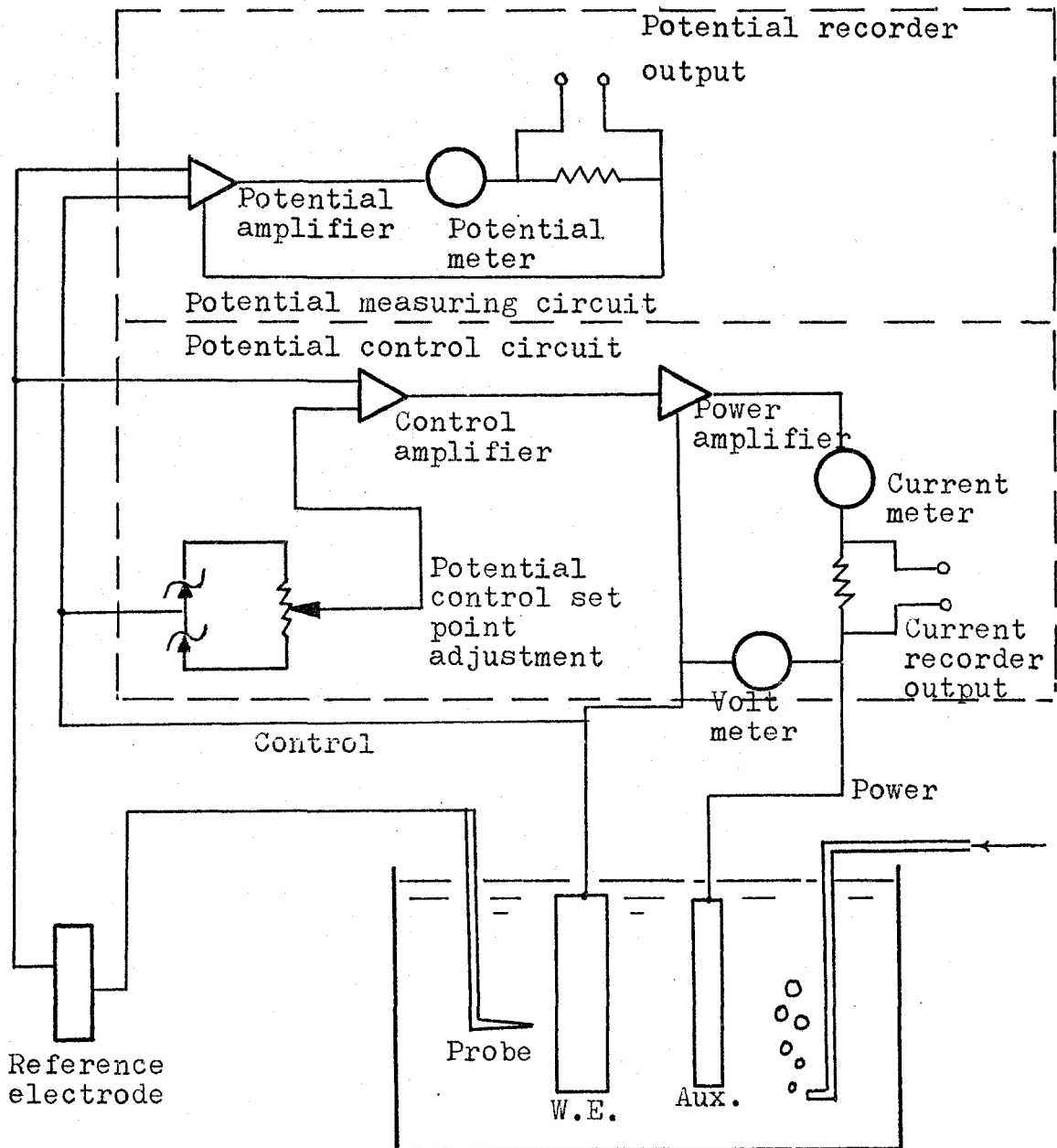
Figure II-3-3. Block Diagram of Model 4700M Magna
Potentiostat

Details of the design of the liquid recycle system
and its accessories have been given in Part One, Chapter IV.

2.   Tubular Electrolysis Cell Design

The construction of the tubular electrolysis cell
is shown in Figure II-3-4. A tin tube of half inch inside
diameter and four inches in length was produced from a
remoulded one inch diameter tin rod.

A pair of spigots were machined from 1.5 inch diameter
polypropylene rod to different dimensions to accommodate the
tin tube as shown in Figure II-3-4.

Both ends of the tin tube were recessed into the spigots
and secured firmly with plastic cement. In addition two
Teflon washers, functioning as watertight seals, were placed
between the end surfaces of tin specimen and the stopping
edges of the spigots.

A capillary tube was machined from 0.25 inch diameter
Teflon rod to the dimensions shown in Figure II-3-4. One end
of the capillary was inserted tightly into a hole drilled
through the wall of the tin tube, and fixed firmly with
plastic cement. This system constituted the probe for the
reference electrode. A salt bridge of saturated KCl solution
contained in a length of Tygon tubing connected the short
capillary tube to the saturated calomel reference electrode.

A portion of the outside surface of the tin tube between
the two connecting polypropylene spigots was exposed for
electrical contact with the control lead of the potentiostat.
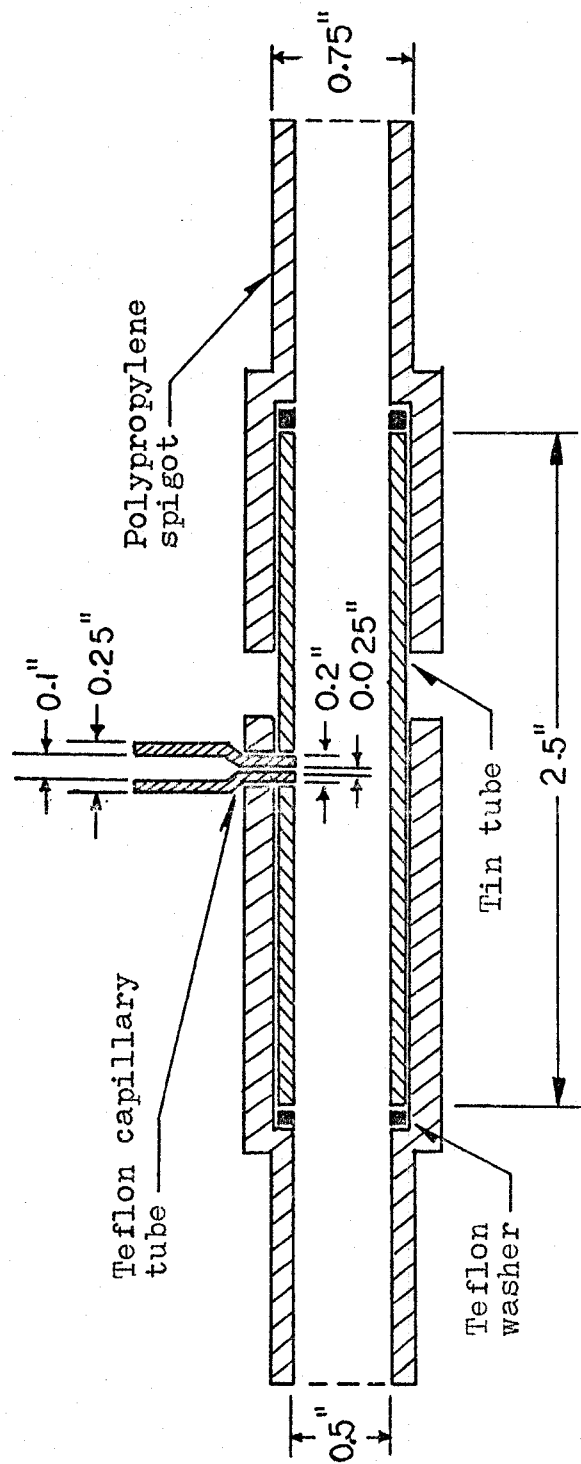
Figure II-3-4. Schematic Diagram of Tubular Electrolysis Cell

3. Design of the Counter Electrode

The construction of the counter electrode is shown in Figure II-3-5. This electrode was a ten inch length of 17 s.w.g. platinum wire. The main body of this platinum wire projected through the centre of the tin tube when the electrolysis cell was assembled. This central location of the counter electrode ensured a uniform electrical field.

One end of the platinum wire was inserted tightly into and led through the wall of a five inch length polypropylene tube. This polypropylene tube was used as a supporting base for the platinum wire.

4. Electrical Circuitry

The electrical circuitry of the assembled electrolytic cell is shown in Figure II-3-6.

C. Materials and Chemicals

A description of the materials and chemical reagents used in this study has been given in Part One, Chapter IV.

D. Procedures for Polarization Measurements and Cathodic Protection Tests Using a Stationary System

The corrosion behaviour of the stationary tin bar was determined by potentiostatic polarization (the variation of current was examined as a function of imposed cathodic or anodic potential).

1. Preparation

Prior to testing, the test cell was filled with 1,000 milliliters of test solution, placed in the constant
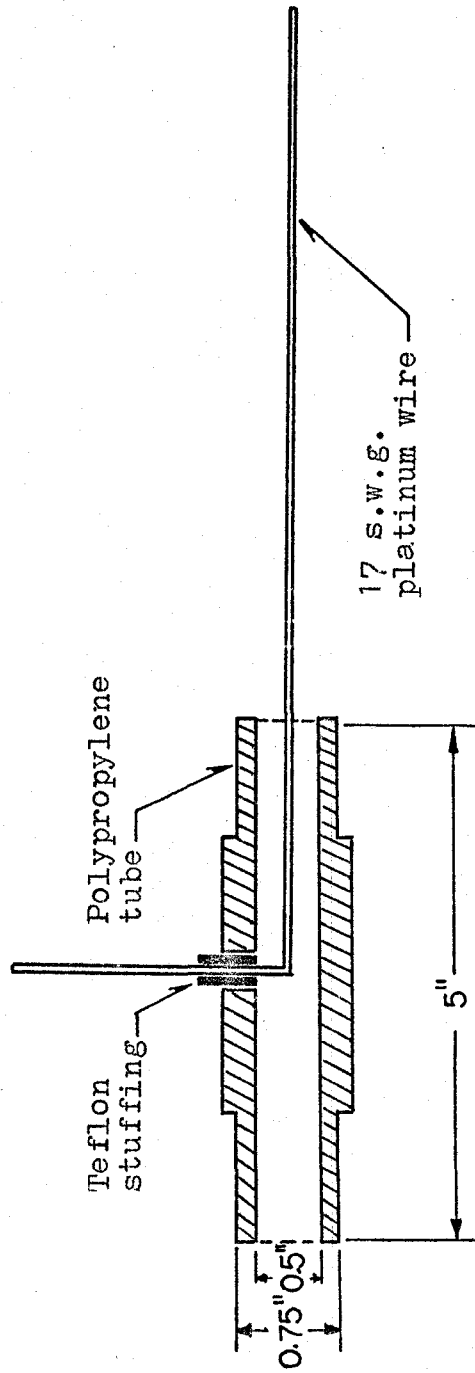
Figure II-3-5. Schematic Diagram of Counter Electrode

114
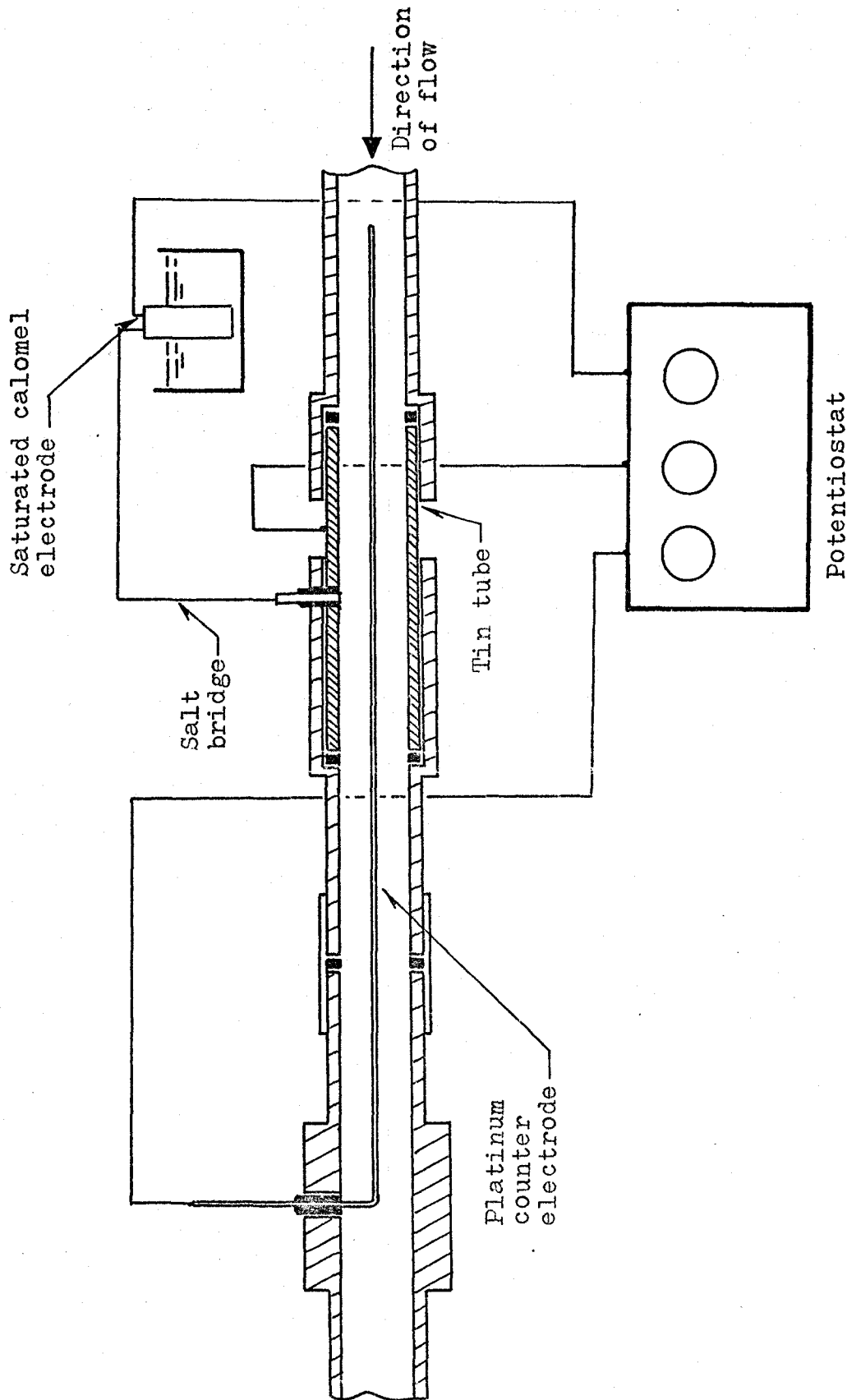
Figure II-3-6. Schematic Diagram of Electrical Circuitry of Flow System

Direction of flow

Saturated calomel electrode

Salt bridge

Tin tube

Potentiostat

Platinum counter electrode

temperature water bath, and saturated with appropriate gas for three hours.

The test electrode(tin bar),polished manually to 3/0 emery paper smoothness, was washed initially with distilled water, then washed with acetone for degreasing, and finally rewashed with distilled water.

The power supply of the potentiostat was then turned on and allowed to warm up in the "standby" position for approximately 30 minutes prior to testing.

The test electrode and counter electrode were then placed in the test cell. The probe of the salt bridge was inserted into the test cell and the probe tip positioned approximately half inch from the test electrode surface. Precautions were taken to ensure that the probe faced the test electrode without blocking the current path from the counter to test electrode.

All electrical leads were then connected as shown in Figure II-3-3. The zeroing of the potential measuring circuit was adjusted prior to the test and approximately every 10 minutes through the test period.

2. Polarization Testing

After the preparatory steps were completed, the potentiostat was first adjusted to the rest potential with respect to the saturated calomel reference electrode and then switched to the "on" position. At the rest potential no current flowed between the test electrode and the counter

·electrode.

The imposed potential of the test electrode was then changed by approximately 50 millivolt increments, allowing the current to stabilize for 5 minutes, and recording the potential and current. This process was repeated until the desired potential range was covered.

3. Cathodic Protection Study

The cathodic protection study was conducted by making the tin sample(test electrode) the cathode as shown in Figure II-3-3. The potential of the test electrode was adjusted to the desired potential which was then maintained between the test electrode and the reference electrode. After the desired potential was reached, a record of current versus time was made.

When the termination point (after 3 hours) of the test was reached, an appropriately sized sample of the corroding solution was withdrawn for routine Atomic Absorption Analysis.

After the test was completed, the potentiostat was switched off, all electrical leads were disconnected and the purge gas was turned off. The test cell was disassembled, cleaned, and the acid solution discarded.

E. Procedures for Polarization Measurements and Cathodic Protection Tests Using a Flow System

1. Preparation

Prior to testing, hydrochloric acid solutions were made up and mixed in the make-up tank as described in Part One,

Chapter IV. A proper volume of the solution was then pumped into the top supply tank. After the solution was saturated with the appropriate gas overnight, the temperature control system and the stirrer in the supply tank were switched on. During the time required for the acid solution to reach the desired temperature, the electrolytic cell was prepared and connected to the flow system. The power supply of the potentiostat was turned on and allowed to warm up in the "standby" position for approximately 30 minutes.

After the acid solution in the supply tank reached the desired temperature, the Dynalab Model 4-MD pump used to deliver the corroding solutions was switched on and the flow rate was regulated. All electrical leads of the electrolytic cell were then connected to the potentiostat as shown in Figure II-3-6.

2. Polarization Measurements

After the preparatory steps as described in the above section were completed, the potentiostat was adjusted to the rest potential with respect to the reference electrode. The imposed potential of the test electrode was then changed by approximately 50 millivolt increments, allowing the current to stabilize for 5 minutes, and recording the potential and current. This process was repeated until the desired potential range was covered.

3. Cathodic Protection Study

After the preparatory steps as described in Section 1

were completed, the test electrode(tin tube) was made cathodic by adjusting its potential to the desired value which was then maintained between the test electrode and the reference electrode. After the desired potential was reached, a record of current versus time was made. Besides the current-time record, an appropriately sized sample of the corroding solution was withdrawn for routine Atomic Absorption Analysis at convenient intervals of time.

4. Shut-down Procedure

When the test was terminated, the potentiostat was switched to the "standby" position, and all power to the circuit was turned off. All electrical leads were then disconnected. The acid solution was drained from the flow system. After the flow system was flushed with water twice, the electrolytic cell was disconnected, cleaned with distilled water, and stored.

CHAPTER IV

EXPERIMENTAL RESULTS AND DISCUSSION

The results obtained from the polarization and cathodic protection studies are presented in this chapter.

For each polarization test, a separate plot of current density versus electrode potential with respect to a saturated calomel electrode was constructed. Current density values at each potential were calculated from the measured current and the exposed surface area of the electrode.

For each cathodic protection test, in addition to the current density-electrode potential plot, a separate plot of metal ion concentration in the corroding solution versus time was made for the purpose of examining the protective effect of the impressed current on the test electrode at each potential.

A. Results of Stationary System Tests

1. Polarization Tests

Preliminary polarization tests were conducted at $25^{\circ}C$ by immersing stationary tin samples in aerated and deaerated solutions over the concentration range 0.0625 to 2.0 M HCl. The results are illustrated by the electrode potential-log(current density) plots shown in Figures II-4-1 and II-4-2. The polarization curves shown in these Figures are of similar form. This similarity in form of the polarization curves confirmed that the electrical circuitry of the electrolytic cell, including the potentiostat,

119
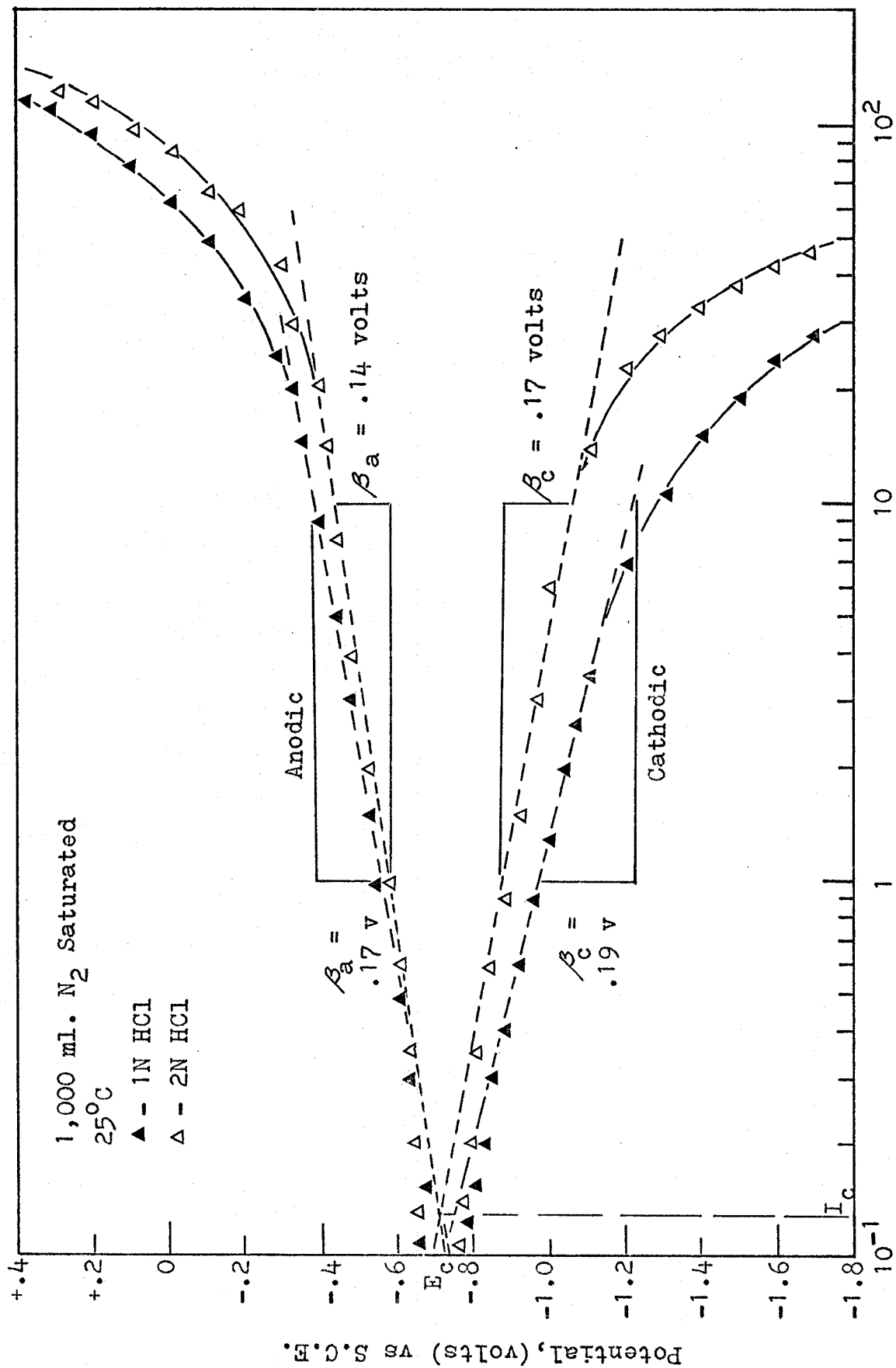
Figure II-4-1. Cathodic and Anodic Polarization of Stationary Tin Samples in Nitrogen Saturated HCl Solutions
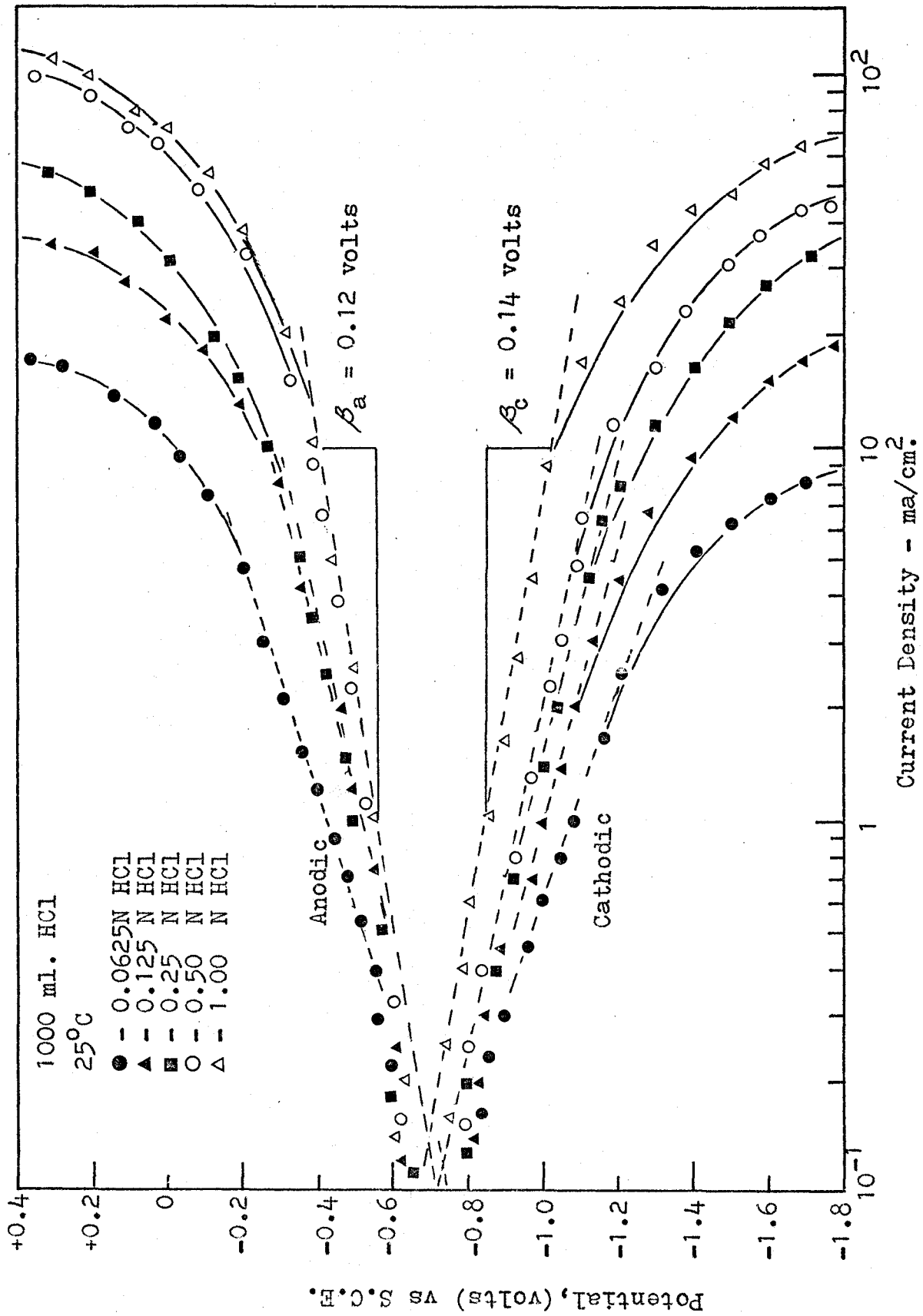
Figure II-4-2. Cathodic and Anodic Polarization of Stationary Tin Samples in Air Saturated HCl Solutions

functioned satisfactorily.

The dashed lines in Figures II-4-1 and II-4-2 are the estimated Tafel lines for the anodic and cathodic processes. These linear portions of the polarization curves are well defined. The intersection of the anodic and cathodic Tafel lines gives both the corrosion current (I_c) and corrosion potential (E_c) as specified by theory[79].

Figure II-4-1 shows that the anodic slopes of the potential-log(current density) plots (β_a in Tafel equation) for tin in 1.0M and 2.0M HCl solutions are 0.17 volt and 0.14 volt, respectively. The cathodic Tafel slopes, β_c, are 0.19 volt and 0.17 volt, respectively. Figure II-4-2 shows that at 25^oC, in aerated 1.0M HCl solution, β_a for tin is 0.12 volt, β_c is 0.14 volt.

A literature survey[19, 64,85] showed that the value of β for electrochemical reactions ranges between 0.05 and 0.15 volt per tenfold increase in current. However, in the presence of readily adsorbed impurities, the values of β may be twice the values quoted above and may also vary irregularly with current density[28,64]. Conway[19] has reported a β value of 0.15 volt for the hydrogen overvoltage of tin in deaerated 1.0M HCl solution at 20^oC, and Potter[64] has given a β value of 0.13 volt for hydrogen overvoltage of tin in deaerated 2.0N H_2SO_4 solution at 20^oC.

When compared with the data in the literature, the presently determined values of β are of the right order of

magnitude.

Figures II-4-1 and II-4-2 indicate that at lower reaction rates(lower current densities), activation polarization appears to be controlling for both anodic and cathodic reactions, because the linear portions of the potential-log(current density) plots are well defined. At higher reaction rates(higher current densities) the effect of concentration polarization becomes significant. It is also noted that the value of current density at which the concentration polarization effect starts to show up is always lower for the cathodic reaction than that for the anodic reaction. For instance, the polarization curves obtained at $25^{\circ}C$, in nitrogen saturated 1.0M HCl solution(as shown in Figure II-4-1) indicate that for the cathodic reaction the effect of concentration polarization starts to show up at a current density of 5 ma/cm^2 , for the anodic reaction the concentration polarization effect starts to show up only when the current density reaches a value of about 20 ma/cm^2.

Both Figures II-4-1 and II-4-2 show that changes in the HCl concentration of the corroding solutions produce no apparent variation in the corrosion current. This behaviour is consistent with the results obtained in Part One.

Theoretically the corrosion current should be directly proportional to the dissolution rate of a metal. In Part One it has been shown experimentally that the dissolution rates of tin are essentially independent of acid concentration over the range 0.10 to 4.0 M HCl.

Figures II-4-1 and II-4-2 also show that the values of the cathodic and anodic Tafel slopes, β_a and β_c , decrease with increasing HCl concentrations in the corroding solutions. This behaviour is consistent with theory which predicts that an increase in HCl concentration generally results in a decrease in the overvoltage of metals.

2. Cathodic Protection Tests

A series of preliminary cathodic protection tests were carried out at $25^\circ C$ by immersing stationary tin samples in air saturated 1.0M HCl solutions. At each test potential, the tin ion concentration in the corroding solution was determined after the test electrode had been immersed in the solution for three hours. The current corresponding to the applied potential was recorded after it became stabilized.

Figure II-4-3 shows these results in the form of a $[Sn]$-potential-protection current density plot. This Figure indicates clearly that the corrosion rate of tin in HCl solutions can be reduced sharply by means of an externally applied electric current.

In Figure II-4-3 the point labeled "from unprotected sample" represents the tin ion concentration obtained by immersing a stationary, unprotected(no external protection current was impressed on the specimen) sample in the corroding solution for three hours.

The main advantage of representing the experimental data according to the plot of Figure II-4-3 is that it reveals the

Figure II-4-3. Cathodic Protection Effects Related to
Protection Current Requirements for
Stationary Tin Sample in Air Saturated
HCl Solutions

optimum region of applied cathodic potential. From this
Figure, it becomes easy to select the most desirable potential
which, if imposed on the test electrode, will offer the most
effective protection and at the same time require the least
protection current. For instance, Figure II-4-3 shows that the
most desirable range of applied cathodic potential is -0.8 to
-0.95 volt for the conditions specified.

B. Results Obtained from Flow System

   1. Polarization Tests

      The cathodic and anodic polarization tests were
conducted at $30^{\circ}C$, in nitrogen, air, and oxygen saturated HCl
solutions, at the following three flow velocities; 2,650 cm./min.,
8,350 cm./min., and 14,300 cm./min. The results are presented
by the potential-log(current density) plots shown in Figures
II-4-4 and II-4-5. The general form and characteristics of
these polarization curves are internally consistent and are
consistent with those for stationary specimens.

      It can be observed that an increase in the fluid velocity,
or an increase in the oxygen concentration of the corroding
solutions lowers the values of the cathodic and anodic Tafel
slopes. It can also be observed that the values of corrosion
currents given by the intersections of these Tafel slopes
increase with an increase in the fluid velocity, or an
increase in the oxygen concentration in the corroding solutions.

      Figures II-4-6 and II-4-7 indicate that the corrosion
current (I_c) obtained from the intersections of the anodic
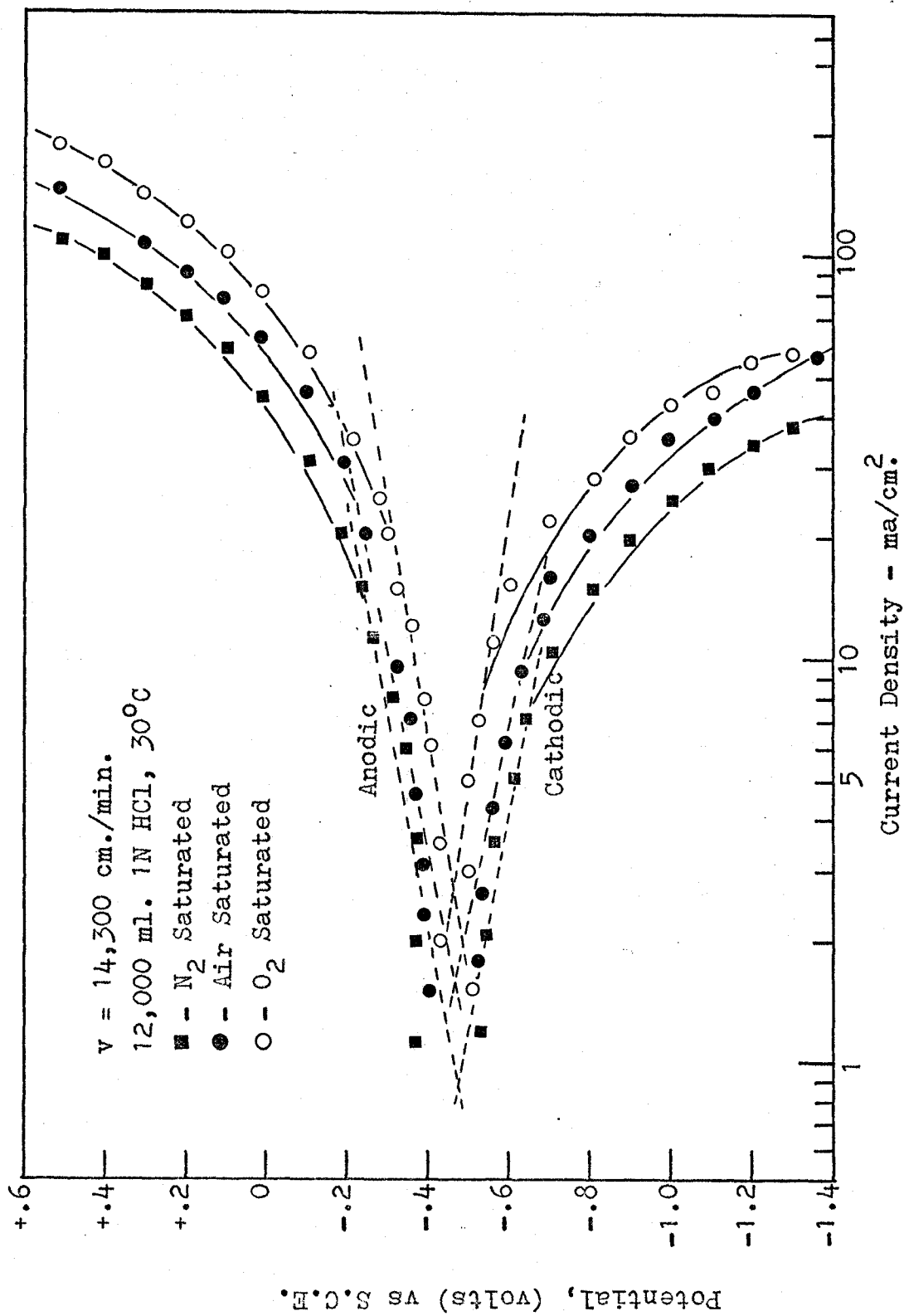
Figure II-4-4. Effect of Oxygen Concentration on Cathodic and Anodic
Polarization of Tin in a Flow System
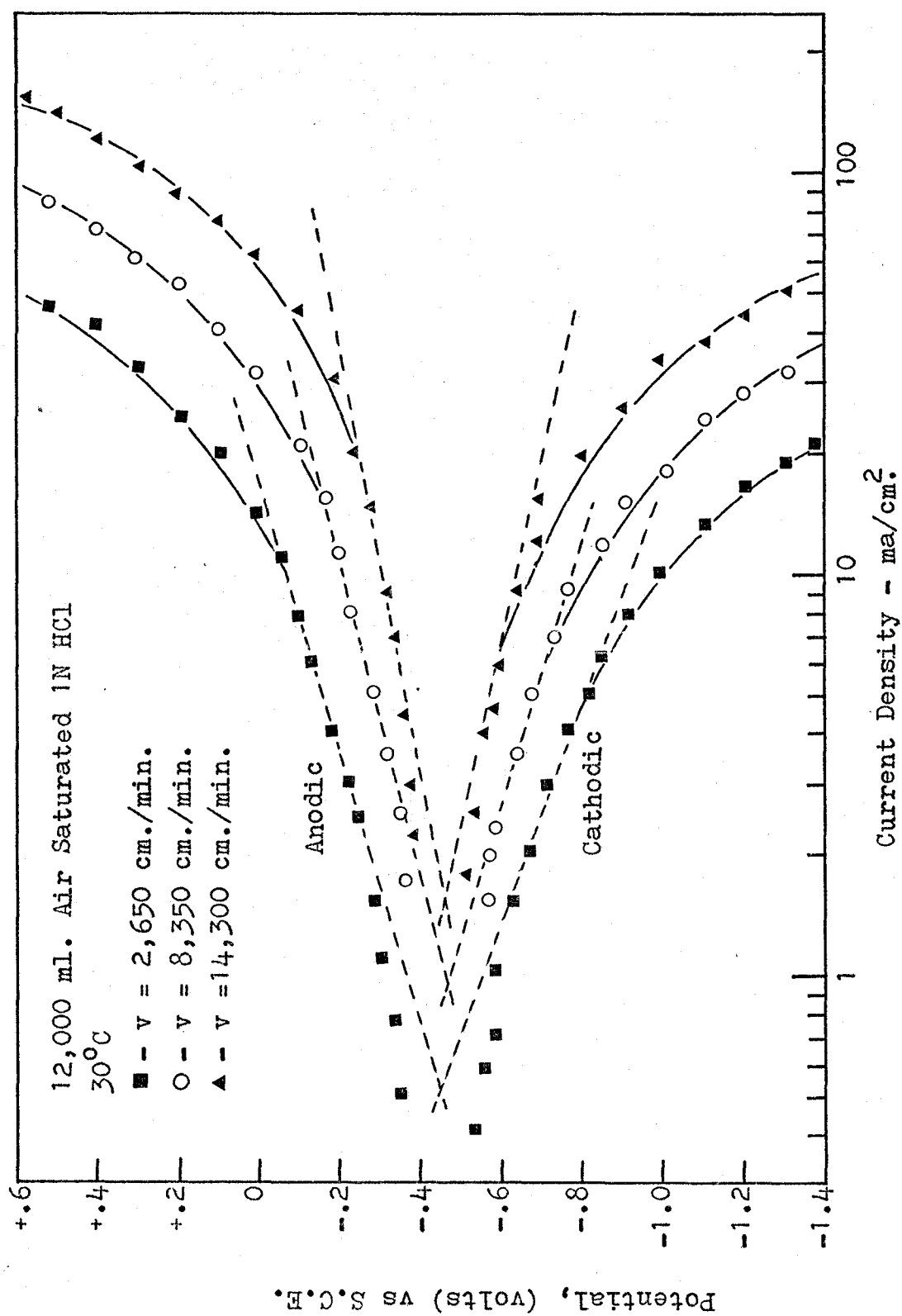
Figure II-4-5. Effect of Fluid Velocity on Cathodic and Anodic Polarization of Tin in a Flow System
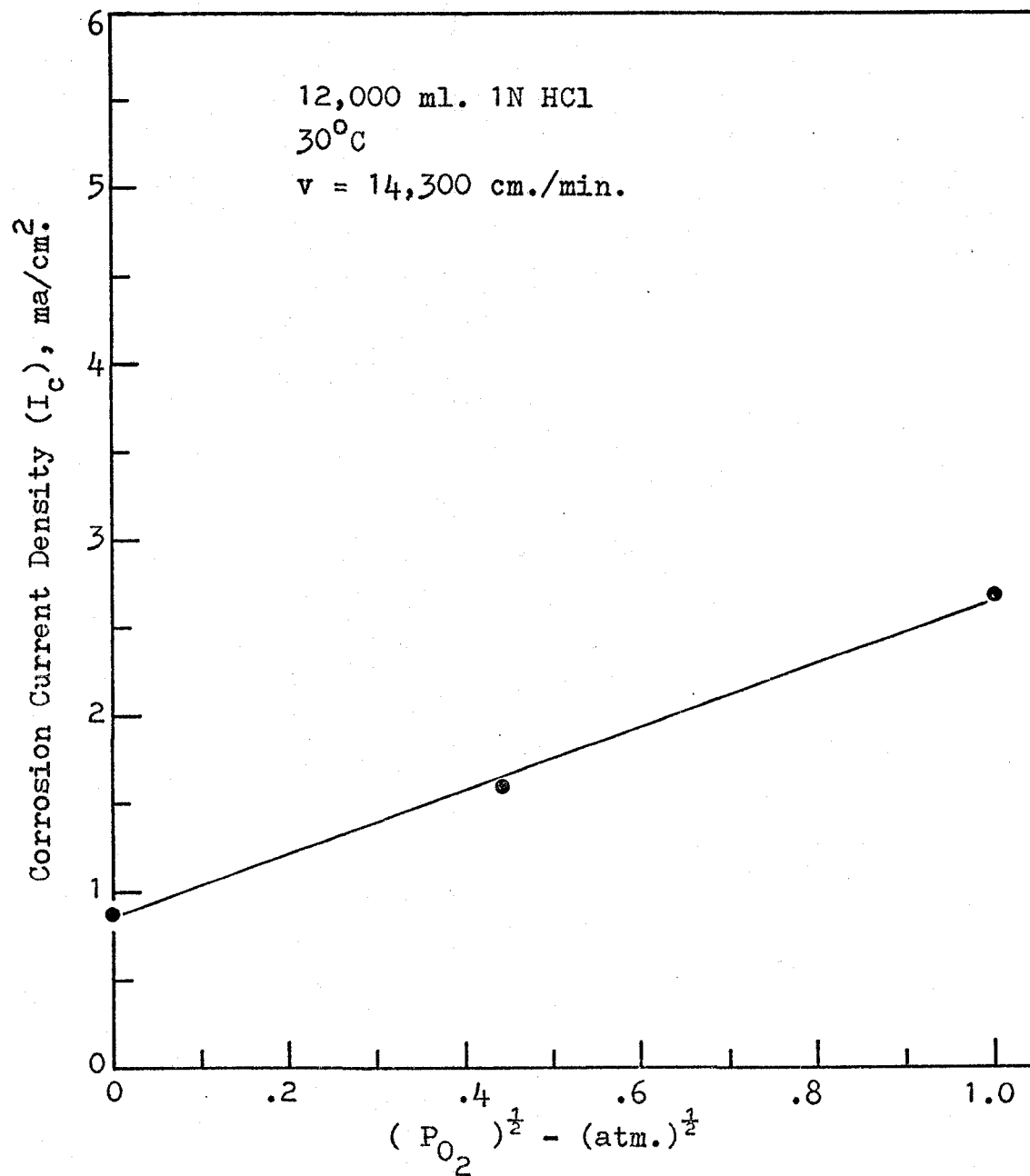
Figure II-4-6. Effect of Oxygen Concentration on
Corrosion Current for Tin in 1N
HCl Solutions

12,000 ml. Air Saturated 1N HCl
30°C
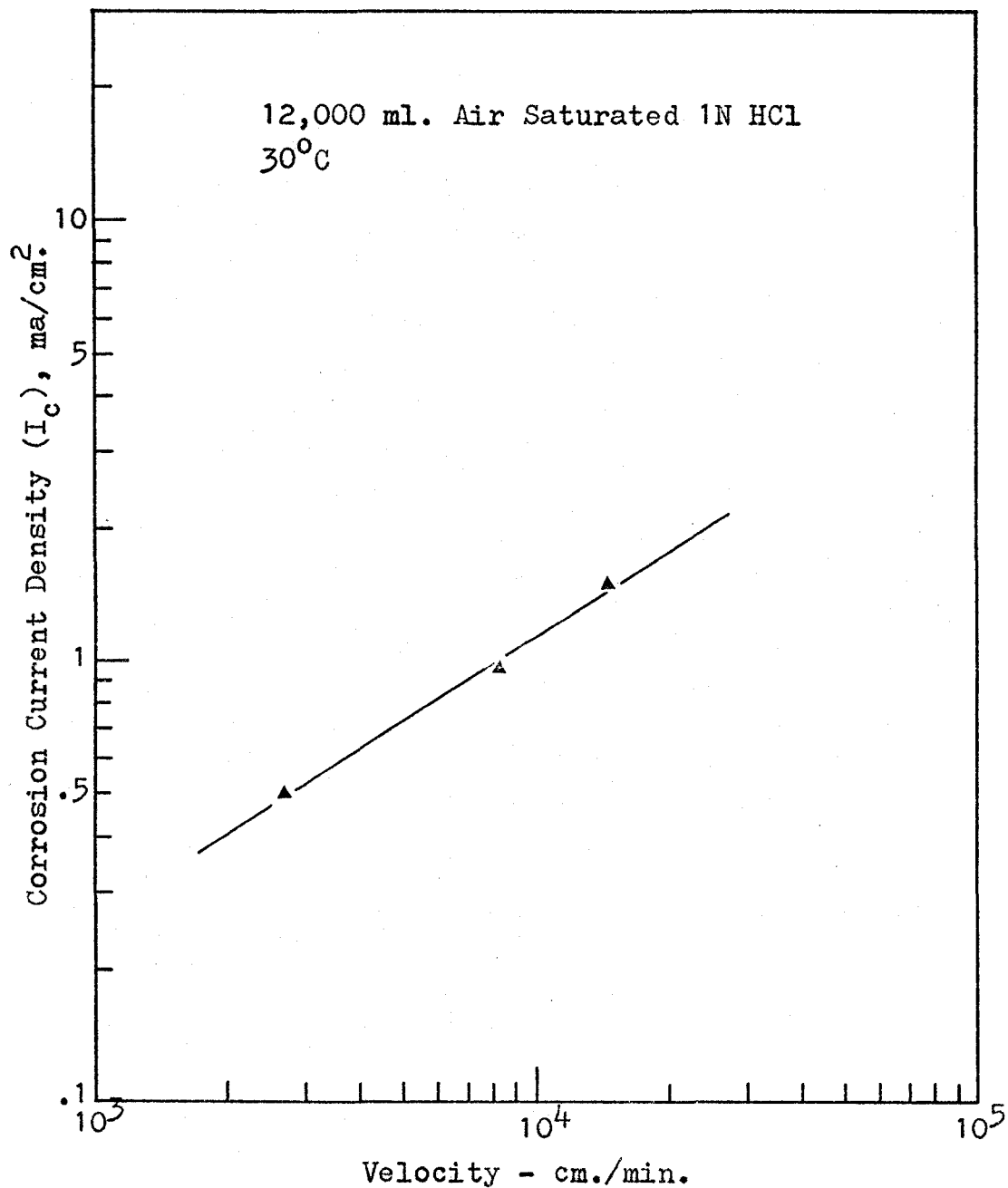
Figure II-4-7. Effect of Fluid Velocity on Corrosion
Current for Tin in Air Saturated 1N
HCl Solutions

and cathodic Tafel lines plotted in Figures II-4-4 and II-4-5, is proportional to the fluid velocity raised to the 0.64 power, and also directly proportional to the square root of the oxygen concentration in the corroding solutions. This behaviour is completely consistent with the results obtained in Part One, which showed similar proportionalities between the spontaneous dissolution rate of tin, fluid velocity, and oxygen concentration in the corroding solution.

2. Cathodic Protection Tests

The cathodic protection tests were carried out at $30^{\circ}C$, in nitrogen, air, and oxygen saturated HCl solutions, and at flow velocities of 2,650 and 14,300 cm./min. The results of these tests are given in Figures II-4-8 through II-4-11 which are presented in pairs. An explanation of Figures II-4-8A and II-4-8B is given here as an example to show how these Figures were constructed.

Figure II-4-8A shows nine plots, of tin ion concentration versus time, which represent the results of a series of nine testing runs conducted at $30^{\circ}C$, in air saturated 1.0M HCl solutions flowing at 14,300 cm./min. Each curve is the result of a separate run conducted by maintaining the test electrode (tin tube) at a pre-assigned potential. These plots clearly indicate that the tin tube received cathodic protection of different effectiveness at different potentials.

In the construction of Figure II-4-8B, the $[Sn]$-electrode potential-protection current density plot, tin ion
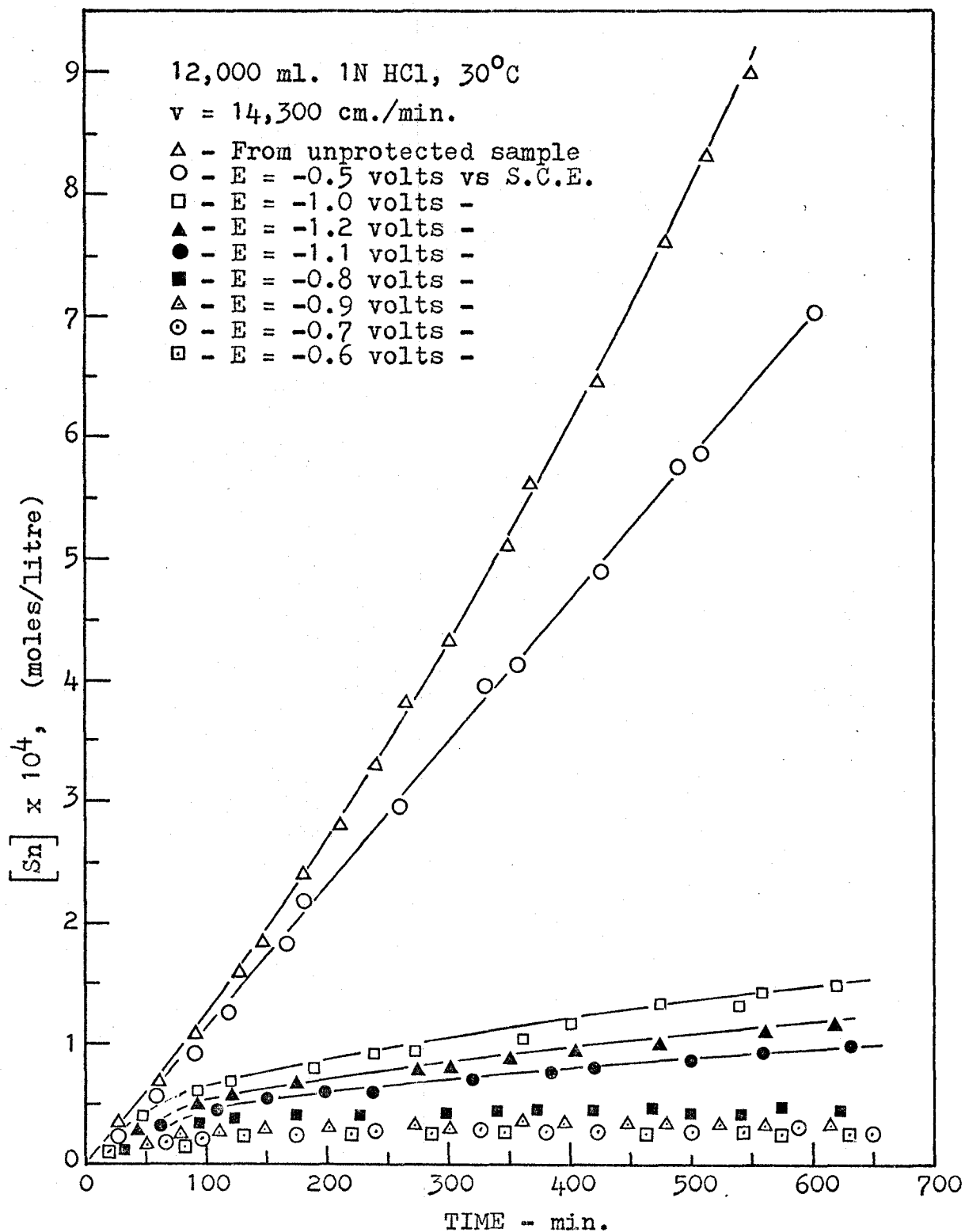
Figure II-4-8A. Cathodic Protection of Tin in High Velocity,
Air Saturated HCl Solutions
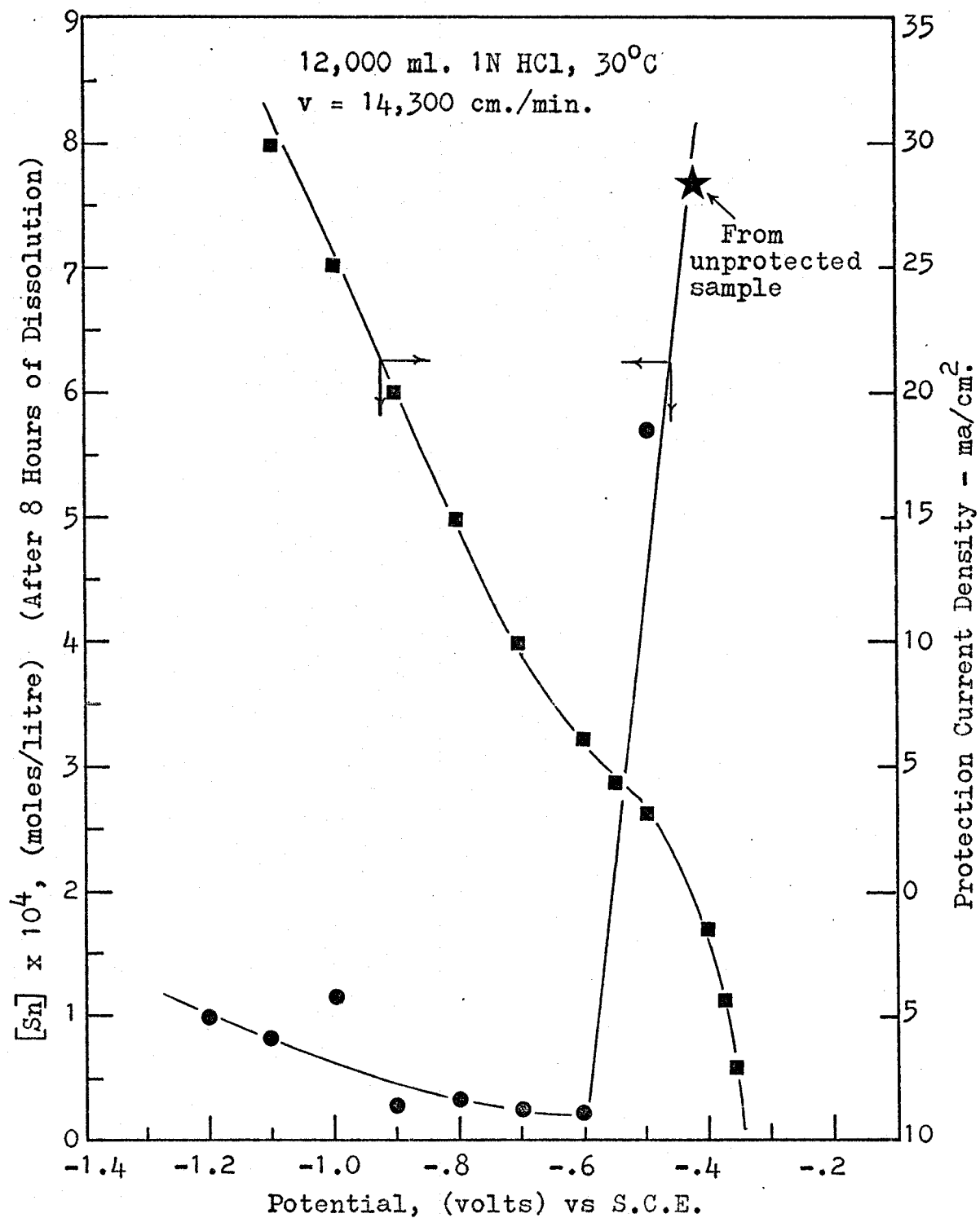
Figure II-4-8B. Cathodic Protection Effects Related
to Protection Current Requirements
for Tin in High Velocity, Air Saturated
HCl Solutions
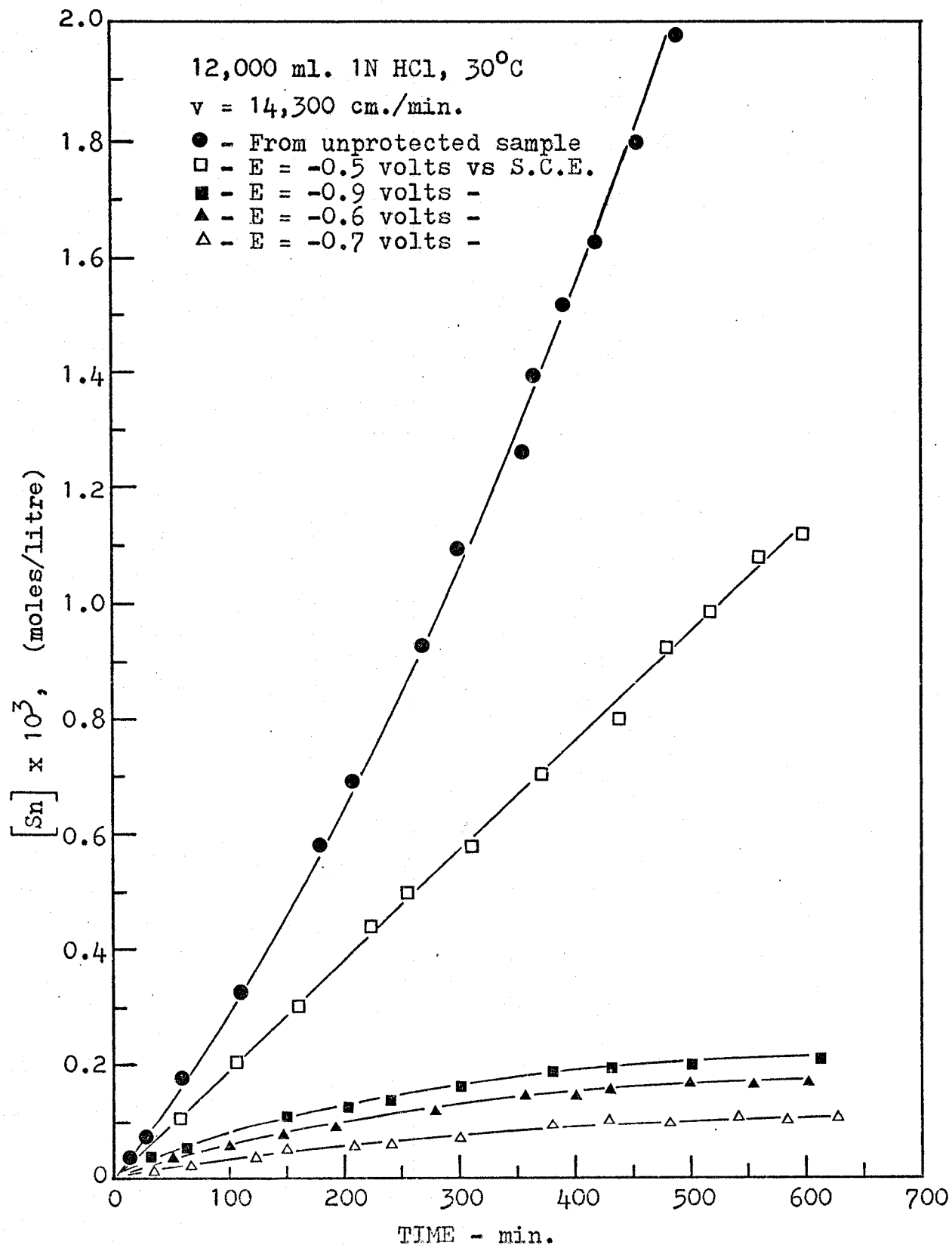
Figure II-4-9A. Cathodic Protection of Tin in High
Velocity, Oxygen Saturated HCl
Solutions
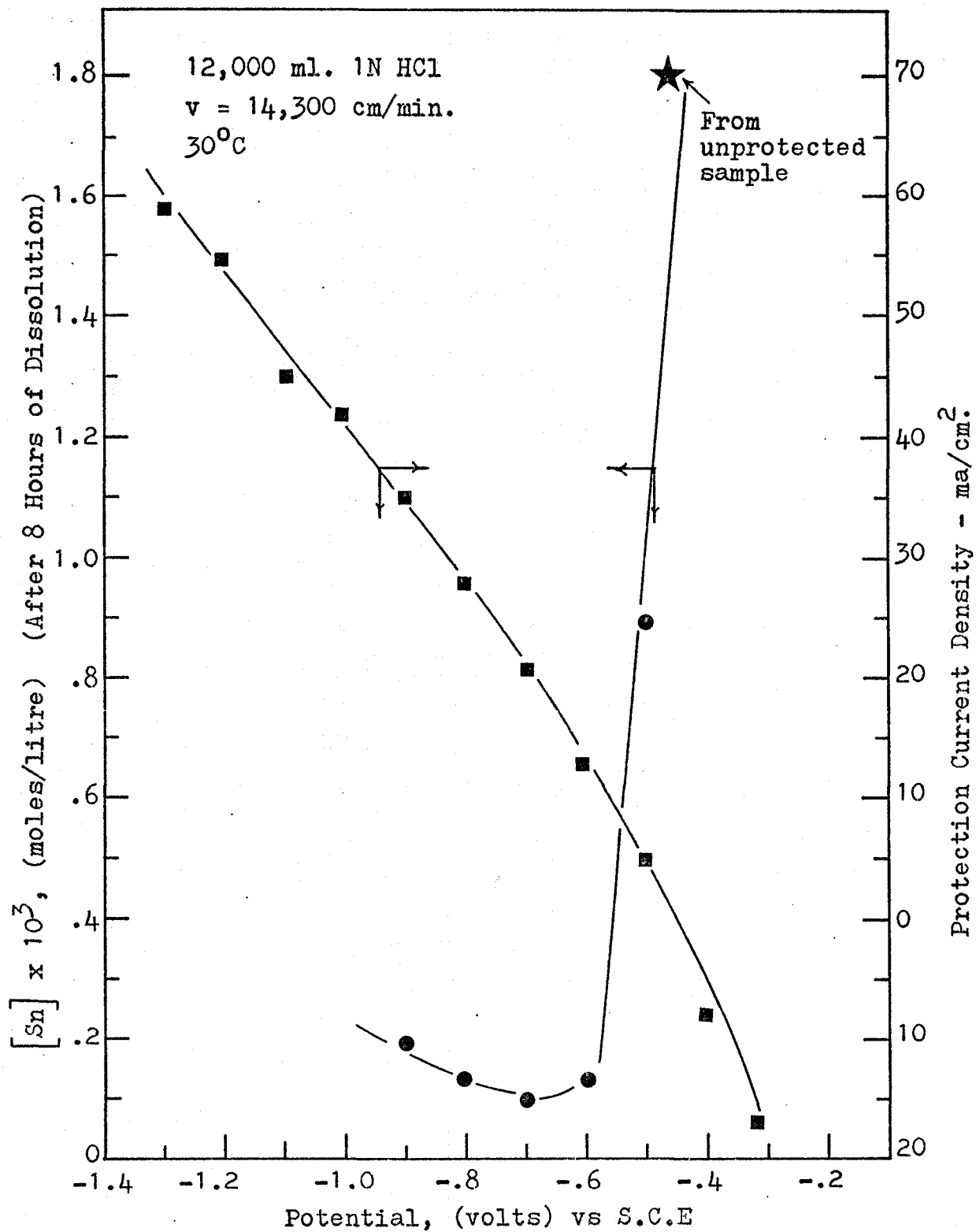
Figure II-4-9B. Cathodic Protection Effects Related to Protection Current Requirements for Tin in High Velocity, Oxygen Saturated HCl Solutions
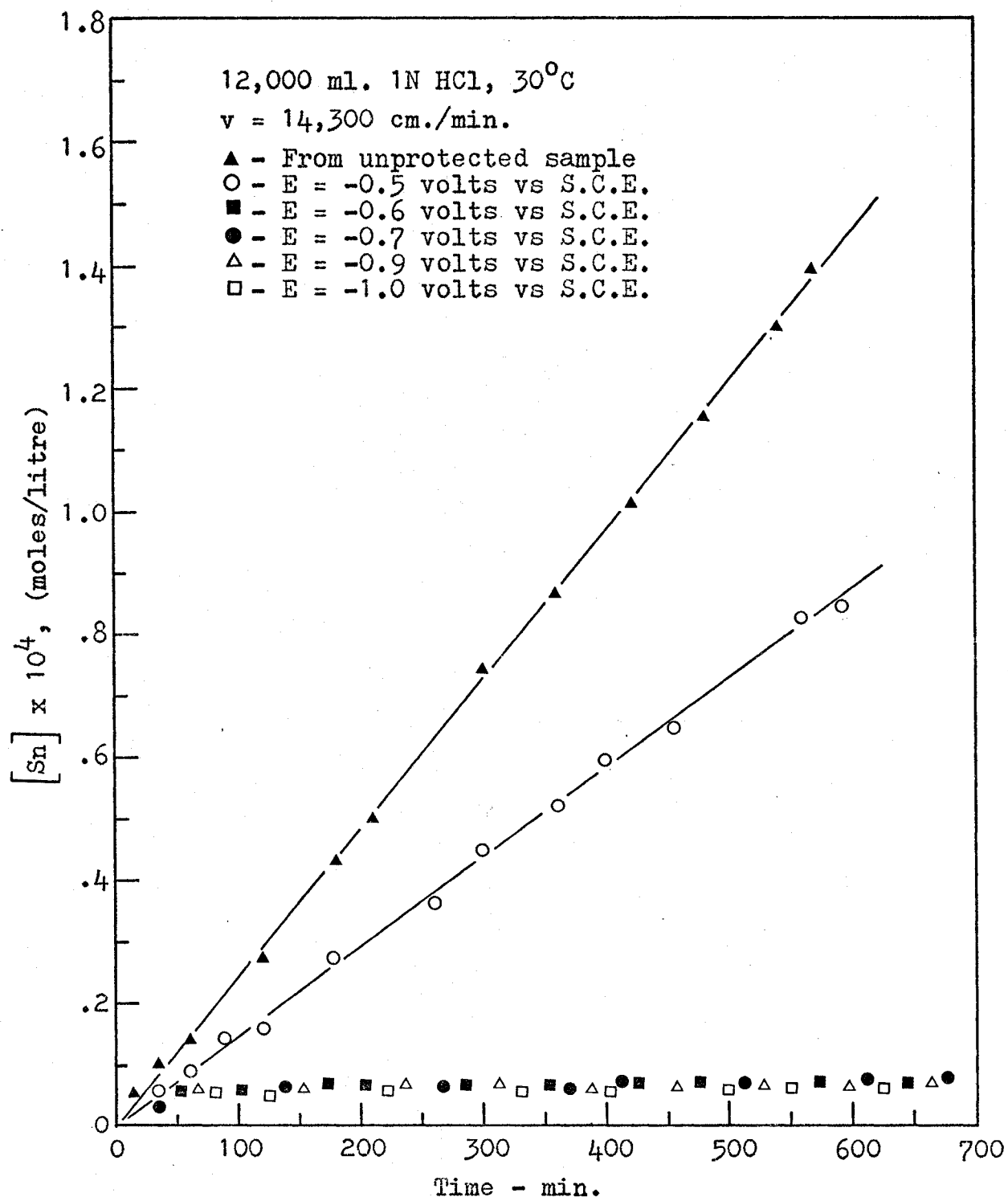
Figure II-4-10A. Cathodic Protection of Tin in High
Velocity, Nitrogen Saturated HCl
Solutions
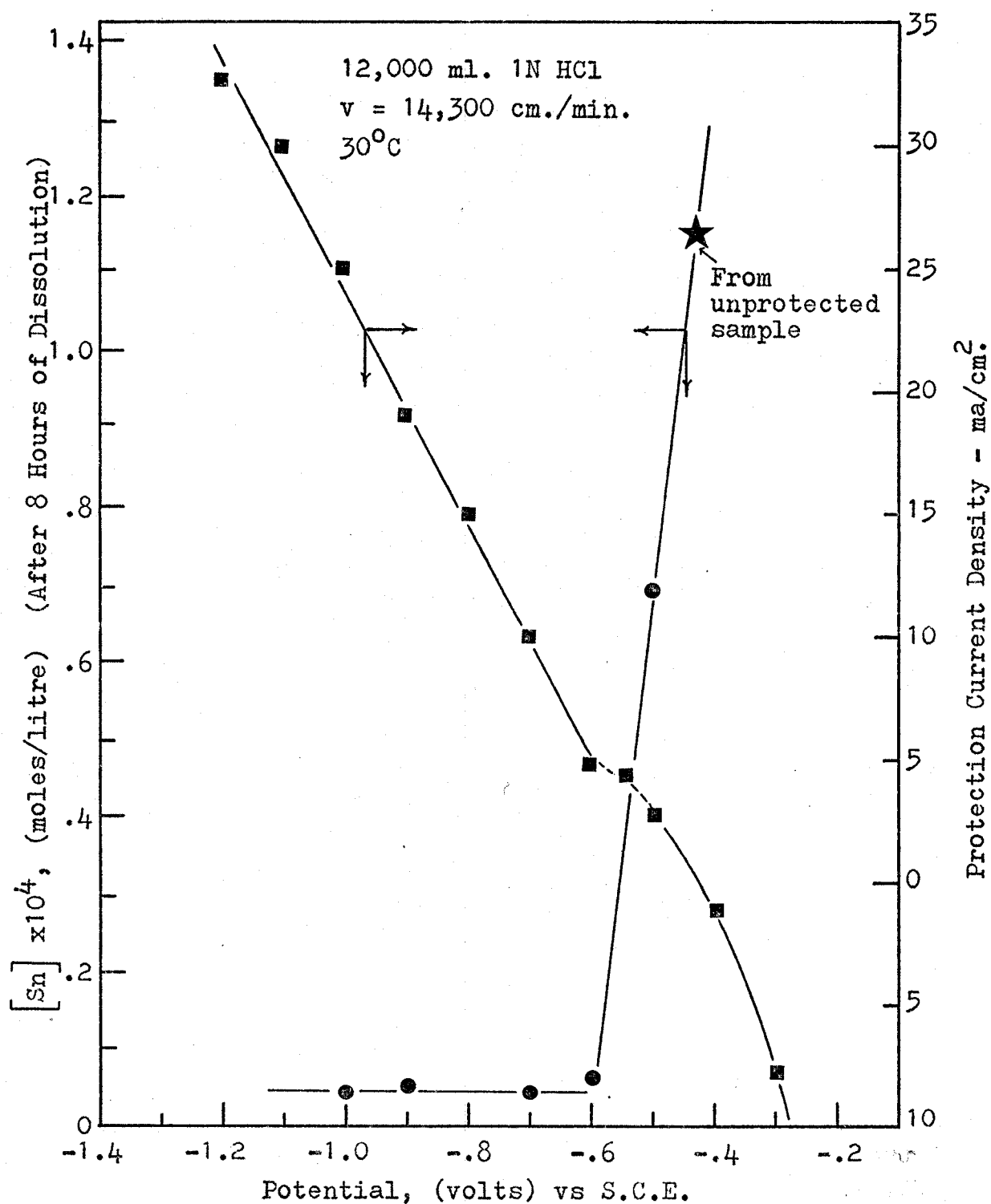
Figure II-4-10B. Cathodic Protection Effects Related to Protection Current Requirements for Tin in High Velocity, N_2 Saturated HCl Solutions
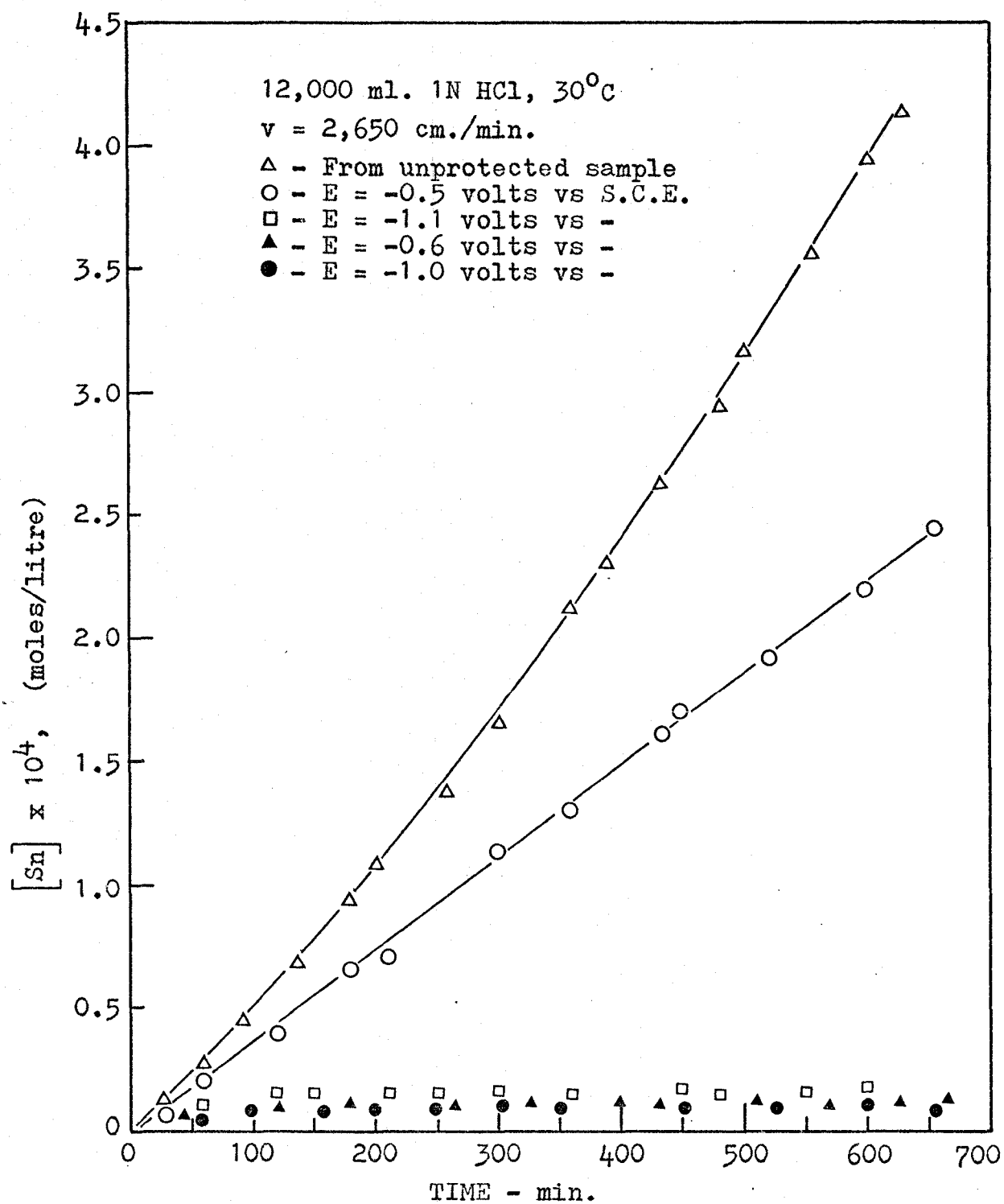
Figure II-4-11A. Cathodic Protection of Tin in Low
Velocity, Air Saturated HCl Solutions
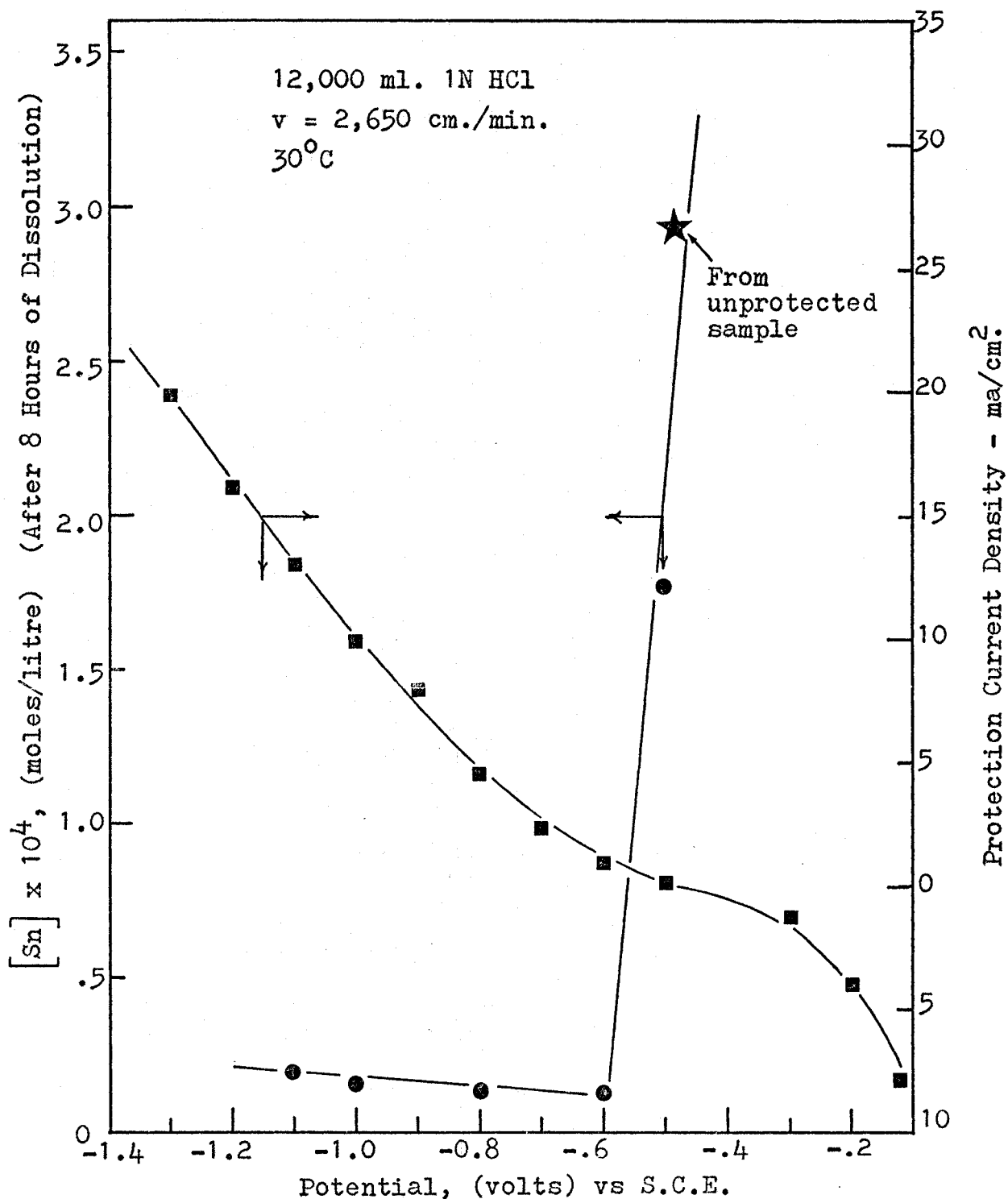
Figure II-4-11B. Cathodic Protection Effects Related
to Protection Current Requirements for
Tin in Low Velocity, Air Saturated
HCl Solutions

concentrations corresponding to 480 minutes of exposure to the corroding solution at the nine different electrode potentials were adopted from Figure II-4-8A. The time of 480 minutes at which the values of tin ion concentrations were taken is purely arbitrary. Figure II-4-8B will show the same general characteristics if tin ion concentrations are taken at any other exposure time. The protection current densities were calculated from the stabilized currents recorded at each potential.

The general form and shape of Figure II-4-8B is consistent with Figure II-4-3. The point labeled "from unprotected sample" in Figure II-4-8B represents the tin ion concentration obtained from a spontaneous dissolution run which was carried out under a condition of no external protection current being impressed on the specimen.

An examination of Figures II-4-8 to II-4-11 reveals the following characteristics:

(a) Cathodic protection of tin can be achieved in both aerated and deaerated hydrochloric acid solutions.

(b) The effect of overprotection appears in certain situations. For instance, Figure II-4-8B shows that, at $30^{\circ}C$, in air saturated 1.0N HCl solution, at a velocity of 14,300 cm./min., when the impressed protection current density exceeds 20 ma/cm^2., instead of the expected decrease in the dissolution rate of tin there may be just the reverse, an increase in the dissolution rate.

This damaging overprotection effect was probably caused by (1) excess alkalies generated at the metal surface. Since tin is one of the amphoteric metals, excess alkalies can damage tin by causing increased attack rather than reduction of corrosion, and (2) mechanical destruction of the protective film and disturbance of diffusional mass transfer layer by the liberation of hydrogen on the electrode. Because the overprotection effect was more significant in the aerated systems, the first reason appears to be the more damaging factor.

(c) The range of electrode potential within which the metal can be satisfactorily protected becomes narrower when the fluid velocity or the oxygen concentration of the corroding solution increases.

3. Protection Current Dependence on Temperature

The protection current dependence on temperature was studied over the range 25 to $55^{\circ}C$, in air saturated 1.0M HCl solutions, at three different velocities and two different potentials. The results presented in Figure II-4-12 show that the protection current density increases with increasing temperature of the corroding solutions at a rate of approximately .12 $ma/cm^2.-^{\circ}K$.

An increase in temperature of electrolyte is usually associated with a fall in hydrogen overvoltage, decrease in viscosity of the solution, and destruction of protective films. These are probably the factors which contribute to the increase
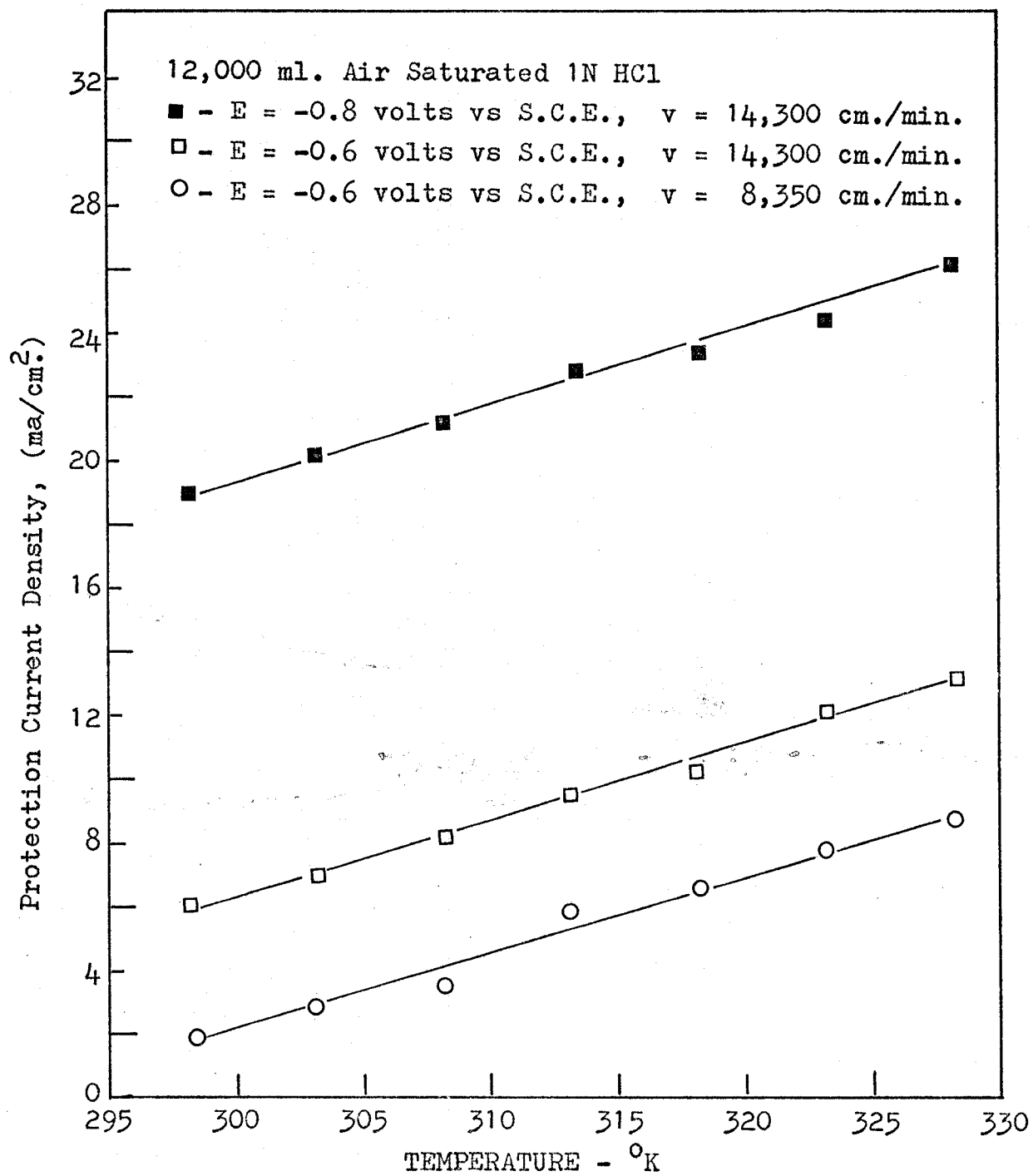
Figure II-4-12. Protection Current Dependence on
Temperature
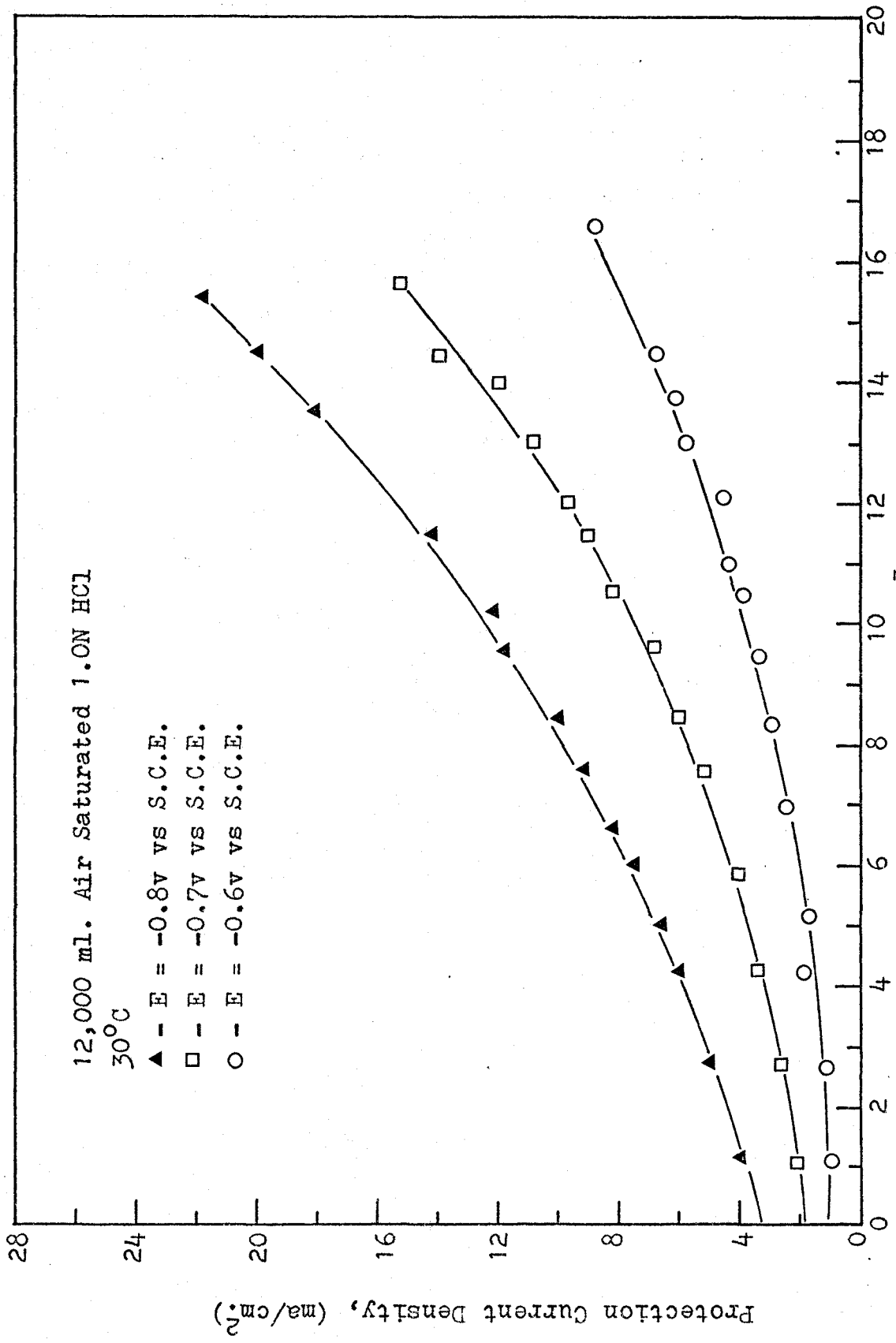
Figure II-4-13. Protection Current Dependence on Fluid Velocity

in the protection current.

4. Protection Current Dependence on Fluid Velocity

The investigation of the protection current dependence on fluid velocity was carried out at $30^{\circ}C$, in air saturated 1.0M HCl solutions, and at three different electrode potentials. The fluid velocity was varied over the range 1,150 to 14,300 cm./min.

The results, as shown in Figure II-4-13, indicate that the protection current increases with increasing flow velocity of corroding solution. This behaviour can be interpreted by the fact that a higher solution velocity can cause a higher degree of turbulence which reduces the thickness of the diffusional mass transfer layer through which the reactants must diffuse. Most previous investigators[59, 78] observed that in highly turbulent fluids substantially higher currents were required to protect metal surfaces.

5. Protection Current Dependence on Oxygen concentration

The protection current dependence on oxygen concentration in the corroding solution was studied at $30^{\circ}C$, in 1.0M HCl solutions, and at two different fluid velocities. The results are presented in Figure II-4-14.

It was found that the protection current increased continuously with increasing oxygen concentration in the acid solutions. The same effect was observed by most other corrosion researchers[59,83].

Because oxygen is a strong depolarizer, its accessibility
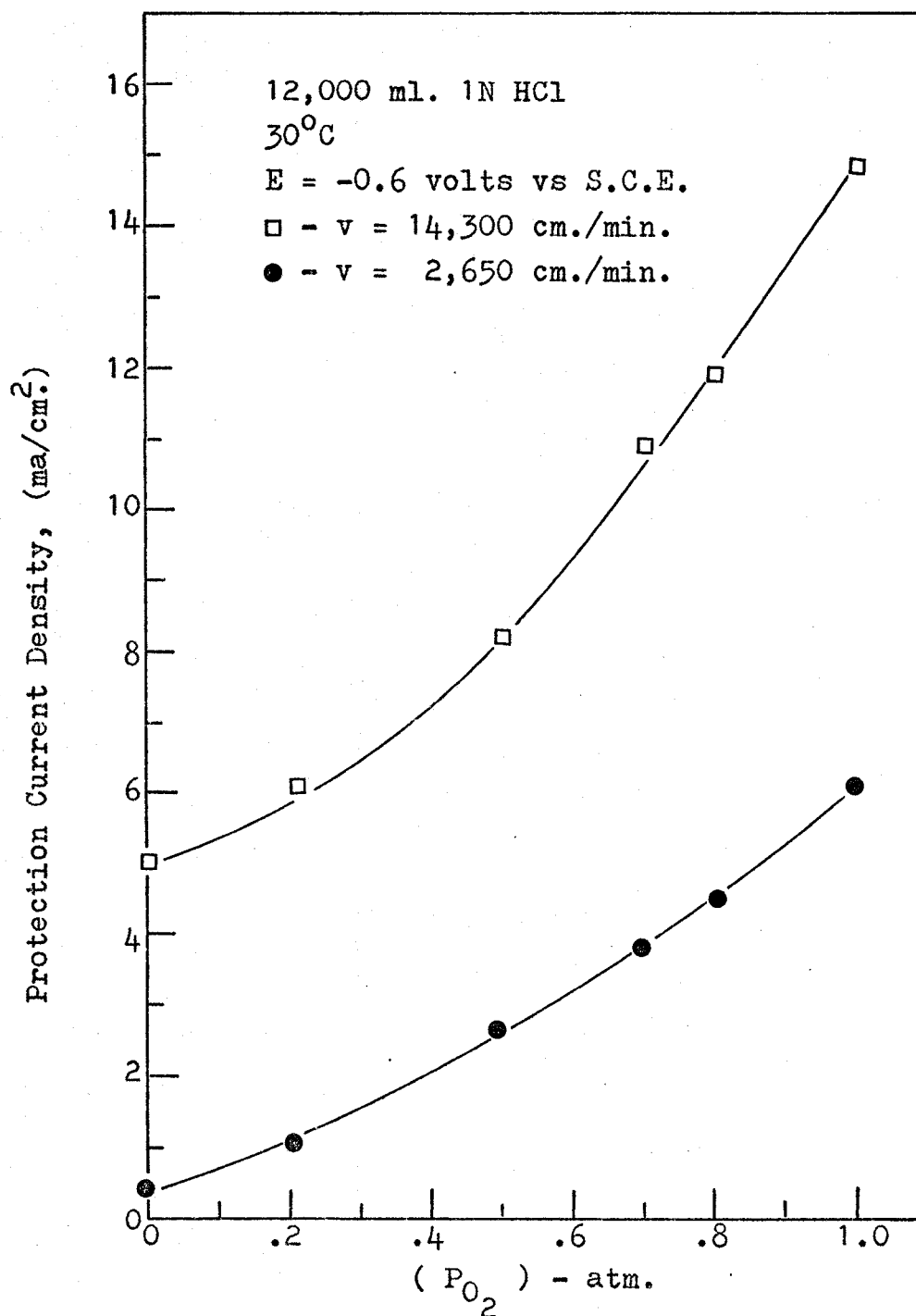
Figure II-4-14. Protection Current Dependence on Oxygen Concentration

12,000 ml. Air Saturated

$30^{\circ}C$, E = -0.6volts vs S.C.E.

● — v = 14,300 cm./min.

□ — v = 9,100 cm./min.

△ — v = 8,350 cm./min.

▲ — v = 2,650 cm./min.

Protection Current Density, $(ma/cm^2.)$

$[HCl]$ — molar
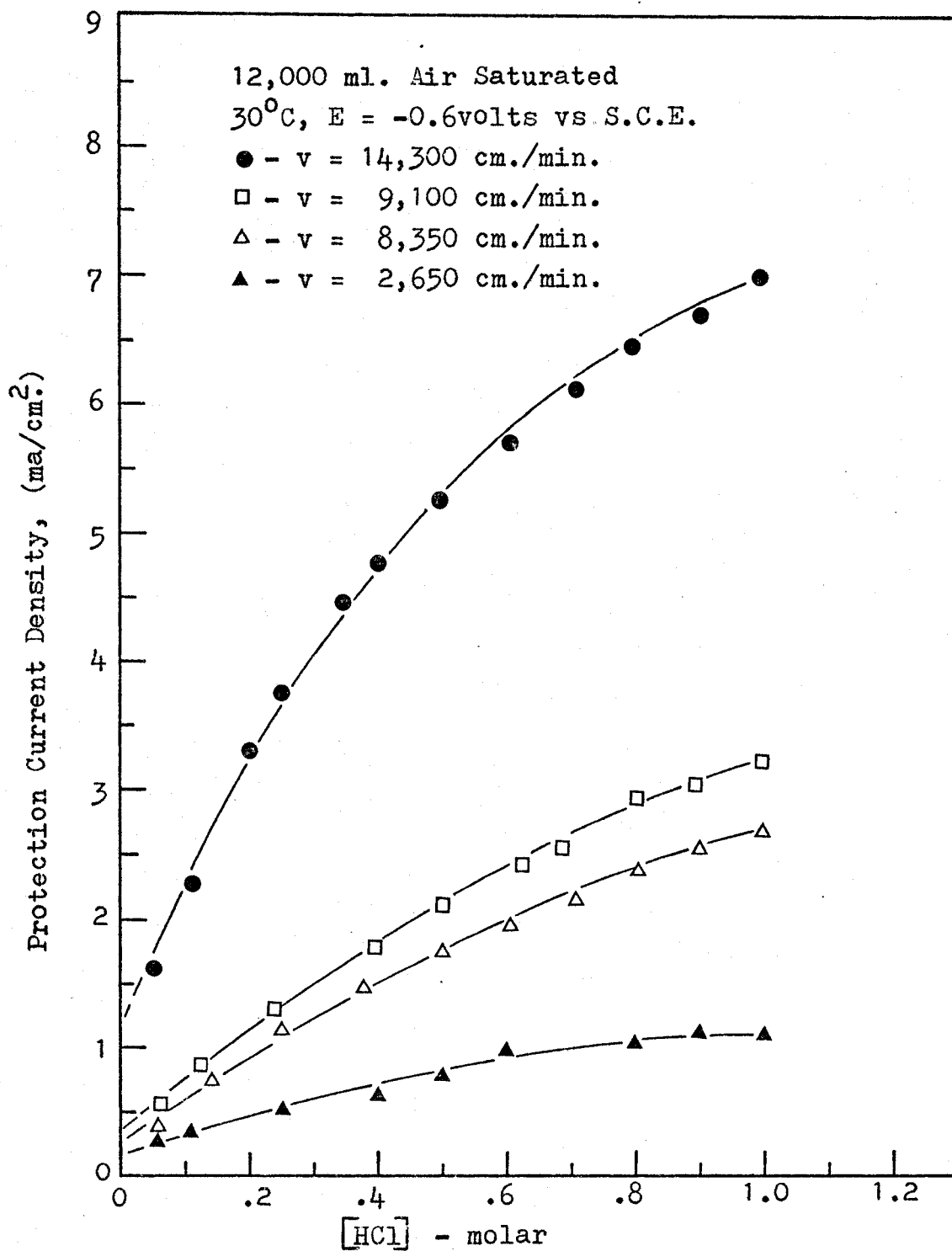
Figure II-4-15. Protection Current Dependence on HCl Concentration

to the metal surface is a very important factor in determining
the density of protection current.

6. Protection Current Dependence on HCl Concentration

The protection current dependence on the HCl
concentration in corroding solution was investigated at $30^{\circ}C$,
in air saturated solutions, and at four different fluid
velocities. The concentration of the HCl solutions was varied
over the range 0.0625 to 1.0M. The results, as plotted in
Figure II-4-15, illustrate that the protection current
initially increases sharply with increasing HCl concentrations.
The rate of increase of the protection current decreases when
the acid concentrations become higher than about 0.3M.

This phenomenon has been observed by many other
investigators[59,73,83]. They pointed out that in acid solutions
in which hydrogen ions can be discharged, the presence of high
concentrations of such acids generally creates a much larger
current requirement for protection of metal surfaces.

CHAPTER V

SUMMARY AND CONCLUSIONS

An examination of the experimental results obtained from the present polarization and cathodic protection studies revealed the following characteristics:

1. The polarization curves (potential-log(current density) plots) are of similar form. They are internally consistent. At lower reaction rates (lower current densities), activation polarization appears to be controlling for both anodic and cathodic reactions, because the linear portions (Tafel lines) of the potential-log(current density) plots are well defined. At higher reaction rates (higher current densities) the effect of concentration polarization becomes significant. It is also noted that the value of current density at which the concentration polarization effects starts to show up is always lower for the cathodic reaction than that for the anodic reaction. For instance, the polarization curves obtained at $30^{\circ}C$, in air saturated 1.0M HCl solution flowing at 14,300 cm./min.(as shown in Figure II-4-5) indicate that for the cathodic reactions the effect of concentration polarization starts to show up at a current density of about 9 ma/cm^2; for the anodic reaction the concentration polarization effect starts to show up only when the current density reaches a value of 20 ma/cm^2.

148

2. The values of Tafel constants, β_a's and β_c's , (0.12 - 0.32 volts as given by the slopes of the Tafel lines) are of the right order of magnitude when compared with the data reported by other investigators[19,64]. The present results show that increasing HCl concentrations, flow velocities, and oxygen concentrations of the corroding solutions lower the values of Tafel constants. This behaviour is an indication that the activation overvoltages for both anodic and cathodic reactions occurring at the tin electrode decrease with increasing HCl concentrations, flow velocities, and oxygen concentrations of the corroding solutions.

3. The corrosion current I_c, as indicated by the intersections of the anodic and cathodic Tafel lines, is found to be proportional to the fluid velocity raised to the 0.64 power, and also directly proportional to the square root of the oxygen concentration; but essentially independent of the HCl concentration. This behaviour is consistent with the results obtained in Part One, which show similar proportionalities between the spontaneous dissolution rates of tin, HCl concentrations, flow velocities, and oxygen concentrations of the corroding solutions.

4. The cathodic protection of tin can be accomplished in both aerated and deaerated hydrochloric acid solutions. To achieve the most effective cathodic protection (maximum protective effect with lowest protection current), optimum regions of applied cathodic potentials under different

conditions have been determined; for the stationary system, the most effective range of applied potential is -0.8 to -0.95 volt, for the flow system the effective range is generally -0.6 to -0.9 volt. The range of applied cathodic potentials within which tin can be satisfactorily protected becomes narrower when the flow velocity or oxygen concentration of the corroding solution increases.

5. Negative effects of overprotection were observed in the flow system with air and oxygen saturated solutions. This damaging overprotection effect was probably caused by (1) excess alkalies generated at the metal surface, and (2) mechanical destruction of the protective film and disturbance of the diffusion layer by the liberation of hydrogen on the cathode. Since tin is one of the amphoteric metals, excess alkalies can damage tin by causing increased attack rather than reduction of corrosion. Because the overprotection effect was more significant in the aerated systems, the first reason appears to be the more damaging factor.

6. The protection current density required to protect the tin tube increases with increasing temperature at a rate of approximately 0.12 ma/cm^2-$^{\circ}$K, and it also increases with increasing hydrochloric acid concentration, flow velocity, and oxygen concentration of the corroding solution.

APPENDIX 1

CALIBRATION OF ROTAMETERS

Two rotameters were used to measure the full range of flow rates of corroding solutions.

1. 12-1000 Brooks Glass Tube Rotameter(Tube:R-12M-25-5)

    Flow capacity: 1.5 - 15 USGPM

    Accuracy: $\pm$ 2% of maximum flow

    Tube: Borosilicate glass

    Packing: Teflon

    Float: Hasteloy B

2. 10-1000 Brooks Glass Tube Rotameter(Tube:R-10M-25-1)

    Flow capacity: .4 - 4 USGPM

    Accuracy: $\pm$ 2% of maximum flow

    Tube: Borosilicate glass

    Packing: Teflon

    Float   Hasteloy B

The rotameters were calibrated by maintaining a particular reading and measuring the volume of effluent collected in a known time interval. The calibration curves are shown in Figures A-1-1 and A-1-2.

151
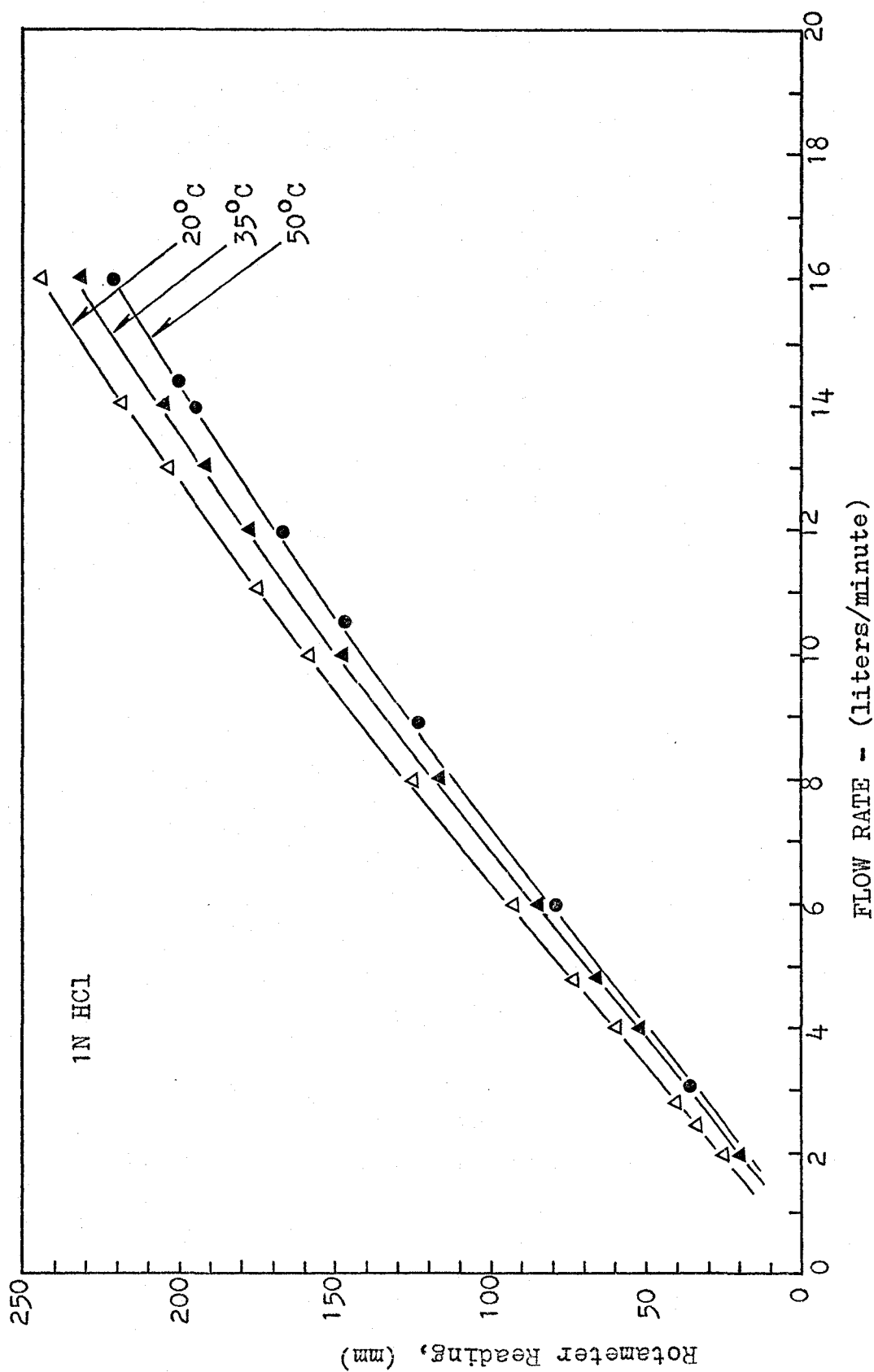
Figure A-1-1. Calibration Curves for Rotameter No.10-1000(Tube:R-10M-25-1)

FLOW RATE - (liters/minute)

Rotameter Reading, (mm)

1N HCl

20°C
35°C
50°C
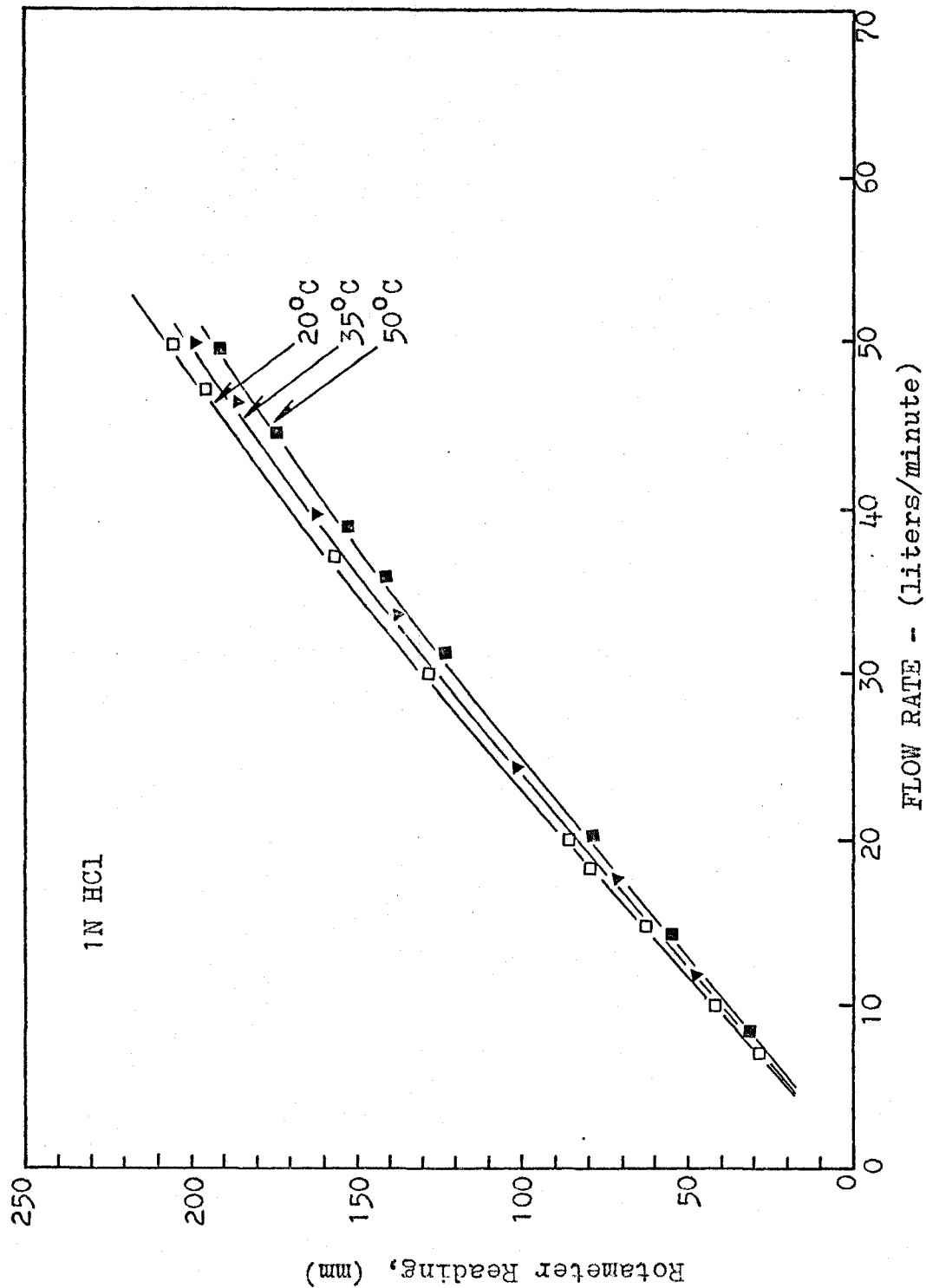
Figure A-1-2. Calibration Curve for Rotameter No.12-1000(Tube:R-12M-25-5)

APPENDIX 2

ANALYTICAL METHODS AND CALIBRATION

A. Instrumentation

A Jarrell-Ash Model 82-526 Maximum Versatility Atomic Absorption Spectrophotometer was used for the analysis of tin ion concentrations in the corroding solutions. This instrument features a 500 mm focal length Ebert Mount Monochrometer with two interchangeable gratings with 1,180 grooves/mm. A choice of three burners is available; a total consumption Hetco burner, a 5 cm. and a 10 cm. slot laminar flow burner. The instrument can simultaneously accommodate two fuels and two oxidants.

B. Analytical Methods

The analysis of tin by the Atomic Absorption Spectrophotometric method has been developed by Allan[5], Agazzi[2], Amas and Willis[6], Capacho-Delgado and Manning[17], Gatehouse and Willis[30], Gibson and Grossman[32], and Vollmer[86].

C. Preparation of Standard Solution

A stock of 2×10^{-3}M tin ion solution was made by dissolving Analar Grade tin bars in 1M HCl. Standard tin ion solutions were prepared by diluting aliquot samples of the stock solution with 1M HCl.

A new calibration curve was drawn each time a series of samples was to be analyzed. The calibration curves were made

154

by plotting tin ion concentration against absorbance on linear scales. A typical calibration curve is shown in Figure A-2-1.

D. Analytical Conditions and Instrument Settings

The 10 cm. laminar flow burner was used in this analytical work. The fuel and oxidant used were hydrogen and air, respectively.

Following are the instrument settings which were used in the analysis of tin:

Wave length:	2246 Å
Hollow cathode current:	12 ma
High voltage:	0.65 kv
H_2 tank regulator pressure:	20 psi
Air tank regulator pressure:	30 psi
H_2 flow:	50 SCFH
Air flow:	17.5 SCFH
Burner height:	10 mm
Damping:	minimum
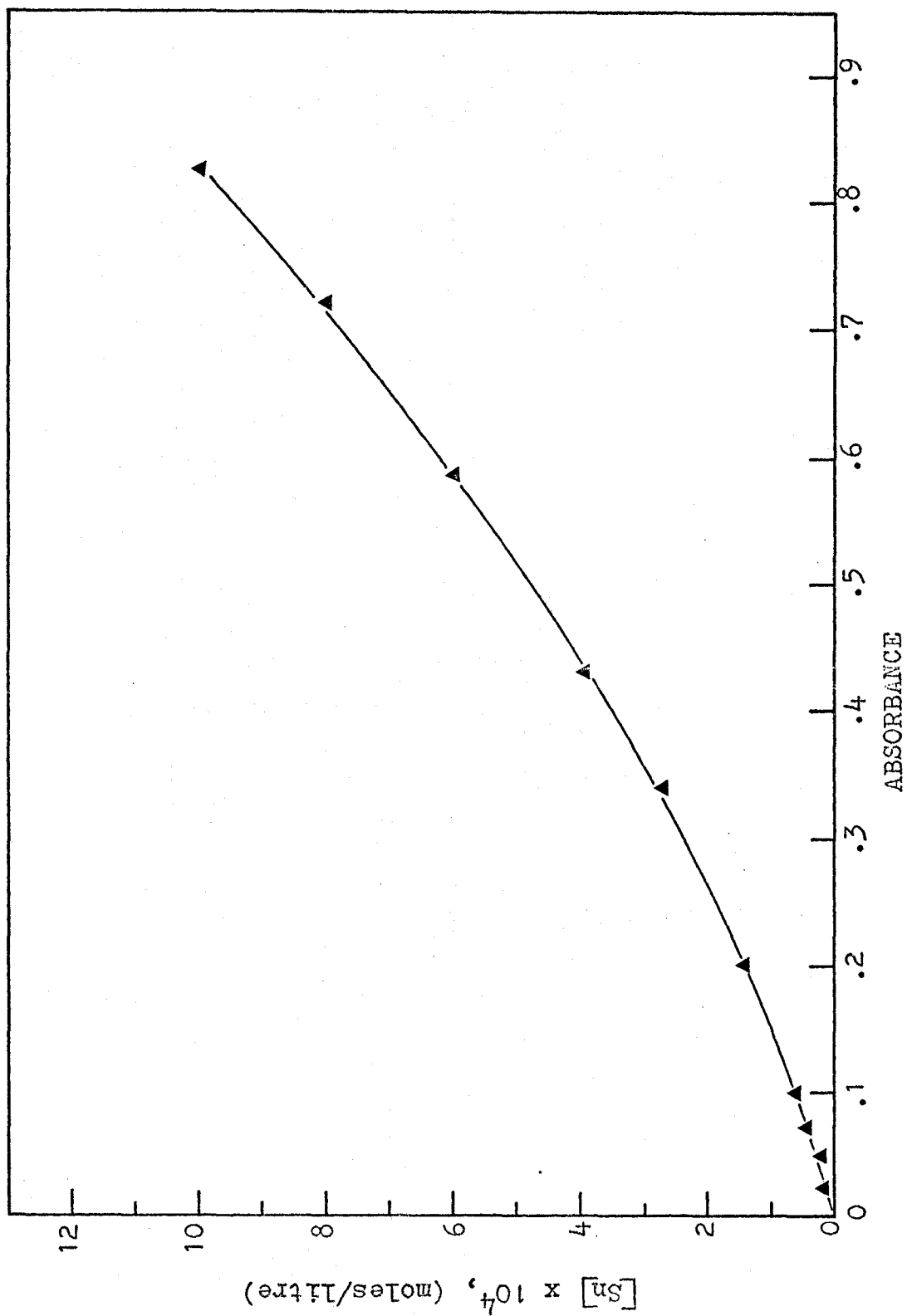
Figure A-2-1. A Typical Calibration Curve for Atomic Absorption Analysis

APPENDIX 3

CALCULATIONS OF RATE CONSTANTS FOR TIN DISSOLUTION

The following equations:

$$k_1^o = (\frac{1}{A}\frac{dSn}{dt})_1 (v)^{-.67}(d)^{.05}(L)^{.30} e^{\frac{4250}{RT}}$$

$$k_2^o = (\frac{1}{A}\frac{dSn}{dt})_2 (v)^{-.59}(d)^{.11}(L)^{.33}(P_{O_2})^{-.5} e^{\frac{5450}{RT}}$$

$$k_3^o = (\frac{1}{A}\frac{dSn}{dt})_3 (v)^{-.61}(d)^{.10}(L)^{.32}(P_{O_2})^{-.5}[Sn]^{-.5} e^{\frac{5800}{RT}}$$

have been used for the determination of k_1^o, k_2^o, and k_3^o to give the average values of these constants, with an average deviation of $\pm$ 4 per cent as shown in Tables A-3-1, A-3-2, and A-3-3.

157

TABLE A-3-1

Evaluation of Velocity Constant

$(k_1^0$ for hydrogen evolution)

$\left(\dfrac{1}{A}\dfrac{dSn}{dt}\right)_1$ $\left(\dfrac{moles}{cm^2\text{-}min}\right)$	v $\left(\dfrac{cm.}{min.}\right)$	d (cm.)	L (cm.)	T (°K)	k_1^0
3.31×10^{-8}	4,700	1.905	7.620	298.15	3.27×10^{-7}
3.97 –	5,730	1.270	10.160	303.15	3.30 –
5.81 –	10,280	– –	– –	– –	3.55 –
2.11 –	2,350	1.902	7.620	298.15	3.42 –
1.35 –	1,175	– –	– –	– –	3.31 –
7.20 –	14,300	1.270	10.160	303.15	3.57 –
7.93 –	16,600	– –	– –	– –	3.37 –
8.89 –	– –	– –	– –	308.15	3.36 –
9.93 –	– –	– –	– –	313.15	3.29 –
1.23×10^{-7}	– –	– –	– –	323.15	3.35 –
7.21×10^{-8}	– –	– –	13.970	303.15	3.37 –
7.42 –	– –	– –	12.700	– – – –	3.39 –
8.25 –	– –	– –	8.900	– –	3.45 –
9.76 –	– –	– –	5.075	– –	3.38 –
4.03 –	5,730	0.953	10.160	– –	3.17 –
3.93 –	– –	1.588	– –	– –	3.43 –
3.84 –	– –	2.540	– –	– –	3.32 –
3.22 –	4,150	1.270	– –	– –	3.19 –
4.87 –	8,500	1.905	7.620	298.15	3.42 –
5.51 –	10,280	– –	– –	– –	3.47 –

Average = 3.37×10^{-7}

TABLE A-3-2

Evaluation of Velocity Constant

(k_2^o for O_2 depolarization)

$(\frac{1}{A} \frac{dSn}{dt})_2$ $(\frac{moles}{cm.^2-min})$	v $(\frac{cm.}{min.})$	d (cm.)	L (cm.)	P_{O_2} (atm.)	T (^oK)	k_2^o
1.10×10^{-7}	4,700	1.905	7.62	0.21	298.15	2.95×10^{-5}
1.37 –	5,730	1.270	10.16	– –	303.15	3.20 –
1.95 –	10,280	– –	– –	– –	– –	3.04 –
7.29×10^{-8}	2,350	1.902	7.62	– –	298.15	3.11 –
4.80 –	1,175	– –	– –	– –	– –	3.15 –
2.38×10^{-7}	14,300	1.270	10.16	– –	303.15	3.10 –
2.61 –	16,600	– –	– –	– –	– –	2.97 –
3.01 –	– –	– –	– –	– –	308.15	3.14 –
3.47 –	– –	– –	– –	– –	313.15	2.98 –
4.56 –	– –	– –	– –	– –	323.15	3.01 –
2.35 –	– –	– –	13.97	– –	303.15	3.09 –
2.42 –	– –	– –	12.70	– –	– –	3.12 –
2.72 –	– –	– –	8.90	– –	– –	2.96 –
3.25 –	– –	– –	5.08	– –	– –	3.13 –
1.42 –	5,730	0.953	10.16	– –	– –	3.00 –
1.35 –	– –	1.588	– –	– –	– –	2.95 –
1.28 –	– –	2.540	– –	– –	– –	2.97 –
1.75 –	4,150	1.270	– –	0.50	– –	3.06 –
2.07 –	– –	– –	– –	0.70	– –	2.90 –
2.47 –	– –	– –	– –	1.00	– –	3.15 –

Average = 3.05×10^{-5}

TABLE A-3-3

Evaluation of Velocity Constant

(k_3^o for autocatalytic reaction)

$(\frac{1}{A}\frac{dSn}{dt})_3$ $(\frac{moles}{cm^2-min})$	v $(\frac{cm.}{min.})$	d (cm.)	L (cm.)	P_{O_2} (atm.)	[Sn] $(\frac{moles}{litre})$	T (°K)	k_3^o
2.15x10⁻⁷	16,600	1.905	7.62	0.21	3.20x10⁻⁴	298.15	6.40x10⁻⁴
2.40 -	- -	- -	- -	- -	4.00 -	- -	6.35 -
2.72 -	- -	- -	- -	- -	5.15 -	- -	6.51 -
3.18 -	- -	- -	- -	- -	7.10 -	- -	6.55 -
3.61 -	- -	- -	- -	- -	9.20 -	- -	6.30 -
1.18 -	8,500	- -	- -	- -	2.00 -	- -	6.22 -
1.70 -	- -	- -	- -	- -	4.45 -	- -	6.14 -
2.20 -	- -	- -	- -	- -	7.20 -	- -	6.65 -
7.80x10⁻⁸	4,700	- -	- -	- -	1.35 -	- -	6.37 -
1.15x10⁻⁷	- -	- -	- -	- -	2.95 -	- -	6.70 -
1.41 -	- -	- -	- -	- -	4.75 -	- -	6.20 -
1.55 -	- -	- -	- -	- -	- -	303.15	6.63 -
3.90 -	1,175	1.270	10.16	- -	1.70 -	- -	6.42 -
6.02 -	2,350	- -	- -	- -	- -	- -	6.46 -
1.06x10⁻⁶	5,700	- -	- -	- -	- -	- -	6.61 -
1.55 -	10,280	- -	- -	- -	- -	- -	6.45 -
4.10x10⁻⁷	15,800	- -	- -	- -	1.20x10⁻³	- -	6.57 -
6.20 -	- -	- -	- -	0.50	- -	- -	6.27 -
8.51 -	- -	- -	- -	1.00	- -	- -	6.39 -
4.35 -	16,600	0.953	- -	0.21	- -	- -	6.30 -
4.05 -	- -	1.588	- -	- -	- -	- -	6.55 -
3.85 -	- -	2.540	- -	- -	- -	- -	6.63 -
3.25 -	- -	1.270	5.08	- -	6.80x10⁻⁴	- -	6.71 -
2.68 -	- -	- -	8.90	- -	- -	- -	6.14 -
2.41 -	- -	- -	12.70	- -	- -	- -	6.65 -
2.32 -	- -	- -	13.97	- -	- -	- -	6.55 -

Average = 6.45x10⁻⁴

APPENDIX 4

An Example of the Application of the Empirical Rate Equation

The application of the empirical rate equation to the prediction of changes in tin ion concentration in corroding solutions may be illustrated by considering the following dissolution conditions:

Solution volume = 12 liters

Fluid velocity = 14,150 cm./min.

Temperature = $30^{\circ}C$

P_{O_2} = 0.21 atm.

$[HCl]$ = 1.0M

Inside diameter of tin tube = 1.27 cm.

Length of tin tube = 10.16cm.

Substitution of these values into the empirical rate equation gives

$$\frac{1}{A}\frac{dSn}{dt} = \frac{V}{A}\frac{d[Sn]}{dt}$$

$$= 7.148 \times 10^{-8} + 2.365 \times 10^{-7} + 2.802 \times 10^{-6}[Sn]^{.5}$$

(A-4-1)

Rearranging gives

$$\frac{d[Sn]}{dt} = \frac{A}{V}(7.148 \times 10^{-8} + 2.365 \times 10^{-7} + 2.802 \times 10^{-6} Sn^{.5})$$

$$= 1.041 \times 10^{-6} + 9.45 \times 10^{-6}[Sn]^{.5}$$ (A-4-2)

hence

$$d[Sn] = (1.041 \times 10^{-6} + 9.45 \times 10^{-6}[Sn]^{.5})dt$$ (A-4-3)

161

and

$$\Delta[\text{Sn}] = (1.041 \times 10^{-6} + 9.45 \times 10^{-6}[\text{Sn}]^{.5})\Delta t \qquad (A-4-4)$$

To calculate the tin ion concentration for the initial period of dissolution, only the first term on the right hand side of Equation(A-4-4) is applied. When the tin ion concentration thus calculated exceeds the value of $.35 \times 10^{-4}$ moles/liter, the second term on the right hand side of Equation(A-4-4) is also applied. By employing appropriate numerical techniques a dissolution curve can be predicted as shown in Figure A-4-1, where an experimental dissolution curve is also drawn for comparison. Figure A-4-1 shows that the rate equation works well even for quite large time increments (about 100 minutes). The accuracy of the prediction can be improved by decreasing the time increments used in the numerical calculations.
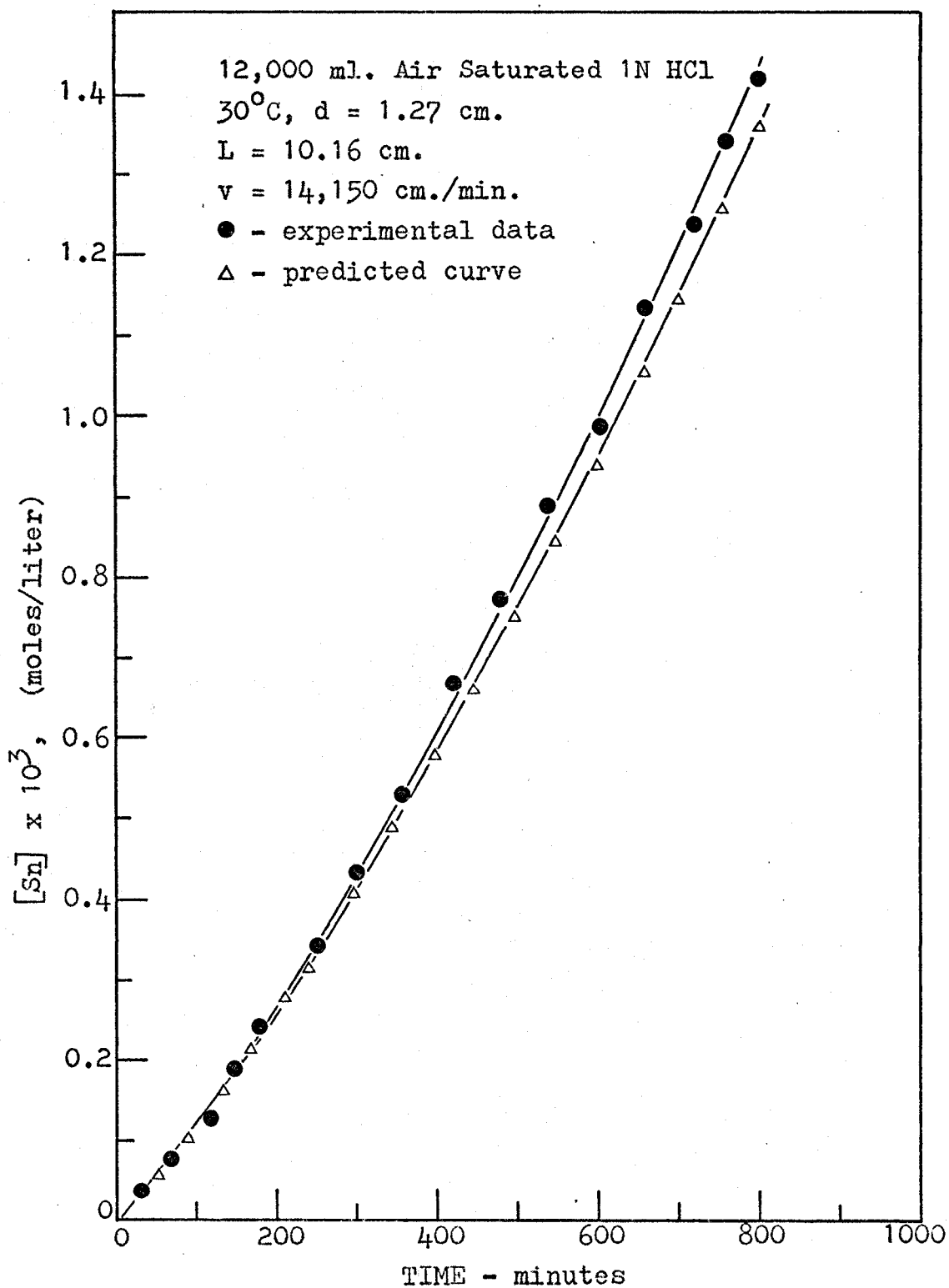
Figure A-4-1. An Example of the Application of the Empirical Rate Equation

APPENDIX 5

Diffusional Mass Transfer Correlations

To appreciate the role of diffusional mass transfer in the dissolution of tin in HCl solutions, it is possible to write

$$\frac{d[Sn]}{dt} = k_L \Delta C \qquad (A-5-1)$$

where k_L is the mass transfer coefficient for the species concerned.

For the purpose of illustration, let us consider the case in which the diffusion of stannous ions from the metal-solution interface to the bulk solution, $Sn_i^{++} \longrightarrow Sn_b^{++}$, is the important physical step, then

$$\Delta C = C_{Sn_i^{++}} - C_{Sn_b^{++}} \qquad (A-5-2)$$

Because the concentration of stannous ion in the bulk of the solution is negligible in comparison to the concentration at the metal-solution interface, $C_{Sn_b^{++}} \ll C_{Sn_i^{++}}$. Also $C_{Sn_i^{++}}$, which is the saturation concentration of stannous ion corresponding to the specific conditions, can be regarded as a constant. Therefore, from Equations (A-5-1) and (A-5-2), we obtain

$$\frac{d[Sn]}{dt} = k_L \cdot const \qquad (A-5-3)$$

By combining Equations (I-6-2) and (A-5-3), we obtain

$$k_L = const_1' \cdot (v)^{.67}(d)^{-.05}(L)^{-.30}$$
$$+ const_2' \cdot (v)^{.59}(d)^{-.11}(L)^{-.33}$$
$$+ const_3' \cdot (v)^{.61}(d)^{-.10}(L)^{-.32} \qquad (A-5-4)$$

164

We further assume that the physical properties of the corroding solution, ρ , μ , and $D_{Sn^{++}}$ are constants, then, Equation(A-5-4) can be changed into the following form by multiplying both sides by d, dividing both sides by D_{Sn^+} , and rearranging slightly:

$$\frac{k_L d}{D_{Sn^+}} = const_1' \left(\frac{dv\rho}{\mu}\right)^{.67}\left(\frac{\mu}{\rho D_{Sn^+}}\right)^{.67}\left(\frac{d^{.28}}{L^{.30}}\right)\frac{1}{(D_{Sn^+})^{.33}}$$

$$+ const_2' \left(\frac{dv\rho}{\mu}\right)^{.59}\left(\frac{\mu}{\rho D_{Sn^+}}\right)^{.59}\left(\frac{d^{.30}}{L^{.33}}\right)\frac{1}{(D_{Sn^+})^{.41}}$$

$$+ const_3' \left(\frac{dv\rho}{\mu}\right)^{.61}\left(\frac{\mu}{\rho D_{Sn^+}}\right)^{.61}\left(\frac{d^{.29}}{L^{.32}}\right)\frac{1}{(D_{Sn^{++}})^{.39}} \qquad (A-5-5)$$

Since the diffusion coefficients of metal ions at the metal-solution interface are generally not measurable, the correlations between dissolution rate constants and $D_{Sn^{++}}$ were not directly investigated. However, for a discussion which requires only characteristic comparison it is quite reasonable to assume that the value of $D_{Sn^{++}}$ is constant. Therefore, the three factors of $D_{Sn^{++}}$ at the right-hand side of Equation(A-5-5) can be combined with their respective constant. Thus, we have

$$\frac{k_L d}{D_{Sn^{++}}} = Nu = c_1' \ (Re)^{.67}(Sc)^{.67}(\tfrac{d}{L})^{.29}$$

$$+ c_2' \ (Re)^{.59}(Sc)^{.59}(\tfrac{d}{L})^{.31}$$

$$+ c_3' \ (Re)^{.61}(Sc)^{.61}(\tfrac{d}{L})^{.30} \qquad (I-6-3)$$

The above equation is consistent in form with Equation (I-6-1), which is the generally accepted form of dimensionless correlations for diffusional mass transfer for a fluid moving through a tube of circular cross-section.

APPENDIX 6

Preparation of Saturated Calomel Electrode

A sketch of the saturated calomel electrode used in this investigation is shown in Figure A-6-1.

First, pure mercury was added to the reference electrode compartment to produce a layer of 1 to 2 cm. depth. This was covered with an equally thick layer of a paste made by stirring equal weights of mercurous and potassium chlorides with a saturated potassium chloride solution containing a large excess of solid salt. After the cell was filled with

Hg

Connection to KCl salt bridge

Saturated KCl solution

Hg_2Cl_2 + KCl (paste)
Mercury pool

Platinum wire
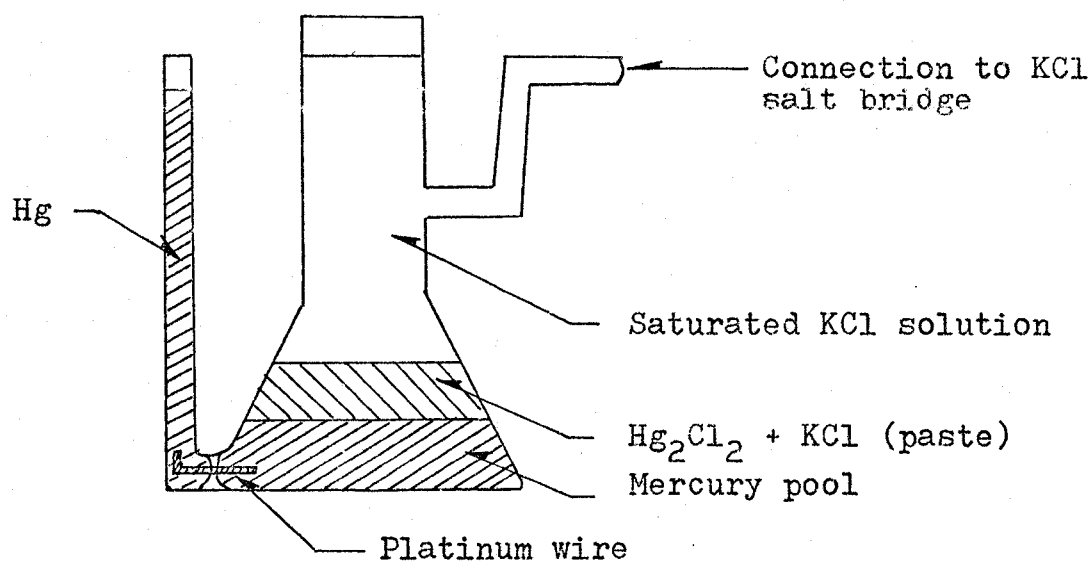
Figure A-6-1. Saturated Calomel Electrode

saturated potassium chloride solution, two days were allowed for the S.C.E. to reach its equilibrium potential.

167

APPENDIX 7

Specifications of the Model 4700M Research Potentiostat

Following are the specifications of the Model 4700M
Research Potentiostat used in this investigation:

Potential control range: $\pm$ 1, 3 and 6 volts.

Potential control stability: $\pm$ 0.5 mv/24 hours.

Potential meter scales: $\pm$ 1, 3 and 6 volts.

Potential recorder output: 0 - 10 mv.

Anodic and cathodic current capacity: 10 amps at $\pm$ 10

volts and 5 amps at $\pm$ 20 volts.

Current meter scales: $\pm$ 100μa to $\pm$ 10 amps in 6 decades.

Current recorder output: 0 - 10 mv.

Voltage meter scales: $\pm$ 10 and 20 volts.

Rise time: less than 2 microseconds at rated currents

into a resistance load over the full $\pm$ 6 volt

potential range.

Noise: less than 150 microvolts RMS

Input impedance: 500,000 ohms at maximum imbalance,

resistance component greater than 100

megohms at balance, constant offset

current over full potential control

range typically 5μa.

168

APPENDIX 8

DATA OF TIN DISSOLUTION

169

EFFECT OF FLUID VELOCITY

12,000 ml. 1M HCl, Air Saturated
25°C, d = 1.905 cm., L = 7.62 cm.

Run 1 1,175 cm./min.		Run 2 4,700 cm./min.		Run 3 8,500 cm./min.		Run 4 13,500 cm./min.		Run 5 16,600 cm./min.	
Time (min.)	$[Sn]$ (mol./l.)	Time (min.)	$[Sn]$ (mol./l.)	Time (min.)	$[Sn]$ (mol./l.)	Time (min.)	$[Sn]$ (mol./l.)	Time (min.)	$[Sn]$ (mol./l.)
30	0.08×10^{-4}	20	0.15×10^{-4}	30	0.28×10^{-4}	30	0.41×10^{-4}	25	0.52×10^{-4}
60	0.15	60	0.36	60	0.52	90	1.05	55	0.75
90	0.24	95	0.57	100	0.98	120	1.52	90	1.24
120	0.29	120	0.76	130	1.12	150	1.94	150	2.11
170	0.48	150	0.89	180	1.75	210	2.85	180	2.75
220	0.62	240	1.63	240	2.44	270	3.86	240	3.86
300	0.81	300	2.08	270	2.78	310	4.35	300	5.03
330	0.87	360	2.58	340	3.65	370	5.41	360	6.25
420	1.15	390	2.82	430	4.65	400	6.22	450	8.14
480	1.27	455	3.31	490	5.46	460	7.08	480	8.82
510	1.44	520	3.82	520	5.95	490	7.61	540	10.22
600	1.75	630	4.93	610	7.11	550	8.77	630	12.36
630	1.87	690	5.46	660	7.89	640	10.65	690	13.75
720	2.21	710	5.75	690	8.35	700	11.75	720	14.62
775	2.37			730	8.94	720	12.51	760	15.12

EFFECT OF FLUID VELOCITY

12,000 ml. Air Saturated 1M HCl
30°C, d = 1.27 cm., L = 10.16 cm.

Run 6
1,175 cm./min.

Time (min.)	[Sn] (mol./l.)
30	0.09x10^{-4}
60	0.14
115	0.29
190	0.47
235	0.62
300	0.81
330	0.89
370	0.97
490	1.36
540	1.54
610	1.73
660	1.92
710	2.11
780	2.33

Run 7
5,730 cm./min.

Time (min.)	[Sn] (mol./l.)
30	0.19x10^{-4}
60	0.37
120	0.81
170	1.21
240	1.81
310	2.33
360	2.87
410	3.35
470	3.95
530	4.53
590	5.21
670	5.86
725	6.48

Run 8
7,075 cm./min.

Time (min.)	[Sn] (mol./l.)
20	0.17x10^{-4}
50	0.41
90	0.67
130	0.96
180	1.52
240	2.09
300	2.69
360	3.33
420	3.98
480	4.66
540	5.35
660	6.80
720	7.55
750	7.94

Run 9
8,300 cm./min.

Time (min.)	[Sn] (mol./l.)
30	0.28x10^{-4}
60	0.49
120	1.07
150	1.34
180	1.68
250	2.35
310	3.11
390	4.05
430	4.45
485	5.22
550	6.11
600	6.81
690	8.06
720	8.49

Run 10
14,150 cm./min.

Time (min.)	[Sn] (mol./l.)
30	0.41x10^{-4}
60	0.69
130	1.55
190	2.42
245	3.37
310	4.39
365	5.43
430	6.54
480	7.67
550	8.92
600	10.05
670	11.35
710	12.33
770	13.65

EFFECT OF FLUID VELOCITY

12,000 ml. Air Saturated 1M HCl

$40^\circ C$, d = 1.27 cm., L = 10.16 cm.

Run 11, 1,175 cm./min.

Time (min.)	[Sn] (mol./l.)
20	0.07×10^{-4}
50	0.17
90	0.31
120	0.39
190	0.63
245	0.85
300	1.09
370	1.35
425	1.59
480	1.85
550	2.14
610	2.39
660	2.66
730	2.95
790	3.25

Run 12, 2,350 cm./min.

Time (min.)	[Sn] (mol./l.)
30	0.17×10^{-4}
60	2.98
120	6.03
190	9.87
230	1.30
290	1.62
350	2.11
430	2.56
490	2.98
540	3.42
600	3.86
660	4.32
720	4.78
750	4.98

Run 13, 4,700 cm./min.

Time (min.)	[Sn] (mol./l.)
30	0.31×10^{-4}
60	0.47
90	0.71
150	1.22
180	1.55
240	2.17
300	2.81
390	3.75
420	4.14
475	4.83
540	5.58
630	6.69
690	7.49
720	7.91

Run 14, 5,730 cm./min.

Time (min.)	[Sn] (mol./l.)
20	0.21×10^{-4}
55	0.49
85	0.81
120	1.11
180	1.75
210	2.09
310	3.25
420	4.77
450	5.17
540	6.44
600	7.32
670	8.23
725	9.15
780	10.11

Run 15, 8,500 cm./min.

Time (min.)	[Sn] (mol./l.)
30	0.42×10^{-4}
60	0.65
120	1.43
180	2.31
240	3.26
300	4.24
360	5.27
420	6.34
480	7.45
550	8.75
600	9.78
690	1.16×10^{-3}
720	1.23
780	1.36

EFFECT OF FLUID VELOCITY

12,000 ml. Air Saturated 1M HCl

$40^{\circ}C$, d = 1.27 cm., L = 10.16 cm.

Run 16 10,280 cm./min.		Run 17 13,500 cm./min.		Run 18 15,800 cm./min.		Run 19 16,600 cm./min.	
Time (min.)	$[Sn]$ (mol./l.)	Time (min.)	$[Sn]$ (mol./l.)	Time (min.)	$[Sn]$ (mol./l.)	Time (min.)	$[Sn]$ (mol./l.)
30	0.44×10^{-4}	20	0.38×10^{-4}	30	0.61×10^{-4}	45	0.76×10^{-4}
60	0.76	50	0.75	60	1.01	90	1.43
120	1.45	80	1.22	90	1.55	120	2.02
180	2.66	130	2.02	120	2.24	150	3.02
210	3.11	190	3.25	150	2.79	210	4.21
250	3.82	270	5.05	180	3.59	240	5.23
310	4.92	360	7.36	240	5.05	300	6.85
400	7.02	420	8.89	300	6.61	330	7.60
490	8.65	510	11.11	360	8.25	390	9.15
550	10.05	600	13.87	420	9.98	425	10.36
660	12.73	690	16.32	480	11.78	490	12.55
730	14.42	720	17.51	570	14.33	550	15.13
780	15.72	750	18.22	660	17.68	630	17.22
810	16.33	780	19.42	690	18.32	690	19.44
				720	19.78		

EFFECT OF TEMPERATURE

12,000 ml. Air Saturated 1M HCl

16,600 cm./min., d=1.27 cm., L=10.16 cm.

Run 20 – 25°C		Run 21 – 30°C		Run 22 – 35°C		Run 23 – 45°C		Run 24 – 50°C	
Time (min.)	$[Sn]$ (mol./l.)	Time (min.)	$[Sn]$ (mol./l.)	Time (min.)	$[Sn]$ (mol./l.)	Time (min.)	$[Sn]$ (mol./l.)	Time (min.)	$[Sn]$ (mol./l.)
30	0.41×10^{-4}	20	0.35×10^{-4}	30	0.53×10^{-4}	30	0.62×10^{-4}	45	0.78×10^{-4}
60	0.67	50	0.66	45	0.65	60	1.15	90	2.15
90	0.92	80	0.94	90	1.33	90	1.82	120	2.98
120	1.34	110	1.42	120	1.65	120	2.45	180	5.06
180	2.28	190	2.68	150	2.42	170	4.13	210	6.05
245	3.17	240	3.77	240	4.45	250	6.14	240	7.18
310	4.12	300	4.89	300	5.80	310	8.06	290	9.44
370	5.12	360	6.08	360	7.22	370	10.11	350	11.85
420	6.13	390	6.66	430	8.72	430	12.26	430	14.48
490	7.19	420	7.32	490	10.28	480	14.53	485	17.22
545	8.30	480	8.61	530	11.21	540	16.87	545	20.04
600	9.44	540	9.95	605	13.58	610	19.36	600	23.03
710	10.95	610	11.34	670	15.34	660	21.93	670	26.13
770	12.84	720	14.25	710	16.14	720	24.59	730	29.65

EFFECT OF TEMPERATURE

12,000 ml. 1M HCl, Air Saturated

10,280cm./min, d = 1.27 cm., L = 10.16 cm.

Run 25 - 25°C	
Time (min.)	$[Sn]$ (mol./l.)
30	0.28×10^{-4}
60	0.45
90	0.71
120	0.98
190	1.68
230	2.28
310	2.95
370	3.64
410	4.22
490	5.10
530	5.62
600	6.65
670	7.46
730	8.32

Run 26 - 30°C	
Time (min.)	$[Sn]$ (mol./l.)
30	0.35×10^{-4}
60	0.55
90	0.84
120	1.12
180	1.94
220	2.35
300	3.49
360	4.32
420	5.18
480	6.08
540	7.01
600	7.95
660	8.94
720	9.94

Run 27 - 35°C	
Time (min.)	$[Sn]$ (mol./l.)
45	0.55×10^{-4}
60	0.64
90	0.98
150	1.72
185	2.28
240	3.17
290	3.95
350	4.98
430	6.22
490	7.23
545	8.34
610	9.49
650	9.97
710	11.05

Run 28 - 45°C	
Time (min.)	$[Sn]$ (mol./l.)
20	0.35×10^{-4}
50	0.75
80	0.96
120	1.81
175	2.98
245	4.36
310	5.69
365	7.10
425	8.58
485	10.12
535	11.05
595	12.95
665	15.12
725	16.90

Run 29 - 50°C	
Time (min.)	$[Sn]$ (mol./l.)
30	0.64×10^{-4}
60	1.01
90	1.48
120	2.10
180	3.61
250	5.12
300	6.66
370	8.33
420	9.98
490	11.93
540	13.85
600	15.85
660	17.92
720	20.07

EFFECT OF TEMPERATURE

12,000 ml. Air Saturated 1M HCl

4,150 cm./min., d = 1.27 cm., L = 10.16 cm.

Run 30 - 25°C		Run 31 - 30°C		Run 32 - 35°C		Run 33 - 45°C		Run 34 - 50°C	
Time (min.)	$[Sn]$ (mol./l.)	Time (min.)	$[Sn]$ (mol./l.)	Time (min.)	$[Sn]$ (mol./l.)	Time (min.)	$[Sn]$ (mol./l.)	Time (min.)	$[Sn]$ (mol./l.)
30	0.16×10^{-4}	30	0.21×10^{-4}	20	0.15×10^{-4}	45	0.25×10^{-4}	30	0.35×10^{-4}
60	0.24	60	0.30	65	0.37	90	0.74	60	0.53
90	0.35	90	0.47	95	0.65	120	1.02	90	0.82
120	0.55	120	0.65	125	0.78	175	1.55	120	1.12
180	0.89	190	1.06	185	1.23	235	2.31	180	1.93
240	1.24	245	1.46	245	1.70	295	2.85	240	2.69
300	1.58	290	1.75	285	2.19	355	3.71	300	3.48
360	1.95	370	2.33	365	2.70	420	4.44	370	4.33
420	2.32	425	2.74	425	3.23	475	5.12	420	5.19
490	2.72	485	3.22	485	3.77	540	5.95	475	6.10
545	3.09	550	3.66	545	4.23	600	6.82	540	7.04
610	3.51	600	4.14	605	4.89	690	8.06	600	8.01
675	3.92	660	4.63	665	5.48	720	8.52	670	8.95
730	4.31	720	5.14	725	6.12	750	8.92	710	9.85

EFFECT OF TEMPERATURE

12,000 ml. Air Saturated 1M HCl

1,175 cm./min., d = 1.27 cm., L = 10.16 cm.

Run 35 - 25°C		Run 36 - 30°C		Run 37 - 35°C		Run 38 - 45°C		Run 39 - 50°C	
Time (min.)	$[Sn]$ (mol./l.)	Time (min.)	$[Sn]$ (mol./l.)	Time (min.)	$[Sn]$ (mol./l.)	Time (min.)	$[Sn]$ (mol./l.)	Time (min.)	$[Sn]$ (mol./l.)
30	0.07×10^{-4}	30	0.08×10^{-4}	20	0.06×10^{-4}	35	0.13×10^{-4}	30	0.14×10^{-4}
60	0.11	60	0.13	50	0.12	65	0.22	60	0.23
90	0.17	90	0.21	80	0.25	95	0.32	90	0.34
120	0.24	125	0.29	115	0.31	125	0.41	120	0.51
180	0.39	190	0.46	175	0.53	185	0.72	180	0.83
210	0.46	245	0.63	235	0.72	245	0.96	240	1.14
300	0.68	310	0.81	295	0.94	310	1.26	300	1.46
330	0.75	365	0.98	355	1.12	365	1.55	390	1.98
420	0.98	430	1.16	415	1.25	420	1.84	420	2.14
490	1.14	485	1.35	480	1.58	490	2.15	450	2.33
540	1.31	550	1.54	540	1.81	545	2.46	530	2.65
600	1.46	610	1.73	600	2.03	620	2.83	610	3.23
630	1.56	665	1.92	655	2.21	670	3.11	670	3.67
720	1.80	730	2.12	715	2.43	730	3.45	720	3.98

EFFECT OF OXYGEN CONCENTRATION

12,000 ml. 1M HCl, 16,600 cm./min.
30°C, d = 1.27 cm., L = 10.16 cm.

Run 40 P_{O_2} = 0 atm.		Run 41 P_{O_2} = 0.21 atm.		Run 42 P_{O_2} = 0.5 atm.		Run 43 P_{O_2} = 0.7 atm.		Run 44 P_{O_2} = 1.0 atm.	
Time (min.)	[Sn] (mol./l.)	Time (min.)	[Sn] (mol./l.)	Time (min.)	[Sn] (mol./l.)	Time (min.)	[Sn] (mol./l.)	Time (min.)	[Sn] (mol./l.)
30	0.08×10^{-4}	30	0.45×10^{-4}	45	0.73×10^{-4}	30	0.82×10^{-4}	30	0.85×10^{-4}
60	0.16	60	0.76	75	1.46	60	1.24	60	1.54
90	0.23	95	0.99	105	2.02	120	2.95	90	2.41
120	0.33	125	1.42	135	2.65	180	4.86	120	3.35
210	0.57	175	2.54	180	4.11	240	6.97	180	5.94
295	0.79	250	3.76	240	5.82	300	9.19	240	8.49
370	0.96	310	4.89	300	7.64	390	12.32	330	11.25
425	1.12	365	6.08	355	9.22	420	13.85	420	17.74
480	1.28	430	7.32	425	11.63	450	15.33	480	20.73
540	1.44	545	9.95	490	13.78	480	16.74	540	24.26
610	1.61	610	11.34	535	15.95	540	19.53	630	31.83
640	1.65	665	12.75	600	18.37	600	22.44	690	33.55
670	1.76	715	13.92	660	20.81	660	25.48	710	34.81
730	1.95	745	14.85	720	23.34	720	28.65	740	36.88

EFFECT OF OXYGEN CONCENTRATION

12,000 ml. 1M HCl, 10,280 cm./min.
30°C, d = 1.27 cm., L = 10.16 cm.

Run 45 P_{O_2} = 0 atm.		Run 46 P_{O_2} = 0.21 atm.		Run 47 P_{O_2} = 0.5 atm.		Run 48 P_{O_2} = 0.7 atm.		Run 49 P_{O_2} = 1.0 atm.	
Time (min.)	[Sn] (mol./l.)	Time (min.)	[Sn] (mol./l.)	Time (min.)	[Sn] (mol./l.)	Time (min.)	[Sn] (mol./l.)	Time (min.)	[Sn] (mol./l.)
30	0.07×10^{-4}	30	0.32×10^{-4}	45	0.65×10^{-4}	30	0.58×10^{-4}	30	0.66×10^{-4}
60	0.12	60	0.55	90	1.34	60	0.95	60	1.12
120	0.24	90	1.14	120	1.75	120	1.96	90	1.83
180	0.34	120	1.23	180	2.94	210	4.11	120	2.45
270	0.52	175	1.94	270	4.74	300	6.45	180	4.11
360	0.71	240	2.70	360	6.73	360	8.10	240	5.98
420	0.82	310	3.49	450	8.85	420	9.81	300	7.88
480	0.96	355	4.12	540	11.13	480	11.55	360	9.90
540	1.05	430	5.18	600	12.72	570	14.46	420	12.03
630	1.23	490	6.12	660	14.35	660	17.47	480	14.29
720	1.41	550	7.05	690	15.15	720	19.58	540	16.64
		610	7.96	720	16.05	780	21.75	600	19.11
		670	8.95					660	21.67
		730	9.95					720	24.34

EFFECT OF OXYGEN CONCENTRATION

12,000 ml. 1M HCl, 4,150 cm./min.

30°C, d = 1.27 cm., L = 10.16 cm.

Run 50 P_{O_2} = 0 atm.		Run 51 P_{O_2} = 0.21 atm.		Run 52 P_{O_2} = 0.5 atm.		Run 53 P_{O_2} = 0.7 atm.		Run 54 P_{O_2} = 1.0 atm.	
Time (min.)	[Sn] (mol./l.)	Time (min.)	[Sn] (mol./l.)	Time (min.)	[Sn] (mol./l.)	Time (min.)	[Sn] (mol./l.)	Time (min.)	[Sn] (mol./l.)
30	0.04×10^{-4}	30	0.18×10^{-4}	45	0.35×10^{-4}	30	0.33×10^{-4}	20	0.29×10^{-4}
60	0.07	60	0.31	90	0.72	60	0.54	65	0.65
120	0.14	90	0.49	120	0.98	90	0.79	120	1.41
180	0.19	120	0.65	210	1.91	120	1.18	180	2.24
240	0.26	180	1.06	270	2.52	180	1.87	270	3.46
300	0.34	245	1.45	330	3.16	240	2.61	330	4.59
390	0.42	310	1.88	360	3.52	300	3.38	420	6.14
480	0.53	485	3.20	420	4.22	360	4.20	510	7.82
540	0.58	540	3.66	480	4.95	420	5.05	600	9.54
600	0.65	570	3.80	570	6.10	480	5.93	660	10.75
660	0.72	600	4.14	630	6.85	540	6.85	720	12.05
730	0.81	660	4.63	720	8.09	600	7.79	750	12.61
		690	4.88			660	8.76		
		720	5.14			720	9.77		

VARIATION OF TUBE DIAMETER

12,000 ml. 1M HCl, Air Saturated
16,600 cm./min., 30°C, L = 10.16 cm.

Run 55, d = 0.953 cm.

Time (min.)	[Sn] (mol./l.)
30	0.35×10^{-4}
60	0.59
120	1.15
180	1.96
240	2.79
300	3.62
360	4.35
420	5.35
480	6.25
540	7.26
600	8.15
660	9.27
720	10.22
780	11.40

Run 56, d = 1.588 cm.

Time (min.)	[Sn] (mol./l.)
30	0.55×10^{-4}
60	0.96
90	1.03
120	1.94
210	3.95
310	6.24
370	7.75
510	11.83
600	14.59
660	16.47
720	18.41
810	21.42

Run 57, d = 1.905 cm.

Time (min.)	[Sn] (mol./l.)
30	0.65×10^{-4}
60	1.14
95	1.86
125	2.35
185	4.10
250	5.86
310	7.66
370	9.68
430	11.95
520	14.55
610	18.10
670	20.65
730	23.22
820	26.55

Run 58, d = 2.54 cm.

Time (min.)	[Sn] (mol./l.)
45	0.98×10^{-4}
75	1.64
105	2.33
130	3.65
190	5.72
250	7.96
310	11.04
370	13.24
460	17.11
550	22.33
580	23.87
610	25.64
670	28.96
730	32.25

Run 59, d = 1.27 cm.

Time (min.)	[Sn] (mol./l.)
30	0.42×10^{-4}
60	0.75
120	1.58
180	2.69
240	3.77
300	4.89
360	6.08
420	7.33
480	8.61
490	8.73
590	10.85
665	12.84
730	14.43
810	16.52

VARIATION OF TUBE DIAMETER

12,000 ml. Air Saturated 1M HCl
5,730 cm./min., 30°C, L=10.16 cm.

Run 60, d = 0.953 cm.

Time (min.)	[Sn] (mol./l.)
30	0.18×10^{-4}
60	0.29
90	0.45
120	0.61
180	0.98
240	1.36
300	1.74
360	2.14
420	2.55
480	2.97
540	3.40
600	3.84
660	4.30
720	4.76

Run 61, d = 1.27 cm.

Time (min.)	[Sn] (mol./l.)
45	0.30×10^{-4}
90	0.62
120	0.81
210	1.56
240	1.81
330	2.59
420	3.43
480	4.01
540	4.60
600	5.21
690	6.15
720	6.48
780	7.13
810	7.43

Run 62, d = 1.588 cm.

Time (min.)	[Sn] (mol./l.)
30	0.28×10^{-4}
60	0.47
120	1.04
180	1.64
270	2.58
360	3.62
420	4.34
480	5.08
540	5.84
630	7.03
720	8.26
750	8.67

Run 63, d = 1.905 cm.

Time (min.)	[Sn] (mol./l.)
30	0.31×10^{-4}
60	0.57
120	1.22
210	2.35
240	2.74
300	3.54
360	4.38
420	5.27
480	6.17
545	7.11
610	8.12
670	9.15
730	10.15
790	11.24

Run 64, d = 2.54 cm.

Time (min.)	[Sn] (mol./l.)
20	0.25×10^{-4}
50	0.58
80	0.89
110	1.45
200	2.98
230	3.42
290	4.43
355	5.66
420	7.17
510	9.05
600	11.11
660	12.51
720	13.95

VARIATION OF TUBE DIAMETER

12,000 ml. Air Saturated 1M HCl

1,175 cm./min., 30°C, L = 10.16 cm.

Run 65, d = 0.953 cm.

Time (min.)	[Sn] (mol./l.)
30	0.06×10^{-4}
60	0.11
120	0.22
185	0.35
250	0.48
300	0.60
365	0.74
420	0.87
485	1.01
540	1.15
610	1.29
670	1.45
730	1.61

Run 66, d = 1.27 cm.

Time (min.)	[Sn] (mol./l.)
30	0.07×10^{-4}
60	0.14
125	0.30
190	0.46
240	0.63
310	0.81
370	0.98
425	1.16
480	1.35
535	1.52
600	1.73
660	1.92
720	2.12
780	2.33

Run 67, d = 1.588 cm.

Time (min.)	[Sn] (mol./l.)
30	0.08×10^{-4}
60	0.16
90	0.25
120	0.37
175	0.55
305	1.01
360	1.22
490	1.69
550	1.93
610	2.17
660	2.42
720	2.67
750	2.80

Run 68, d = 1.905 cm.

Time (min.)	[Sn] (mol./l.)
30	0.11×10^{-4}
60	0.21
120	0.44
175	0.64
235	0.89
295	1.15
355	1.42
415	1.71
475	2.03
535	2.22
655	2.85
715	3.12
775	3.44

Run 69, d = 2.54 cm.

Time (min.)	[Sn] (mol./l.)
30	0.14×10^{-4}
60	0.27
90	0.41
125	0.56
190	0.91
245	1.25
365	1.97
485	2.73
545	3.12
600	3.53
660	3.95
720	4.37
780	4.80

VARIATION OF TUBE LENGTH

12,000 ml. Air Saturated 1M HCl

16,600 cm./min., 30°C, d = 1.27 cm.

Run 70, L = 13.97 cm.

Time (min.)	[Sn] (mol./l.)
30	0.49×10^{-4}
60	0.98
90	1.44
120	2.16
180	3.44
270	5.52
330	7.10
420	9.52
480	11.23
540	13.01
600	14.86
660	16.78
720	18.76

Run 71, L = 12.7 cm.

Time (min.)	[Sn] (mol./l.)
30	0.47×10^{-4}
60	0.92
125	1.95
190	3.20
245	4.49
310	5.85
360	7.29
425	8.79
490	10.37
545	12.01
610	13.72
670	15.45
730	17.27
760	18.75

Run 72, L = 8.9 cm.

Time (min.)	[Sn] (mol./l.)
45	0.56×10^{-4}
90	1.12
120	1.53
180	2.43
240	3.39
300	4.40
365	5.46
425	6.57
485	7.72
545	8.92
605	10.15
665	11.42
725	12.73
785	14.08

Run 73, L = 6.35 cm.

Time (min.)	[Sn] (mol./l.)
30	0.29×10^{-4}
60	0.55
90	0.85
120	1.16
190	1.89
250	2.65
310	3.38
370	4.17
430	5.02
490	5.88
550	6.76
610	7.68
730	9.59

Run 74, L = 5.075 cm

Time (min.)	[Sn] (mol./l.)
30	0.24×10^{-4}
60	0.47
120	1.01
180	1.58
240	2.19
300	2.83
360	3.50
420	4.19
480	4.89
540	5.64
600	6.39
630	6.77
720	7.96
750	8.37

VARIATION OF TUBE LENGTH

12,000 ml. Air Saturated 1M HCl

8,300 cm./min., 30°C, d = 1.27 cm.

Run 75, L = 13.97 cm.

Time (min.)	$[Sn]$ (mol./l.)
30	0.32×10^{-4}
60	0.63
120	1.32
180	2.14
245	2.98
305	3.86
365	4.78
425	5.75
485	6.73
545	7.78
605	8.84
665	9.95
725	11.07
755	11.65

Run 76, L = 11.42 cm.

Time (min.)	$[Sn]$ (mol./l.)
30	0.28×10^{-4}
60	0.54
90	0.82
120	1.16
175	1.80
240	2.55
300	3.29
360	4.02
450	5.33
540	6.54
600	7.49
660	8.41
750	9.76

Run 77, L = 8.9 cm.

Time (min.)	$[Sn]$ (mol./l.)
45	0.32×10^{-4}
60	0.45
120	0.95
185	1.52
250	2.10
310	2.71
370	3.35
430	4.01
490	4.69
550	5.39
610	6.18
670	6.97
730	7.88

Run 78, L = 6.35 cm.

Time (min.)	$[Sn]$ (mol./l.)
30	0.18×10^{-4}
60	0.34
120	0.71
190	1.23
245	1.65
305	2.11
360	2.58
420	3.06
510	3.64
570	4.37
660	5.21
720	5.78
750	6.06

Run 79, L = 5.075 cm.

Time (min.)	$[Sn]$ (mol./l.)
20	0.11×10^{-4}
60	0.32
90	0.53
125	0.65
185	1.07
245	1.37
310	1.78
370	2.17
430	2.62
490	3.11
550	3.48
610	3.97
670	4.45
730	4.86

VARIATION OF TUBE LENGTH

12,000 ml. Air Saturated 1M HCl

2,350 cm./min., 30°C, d = 1.27 cm.

Run 80, L = 13.95 cm.

Time (min.)	$[Sn]$ (mol./l.)
30	0.15x10^{-4}
60	0.28
90	0.41
120	0.58
180	0.92
240	1.26
300	1.62
360	1.98
420	2.37
480	2.76
540	3.16
600	3.33
720	4.45
750	4.62

Run 81, L = 12.7 cm.

Time (min.)	$[Sn]$ (mol./l.)
30	0.14x10^{-4}
60	0.26
120	0.54
185	0.85
245	1.17
305	1.51
365	1.74
425	2.22
485	2.45
545	2.94
605	3.25
610	3.33
730	4.18
760	4.45

Run 82, L = 8.9 cm.

Time (min.)	$[Sn]$ (mol./l.)
45	0.13x10^{-4}
60	0.19
90	0.26
120	0.40
175	0.66
235	0.89
295	1.14
310	1.22
365	1.35
425	1.71
490	1.98
550	2.38
610	2.52
670	2.85
730	3.17

Run 83, L = 7.62 cm.

Time (min.)	$[Sn]$ (mol./l.)
30	0.10x10^{-4}
60	0.18
120	0.37
180	0.57
240	0.80
300	1.04
360	1.15
420	1.52
480	1.63
540	1.98
600	2.32
660	2.36
720	2.78
780	2.95

Run 84, L = 5.075cm.

Time (min.)	$[Sn]$ (mol./l.)
30	0.07x10^{-4}
60	0.13
90	0.20
125	0.27
185	0.44
250	0.61
310	0.76
370	0.93
430	1.11
490	1.24
550	1.50
610	1.59
730	2.05

VARIATION OF TUBE LENGTH

12,000 ml. 1M HCl, Air Saturated

16,600 cm./min., 40°C, d = 1.27 cm.

Run 85, L = 13.95 cm.

Time (min.)	[Sn] (mol./l.)
30	0.69×10^{-4}
60	1.32
90	1.96
120	2.81
210	5.77
300	8.75
360	11.92
420	13.50
485	15.55
545	18.72
605	22.05
665	23.87
725	27.24
755	28.54

Run 86, L = 11.42 cm.

Time (min.)	[Sn] (mol./l.)
35	0.60×10^{-4}
65	1.15
125	2.52
185	4.08
245	5.75
305	7.53
365	9.22
425	11.56
485	13.12
550	14.85
610	18.10
670	20.35
730	22.85

Run 87, L = 8.9 cm.

Time (min.)	[Sn] (mol./l.)
30	0.49×10^{-4}
60	0.94
90	1.45
120	1.85
210	4.05
300	6.15
390	8.42
450	9.65
540	12.68
600	14.44
690	17.10
750	19.25

Run 88, L = 6.35 cm.

Time (min.)	[Sn] (mol./l.)
45	0.38×10^{-4}
90	1.10
120	1.62
180	2.55
240	3.45
300	4.71
360	5.82
420	6.94
480	8.35
540	9.54
600	10.88
690	12.90
750	14.38

Run 89, L = 5.075 cm.

Time (min.)	[Sn] (mol./l.)
30	0.32×10^{-4}
60	0.62
90	0.95
120	1.24
190	2.17
250	3.02
310	3.85
370	4.86
430	5.91
490	6.95
580	8.33
670	10.55
760	11.85

VARIATION OF SOLUTION VOLUME

Air Saturated 1M HCl , 8,500 cm./min.

30°C, d = 1.27 cm., L = 10.16 cm.

Run 90
V = 14,000 ml.

Time (min.)	$[Sn]$ (mol./l.)
30	0.22×10^{-4}
60	0.42
120	0.85
180	1.46
240	2.03
330	2.92
420	3.88
510	4.86
600	5.94
660	6.66
720	7.25
780	8.18

Run 91
V = 13,000 ml.

Time (min.)	$[Sn]$ (mol./l.)
30	0.24×10^{-4}
60	0.46
90	0.75
120	0.98
210	1.88
300	2.82
390	3.80
480	4.89
540	5.64
630	6.73
690	7.55
750	8.35

Run 92
V = 11,000 ml.

Time (min.)	$[Sn]$ (mol./l.)
45	0.40×10^{-4}
90	0.81
125	1.10
185	1.88
245	2.49
305	3.24
425	4.96
485	5.75
545	6.66
670	8.45
730	9.32
760	9.82

Run 93
V = 10,000 ml.

Time (min.)	$[Sn]$ (mol./l.)
30	0.32×10^{-4}
60	0.61
90	0.95
120	1.25
185	2.05
250	2.85
310	3.67
370	4.66
460	6.12
550	7.35
610	8.55
670	9.46
730	10.65

Run 94
V = 8,000 ml.

Time (min.)	$[Sn]$ (mol./l.)
30	0.38×10^{-4}
60	0.75
120	1.55
180	2.55
240	3.56
300	4.58
360	5.45
420	6.82
510	8.55
600	10.39
690	12.25
750	13.65

VARIATION OF HCl CONCENTRATION

12,000 ml. Air Saturated, 30°C

16,600 cm./min., d = 1.27 cm., L = 10.16 cm.

Run 95 HCl = 0.1M		Run 96 HCl = 0.25M		Run 97 HCl = 0.5M		Run 98 HCl = 2.0M		Run 99 HCl = 4.0M	
Time (min.)	[Sn] (mol./l.)	Time (min.)	[Sn] (mol./l.)	Time (min.)	[Sn] (mol./l.)	Time (min.)	[Sn] (mol./l.)	Time (min.)	[Sn] (mol./l.)
30	0.41×10^{-4}	45	0.64×10^{-4}	20	0.24×10^{-4}	30	0.45×10^{-4}	30	0.38×10^{-4}
60	0.78	90	1.15	50	0.65	60	0.75	60	0.75
120	1.65	125	1.24	80	0.95	115	1.69	90	1.22
210	3.18	185	2.75	130	1.68	175	2.69	150	1.95
300	4.88	245	3.89	190	2.65	235	3.76	240	3.75
390	6.64	310	5.22	250	3.74	295	4.89	330	5.44
480	8.62	370	6.35	310	4.88	355	6.07	420	7.32
540	9.84	430	7.62	370	6.08	475	8.62	510	9.21
600	11.33	520	9.35	430	7.32	535	9.95	600	11.55
660	12.65	610	11.85	490	8.62	595	11.33	660	12.95
720	13.98	730	14.77	580	10.45	655	12.78	720	14.35
750	14.95	790	16.45	670	12.76	715	14.25	780	15.65
				760	14.89	775	15.77		

EFFECT OF FLUID VELOCITY

12,000 ml. N_2 Saturated 1M HCl

25°C, d = 1.905 cm., L = 7.72 cm.

Run 100, 1,175 cm./min.		Run 101, 4,700 cm./min.		Run 102, 85,00 cm./min.		Run 103, 13,500 cm./min.		Run 104, 16,600 cm./min.	
Time (min.)	[Sn] (mol./l.)	Time (min.)	[Sn] (mol./l.)	Time (min.)	[Sn] (mol./l.)	Time (min.)	[Sn] (mol./l.)	Time (min.)	[Sn] (mol./l.)
30	0.17×10^{-5}	45	0.57×10^{-5}	30	0.55×10^{-5}	30	0.82×10^{-5}	20	0.62×10^{-5}
60	0.30	90	1.10	60	1.12	60	1.48	80	2.21
120	0.62	120	1.51	90	1.65	90	2.22	120	3.43
210	1.11	190	2.27	120	2.22	120	3.02	180	5.14
300	1.51	310	3.78	235	4.45	190	4.51	300	8.58
390	1.95	415	5.28	370	6.65	305	7.50	420	12.01
480	2.45	475	6.04	485	8.88	430	10.50	540	15.44
540	2.76	610	7.55	600	11.15	550	13.52	595	17.15
660	3.34	655	8.31	670	12.21	665	16.50	730	20.59
720	3.65	730	9.16	775	14.43	720	18.02	790	22.31
780	3.98					780	19.50		

EFFECT OF FLUID VELOCITY

12,000 ml. N_2 Saturated 1M HCl

30°C, d = 1.27 cm., L = 10.16 cm.

Run 105 1,175 cm./min.		Run 106 5,730 cm./min.		Run 107 7,075 cm./min.		Run 108 8,300 cm./min.		Run 109 14,150 cm./min.	
Time (min.)	[Sn] (mol./l.)	Time (min.)	[Sn] (mol./l.)	Time (min.)	[Sn] (mol./l.)	Time (min.)	[Sn] (mol./l.)	Time (min.)	[Sn] (mol./l.)
30	0.15×10^{-5}	30	0.41×10^{-5}	30	0.48×10^{-5}	30	0.52×10^{-5}	30	0.75×10^{-5}
60	0.29	60	0.79	60	0.92	60	1.02	60	1.44
130	0.58	90	1.25	120	1.84	90	1.55	90	2.15
190	0.86	120	1.61	240	3.69	120	2.05	250	5.79
310	1.44	235	3.22	360	5.54	235	4.10	310	7.24
430	2.12	370	4.83	420	6.46	370	6.14	370	8.69
550	2.58	490	6.45	480	7.38	475	8.19	430	10.14
600	2.87	610	8.05	605	9.23	610	10.24	550	13.14
660	3.16	730	9.66	670	10.15	660	11.26	670	15.95
720	3.45	790	10.48	730	11.12	720	12.29	730	17.44
750	3.58					780	13.31	760	17.58

191

EFFECT OF FLUID VELOCITY

12,000 ml. N_2 Saturated 1M HCl

40°C, d = 1.27 cm., L = 10.16 cm.

Run 110 1,175 cm./min.		Run 111 2,350 cm./min.		Run 112 4,700 cm./min.		Run 113 5,730 cm./min.		Run 114 8,500 cm./min.	
Time (min.)	$\left[\text{Sn}\right]$ (mol./l.)	Time (min.)	$\left[\text{Sn}\right]$ (mol./l.)	Time (min.)	$\left[\text{Sn}\right]$ (mol./l.)	Time (min.)	$\left[\text{Sn}\right]$ (mol./l.)	Time (min.)	$\left[\text{Sn}\right]$ (mol./l.)
30	0.20×10^{-5}	30	0.31×10^{-5}	45	0.66×10^{-5}	30	0.55×10^{-5}	30	0.66×10^{-5}
60	0.36	60	0.56	90	1.15	60	1.01	60	1.25
120	0.70	90	0.85	135	1.81	120	2.01	90	1.85
195	1.12	180	1.13	235	3.54	240	4.03	180	3.91
245	1.44	240	2.25	295	4.43	360	6.12	300	6.52
365	2.16	365	3.39	415	6.15	480	8.07	360	7.82
425	2.52	430	3.95	535	7.98	540	9.11	420	9.12
485	2.88	490	4.52	600	8.86	600	10.21	540	11.72
550	3.24	610	5.65	660	9.75	660	11.09	630	13.60
610	3.62	725	6.78	720	10.63	720	12.11	750	16.22
730	4.35	785	7.34	780	11.52	780	13.20	870	18.75
760	4.54								

EFFECT OF FLUID VELOCITY

12,000 ml. N_2 Saturated 1M HCl

40°C, d = 1.27 cm., L = 10.16 cm.

Run 115 10,280 cm./min.		Run 116 13,500 cm./min.		Run 117 15,800 cm./min.		Run 118 16,600 cm./min.	
Time (min.)	[Sn] (mol./l.)	Time (min.)	[Sn] (mol./l.)	Time (min.)	[Sn] (mol./l.)	Time (min.)	[Sn] (mol./l.)
30	0.75×10^{-5}	30	0.91×10^{-5}	45	1.45×10^{-5}	30	1.02×10^{-5}
60	1.47	60	1.76	90	2.84	60	2.01
120	2.95	90	2.65	135	3.96	120	4.10
180	4.42	120	3.51	180	5.85	240	8.05
300	7.37	210	6.11	225	6.75	360	12.12
390	9.44	310	8.82	360	11.69	450	15.10
480	11.79	430	12.33	480	15.59	540	18.12
570	13.85	550	15.85	540	17.54	600	20.13
660	16.22	610	17.62	630	20.45	690	23.11
750	18.35	730	21.12	720	23.40	725	24.15
780	19.21	790	22.95	765	24.44	785	26.17

VARIATION OF TEMPERATURE

12,000 ml. N_2 Saturated 1M HCl

16,600 cm./min., d = 1.27 cm., L = 10.16 cm.

Run 119 - 25°C		Run 120 - 30°C		Run 121 - 35°C		Run 122 - 45°C		Run 123 - 50°C	
Time (min.)	[Sn] (mol./l.)	Time (min.)	[Sn] (mol./l.)	Time (min.)	[Sn] (mol./l.)	Time (min.)	[Sn] (mol./l.)	Time (min.)	[Sn] (mol./l.)
30	0.75×10^{-5}	20	0.60×10^{-5}	30	0.95×10^{-5}	30	1.2×10^{-5}	30	1.35×10^{-5}
60	1.41	50	1.55	60	1.81	60	2.01	60	2.45
120	2.85	80	2.21	120	3.60	90	3.32	120	4.96
210	4.95	170	4.82	240	7.14	120	3.95	180	7.46
300	7.14	235	6.43	360	10.75	210	7.04	270	11.32
420	9.95	355	9.64	420	12.65	355	11.55	360	14.92
510	12.10	475	1.25×10^{-4}	480	14.33	415	13.84	480	19.89
600	14.25	595	1.62	600	18.02	545	18.11	570	23.44
660	15.70	655	1.76	660	19.75	665	22.14	630	25.35
720	17.13	715	1.92	750	22.45	725	24.16	720	29.84
750	17.66	745	1.97	780	23.42	755	25.65	750	31.08

VARIATION OF TEMPERATURE

12,000 ml. N_2 Saturated 1M HCl

10,280 cm./min., d = 1.27 cm., L = 10.16 cm.

Run 124 - 25°C		Run 125 - 30°C		Run 126 - 35°C		Run 127 - 45°C		Run 128 - 50°C	
Time (min.)	[Sn] (mol./l.)	Time (min.)	[Sn] (mol./l.)	Time (min.)	[Sn] (mol./l.)	Time (min.)	[Sn] (mol./l.)	Time (min.)	[Sn] (mol./l.)
30	0.55×10^{-5}	30	0.64×10^{-5}	45	0.70×10^{-5}	30	0.85×10^{-5}	30	0.98×10^{-5}
60	1.04	60	1.15	90	1.35	60	1.64	60	1.81
120	2.10	90	1.75	135	1.98	120	3.25	90	2.65
180	3.12	120	2.35	195	3.96	210	5.65	180	5.45
270	4.65	210	4.11	310	6.61	300	8.21	240	7.28
370	6.28	300	5.88	430	9.24	390	10.55	330	9.55
485	8.36	430	8.25	475	10.35	480	13.13	420	12.75
545	9.41	545	10.59	630	13.75	545	14.77	510	15.33
610	10.45	665	12.95	690	15.22	595	16.42	600	18.22
730	12.66	720	14.12	725	15.83	670	18.15	690	20.95
780	13.59	750	14.55	755	16.42	760	20.85	750	22.33

VARIATION OF TEMPERATURE

12,000 ml. N_2 Saturated 1M HCl

4,150 cm./min., d = 1.27 cm., L = 10.16 cm.

Run 129 - 25°C		Run 130 - 30°C		Run 131 - 35°C		Run 132 - 45°C		Run 133 - 50°C	
Time (min.)	$[Sn]$ (mol./l.)	Time (min.)	$[Sn]$ (mol./l.)	Time (min.)	$[Sn]$ (mol./l.)	Time (min.)	$[Sn]$ (mol./l.)	Time (min.)	$[Sn]$ (mol./l.)
30	0.30×10^{-5}	30	0.35×10^{-5}	45	0.58×10^{-5}	30	0.48×10^{-5}	30	0.58×10^{-5}
60	0.57	60	0.65	90	1.05	60	0.91	60	1.01
120	1.15	90	0.98	135	1.45	120	1.75	90	1.45
180	1.74	210	2.32	180	2.19	240	3.58	180	3.10
270	2.52	300	3.26	270	3.33	360	5.45	270	4.55
360	3.45	390	4.22	360	4.39	450	6.67	370	6.10
430	4.12	485	5.21	450	5.50	540	8.19	460	7.65
550	5.33	615	6.52	540	6.58	600	9.11	550	9.10
670	6.38	680	7.45	660	8.05	690	10.55	670	11.12
725	6.95	735	7.83	750	9.02	720	10.92	715	12.22
775	7.45	765	8.25	780	9.520	810	12.25	745	12.55

VARIATION OF TEMPERATURE

12,000 ml. N_2 Saturated 1M HCl

1,175 cm./min., d = 1.27 cm., L = 10.16 cm.

Run 134 - 25°C

Time (min.)	$[Sn]$ (mol./l.)
30	0.15×10^{-5}
60	0.26
120	0.51
210	0.89
300	1.28
390	1.66
480	2.04
540	2.29
600	2.55
660	2.75
720	2.98
750	3.15

Run 135 - 30°C

Time (min.)	$[Sn]$ (mol./l.)
30	0.16×10^{-5}
60	0.29
150	0.70
240	1.15
310	1.44
430	2.01
545	2.58
675	3.16
720	3.45
780	3.74

Run 136 - 35°C

Time (min.)	$[Sn]$ (mol./l.)
45	0.24×10^{-5}
90	0.43
135	0.65
225	1.12
305	1.61
425	2.25
485	2.58
545	2.85
665	3.54
730	3.88
760	4.10

Run 137 - 45°C

Time (min.)	$[Sn]$ (mol./l.)
30	0.25×10^{-5}
60	0.40
90	0.61
180	1.21
270	1.80
360	2.42
440	3.11
500	3.35
590	3.95
650	4.42
740	4.95

Run 138 - 50°C

Time (min.)	$[Sn]$ (mol./l.)
30	0.25×10^{-5}
60	0.44
120	0.89
180	1.33
270	1.96
360	2.59
450	3.32
540	4.02
600	4.44
660	4.89
730	5.33
760	5.54
790	5.95

VARIATION OF TUBE DIAMETER

12,000 ml. N_2 Saturated 1M HCl

16,600 cm./min., 30°C, L = 10.16 cm.

Run 139, d = 0.953 cm.

Time (min.)	$[Sn]$ (mol./l.)
30	0.65×10^{-5}
60	1.22
120	2.35
210	4.37
300	6.11
390	7.95
450	9.15
510	10.32
600	12.22
660	13.45
720	14.68

Run 140, d = 1.588 cm.

Time (min.)	$[Sn]$ (mol./l.)
30	0.11×10^{-5}
60	1.95
90	2.75
180	5.96
240	7.85
330	10.43
420	13.98
540	17.85
660	21.86
730	23.85
760	24.44
810	26.80

Run 141, d = 1.905 cm.

Time (min.)	$[Sn]$ (mol./l.)
30	1.22×10^{-5}
60	2.33
120	4.72
210	8.25
270	10.25
360	14.17
430	16.53
545	21.26
610	23.62
690	27.11
750	29.33

Run 142, d = 2.54 cm.

Time (min.)	$[Sn]$ (mol./l.)
45	2.22×10^{-5}
90	4.15
135	6.32
190	9.31
310	15.52
430	21.73
550	27.94
610	31.05
670	34.15
730	37.25
790	41.35

Run 143, d = 1.27 cm.

Time (min.)	$[Sn]$ (mol./l.)
45	1.25×10^{-5}
90	2.40
135	3.24
225	5.55
315	8.03
425	11.25
545	14.46
605	15.58
665	17.85
725	19.28
785	20.89

VARIATION OF TUBE DIAMETER

12,000 ml. N_2 Saturated 1M HCl

5,730 cm./min., 30°C, L = 10.16 cm.

Run 144 d = 0.953 cm.		Run 145 d = 1.27 cm.		Run 146 d = 1.588 cm.		Run 147 d = 1.905 cm.		Run 148 d = 2.54 cm.	
Time (min.)	$[Sn]$ (mol./l.)	Time (min.)	$[Sn]$ (mol./l.)	Time (min.)	$[Sn]$ (mol./l.)	Time (min.)	$[Sn]$ (mol./l.)	Time (min.)	$[Sn]$ (mol./l.)
30	0.33×10^{-5}	45	0.63×10^{-5}	30	0.54×10^{-5}	30	0.65×10^{-5}	30	0.80×10^{-4}
60	0.61	90	1.15	60	0.98	60	1.18	60	1.55
120	1.22	135	1.86	90	1.50	120	2.35	150	3.85
180	1.82	195	2.42	120	1.85	210	4.12	240	6.22
270	2.74	300	4.03	210	3.48	300	5.91	330	8.45
330	3.33	365	4.82	300	4.97	420	8.28	390	10.45
450	4.60	455	5.95	390	6.45	485	9.46	460	11.95
570	5.82	545	7.24	480	7.96	545	10.65	550	14.22
630	6.24	620	8.05	570	9.43	610	11.83	640	16.50
720	7.35	650	8.80	660	10.94	670	12.95	700	18.32
750	7.62	715	9.62	750	12.55	730	14.19	760	19.55
		745	9.85			760	14.85		

VARIATION OF TUBE DIAMETER

12,000 ml. N_2 Saturated 1M HCl

1,175 cm./min., 30°C, L = 10.16 cm.

Run 149, d = 0.953 cm.

Time (min.)	[Sn] (mol./l.)
30	0.12×10^{-5}
60	0.21
90	0.30
120	0.43
210	0.75
330	1.15
450	1.66
540	1.97
600	2.18
660	2.35
720	2.62

Run 150, d = 1.27 cm.

Time (min.)	[Sn] (mol./l.)
30	0.15×10^{-5}
60	0.28
120	0.57
210	1.54
300	1.62
390	1.88
420	2.01
510	2.45
630	3.05
690	3.30
750	3.60
780	3.74

Run 151, d = 1.588 cm.

Time (min.)	[Sn] (mol./l.)
30	0.20×10^{-5}
60	0.35
120	0.71
180	1.06
270	1.58
330	1.90
420	2.48
540	3.19
600	3.55
670	3.90
730	4.33

Run 152, d = 1.905 cm.

Time (min.)	[Sn] (mol./l.)
30	0.25×10^{-5}
60	0.42
90	0.71
120	0.82
240	1.68
330	2.33
425	2.95
545	3.81
605	4.22
665	4.64
755	5.25

Run 153, d = 2.54 cm.

Time (min.)	[Sn] (mol./l.)
30	0.30×10^{-5}
60	0.55
120	1.11
180	1.65
240	2.15
360	3.33
480	4.35
540	4.98
600	5.52
660	6.05
720	6.46
750	6.96

VARIATION OF TUBE LENGTH

12,000 ml. N_2 Saturated 1M HCl

16,600 cm./min., 30°C, d = 1.27 cm.

Run 154, L = 13.97 cm.

Time (min.)	[Sn] (mol./l.)
30	1.10×10^{-5}
60	2.00
120	3.95
180	6.02
270	9.33
330	1.12×10^{-4}
420	1.40
480	1.55
540	1.80
610	2.11
670	2.25
730	2.41

Run 155, L = 12.7 cm.

Time (min.)	[Sn] (mol./l.)
30	0.95×10^{-5}
60	1.85
90	2.65
120	3.70
210	6.55
330	10.42
390	12.12
510	16.44
600	18.78
660	20.66
720	22.54
780	24.42

Run 156, L = 8.9 cm.

Time (min.)	[Sn] (mol./l.)
45	1.15×10^{-5}
90	1.95
135	2.96
225	5.28
315	7.56
405	9.55
465	11.24
525	12.85
585	13.96
645	15.43
735	18.02
765	18.95

Run 157, L = 6.35 cm.

Time (min.)	[Sn] (mol./l.)
45	0.90×10^{-5}
90	1.74
120	2.31
210	4.05
300	5.78
390	7.43
450	8.65
540	10.40
600	11.56
630	12.22
720	13.85
750	14.32

Run 158, L = 5.075 cm.

Time (min.)	[Sn] (mol./l.)
30	0.54×10^{-5}
60	0.98
120	1.95
210	3.45
270	4.44
360	5.93
450	6.45
510	8.33
570	9.42
660	10.87
750	12.45
780	12.85

Reproduced with permission of the copyright owner. Further reproduction prohibited without permission.

VARIATION OF TUBE LENGTH

12,000 ml. N_2 Saturated 1M HCl

83,00 cm./min., 30°C, d = 1.27 cm.

Run 159, L = 13.97 cm.

Time (min.)	$[Sn]$ (mol./l.)
30	0.65×10^{-5}
60	1.15
120	2.55
210	4.45
300	6.39
390	8.42
480	10.24
510	10.65
600	12.79
690	14.66
750	15.86

Run 160, L = 11.42 cm.

Time (min.)	$[Sn]$ (mol./l.)
30	0.56×10^{-5}
60	1.11
90	1.50
120	2.20
180	3.25
300	5.55
420	7.78
540	9.96
630	11.55
710	13.22
740	13.65

Run 161, L = 8.9 cm.

Time (min.)	$[Sn]$ (mol./l.)
30	0.50×10^{-5}
60	0.93
120	1.85
240	3.71
330	5.05
420	6.53
510	7.92
600	9.33
660	10.26
720	11.15

Run 162, L = 6.35 cm.

Time (min.)	$[Sn]$ (mol./l.)
30	0.40×10^{-5}
60	0.73
150	1.80
245	2.92
305	3.68
395	4.82
485	5.89
545	6.63
605	7.35
695	8.42
755	9.15

Run 163, L = 5.075 cm.

Time (min.)	$[Sn]$ (mol./l.)
30	0.34×10^{-5}
60	0.63
120	1.26
245	2.45
305	3.15
365	3.75
455	4.70
575	6.00
635	6.55
725	7.54
785	8.15

VARIATION OF TUBE LENGTH

12,000 ml. N_2 Saturated 1M HCl

2,350 cm./min., 30°C, d = 1.27 cm.

Run 164 L = 13.95 cm.		Run 165 L = 12.7 cm.		Run 166 L = 8.9 cm.		Run 167 L = 7.62 cm.		Run 168 L = 5.075 cm.	
Time (min.)	[Sn] (mol./l.)	Time (min.)	[Sn] (mol./l.)	Time (min.)	[Sn] (mol./l.)	Time (min.)	[Sn] (mol./l.)	Time (min.)	[Sn] (mol./l.)
30	0.30×10^{-5}	30	0.28×10^{-5}	30	0.24×10^{-5}	45	0.30×10^{-5}	30	0.18×10^{-5}
60	0.56	60	0.51	60	0.41	90	0.55	60	0.32
120	1.12	90	0.83	120	0.80	135	0.73	120	0.61
210	1.93	180	1.55	240	1.55	225	1.22	180	0.96
300	2.75	270	2.32	300	2.05	315	1.85	300	1.62
390	3.56	360	3.16	370	2.50	405	2.35	420	2.27
430	3.95	450	3.80	425	2.87	435	2.67	510	2.65
520	4.88	540	4.74	545	3.69	495	2.95	600	3.24
610	5.63	630	5.55	610	4.15	585	3.55	660	3.57
670	6.22	720	6.32	665	4.52	645	3.92	720	3.89
760	7.15	750	6.57	725	4.93	735	4.45		

VARIATION OF TUBE LENGTH

12,000 ml. N_2 Saturated 1M HCl

16,600 cm./min., 40°C, d = 1.27 cm.

Run 169
L = 13.95 cm.

Time (min.)	[Sn] (mol./l.)
30	1.35×10^{-5}
60	2.50
120	4.95
190	7.55
250	10.05
340	14.54
430	17.65
460	18.95
550	22.62
640	26.75
730	30.55
760	31.32

Run 170
L = 11.42 cm.

Time (min.)	[Sn] (mol./l.)
30	1.15×10^{-5}
60	2.15
150	5.45
240	8.65
330	11.95
420	15.29
480	17.48
570	20.05
660	24.10
750	27.30

Run 171
L = 8.9 cm.

Time (min.)	[Sn] (mol./l.)
30	0.95×10^{-5}
60	1.82
90	2.55
180	5.45
270	8.16
360	11.02
450	13.65
540	16.45
630	19.22
720	22.00
780	23.65

Run 172
L = 6.35 cm.

Time (min.)	[Sn] (mol./l.)
45	0.75×10^{-5}
90	1.45
135	2.05
225	2.75
315	3.35
405	4.20
435	8.95
525	11.55
615	14.45
705	16.55
735	17.85

Run 173
L = 5.075 cm.

Time (min.)	[Sn] (mol./l.)
30	0.66×10^{-5}
60	1.20
120	2.45
210	4.35
300	6.19
390	8.05
480	9.90
570	11.64
660	13.62
750	15.22

204

VARIATION OF HCl CONCENTRATION

12,000 ml., N_2 Saturated, 16,600 cm./min.

30°C, d = 1.27 cm., L = 10.16 cm.

Run 174 HCl = 0.1M Time (min.)	[Sn] (mol./l.)	Run 175 HCl = 0.25M Time (min.)	[Sn] (mol./l.)	Run 176 HCl = 0.5M Time (min.)	[Sn] (mol./l.)	Run 177 HCl = 2.0M Time (min.)	[Sn] (mol./l.)	Run 178 HCl = 4.0M Time (min.)	[Sn] (mol./l.)
30	0.85×10^{-5}	30	0.78×10^{-5}	30	0.80×10^{-5}	30	0.85×10^{-5}	45	1.21×10^{-5}
60	1.55	60	1.50	60	1.60	60	1.64	90	2.35
90	2.35	130	3.22	115	3.15	90	2.45	135	3.55
120	3.10	190	4.82	175	4.88	180	4.83	225	5.45
210	5.55	310	8.04	295	8.12	240	6.42	315	8.34
300	8.03	430	11.25	415	11.34	300	8.11	405	10.50
390	11.00	550	14.46	535	14.35	360	9.64	495	13.21
480	12.85	610	16.07	595	15.95	480	12.85	585	15.25
570	15.12	670	17.67	655	17.80	570	15.15	675	18.35
660	17.67	730	19.28	715	19.55	660	17.67	765	19.85
750	19.98	790	20.89	775	21.00	720	19.33	795	21.00
						750	20.32		

APPENDIX 9

DATA OF POLARIZATION AND CATHODIC POLARIZATION TESTS

206

EFFECT OF HCl CONCENTRATION ON THE POLARIZATION OF
TIN IN NITROGEN SATURATED ACID SOLUTIONS

Stationary Tin Cylinders; d = 0.762 cm., L = 7.62 cm.

25°C, 1000 ml. N_2 Saturated HCl

Cathodic Polarization

E, (volts) vs S.C.E.	i, (ma/cm²) 1M HCl	2M HCl
-1.80	30.00	46.20
-1.70	27.50	46.10
-1.60	24.00	44.00
-1.50	20.50	40.20
-1.40	15.00	35.30
-1.30	11.20	28.00
-1.20	7.20	22.50
-1.10	3.50	14.00
-1.05	2.20	10.15
-1.00	1.30	6.25
-0.95	0.80	3.50
-0.90	0.45	1.30
-0.85	0.30	0.82
-0.80	0.15	0.31
-0.75	0.11	0.14

Anodic Polarization

E, (volts) vs S.C.E.	i, (ma/cm²) 1M HCl	2M HCl
-0.65	0.15	0.13
-0.60	0.50	0.60
-0.55	1.20	2.20
-0.50	2.10	3.60
-0.45	5.30	11.55
-0.40	9.20	20.00
-0.35	14.00	30.50
-0.30	21.20	40.15
-0.20	33.20	53.85
-0.10	48.00	68.00
0.00	60.40	84.50
+0.10	75.85	95.50
+0.20	89.50	114.20
+0.30	105.50	129.50
+0.40	120.00	144.70
+0.50	137.00	155.50
+0.60	145.50	168.00
+0.70	154.50	175.80
+0.80	160.55	180.00

EFFECT OF HCl CONCENTRATION ON THE POLARIZATION OF TIN IN AIR SATURATED ACID SOLUTIONS

Stationary Tin Cylinders; d = 0.762 cm., L = 7.62 cm.
25°C, 1000 ml. Air Saturated HCl

Cathodic Polarization

E, (volts) vs S.C.E.	i, (ma/cm.^{2})				
	0.0625M HCl	0.125M HCl	0.25M HCl	0.5M HCl	1.0M HCl
-1.80	10.30	21.50	38.40	48.50	69.50
-1.70	9.25	18.50	34.20	42.96	64.30
-1.60	7.60	15.50	27.50	36.00	56.00
-1.50	6.30	12.45	22.00	29.85	48.50
-1.40	5.00	9.50	16.40	23.50	40.00
-1.30	3.70	6.80	12.30	16.50	34.00
-1.20	2.40	4.40	7.60	11.00	24.60
-1.10	1.20	2.40	3.80	4.60	16.00
-1.00	0.62	1.00	1.40	2.00	7.60
-0.95	0.45	0.72	0.95	1.30	5.30
-0.90	0.35	0.54	0.60	0.70	2.20
-0.85	0.25	0.33	0.35	0.40	1.30
-0.80	0.14	0.18	0.13	0.25	0.60
-0.75	0.12	0.14	0.12	0.15	0.17

EFFECT OF HCl CONCENTRATION ON THE POLARIZATION OF TIN IN AIR SATURATED ACID SOLUTIONS

Stationary Tin Cylinders; d = 0.762 cm., L = 7.62 cm.
25°C, 1000 ml. Air Saturated HCl

Anodic Polarization

E, (volts) vs S.C.E.	i, (ma/cm^2)				
	0.0625M HCl	0.125M HCl	0.25M HCl	0.5M HCl	1.0M HCl
-0.65	0.12	0.13	0.18	0.16	0.20
-0.60	0.22	0.25	0.32	0.48	0.50
-0.55	0.45	0.56	0.64	1.22	1.45
-0.50	0.72	1.10	1.30	2.30	2.70
-0.45	0.86	1.75	3.60	5.40	6.30
-0.40	1.20	2.44	4.20	8.80	11.20
-0.35	1.76	4.65	6.30	12.50	15.45
-0.30	2.50	7.10	9.10	18.00	20.50
-0.20	4.80	11.50	15.50	28.50	37.00
-0.10	6.95	15.95	21.40	42.00	49.50
0.00	9.20	21.00	31.50	52.00	66.10
+0.10	11.50	25.85	39.00	66.75	81.00
+0.20	13.65	31.00	48.00	81.50	98.50
+0.30	16.00	35.85	58.00	95.00	111.50
+0.40	17.85	42.10	67.55	110.00	127.50
+0.50	19.50	46.20	77.55	121.50	144.30
+0.60	22.00	49.70	86.80	133.40	155.30
+0.70	23.80	53.00	93.00	143.30	164.80
+0.80	25.00	56.00	98.00	145.50	172.00

CATHODIC PROTECTION EFFECTS RELATED TO PROTECTION
CURRENT REQUIREMENTS IN AIR SATURATED HCl SOLUTIONS

Stationary Tin Cylinders; d = 0.762 cm., L = 7.62 cm.
25°C, 1000 ml. Air Saturated 1M HCl

Applied Potential E, (volts) vs S.C.E.	Protection Current Density, i, (ma/cm²)	[Sn] in Corroding Solution (After 3 hours of immersion), (mol./l.)
-1.50	47.85	0.25×10^{-5}
-1.40	39.55	0.25 -
-1.30	34.00	0.25 -
-1.20	23.85	0.25 -
-1.10	16.00	0.25 -
-1.00	7.60	0.25 -
-0.90	2.20	0.32 -
-0.80	0.60	0.45 -
-0.75	0.16	5.00×10^{-5}
-0.70	0.00	1.40×10^{-4}
-0.64	0.00	1.78 -

EFFECT OF OXYGEN CONCENTRATION ON CATHODIC AND
ANODIC POLARIZATION OF TIN IN A FLOW SYSTEM

Tin tube; d = 1.27 cm., L = 10.16 cm., 30°C

14,300 cm./min., 12,000 ml. 1M HCl

Cathodic Polarization

E,(volts) vs S.C.E.	i,(ma/cm²) P_{O_2} =.21 atm.	P_{O_2} = 1 atm.	P_{O_2} = 0 atm.
-1.60	76.85	64.30	49.20
-1.50	65.55	62.00	46.30
-1.40	59.80	60.15	41.50
-1.30	52.75	56.20	38.10
-1.20	46.00	52.05	33.00
-1.10	38.95	46.25	28.90
-1.00	31.55	40.50	24.00
-0.95	28.55	37.15	21.75
-0.90	25.00	34.20	18.90
-0.85	22.15	31.00	16.55
-0.80	18.50	28.30	14.10
-0.75	17.25	25.30	12.00
-0.70	15.10	17.85	10.05
-0.65	12.22	16.90	7.50
-0.60	7.05	15.00	5.10
-0.55	2.60	3.20	1.51

Anodic Polarization

E,(volts) vs S.C.E.	i,(ma/cm²) P_{O_2} = 0 atm.	P_{O_2} =.21 atm.	P_{O_2} = 1 atm.
-0.45	1.50	2.30	2.20
-0.40	2.30	3.50	5.95
-0.35	4.25	5.55	12.5
-0.30	6.20	10.08	22.85
-0.25	10.55	18.55	28.65
-0.20	17.50	30.10	39.50
-0.15	23.75	35.50	48.65
-0.10	31.00	41.85	57.85
0.00	41.85	55.15	77.00
+0.10	55.10	69.86	95.35
+0.20	66.75	86.10	118.85
+0.30	81.05	105.25	145.22
+0.40	95.55	121.15	168.35
+0.50	113.20	144.90	189.66
+0.60	129.55	163.85	215.75
+0.70	144.85	185.00	233.25
+0.80	163.00	201.75	245.89
+0.90	174.85	217.50	255.00
+1.00	185.15	230.15	265.00

EFFECT OF FLUID VELOCITY ON CATHODIC POLARIZATION
OF TIN IN A FLOW SYSTEM

Tin tube; d = 1.27 cm., L = 10.16 cm., 30°C

12,000 ml. Air Saturated 1M HCl

E, (volts) vs S.C.E.	i, (ma/cm^2)		
	2,650 cm./min.	8,350 cm./min.	14,300 cm./min.
-1.60	30.15	48.95	74.50
-1.50	26.22	43.00	66.00
-1.40	22.50	37.50	57.80
-1.30	19.00	31.85	52.00
-1.20	16.25	27.35	44.30
-1.10	12.95	23.00	38.10
-1.00	10.05	18.00	31.00
-0.95	8.95	15.55	27.50
-0.90	7.80	13.50	24.20
-0.85	6.33	11.70	21.50
-0.80	4.70	10.00	18.00
-0.75	3.55	8.50	15.30
-0.70	2.50	6.00	12.00
-0.65	3.05	4.30	9.50
-0.60	1.40	2.80	6.80
-0.55	0.60	1.50	2.50

EFFECT OF FLUID VELOCITY ON ANODIC POLARIZATION
OF TIN IN A FLOW SYSTEM

Tin tube; d = 1.27 cm., L = 10.16 cm., 30°C

12,000 ml. Air Saturated 1M HCl

E, (volts) vs S.C.E.	i, (ma/cm^2)		
	2,650 cm./min.	8,350 cm./min.	14,300 cm./min.
-0.35	0.49	1.20	5.10
-0.30	1.50	3.90	9.50
-0.25	2.20	6.50	19.55
-0.20	3.10	9.00	30.00
-0.15	4.60	14.30	44.60
-0.10	7.20	21.00	60.00
-0.05	10.50	26.30	62.30
-0.00	14.25	30.00	65.50
0.00	19.00	40.00	72.30
+0.10	25.00	49.55	88.00
+0.20	33.50	61.60	105.50
+0.30	41.20	74.00	120.00
+0.40	48.50	86.85	138.85
+0.50	57.50	99.55	159.50
+0.60	65.00	114.30	178.80
+0.70	71.00	125.50	200.00
+0.80	78.00	135.50	215.00
+0.90	85.00	150.00	230.00

CATHODIC PROTECTION OF TIN IN HIGH VELOCITY, AIR SATURATED HCl SOLUTIONS

Tin tube; d = 1.27 cm., L = 10.16 cm.
30°C, 12,000 ml. 1M HCl, 14,300 cm./min.

From Unprotected Sample

Time (min.)	$[Sn]$ (mol./l.)
60	0.65×10^{-4}
90	1.15
150	1.83
210	2.77
300	4.26
360	5.26
390	5.75
450	6.95
510	8.15
540	8.75
600	9.42
630	11.05

E = -1.2 volts vs S.C.E. i = 44.30 ma/cm²

Time (min.)	$[Sn]$ (mol./l.)
30	0.24×10^{-4}
60	0.36
90	0.49
120	0.55
150	0.64
240	0.70
300	0.80
330	0.84
390	0.89
450	0.95
510	1.04
570	1.09
600	1.14
660	1.20

E = -1.1 volts vs S.C.E. i = 32.50 ma/cm²

Time (min.)	$[Sn]$ (mol./l.)
30	0.20×10^{-4}
60	0.35
90	0.45
120	0.50
180	0.54
210	0.60
270	0.65
300	0.68
360	0.72
390	0.76
480	0.85
540	0.90
570	0.95
600	0.97
630	1.00
650	1.02

E = -1.0 volt vs S.C.E. i = 27.50 ma/cm²

Time (min.)	$[Sn]$ (mol./l.)
30	0.25×10^{-4}
60	0.46
90	0.65
120	0.70
150	0.75
210	0.82
270	0.95
330	1.04
390	1.12
450	1.24
510	1.33
570	1.40
630	1.50

E = -0.9 volts vs S.C.E. i = 24.20 ma/cm²

Time (min.)	$[Sn]$ (mol./l.)
30	0.20×10^{-4}
60	0.25
90	0.29
120	0.29
210	0.29
240	—
300	—
360	—
420	—
480	—
510	—
540	—
600	—
660	—

CATHODIC PROTECTION OF TIN IN HIGH VELOCITY, AIR SATURATED HCl SOLUTIONS

Tin tube; d = 1.27 cm., L = 10.16 cm.
30°C, 12,000 ml. 1M HCl, 14,300 cm./min.

E = -0.5 volts vs S.C.E. i = 2.50 ma/cm²	
Time (min.)	[Sn] (mol./l.)
30	0.24x10⁻⁴

E = -0.5 volts vs S.C.E., i = 2.50 ma/cm²	
Time (min.)	[Sn] (mol./l.)
30	0.24×10^{-4}
60	0.65
120	1.20
180	2.15
240	2.70
300	3.65
360	4.15
420	4.90
480	5.74
540	6.34
600	7.05
620	7.22
650	7.56

E = -0.6 volts vs S.C.E., i = 6.80 ma/cm²	
Time (min.)	[Sn] (mol./l.)
30	0.10×10^{-4}
60	0.15
90	0.20
150	--
180	--
240	--
270	--
330	--
390	--
435	--
495	--
525	--
585	--
645	--

E = -0.7 volts vs S.C.E., i = 11.90 ma/cm²	
Time (min.)	[Sn] (mol./l.)
30	0.20×10^{-4}
60	0.24
120	0.30
150	--
210	--
270	--
300	--
360	--
420	--
450	--
480	--
510	--
570	--
630	--

E = -0.8 volts vs S.C.E., i = 18.00 ma/cm²	
Time (min.)	[Sn] (mol./l.)
30	0.2×10^{-4}
60	0.42
90	0.40
120	0.42
150	--
180	--
210	--
270	--
330	--
390	--
450	--
510	--
570	--
630	--
660	--

CATHODIC PROTECTION OF TIN IN HIGH VELOCITY,
OXYGEN SATURATED HCl SOLUTIONS

Tin tube; d = 1.27 cm., L = 10.16 cm.
30°C, 12,000 ml. 1M HCl, 14,300 cm./min.

From Unprotected Sample

Time (min.)	$[Sn]$ (mol./l.)
30	0.55×10^{-4}
60	1.21
90	2.80
120	3.95
130	4.10
190	6.20
220	7.30
280	10.15
340	12.85
370	13.45
430	16.95
490	20.35
550	25.68
610	31.20

E = -0.9 volts vs S.C.E. i = 34.2 ma/cm²

Time (min.)	$[Sn]$ (mol./l.)
30	0.20×10^{-4}
60	0.25
90	0.65
120	0.74
180	1.10
240	1.42
300	1.62
330	1.75
390	1.95
450	1.95
510	1.97
570	2.02
630	2.02
670	2.06

E = -0.7 volts vs S.C.E. i = 18.25 ma/cm²

Time (min.)	$[Sn]$ (mol./l.)
30	0.10×10^{-4}
60	0.20
120	0.45
150	0.50
210	0.56
270	0.65
330	0.80
390	0.95
450	1.06
510	1.04
570	1.05
600	1.05
630	1.05
675	1.05

E = -0.6 volts vs S.C.E. i = 14.50 ma/cm²

Time (min.)	$[Sn]$ (mol./l.)
30	0.20×10^{-4}
60	0.35
90	0.50
120	0.60
180	0.85
210	1.05
270	1.15
300	1.20
360	1.45
400	1.50
430	1.55
500	1.65
600	1.70
630	1.70
670	1.75

E = -0.5 volts vs S.C.E. i = 4.5 ma/cm²

Time (min.)	$[Sn]$ (mol./l.)
45	0.75×10^{-4}
110	2.05
170	3.15
220	4.15
260	4.90
310	5.75
370	6.80
440	5.95
520	5.75
570	9.75
590	10.75
660	11.10
	12.25

CATHODIC PROTECTION OF TIN IN HIGH VELOCITY, NITROGEN SATURATED HCl SOLUTIONS

Tin tube; d = 1.27 cm., L = 10.16 cm.

30°C, 12,000 ml. 1M HCl, 14,300 cm./min.

From Unprotected Sample

Time (min.)	[Sn] (mol./l.)
30	0.20x10^{-4}
60	0.25
120	0.35
200	0.74
230	0.85
300	1.10
360	1.25
420	1.54
500	1.82
530	1.90
560	2.05
600	2.15
670	2.35

E = -1.0 volt vs S.C.E. i = 24 ma/cm²

Time (min.)	[Sn] (mol./l.)
30	0.35x10^{-5}
60	0.55
90	0.65
120	0.75
130	-
220	-
280	-
340	-
430	-
490	-
550	-
610	-
640	-
670	-

E = -0.7 volts vs S.C.E. i = 10.05 ma/cm²

Time (min.)	[Sn] (mol./l.)
30	0.35x10^{-5}
60	0.42
90	0.55
150	0.70
240	-
300	-
360	-
400	-
460	-
520	-
580	-
660	-

E = -0.6 volts vs S.C.E. i = 5.10 ma/cm²

Time (min.)	[Sn] (mol./l.)
45	0.40x10^{-5}
90	0.65
135	1.20
195	-
225	-
255	-
315	-
375	-
435	-
495	-
555	-
615	-
645	-

E = -0.5 volts vs S.C.E. i = 2.50 ma/cm²

Time (min.)	[Sn] (mol./l.)
30	0.12x10^{-4}
60	0.14
90	0.30
120	0.31
180	0.44
240	0.62
300	0.75
320	0.80
365	0.90
450	1.12
480	1.24
560	1.34
600	1.52
660	1.65

CATHODIC PROTECTION OF TIN IN LOW VELOCITY, AIR SATURATED HCl SOLUTIONS

Tin tube; d = 1.27 cm., L = 10.16 cm.

30°C, 12,000 ml. 1M HCl, 2,650 cm./min.

From Unprotected Sample

Time (min.)	$[Sn]$ (mol./l.) 0.13×10^{-4}
30	0.13
60	0.22
90	0.45
120	0.54
130	0.58
210	1.06
270	1.22
330	1.85
390	2.38
450	2.75
540	3.45
600	3.93
630	4.20

E = -1.1 volts vs S.C.E. i = 12.95 ma/cm^2

Time (min.)	$[Sn]$ (mol./l.) 0.45×10^{-5}
30	0.45
60	0.72
90	0.93
120	1.30
190	–
250	–
340	–
370	–
400	–
430	–
460	–
490	–
570	–
630	–
660	–

E = -1.0 volt vs S.C.E. i = 10.05 ma/cm^2

Time (min.)	$[Sn]$ (mol./l.) 0.30×10^{-5}
30	0.30
60	0.45
120	0.70
130	–
190	–
220	–
250	–
340	–
400	–
460	–
520	–
600	–
630	–

E = -0.6 volts vs S.C.E. i = 1.40 ma/cm^2

Time (min.)	$[Sn]$ (mol./l.) 0.35×10^{-5}
30	0.35
60	0.42
90	0.50
120	0.72
210	–
270	–
330	–
390	–
450	–
540	–
600	–
630	–

E = -0.5 volts vs S.C.E. i = 0 ma/cm^2

Time (min.)	$[Sn]$ (mol./l.) 0.10×10^{-4}
30	0.10
60	0.17
120	0.38
210	0.70
300	1.12
330	1.22
400	1.45
450	1.65
510	1.84
600	2.30
660	2.48

PROTECTION CURRENT DEPENDENCE ON TEMPERATURE FOR TIN IN AIR SATURATED HCl SOLUTIONS

Flow system, 12,000 ml. Air Saturated 1M HCl

Tin tube; d = 1.27 cm., L = 10.16 cm.

E = -0.8 volts vs S.C.E.
v = 14,300 cm./min.

T (°C)	Protection Current Density, (ma/cm²)
25	17.40
30	20.05
35	21.20
40	22.65
45	23.44
50	24.35
55	26.10

E = -0.6 volts vs S.C.E.
v = 14,300 cm./min.

T (°C)	Protection Current Density, (ma/cm²)
25	6.10
30	7.05
35	8.22
40	9.45
45	10.35
50	12.00
55	12.90

E = -0.6 volts vs S.C.E.
v = 8,350 cm./min.

T (°C)	Protection Current Density, (ma/cm²)
25	1.50
30	2.60
35	3.22
40	5.65
45	6.30
50	7.70
55	8.75

PROTECTION CURRENT DEPENDENCE ON FLUID VELOCITY FOR TIN IN AIR SATURATED HCl SOLUTIONS

Flow system, 12,000 ml. Air Saturated 1M HCl

Tin tube; d = 1.27 cm., L = 10.16 cm., 30°C

E = -0.8 volts vs S.C.E.		E = -0.7 volts vs S.C.E.		E = -0.6 volts vs S.C.E.	
v, (cm./min.)	i, (ma/cm^2.)	v, (cm./min.)	i, (ma/cm^2.)	v, (cm./min.)	i, (ma/cm^2.)
1,170	4.10	1,170	2.25	1,175	0.95
2,650	4.95	2,650	2.55	1,900	1.15
4,150	5.75	3,600	3.15	2,650	1.22
5,950	7.05	4,250	3.62	4,250	1.80
6,700	8.45	5,850	4.25	5,050	2.05
8,350	9.95	7,730	5.15	6,950	2.35
9,550	11.80	8,350	5.90	8,350	3.05
10,280	12.30	9,700	7.10	9,500	3.55
11,550	14.35	10,450	8.35	10,550	3.80
13,500	18.30	11,450	9.22	10,850	4.55
14,300	19.90	13,200	10.85	12,100	4.65
		13,950	12.20	13,550	6.25
		14,300	13.95	14,300	6.90

PROTECTION CURRENT DEPENDENCE ON OXYGEN CONCENTRATION FOR TIN IN HCl SOLUTIONS

Flow system, 12,000 ml. 1M HCl, 30°C

Tin tube; d = 1.27 cm., L = 10.16 cm.

E = -0.6 volts vs S.C.E.

v = 14,300 cm./min.	
P_{O_2}, (atm.)	i, (ma/cm²)
0.00	4.95
0.21	6.15
0.50	8.30
0.70	10.85
0.80	11.90
1.00	14.95

v = 2,650 cm./min.	
P_{O_2}, (atm.)	i, (ma/cm²)
0.00	0.45
0.21	1.15
0.50	2.65
0.70	3.85
0.80	4.20
1.00	6.15

PROTECTION CURRENT DEPENDENCE ON HCl CONCENTRATION FOR TIN IN AIR SATURATED HCl SOLUTIONS

Flow system, 12,000 ml. Air Saturated HCl

Tin tube; d = 1.27 cm., L = 10.16 cm.

E = -0.6 volts vs S.C.E., 30°C

v = 14,300 cm./min.		v = 9,100 cm./min.		v = 8,350 cm./min.		v = 2,650 cm./min.	
[HCl] (molar)	i (ma/cm²)	[HCl] (molar)	i (ma/cm²)	[HCl] (molar)	i (ma/cm²)	[HCl] (molar)	i (ma/cm²)
0.0625	1.65	0.0625	0.55	0.0625	0.45	0.0625	0.30
0.1250	2.30	0.125	0.84	0.125	0.60	0.125	0.45
0.25	3.65	0.25	1.30	0.25	1.20	0.25	0.55
0.40	4.75	0.40	1.80	0.40	1.55	0.45	0.65
0.50	5.30	0.50	2.15	0.50	1.65	0.60	1.00
0.60	5.65	0.60	2.45	0.72	2.24	0.80	1.10
0.72	6.10	0.72	2.65	0.90	2.35	0.90	1.15
0.80	6.45	0.90	3.12	1.00	2.80	1.00	1.20
1.00	6.95	1.00	3.20				

REFERENCES

1. Abramova, T.M., I.I. Gankina, and A.S. Fomenko, Doklady Akad, Nauk U.S.S.R., 129,820(1959).

2. Agazzi, E.J., Anal. Chem., 37, 364(1965).

3. Akimov, G.V., "Theory and Methods for Investigating Corrosion of Metals," Moscow Academy of Sciences,(1945).

4. Akimov, G.V., Proceedings of the Zhukovskii Central Aero-Hydrodynamic Institute, No. 70,(1931).

5. Allan, J.E., Spectrochim. Acta, 18, 259(1962).

6. Amas, M.D., and J.B. Willis, Spectrochim. Acta, 22, 1325(1966).

7. Bekier, E., and A. Basinski, J. Chim. Phys., 27,256(1930).

8. Berzelius, J.J., Ann. Chim. Phys., 87, 50(1817).

9. Berzelius, J.J., Ann. Chim. Phys., 5, 149(1813).

10. Bockris, J.O'M., and B.E. Conway(Eds.), "Modern Aspects of Electrochemistry," No.1, Butterworths, (1954).

11. Bockris, J.O'M., and B.E. Conway(Eds.), "Modern Aspects of Electrochemistry," No.3, Butterworths, (1964).

12. Bodner, J.J., M.A.Sc. Thesis, University of Windsor,(1964).

13. Bond, G.C., "Catalysis by Metals," Academic Press, New York,(1962).

14. Brennert, S., Ueber die Korrosion Von Zinn und Verzinnten Materialen Unter Bildung Schwarzer Flecken(Thesis), Stockholm, (1935).

15. Britton, S.C., and D.G. Michael, J. Appl. Chem., 7, 349(1957).

16. Bumbulis, J., and W.F. Graydon, J. Electrochem. Soc., 109,1130(1962).

17. Capacho-Delgado, L., and D.C. Manning, Spectrochim. Acta, 22, 1505(1966).

223

18. Clement, J.K., and L.V. Walker, Trans. Electrochem. Soc., 69, 153(1936).

19. Conway, B.E., "Electrochemical Data," Elsevier, New York, (1952).

20. Cornet, I., E.A. Barrington, and G.U. Behrsing, J. Electrochem. Soc., 108, 947(1961).

21. Cornet, I., and R. Kappesser, Symosium on Corrosion, Tripartite Chemical Engineering Conference, Montreal, (1968).

22. Davy, H., Philosophical Trans. Royal Soc., 114, 151(1824).

23. Delahay, P., "Double Layer and Electrode Kinetics," Interscience, New York, (1965).

24. Dugale, I., J. App. Chem., 13, 42(1963).

25. Eisenberg, M., C.W. Tobias, and C.R. Wilke, J. Electrochem. Soc., 101, 306(1954).

26. Elder, P.J., and G. Wranglen, Electrochemical Technology, 2, No. 1-2(1964).

27. Evans, U.R., "Metallic Corrosion, Passivity, and Protection," Edward Arnold and Co., London, (1948).

28. Fontana, M.G., and N.D. Greene, "Corrosion Engineering," McGraw-Hill, New York, (1967).

29. Friend, J.A.N, J. Chem. Soc., 119, 932(1921).

30. Gatehouse, B.M., and J.B. Willis, Spectrochim. Acta, 17, 710(1961).

31. Gatty, O., and E.C. Spooner, "Electrode Potential Behaviour of Corroding Metals in Aqueous Solutions," Oxford University Press, London, (1938).

32. Gibson, J.H., W.E.L. Grossman, and W.D. Cooke, Anal. Chem., 35, 266(1963).

33. Gnyp, A.W., Ph.D. Thesis, University of Toronto, (1958).

34. Hagymas, G., and M. Quintin, J. Chim. Phys. et Phys. Chim. Biol., 61, 541(1964).

35. Hampson, N.A., and N.E. Spencer, Br. Corros. J., 3, 2(1968).

36. Harker, G., and J. McNamara, J. Soc. Chem. Ind., 29, 1286(1910).

37. Hatch, G.B., and O. Rice, Ind. Eng. Chem., 37, 752(1945).

38. Hoar, T.P., Trans. Faraday Soc., 33, 1152(1937).

39. Ibl, N., Electrochem. Acta, 1, 117(1959).

40. Kagetsu, T.J., and W.F. Graydon, J. Electrochem. Soc., 110, 709(1963).

41. Kalbanov, B.N., and D.V. Kokoulina, Proceedings of the U.S.S.R. Academy of Science, 120, 558(1958).

42. Kerr, R., J. Soc. Chem. Ind., 57, 405(1938).

43. Khitrov, V.A., and V.I. Shatalov, Tsvetn. Metel.,35, 95(1962).

44. Kohman, E.F., and N.H. Sanborn, Ind. Eng. Chem., 20, 1373(1928).

45. Krasilshchikov, A.I., and V.A. Andreeva, J. Phys. Chem. U.S.S.R., 20, 1199(1946).

46. Lange, E., and K. Nagel, Z. Electrochem., 53, 21(1949).

47. Leveque, J., Ann. Mines, 13, 201, 305, 381(1928).

48. Levich, V.G., "Physicochemical Hydrodynamics," Prentice-Hall, New Jersey, (1962).

49. Levitch, B., Discussion Faraday Soc., No.1, 37(1947).

50. Lin, C.S., E.B. Denton, H.S. Gaskill, and G.L. Putnam, Ind. Eng. Chem., 43, 2136(1951).

51. Lu, B.C-Y., and W.F. Graydon, J. Am. Chem. Soc., 77, 6136(1955).

52. Lu, B.C-Y., and W.F. Graydon, Can. J. Chem., 32, 153(1954).

53. Lui, A.W.K., Ph.D. Thesis, University of Windsor, (1964).

54. Makrides, A.C., J. Electrochem. Soc., 107, 869(1960).

55. Makrides, A.C., and N. Hackerman, J. Electrochem. Soc., 105, 156(1958).

56. Marshkov, J.K., Ya.A. Ugai, and V.I. Vigdorovich, J. Appl. Chem. U.S.S.R., 38, 1101(1965).

57. Mears, R.B., and R.H. Brown, Trans. Electrochem. Soc., 74, 519(1938).

58. Mears, R.B., and R.H. Brown, Trans. Electrochem. Soc., 81, 455(1942).

59. Morgan, J.H., "Cathodic Protection," Leonard Hill Books Limited, London(1959).

60. Muller, E., Schwabe Z. Electrochem., 37, 185(1931).

61. Nernst, H.W., Z. Phys. Chem., 47, 55(1904).

62. Perry, J.H., "Chemical Engineers' Handbook," 3rd. ed., McGraw-Hill, New York, (1950).

63. Poa, D.S-P., M.A.Sc. Thesis, University of Windsor, (1967)

64. Potter, E.C., "Electrochemistry," MacMillan, London,(1956)

65. Pourbaix, M.,"Ailas D'Equilibres Electrochemiques a 25°C," Gauthier Villars, Paris,(1963).

66. Pryor, M.J., and D.S. Keir, J. Electrochem. Soc., 102, 609(1955).

67. Reichert, S.A., M.C. Neight, and H.W. Reidel, Ind. Eng. Chem., 11, 194(1939).

68. Riddiford, A.C., and L.L. Bircumshaw, J. Chem. Soc., 1, 697(1952).

69. Romeo, A.J., R.T. Skrinde, and R. Eliassen, Proc. Amer. Soc. Civ. Engrs., 84, Paper 1702,(1958).

70. Ross, T.K., and C. Firouis, Electrochem. Acta, 8, 877(1963).

71. Ross, T.K., and D.H. Jones, J. Appl. Chem., 12, 314(1962).

72. Rothelli, J., and T.R. Brown, Ind. Eng. Chem., 23, 1010(1931).

73. Shreir, L.L.(Ed.), "Corrosion," John Wiley and Sons, New York,(1963).

74. Slomyanskaya, F.B., Corrosion and Prevention, 4,332(1936).

75. Speller, F.N., and V.V. Kendall, Ind. Eng. Chem., 15, 134(1923).

76. Stender, V.V., B.P. Artamonov, and K.Yu. Bogoyavlenskii, J. Appl. Chem. U.S.S.R., 3, 414(1937).

77. Stern, M., Corrosion, $\underline{14}$, 440t(1958).

78. Stern, M., "Symposium on Corrosion Fundamentals,"
University of Tennessee Press, 84(1956).

79. Stern, M., and A.L. Geary, J. Electrochem. Soc., $\underline{104}$,
56(1957).

80. Stone, F.S.,Adv. Catalysis, $\underline{13}$, 1(1962).

81. Tafel, J., Z. Phys. Chem., $\underline{50}$, 641(1905).

82. Taneja, J.N., M.A.Sc. Thesis, University of Windsor,(1967).

83. Tomashov, N.D., "Theory of Corrosion and Protection of
Metals," MacMillan, New York,(1966).

84. Uhlig, H.H., J. Electrochem. Soc., $\underline{111}$, 13(1964).

85. Uhlig, H.H., "Corrosion and Corrosion Control," John Wiley
and Sons, New York,(1965).

86. Vollmer, J., Atomic Absorption Newsletter, $\underline{5}$, 35(1966).

87. Von Shaw, P., L.P. Reiss, and T.J. Hanratty, J. A. I. Ch.
E., $\underline{9}$, 362(1963).

88. Wagner, C., and Traud, W., Z. Electrochem, $\underline{44}$, 391(1938).

89. Weeks, J.R., and G.R. Hill, J. Electrochem. Soc., $\underline{103}$,
203(1956).

90. West, J.M., Br. Corros. J., $\underline{5}$, 65(1970).

91. Whitman, W.G., Chem. Reviews, $\underline{2}$, 419(1925).

92. Whitman, W.G., and R.P. Russell, Ind. Eng. Chem., $\underline{17}$,
348(1925).

93. Wilke, C.R., M. Eisenberg, and C.W. Tobias, J. Electrochem.
Soc., $\underline{100}$, 513(1953).

94. Wilson, R.E., Ind. Eng. Chem., $\underline{15}$, 127(1923).

95. Wranglen, G., and O. Nilsson, Electrochem. Acta, $\underline{7}$, 121
(1962).

NOMENCLATURE

A   apparent surface area of specimen, cm^2.

a activity

$a_{oxd.}$ activity of oxidized species

$a_{red.}$ activity of reduced species

C   concentration, moles/liter

C_M concentration of metal ion, moles/liter

D   diffusion coefficient, sq.cm./sec.

D_M diffusion coefficient of metal ion, sq.cm./sec.

d   diameter of specimen, cm.

E   electrode potential, volts

E^o standard electrode potential, volts

E_c corrosion potential, volts

$E_{eq.}$ equilibrium potential, volts

E_i polarized potential, volts

F   Faraday, 23,063 cal./volt-mole(96,500 coulomb/equiv.)

G   Gibbs free energy, cal.

g   gravitational acceleration, 980.665 $cm./sec^2$.

I_c corrosion current density, $amp./cm^2$.

i   current density, $amp./cm^2$.

$i_{app.}$ applied current density, $amp./cm^2$.

i_L limiting current density, $amp./cm^2$.

i_o exchange current density, $amp./cm^2$.

k_1^o reaction rate constant for hydrogen evolution

k_2^o reaction rate constant for oxygen depolarization

k_3^o reaction rate constant for autocatalytic reaction

k_j mass transfer coefficient of species j, cm./sec.

k_L mass transfer coefficient, cm./sec.

L   length of specimen, cm.

M   an atom of metal

N   mass transfer flux, moles/cm^2-sec.

N_j mass transfer flux of species j, moles/cm^2-sec.

N_M mass transfer flux of metal ion, moles/cm^2-sec.

n   number of electrons transferred in a reaction

P_{O_2} partial pressure of oxygen, atm.

R   gas constant, 1.987 cal./deg-mole

r_1 reaction rate of hydrogen evolution, moles/cm^2-min.

r_2 reaction rate of oxygen depolarization, moles/cm^2-min.

r_3 reaction rate of autocatalytic reaction, moles/cm^2-min.

Sn   tin ions in solution, moles

[Sn]   tin ion concentration, moles/liter

$\Delta[Sn]_1$ tin ion concentration resulted from H_2 evolution, moles/liter

$\Delta[Sn]_2$ tin ion concentration resulted from oxygen depolarization, moles/liter

$\Delta[Sn]_3$ tin ion concentration resulted from autocatalytic reaction, moles/liter

$\underset{*}{Sn}$ active sites on a tin surface

T   absolute temperature, ^oK

t   time

u_j mobility of species j, cm^2-mole/joule-sec.

V	solution volume, liter
v	fluid velocity, cm./min.
z_j	charge number of species j

GREEK SYMBOLS

α	constant
γ	constant
ς	constant
ϵ	constant
φ	constant
β	Tafel constant
β_a	anodic Tafel constant
β_c	cathodic Tafel constant
δ	diffusion layer thickness, cm.
ρ	density, gm./cm.^{3}
μ	viscosity, gm./cm.-sec.
ν	kinematic viscosity, cm.^{2}/sec.
ψ	name of function
Ψ	name of function
η	overvoltage, volts
η_A	activation overvoltage, volts
η_C	concentration overvoltage, volts
η_R	resistance overvoltage, volts
η_T	total overvoltage, volts
ω	angular velocity, r.p.m.
θ	angle, radians

Φ electrostatic potential

SUBSCRIPTS

A   activation

a   anodic

b   bulk solution

C   concentration

c   cathodic or corrosion

i   interface

j   jth species

M   metal atom or ion

R   resistance

r   radial direction of tube

s   surface

T   total

t   time

z   axial direction of tube

DIMENSIONLESS GROUPS

Gr   Grashof number, $\dfrac{gL^3 \Delta \rho}{\rho} \left(\dfrac{\rho}{\mu} \right)^2$

Nu   Nusselt number for mass transfer, $\dfrac{kL}{D}$

Re   Reynolds number, $\dfrac{Lv\rho}{\mu}$

Sc   Schmidt number, $\dfrac{\mu}{\rho D}$

Sh   Sherwood number, $\dfrac{kL}{D}$

VITA AUCTORIS

Birthplace:	Shantung, China
Date of Birth:	February 18, 1938
Education:	Provincial Yunlin High School, Taiwan, China, 1955-1958, diploma.
	National Taiwan University, Taiwan, China, 1958-1962, B.S. degree.
	University of Windsor, Ontario, Canada, 1965-1967, M.A.Sc. degree.
	University of Windsor, Ontario, Canada, 1967-present, Ph.D. candidate.
Experience:	Taiwan Fertilizer Co., Factory No. 6, Ammonia Plant, Oct. 1962 – Oct. 1965, Shift Supervisor.